AGARD-AR-287

AGARD
ADVISORY GROUP FOR AEROSPACE RESEARCH & DEVELOPMENT
7 RUE ANCELLE 92200 NEUILLY SUR SEINE FRANCE

AGARD ADVISORY REPORT 287

Propulsion and Energetics Panel Working Group 21 on Terminology and Assessment Methods of Solid Propellant Rocket Exhaust Signatures

(Méthodes d'Evaluation des Signatures des Propulseurs à Propergol Solide)

This Advisory Report was prepared at the request of the Propulsion and Energetics Panel of AGARD.

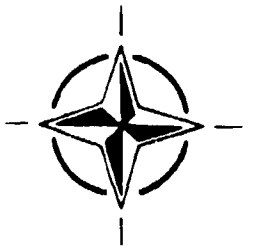

NORTH ATLANTIC TREATY ORGANIZATION

Published February 1993

Distribution and Availability on Back Cover

AGARD

ADVISORY GROUP FOR AEROSPACE RESEARCH & DEVELOPMENT

7 RUE ANCELLE 92200 NEUILLY SUR SEINE FRANCE

AGARD ADVISORY REPORT 287

Propulsion and Energetics Panel Working Group 21 on Terminology and Assessment Methods of Solid Propellant Rocket Exhaust Signatures

(Méthodes d'Evaluation des Signatures des Propulseurs à Propergol Solide)

This Advisory Report was prepared at the request of the Propulsion and Energetics Panel of AGARD.

North Atlantic Treaty Organization
Organisation du Traité de l'Atlantique Nord

The Mission of AGARD

According to its Charter, the mission of AGARD is to bring together the leading personalities of the NATO nations in the fields of science and technology relating to aerospace for the following purposes:

- Recommending effective ways for the member nations to use their research and development capabilities for the common benefit of the NATO community;
- Providing scientific and technical advice and assistance to the Military Committee in the field of aerospace research and development (with particular regard to its military application);
- Continuously stimulating advances in the aerospace sciences relevant to strengthening the common defence posture;
- Improving the co-operation among member nations in aerospace research and development;
- Exchange of scientific and technical information;
- Providing assistance to member nations for the purpose of increasing their scientific and technical potential;
- Rendering scientific and technical assistance, as requested, to other NATO bodies and to member nations in connection with research and development problems in the aerospace field.

The highest authority within AGARD is the National Delegates Board consisting of officially appointed senior representatives from each member nation. The mission of AGARD is carried out through the Panels which are composed of experts appointed by the National Delegates, the Consultant and Exchange Programme and the Aerospace Applications Studies Programme. The results of AGARD work are reported to the member nations and the NATO Authorities through the AGARD series of publications of which this is one.

Participation in AGARD activities is by invitation only and is normally limited to citizens of the NATO nations.

Published February 1993

ISBN 92-835-0699-5

Printed by Specialised Printing Services Limited
40 Chigwell Lane, Loughton, Essex IG10 3TZ

Recent Publications of the Propulsion and Energetics Panel

CONFERENCE PROCEEDINGS (CP)

Heat Transfer and Cooling in Gas Turbines
AGARD CP 390, September 1985

Smokeless Propellants
AGARD CP 391, January 1986

Interior Ballistics of Guns
AGARD CP 392, January 1986

Advanced Instrumentation for Aero Engine Components
AGARD CP 399, November 1986

Engine Response to Distorted Inflow Conditions
AGARD CP 400, March 1987

Transonic and Supersonic Phenomena in Turbomachines
AGARD CP 401, March 1987

Advanced Technology for Aero Engine Components
AGARD CP 421, September 1987

Combustion and Fuels in Gas Turbine Engines
AGARD CP 422, June 1988

Engine Condition Monitoring — Technology and Experience
AGARD CP 448, October 1988

Application of Advanced Material for Turbomachinery and Rocket Propulsion
AGARD CP 449, March 1989

Combustion Instabilities in Liquid-Fuelled Propulsion Systems
AGARD CP 450, April 1989

Aircraft Fire Safety
AGARD CP 467, October 1989

Unsteady Aerodynamic Phenomena in Turbomachines
AGARD CP 468, February 1990

Secondary Flows in Turbomachines
AGARD CP 469, February 1990

Hypersonic Combined Cycle Propulsion
AGARD CP 479, December 1990

Low Temperature Environment Operations of Turboengines (Design and User's Problems)
AGARD CP 480, May 1991

CFD Techniques for Propulsion Applications
AGARD CP 510, February 1992

Insensitive Munitions
AGARD CP 511, July 1992

Combat Aircraft Noise
AGARD CP 512, April 1992

Heat Transfer and Cooling in Gas Turbines
AGARD CP 527 (to be published in 1993)

Airbreathing Propulsion for Missiles and Projectiles
AGARD CP 526, September 1992

ADVISORY REPORTS (AR)

Suitable Averaging Techniques in Non-Uniform Internal Flows *(Results of Working Group 14)*
AGARD AR 182 (in English and French), June/August 1983

Producibility and Cost Studies of Aviation Kerosines *(Results of Working Group 16)*
AGARD AR 227, June 1985

Performance of Rocket Motors with Metallized Propellants *(Results of Working Group 17)*
AGARD AR 230, September 1986

Recommended Practices for Measurement of Gas Path Pressures and Temperatures for Performance Assessment of Aircraft Turbine Engines and Components *(Results of Working Group 19)*
AGARD AR 245, June 1990

The Uniform Engine Test Programme *(Results of Working Group 15)*
AGARD AR 248, February 1990

Test Cases for Computation of Internal Flows in Aero Engine Components *(Results of Working Group 18)*
AGARD AR 275, July 1990

Test Cases for Engine Life Assessment Technology *(Results of Working Group 20)*
AGARD AR 308, September 1992

Terminology and Assessment Methods of Solid Propellant Rocket Exhaust Signatures *(Results of Working Group 21)*
AGARD AR 287, February 1993

LECTURE SERIES (LS)

Ramjet and Ramrocket Propulsion Systems for Missiles
AGARD LS 136, September 1984

3-D Computation Techniques Applied to Internal Flows in Propulsion Systems
AGARD LS 140, June 1985

Engine Airframe Integration for Rotorcraft
AGARD LS 148, June 1986

Design Methods Used in Solid Rocket Motors
AGARD LS 150, April 1987
AGARD LS 150 (Revised), April 1988

Blading Design for Axial Turbomachines
AGARD LS 167, June 1989

Comparative Engine Performance Measurements
AGARD LS 169, May 1990

Combustion of Solid Propellants
AGARD LS 180, July 1991

Steady and Transient Performance Prediction of Gas Turbine Engines
AGARD LS 183, May 1992

AGARDOGRAPHS (AG)

Measurement Uncertainty within the Uniform Engine Test Programme
AGARD AG 307, May 1989

Hazard Studies for Solid Propellant Rocket Motors
AGARD AG 316, September 1990

Advanced Methods for Cascade Testing
AGARD AG 328 (to be published in 1993)

REPORTS (R)

Application of Modified Loss and Deviation Correlations to Transonic Axial Compressors
AGARD R 745, November 1987

Rotorcraft Drivetrain Life Safety and Reliability
AGARD R 775, June 1990

Abstract

The Propulsion and Energetics Panel's Specialists' Meeting in autumn 1985 on Smokeless Propellants demonstrated that no common standard was available in this field and that the lack of common understanding led to misunderstanding amongst the NATO community.

After some preparatory discussion, the Panel, therefore, formed Working Group Number 21 with the objectives of defining methods for the assessment of rocket motor exhaust optical properties in the visible and in the infrared range, and of recommending a terminology based on quantitative criteria.

The Working Group discussed the subject in a total of eight sessions and prepared this Advisory Report. Following an Introduction and Summary there are six chapters, commencing with an Overview and continuing with Propellant Smoke Classification, Plume Primary Smoke, Plume Secondary Smoke, Plume Radiation and Plume Microwave Properties. In most cases, the conclusions and recommendations follow the chapters and are not repeated at the end of the Report.

Résumé

La réunion de spécialistes organisée par le Panel AGARD de Propulsion et d'Energétique au printemps de 1985 sur le thème des propergols non générateurs de fumée a démontré qu'il n'existait aucune norme universellement reconnue dans ce domaine et que ce manque d'entendement pourrait donner lieu à une mauvaise compréhension au sein de la communauté de l'OTAN.

Suite à des discussions préliminaires le Panel a donc décidé de créer le groupe de travail No. 21, en vue de définir des méthodes d'évaluation des propriétés optiques des gaz éjectés des moteurs-fusée dans le domaine du visible et de l'infrarouge afin de fournir des recommandations concernant une terminologie appropriée, basée sur des critères quantitatives.

Le groupe s'est réuni huit fois pour l'élaboration de ce rapport consultatif. Suite à l'introduction et au résumé, le rapport est organisé en six chapitres, à savoir; préambule, la classification des fumées émises par les propergols, la fumée primaire du jet de propulseur, la fumée secondaire du jet de propulseur, le rayonnement du jet de propulseur, et les caractéristiques hyperfréquences du jet de propulseur. Les conclusions et les recommandations se trouvent en général à la fin de chaque chapitre et ne sont donc pas reprises en annexe du rapport.

Propulsion and Energetics Panel
Working Group 21

Chairman: Dr Bernard M. Zeller
Vice-President for North American Operations
SNPE
Washington Office
1111 Jefferson Davis Highway, Suite 700
Arlington, Virginia,
United States

MEMBERS

Canada
Mr B.L. Jones
Bristol Aerospace Ltd
P.O. Box 874
Winnipeg, R3C 294

France
Mr E. Adjari
Société nationale des Poudres
et Explosifs
Centre de recherches du Bouchet
91710 Vert-le-Petit

Mr G. Mellon
Aérospatiale
Département E/EPR
2, rue Béranger
92320 — Châtillon/Bagneux

Mr J Sauvel
CAEPE
B.P.2
33165 Saint-Medard-en-Jalles

Mr J. Souletis
SNPE des Poudres et Explosifs
91710-Vert-le-Petit

Germany
Dip. Ing. B. Crispin
Deutsche Aerospace
Abteilung KY25
Postfach 80 11 69
D-8000 München 80

Dr R. Dirscherl
Deutsche Aerospace
Abteilung VAR 331
Postfach 80 11 49
D-8000 München 80

Mr W. Liehmann
Fraunhofer Institut für
Chemische Technologie
Postfach 1240
D-7507 Pfinztal 1

Greece
Lt Col. I. Pagonis
Hellenic Air Force
Technology Research Center (KETA)
Terpsithea Post Office
16501 Glyfada
Athens

Italy
Ing. R. Brignola
SNIA
BPD
Colleferro (Roma)

Prof. L. De Luca
Dipartimento di Energetica
Politecnico di Milano
Piazza Leonardo da Vinci 32
20133 Milano

Mr R. De Amicis
BPD
Difesa e Spazio
Corso Garibaldi, 22
00034 Colleferro (Roma)

Spain
Mr D.M. Barreiros
Departemento Energia y
Propulsion
INTA
28850 Torrejon de Ardoz
Madrid

United Kingdom
Mr A. Cruttenden
Assistant Director (Projects)
Royal Ordnance
Explosives Division
Westcott, Aylesbury
Bucks HP18 0NZ

Mr G.I. Evans
Royal Ordnance
Rocket Motor Division
Summerfield
Kidderminster
Worcestershire DY11 7RZ

Mr R.E. Lawrence
RARDE, Westcott
Aylesbury
Bucks HP18 0NZ

Mr P.K. Smith
Royal Ordnance
Rocket Motor Division
Summerfield
Kidderminster
Worcestershire DY11 7RZ

Mr A. Whitehouse
Royal Ordnance
Rocket Motor Division
Summerfield
Kidderminster
Worcestershire DY11 7RZ

United States
Mr C.R. Darlington
SVERDRUP
Techn. Inc.
Mail Stop 900
Arnold Air Force Base
Tennessee 37389

Prof. D.W. Netzer
Dept of Aeronautics and
Astronautics
Code AA/NT, Naval Post
Graduate School
Monterey, CA 93943-5000

Mr A.C. Victor
Victor Technology
712 N. Peg. St
Ridgecrest, CA 93555

Mr L.B. Thorn
Advanced Propellant Technology
MICOM
Function, US Army MICOM
Code AMSMI-RD-PR-T
Redstone Arsenal
Huntsville
Alabama 35898-5000

PANEL EXECUTIVE

Dr E. Riester (GE)

Mail from Europe:
AGARD—OTAN
Attn: PEP Executive
7, rue Ancelle
F-92200 Neuilly-sur-Seine
France

Mail from US and Canada:
AGARD—NATO
Attn: PEP Executive
Unit 21551
APO AE 09777

Tel: 33(1)47 38 57 85/87
Telex: 610176 (France)
Telefax: 33 (1) 47 38 57 99

Contents

Introduction and Summary

The question of terminology in the field of solid propellant rocket motors exhaust products has always been a difficult one. In autumn 1985, AGARD held a specialist meeting in Florence on the subject of "Smokeless Propellants". The technical evaluator of this meeting, Geoffrey Evans, stated in his final report that "There is a need for an agreed quantitative measure and methodology for defining smoke properties of propellants." In fact, the classification generally used for propellants as "smoky, reduced smoke, low smoke, minimum smoke and smokeless" is much too imprecise and broad-brush to serve as a meaningful or quantitative guide.

The statements triggered a proposal from AGARD-PEP that a common language be developed within the NATO community in this specific field.

After approval of the AGARD National Delegates Board, Working Group 21 of the Propulsion and Energetics Panel was created in order to study, develop, and recommend a common terminology in the field of solid propellant rocket exhaust signatures. Its objective was also to define methods for assessing rocket motor exhausts in various wavelength regions of the electromagnetic spectrum.

The first official meeting of WG 21 was held on 30 and 31 May 1988, but two preliminary meetings took place earlier in spring and autumn 1987. Additional meetings were held every six months until the final one in autumn 1990 in Brussels, so that a total of eight meetings were held.

As a result of this work, the group has written a detailed report which appears now as an advisory report. The main results and conclusions of the group are summarised herein.

A new terminology is proposed in the field of solid propellant combustion exhaust products. This terminology, which makes a distinction between primary and secondary smokes, is based on parameters linked to solid propellant combustion products.

For primary smokes, three categories are proposed in this new classification: A, B and C (A the least smoky, C the most smoky). It has to be emphasised that the classification is intended **only for propellants**, and **not for motors**. The classification number which was selected is related to the obscuration coefficient, defined as 1-Tr, where Tr is the transmittance through a cloud of condensables in the exhaust. The value of Tr, for a given propellant, is related to the mass percentage and specific gravity of the condensables in the propellant combustion products calculated for standard conditions. An obscuration number close to 1 corresponds to a "C" propellant; close to 0, it corresponds to an "A" propellant.

For secondary smokes, three categories are also proposed: A, B and C (A the least smoky, C the most smoky). The classification approach selected is related to the minimum relative humidity of ambient air at which saturation (secondary smoke formation) will occur for a mixture of one part of calculated propellant products (H_2O, HCl, HF etc) diluted with 1,000 parts air at a mixture temperature of 0°C (273.15K) standard atmospheric pressure. A propellant classified "A" gives secondary smoke condensation only at high relative humidity. A propellant classified "C" gives secondary smoke even at low relative humidity.

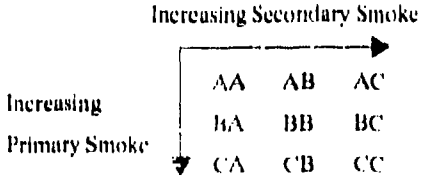

Therefore propellant classification involves two letters. A very low smoke propellant is classified AA; a very smoky propellant is classified CC. A propellant which gives very little primary smoke, but intense secondary smoke is AC, etc.

It is proposed that this new quantitative classification be widely accepted to characterise a solid propellant. However, one has to remember that this classification is related to propellant only. It cannot be assumed that because a fully assembled rocket motor contains a class AA propellant its exhaust plume will be unquestionably satisfactory for all transmittance requirements. Other design parameters, such as ignitor, liner, insulator, nozzle materials and configuration must also be considered.

In addition to this proposal for a new exhaust-smoke classification terminology, the Group also examined the various methods and facilities used in some NATO countries for measuring and predicting solid propellant motor exhaust products, their behaviour and effects. Some are recommended for agencies or companies wishing to establish such capabilities. No standard measurement methods are proposed which would classify propellants or rocket motor experimental techniques because questions of smoke measurement, transmission, emission, and scattering which arise during the development of a given rocket motor are so specific that standardised methods would be inadequate.

The main topics addressed in this report are phenomenology and operational considerations (overview), smoke classification, primary smoke, secondary smoke, plume radiation, and plume microwave properties.

In addition, there is a glossary of terms used in the plume technology field, as well as information about modelling codes and agencies and companies active in this field.

One will also find in this report information about solid propellant rocket motor exhausts which, as far as it is known, has not been available until now; consequently the report will be useful to those entering this field of activity.

For each topic, a member of WG21 was appointed as a pilot and was therefore responsible for that topic, which gave birth to a chapter of the report after discussions with other WG members.

The members of WG21 were:

Bernard ZELLER*	France, Chairman
Barry JONES	Canada
Emmanuel ADJARI	France
Gerard MELLON	France
Jacques SAUVEL	France
Jacques SOULETIS	France
Brunhardt CRISPIN*	Germany
Reinhardt DIRSCHERL	Germany
Wolfgang LIEHMANN	Germany
Lt Col. I PAGONIS*	Greece
Renato BRIGNOLA	Italy
Roberto DE AMICIS	Italy
Prof. Luigi DE LUCA*	Italy
Manuel BARREIROS	Spain
Alan CRUTTENDEN*	United Kingdom
Geoffrey EVANS	United Kingdom
Ronald LAWRENCE	United Kingdom
Peter K SMITH	United Kingdom
Anthony WHITEHOUSE*	United Kingdom
C R DARLINGTON	United States
David NETZER*	United States
Lawrence B THORN	United States
Andrew VICTOR	United States

The writing of this report was a joint effort of the Working Group. We have tried to avoid mistakes or misunderstandings. Please address questions or comments regarding this report to:

AGARD
Executive, Propulsion and Energetics Panel
7, rue Ancelle
92200 Neuilly-sur-Seine, France

or Mr Bernard Zeller
Direction de la Strategie
Division Défense Espace
SNPE
12 Quai Henri IV
75004 Paris, France

*PEP Members

CHAPTER 1

Overview

CHAPTER 1

Overview

TABLE OF CONTENTS

1.0 INTRODUCTION

It is the working group's intention that this overview should provide a useful background framework for understanding the specific technical chapters and recommendations that follow in the remainder of this AGARD Advisory Report.

Exhaust plumes have been a concern in rocket propulsion technology for over four decades. The early concerns involved plume interference with microwave guidance signals for beam-rider and semi-active systems. Subsequent concerns involved exhaust detectability due to primary and secondary smoke and the effects of smoke on some kinds of missile optical guidance systems. The recent emergence of autonomous electro-optical detection and tracking systems has introduced strong concern about increased missile and launch-platform vulnerability due to the entire spectrum of exhaust plume emissions. This becomes even more important as other missile signatures, such as body emissions, body scattering, and body radar cross section (RCS), are reduced by application of new materials technology and non-axisymmetric geometry [1].

Overriding all exhaust plume measurements and predictions is a requirement to quantitatively specify required signature levels for current and future missile missions. Straightforward as this sounds, it has never been adequately done for any tactical missile plume. There is no question that it should be done to set realistic goals and to prioritize research and development (R&D) efforts for plume detection, identification, tracking, targeting, and control. In addition, required signature levels must be identified with specific operational time-frames to correlate with projected enemy detection capabilities. It is also critical that signature be scored or ranked as to its value for any mission, also the relative value of each type of signature for that mission (e.g., IR, UV, smoke, flash, RCS). Other plume effects (e.g. guidance interference and plume impingement effects) are performance issues that must be solved for deployment. Once a set of prioritized signature goals has been established, it may be possible to prioritize the Research and Development required to reach the goals.

Those missiles for which "reduced" and "minimum smoke" propellants have been developed over the past decades have an overriding identified need for signature control. In general controlled smoke propellants are intended to prevent timely countermeasures by the target and/or to prevent interference with some optical guidance, detection, or tracking systems. For missiles launched from covert sites, there are compelling reasons to reduce launch plume signature to undetectable levels. New terminology for controlled smoke propellants is given in Chapter 2.

In general, pertinent ranges for detection will be of the same order of magnitude as the related engagement ranges. When the ranges are short, time becomes an important parameter. Time is also involved in the short burn durations of many rocket motors, limiting the time available for detection of radiative emissions.

Body and exhaust plume IR radiations have been used for decades for detection and targeting by a number of missile guidance systems. For complex engagements, involving many launch platforms and therefore many targets, IR rocket exhaust signatures may be used in the near future to detect and target launch platforms as the launch takes place. In such scenarios one is concerned about highly capable detection systems and detection ranges out to hundreds of kilometres. All signatures encounter some degree of atmospheric interference (Fig. 1-1).

Under clear sky, high visibility daylight conditions plume smoke is visible from ranges comparable to advanced IR detection capabilities. In addition, plume smoke persists and creates an "arrow" from the missile back to its launch point. Primary smoke is the result of particulate rocket motor effluent that forms during cooling of the combustion gases at any ambient atmospheric condition. Secondary smoke is the condensed vapour contrail of a missile plume; its formation depends upon both the nature of the gaseous rocket motor effluent and the prevailing ambient atmospheric temperature and humidity conditions. Missile contrails form under all conditions that support jet aircraft contrail formation. In addition, the HCl product of ammonium perchlorate combustion causes an extremely persistent (and often continuously growing) contrail to form at conditions much warmer and much less humid than those required for the formation of aircraft contrails. It takes some time for the full development of a secondary smoke contrail, and depends upon the ambient conditions and the specific exhaust structure. This can affect its importance to a particular scenario. In addition the optical density (and hence visibility and transmissivity) of the secondary smoke contrail from a given motor strongly depends on ambient conditions. In Chapter 2 of this report (PROPELLANT SMOKE CLASSIFICATION)

new terminology developed by this working group is proposed to replace the qualitative terms "reduced smoke" and "minimum smoke" with quantitative definitions that can be used to relate initial specifications of solid propellant requirements to defined levels of primary and secondary smoke.

Much of the effort of the past two decades in plume technology has been directed towards developing and refining analytical prediction methods. Most of these methods are now exercised as digital-computer programs. When these computer programs accurately predict plume effects, considerable time and expense associated with flight testing to determine plume properties of specific missile exhausts can be avoided. However, it is necessary to prove the validity of any computer program by comparing its calculated results with measured data. The advantage of the computer program is that once its validity is demonstrated, it is possible to apply it to many situations for which measurements have not been made. A strong caution must be made here; validation of a computer program within a limited range of rocket motor propellants and flight environments does not guarantee validity outside that range. In fact, there are many instances of "verified" computer programs failing in subsequent comparisons with data.

Plume predictions are routinely made for IR signature, smoke visibility and obscuration, and RF-guidance signal attenuation. In addition, the analytical techniques available can be used to predict plume impingement effects, and, with various modifications, RF-guidance signal noise-modulation and radar cross-section (RCS), emitted visible and ultraviolet (UV) signature. Despite this state-of-the-art there are clear areas in the modelling which are incomplete and show up as limitations in the accuracy of some predictions, and obvious failures of some others. The major weaknesses responsible for these results are believed to be in flowfield modelling and include :-

(i) lack of turbulence-combustion coupling
(ii) inadequate treatment of baseflow recirculation with chemical reactions
(iii) lack of particle combustion modelling, including multi-phase flow interactions
(iv) lack of reliable data regarding particle size distribution of metal oxides and their complex index of refraction
(v) inadequate criteria for predicting ignition of afterburning in some plume flows
(vi) lack of models for turbulence introduction into the flow
(vii) lack of models for three-dimensional chemically-reacting plume flow fields
(viii) failure of current models to account for time dependent plume signature effects.

Elimination of these weaknesses will require major investigations of both an experimental and theoretical nature. Research to understand and control physical processes (propellant chemistry, fluid dynamics/combustion interactions, signatures) is critical for plume signature reduction. Afterburning of fuel species, such as carbon monoxide and hydrogen, in missile rocket exhausts, is the major contributor to plume IR, UV and RF signature effects. Programmes to investigate these areas are the purview of an individual nation's research and development programmes, and the subject of several collaborative efforts.

It is important to acknowledge the existence of advanced research codes that reflect the latest technology and methods, such topics as baseflow recirculation and three dimensional, multiphase flow with finite rate chemistry etc. These codes attract high investment costs and some may involve sensitive national interests which preclude their general release. Less sophisticated but more readily available, are codes such as the U.S. production suite SPF/SIRRUM and others. These are less exact but model plume properties in a satisfactory manner.

One of the major benefits of predictive modelling is the insight it provides for understanding the effects that different rocket motors and mission variables have on exhaust plume properties and effects. Even when computer programs fail to accurately predict missile plume effects, they may provide important information about the relative importance of many of the different variables that affect exhaust plume properties.

2.0 OPERATIONAL CONSIDERATIONS

This section examines some of the factors that link operational requirements to solid rocket exhaust plume considerations. These factors fall into two major areas :-

(i) Physical Interactions :- This covers such physical interactions of the plume as gas and particle impingement on surfaces and gas dynamic interactions

(such as those between two rockets on closely parallel or serial courses or the effect of rocket exhaust on aircraft jet engine performance, including flameout).

(ii) Radiation interactions :- This covers the areas of plume signature and guidance interference effects that are caused by emitted plume radiation or interactions of plumes with radiation from other sources. Our interest in these interactions can be grouped into the following two categories.

a. Detection requirements :- These are related to threat (enemy) plume signatures and determine our requirements for detection capability and countermeasures.

b. Signature requirements :- These include requirements for "stealth," for missile guidance, and any other operational parameters that are affected by our missile plumes and thus affect the design of our own rocket motors.

Operational requirements regarding exhaust plumes are usually a critical part of a weapon system's design requirements. The rest of this section gives specific examples of such requirements in relation to the above.

2.1 Physical Interactions

In this area we are concerned with the design of a rocket motor to assure that the physical interactions of its plume do not cause operational problems. Although physical interactions are not part of the working group's mandate, they will be discussed briefly herein for completeness and to alert the specialist to the need to consider aspects other than just the signature characteristics of the plume. Three problem areas are considered as examples :-

(i) First, consider plume impingement situations such as those often encountered when a missile is launched from an aircraft or ship, or perhaps our concern is a small shoulder-launched battlefield missile. The geometry of each situation is well known. The first step in solving the design problem is to determine how the missile plume fits into the known launcher geometry. Existing rocket exhaust plume flowfield computer codes are ideal for determining this. The next step is to define the temperatures, pressures, and particle impingement induced by the plume onto launcher surfaces, and to determine whether or not there will be a threat to the launch vehicle or person. To accomplish this, one must use the plume flowfield computer output parameters of gas density, species, temperatures, particle sizes and number densities, and gas and particle velocities and then determine impact forces and heating rates on involved surfaces. The degradation of launcher surfaces can then be determined analytically. Experimental verification of the predictions can be obtained by submerging well instrumented materials into the exhausts of statically fired rocket motors and comparing the results with code predictions. If the predictions are good, they can be extrapolated to other, non-static, rocket motor firing conditions with reasonable assurance of accuracy. Even fairly simple prediction methods have been successful for surface-launched missile launcher impingement problems [2,3].

(ii) Let us consider a barrage rocket system; typically such a system uses unguided rocket powered missiles launched in parallel or series from launchers that contain substantial numbers of weapons. In either parallel or series firing modes the gas dynamic effects of the exhaust jet from one rocket can affect the trajectories of neighbouring rounds. The problem is to determine the magnitude of that interference and whether it causes trajectory errors greater than allowable by the aim-point-accuracy, miss-distance and kill-probability requirements for the weapon system. The pertinent analysis can be done with one of the existing rocket exhaust plume flowfield computer codes. If it is determined that an operational problem exists, it may be possible to redesign the rocket nozzle or the missile exterior to reduce the problem. Another approach might be to devise a tactical firing strategy that minimizes the interference

problem.

(iii) Another very serious problem involving physical interactions is aircraft jet engine flameout caused by the ingestion of rocket exhaust products. There is a history of this problem with afterburning rocket exhausts. In fact, the use of a potassium sulphate "salt-rod" in some early air-launched rockets was implemented just to eliminate the afterburning that caused this problem. The same problem has been encountered more recently during air-launch of some air-to-air tactical guided missiles, particularly when gas-dynamic or autonomous missile guidance effects cause the rocket to cross the aircraft path with resulting engine ingestion of hot exhaust gases. At least three solutions are obvious :- (1) eliminate afterburning in the rocket exhaust (not easy with modern high-performance composite propellants), (2) relocate missile launcher on the aircraft, or (3) delay the start of autonomous guidance of the missile until it is farther from the launch aircraft. Even some of the older rocket exhaust plume computer codes (such as LAPP) have been applied very successfully to this problem.

2.2 Radiation Interactions

2.2.1 Detection Requirements

This area concerns information on plume signatures of threat (enemy) weapons, both aircraft and missiles. It is information that may be difficult to obtain, particularly that needed to predict the signatures of threat aircraft and missiles. Such information is usually highly classified by each nation and handled on a "need-to-know" basis because it has direct implications on weapon design, tactical procedures, and critical technology. However, certain principles that are obvious will be discussed here.

The objective is to perform some military operation at minimum risk and with maximum chance of success. Quite obviously, sensing emissions radiated from the exhaust plume of a target aircraft or missile is an ideal means of locating, identifying, tracking, and possibly targeting (or terminal homing). Therefore, we can start the design of a passive "detection system" based on this method. A number of unknown parameters are immediately evident :-

(i) At what distance must we detect the target?
(ii) At what aspects (relative flight paths, angles, etc.) must we detect the target?
(iii) Over what range of atmospheric conditions must we detect the target?
(iv) Over what range of absolute and relative velocities must we detect the target?
(v) What sensor capabilities do we have and how can they be used?
(vi) What are the target signature characteristics?
(vii) Can the intercepting missile onboard sensor(s) distinguish between plume and target?

It is possible, using modern exhaust plume computer codes and other analytical techniques to get answers to all these questions. However, one must be cautious because all the analytical techniques are based on assumptions that may hide parts of reality. For example, the strongest feature of current plume computer codes is their prediction of steady-state levels of total and spatially resolved radiation. However, the distinction between the target and its plume may be more apparent in the time dependent regime due to such features as turbulence structure and Doppler shifts in radiation, than in the steady-state regime.

For target detection and tracking, the total steady-state radiation levels are of primary importance. At the required maximum operational launch range, the sensor/detector portion of the guidance system must be capable of distinguishing the target plume from background radiation and from spurious local radiation sources. Intervening atmospheric attenuation of the target signature must be accounted for when the maximum operational launch range is determined, this includes accounting for possible variations in atmospheric attenuation over the missile launch envelope. The guidance system must be capable of locking on to the target plume, keeping lock as the missile approaches its target and must include algorithms to overcome any momentary loss of lock .

As the missile approaches its target, the field-of-view of the sensor/detector sub-system will become filled with the target plume and an autonomous decision must be made to transfer lock to a particular part of the signature. Ideally,

this would involve transferring lock from the plume to the target itself and may require inclusion of a bias or shift of lock from the location of maximum plume signature to the expected location of the target. This is not too difficult to do if the missile is using a proportional guidance scheme. In fact, the bias could be built into the missile guidance system to operate from launch onward, and be based on plume signature computer calculations ; however, such calculated values would be strongly dependent on target type, target velocity, and target altitude. The danger of this approach is clear, the range of variation could be large if the bias is preprogrammed, and the resulting average miss distance could also be large. If distinguishing characteristics of the target-plume interface can be identified, transfer of lock would ideally involve switching from the total plume or location of maximum emission in the plume, to those characteristics of the interface. Distinguishing features of this interface may be time-dependent rather than steady-state. The plume gases are at their maximum velocity very close to the target exhaust exit, therefore some guidance solution based upon Doppler shift in the signature might be used. Also, the plume will have a turbulent structure not exhibited by the target surface. This turbulence might be used to distinguish between the target body and its plume. However, the turbulence will probably be a minimum near the target and a maximum at the location of maximum plume temperature and afterburning ; this would tend to mitigate against using turbulence to distinguish between the target and plume. The target signature near the nozzle may be expected to be a combination of hot body radiation and scattered ambient radiation that could distinguish it spectrally from the plume. This report does not consider any "hard-body" signature sources or effects.

2.2.2 Signature Requirements

This area is related to the design of solid rocket motors. The design objective is to minimize the signature of a missile exhaust plume for one or more reasons. Detailed information in this area is usually highly classified to prevent its acquisition by potential threat nations. However, as with the previous section, the principles involved are available in the open literature, and it is from that basis that the following discussion proceeds. There is one primary goal and that is to minimize the deleterious operational effects of our own missile plume signatures. There are however two primary design goals :-

(i) to minimize the detectability of one's own missiles in certain scenarios.

(ii) to minimize any interference of the plume on missile guidance.

Plumes may be detected by sensing either their emitted radiation or their concentration of ambient radiation. Plumes emit significant quantities of electromagnetic radiation over a wide range, from the ultraviolet (UV) at the short wavelength end of the spectrum, through the visible, infrared (IR) and millimetric wave regions down into the high radio frequency (RF) and longer wavelength end of the spectrum. There may be trace amounts of radiation at shorter and longer wavelengths, however, these are usually not considered viable for tactical purposes.

Particles in plumes, often referred to as plume smoke, are a major cause of concentrated ambient radiation which usually becomes apparent as it is scattered from the plume to some detector. The smoke trails of plumes are easily detected visually because they scatter sunlight and the less intense skylight. Scattering of the earth's albedo may also be detectable, particularly when the ground is very bright (for example, when covered with snow). There is also a component of scattered sunlight, usually less than $5\mu m$ in wavelength, that may cause detection or interference problems with electro-optical systems operating at mid-IR wavelengths. Plume smoke can interfere with guidance systems that operate in the visible or near-IR regimes if propagation through the plume is required in tactical scenarios.

The gas-density variations in plume wakes may cause disturbances in ambient RF fields. Although such disturbances can be detected (as can clear-air turbulence, which is the same phenomenon), it is not obvious that such detections can be useful in tactical battlefield conditions.

Electronically charged species in plumes (particularly free electrons, although ions may also contribute significantly at the longer wavelengths) attenuate, scatter, and refract or "focus" impinging RF radiation in the megahertz and gigahertz regimes. For very highly ionized plumes, this can cause a detectable increase in the missile radar cross section (RCS). Even moderate levels of ionization can cause RF interference for beam rider and semi-active guidance systems.

The temperature of the plume is the single

most important factor contributing to signature levels involving emitted radiation and RF interactions. Particles exhausted from the rocket nozzle form particle laden contrails (primary smoke) detectable for many kilometres behind a flying missile. Water-soluble gaseous and condensed species combined with water exhausted from the nozzle and water present naturally in the atmosphere can result in the formation of water-droplet contrails (secondary smoke) that persist for many kilometres over a wide range of ambient conditions, although there are conditions when water-droplets do not form. The criterion for the formation of secondary smoke involves the nature and concentrations of the exhaust species, the temperature and behaviour of the plume (does it afterburn, for example?), as well as the ambient temperature and atmospheric moisture content (i.e., relative humidity).

In the following discussion, methods are given for arriving at solid rocket motor or propellant design requirements to achieve operational goals.

If the level of emitted radiation from a missile plume is to be reduced to a level that prevents detection of the missile, it is first necessary to determine what that level is and the benefits, if any, of partial signature reduction. Required signature levels must be identified with specific operational timeframes to correlate with projected enemy detection capabilities. It is also critical that a signature be scored or ranked as to its value for each mission together with the relative value of each type of signature (e.g., UV, IR, smoke, visible flash, RCS, etc.). The plume effects that involve missile guidance, such as RF and plume smoke interference are overriding performance issues that must be solved for system deployment.

The first step is to determine the range from which non-detectability is needed and the radiation wavelengths involved. No guidelines have been established for this. It would be desirable to have a plume and missile that is undetectable at all ranges, however this is clearly not possible. The following guidelines are believed to be appropriate :-

(i) Initial detection of supersonic missile plumes at ranges of less than 6km is not important because the short engagement times available do not permit effective countermeasures.

(ii) Detection ranges greater than 75km are ambiguous in one-on-one engagements.

(iii) Plume RCS should be controlled to keep detection probability of the plume less than that of the missile alone.

(iv) The need for guidance interference control is determined by the "marginal excess capability" of the guidance system without interference (that is, the ability of the guidance system to operate beyond the maximum missile envelope). For example, if the guidance signals have a power margin of 10db at the maximum operational range, then plume signal interference up to 10db might be tolerable. This is most applicable to RF guidance interference. Plume induced RF noise must be kept to levels that will not be interpreted by the guidance system as false targets or otherwise confuse the guidance system.

(v) Plume smoke must be controlled for those missions in which it can compromise the launch platform or interfere with electro-optical guidance. It is also important, but less critical to avoid detection of the missile itself. There will always be possible scenarios in which secondary smoke can form, and the probabilities of such occurrence should be known. For this reason, this AGARD working group has provided a climate database which permits the prediction of the occurrence of secondary smoke on a common basis. (Appendix 4 to this report).

(vi) Missile plume signatures that can contribute to the detectability of an otherwise covert and vulnerable launch platform may need to be controlled at all costs. This is particularly true of plume smoke trails from missiles launched from stationary or slow-moving platforms, since the smoke trails persist for a long time.

The following three fictitious examples of plume signature problems are included to give some idea of design considerations that are influenced by rocket exhaust plumes.

Example 1 :-

The missile is guided along a line of sight. The guidance system minimizes the angle formed by the target, the launch platform, and the guided missile. Designation of the target is done by an operator who must continuously designate the target until the missile hits it. The missile is located during flight by a beacon that radiates in the near-IR.

The exhaust plume can disturb the guidance system by :-

(i) obscuring the target from the operator due to smoke. The target is seen in a natural environment by a contrast defined as :-

$$C = \frac{B_t - B_b}{B_t} \text{ where}$$

C = contrast
B_t = target brightness
B_b = background brightness

The attenuation (which must be less than a factor 10) is defined as :-

$$A = \frac{C1}{C2} \text{ where}$$

A = attenuation
C1 = contrast without motor exhaust
C2 = contrast with motor exhaust

(ii) obscuring the missile from the operator due to smoke. With the same definitions as the previous paragraph, the attenuation must be less than a factor 20.

(iii) saturation of the light amplifier used for night firing, due to plume radiation. To avoid saturation of the light amplifier the spectral radiance of the plume must be less than 1×10^3 Watt/m^2/sr/m.

(iv) a higher level of radiation from the plume than from the beacon. This point is satisfied if the previous one is satisfied.

Plume smoke can also reveal the missile trajectory and the launch position. This point has not been quantified at the present time. Considering this further, imagine a scenario where conflict occurs in a desert climate in which the first combatant uses an all-climate missile (obtained from a major power arms source) with a rocket propellant (commonly known as a "minimum-smoke" propellant) containing no ammonium perchlorate (AP), which is responsible for secondary smoke formation in cool, humid climates, and the second combatant, realizing it will never use anti-tank missiles elsewhere, has chosen to produce and use a composite propellant with no metal but high AP levels in the rocket motors of its anti-tank missiles. The second combatant will have an advantage in performance (total impulse) in the desert environment, or the option of selecting a smaller and lighter missile design. He may also, in general, have a rocket motor with improved service life and handling, transport, and storage safety.

Example 2 :-

In another situation, consider a goal involving reduced plume-IR signature in the 3μm to 5μm wavelength band. Suppose existing data indicate that with likely enemy detectors, the steady-state IR signature of a current motor capable of meeting the performance goals can be detected at ranges from 30km to 250km depending on plume and detector altitudes, and atmospheric and background conditions. Studies show that a motor might be designed and fabricated with only 10% of the IR signature of the current motor. However, calculations show that this will reduce detection to ranges between 25km and 200km, for identical conditions; a trivial change, and not an improvement in the operational context. Another option is a liquid-organic fuelled ramjet engine, which, after its rocket booster is exhausted, will have a signature only one-fortieth that of the current rocket. Because the ramjet-powered missile will fly at different aspects to expected detector platforms, it is assumed that an IR signature only 1% of the current rocket plume can be achieved. With this condition, the IR detection range can be reduced to a range between 19km and 100km, for identical conditions. If the operational goal had been identified as no detections beyond 50km, that goal is now achievable for a significant percentage of encounters, and the value of these versus other operational parameters must be determined to optimize the system design.

Example 3 :-

As the final example, consider a plume-radar guidance problem. Everything possible has

been done to reduce signal attenuation. Afterburning is suppressed as much as possible considering the performance needed, the rocket motor nozzle lip (missile base) thickness has been minimized by boat-tailing the external missile-cylinder wall, the two receiver antennas for the semi-active radar-guidance system are forward on the missile body to minimize the influence of direct signal-interference paths through the motor exhaust plume. At least one antenna always has a signal attenuation less than the 10dB required for adequate signal-to-noise ratio at maximum thrusting range. Yet the missile sometimes has midcourse guidance problems that cause it to miss its target. After much deliberation, and analysis of expensive telemetry data (which would not otherwise have been obtained), the project team comes to the awful conclusion that the antenna selector in the guidance system is selecting the wrong antenna for guidance. The system is programmed to select the antenna receiving the larger signal, which it is doing; but analysis of the telemetry data indicates that at the time of selection much of that signal is plume- induced noise on the carrier signal scattered into the antenna making it appear to be the larger signal. The problem is now severe, especially since the system has been deployed. Earlier in the design of the system it would have been possible to include noise-discrimination circuitry in the guidance system, or an independent missile orientation sensor that could have eliminated or reduced this problem.

Detailed design guidelines must be worked out for each proposed missile system on the basis of how and where it is to be used, and the relative value of the different contributing factors such as range, velocity, guidance type, mission value, launch platform value, and technology availability. The objective of this design effort is to quantify the available tradeoff options between all the various requirements and goals, and to optimize them for the missile system under consideration. If all operational conditions are considered fairly, some surprises are likely to emerge.

3.0 TECHNICAL CONSIDERATIONS

This section of the overview describes major plume properties and effects of concern, starting with the flow of rocket motor combustion products from the combustion chamber through the nozzle and into the atmosphere as far as necessary for the properties and effects of interest to manifest. Critical design features of solid rocket motors as they affect plumes are addressed, they include design principles and the contributions made by propellants, liners, insulation, nozzles and igniters. Plume effects are described from a theoretical basis. This is necessary since it is the only way to approach an understanding of the phenomena involved. Existing data on plume effects tend to confirm the theoretical principles, if not the specific details of calculations based upon them.

3.1 Solid Propellant Rocket Motors

Solid rocket motors appear to be rather simple devices. Generally they have no moving mechanical parts (although some modern systems are fitted with moving nozzle thrust vector control systems, and adjustable pintel nozzles have been designed and tested). However, this apparent simplicity is deceptive. It is more appropriate to visualize a solid rocket motor as an engine which has all the design requirements "frozen" into the necessary chemical and physical forms.

3.1.1 Motor Design Principles

Figure 1-2 shows a typical tactical rocket motor including the major design features. The solid propellant is cast or extruded as a "grain." The propellant is selected to contain the necessary chemical energy, delivered at an appropriate rate, to accomplish the missile mission. This requires that the following conditions be met :-

(i) The density of the propellant must be sufficiently high to package the needed energy into the available volume.

(ii) The burning rate of the propellant must be such that energy is delivered at the required rate.

(iii) The burning rate slope (n in the burning rate equation $r=aP_c^n$) must be sufficiently low that mild pressure excursions do not lead to unstable burning or runaway (possibly explosive) pressure increases.

(iv) The burning rate of the propellant is usually dependent on temperature, being higher at higher temperatures. Since tactical solid rocket motors must operate over a wide range of ambient (and thus propellant) temperatures, it is important that the performance of the missile should be similar throughout the entire specified operating

temperature range.

(v) The propellant grain is configured to give the desired thrust-time profile. In the motor of Figure 1-2, this is accomplished by "perforating" the grain so that burning occurs internally on the exposed faces. With the internal perforation or bore shown in the figure, the burning surface area remains nearly constant during the entire burn, and thus the thrust is nearly constant. In contrast, a simple circular bore would initially have a smaller burning surface that would grow progressively during combustion. The chamber pressure and the thrust would also grow, although not proportionally, unless the burning rate had no dependence on pressure. The port must be of a size large enough to prevent choking of combustion gas flow upstream of the nozzle throat, and to minimize erosive burning of the propellant surface. As burning reaches the outer insulation of the motor, the burning surface and hence, the thrust, begin to decrease (tailoff). Since motor performance is reduced during tailoff, and an extended burnout phase requires extra internal case insulation, good motor designs minimize the duration of the decrease by attempting to burn out all of the propellant simultaneously.

Some grains or head-end parts of grains are not perforated and burn on the surface facing the nozzle. These are known as end-burning, or restricted, or cigarette-burning grains. It is possible to achieve constant thrust-time curves with such grains. Motors with end-burning grains require more internal case insulation than those with internal-burning grains to prevent exposure of the nozzle end of the motor case to the high-temperature combustion within. End-burning grains also require some internal stress-relief mechanism to prevent cracking due to thermal expansion. Some boost-sustain rocket motors use an internally perforated grain configuration near the nozzle for a short duration, high thrust, boost or acceleration phase, and an end burning configuration to provide longer-duration, lower sustain thrust to maintain constant velocity of the missile. Figure 1-3 shows typical thrust and pressure versus time curves for such a boost-sustain rocket motor. Other, more complex grain shapes are not uncommon.

(vi) The igniter must ignite the entire propellant surface quickly and bring the motor to its design operating pressure. It must be designed so that ignition does not mechanically damage the propellant grain.

(vii) The propellant must have mechanical properties that prevent it from cracking, or other damage when initially pressurized by the igniter, or under forces (loads) of accelerating flight, or of normal handling.

(viii) The liner bonds the propellant grain to the case or insulation. The liner bonds must not separate or burning may creep into the bond region and quickly destroy the motor case. Inhibitors may be used to prevent combustion of some propellant surfaces: these may be slow-burning.

(ix) The insulation must keep the heat from a burned-out motor grain from damaging the case during the final stages of unpowered flight (coast). The insulation must also prevent excessive temperatures and temperature gradients (due to aerothermal heating or other ambient influences) from damaging the propellant or the liner bond.

(x) The nozzle throat must be sized to constrict the flow so that the design burn rate and chamber pressure are reached and maintained in the combustion chamber. Flow in the nozzle throat is choked to sonic velocity which prevents any possible feed back from the nozzle cone or downstream regions from influencing the chamber combustion.

(xi) The nozzle expansion cone angle employed (a conical expansion is usually used in tactical missiles) is a tradeoff between the nozzle length and weight and the expansion efficiency. The sonic gases in the nozzle throat

accelerate in the expansion cone. Maximum performance efficiency is achieved if the exhaust gases just reach ambient pressure at the nozzle exit. However, since many tactical missiles operate over a wide range of altitudes, and hence ambient pressures, a compromise nozzle exit radius is usually chosen based on many factors. The expansion cone half-angle is usually chosen to be between 12 and 20 degrees ; this is a nozzle tradeoff. The smaller the expansion angle, the greater is the axial component of momentum (thrust) that acts to propel the missile ; however, the longer the nozzle, the greater the wall friction and turbulent boundary layer losses in the nozzle and the greater the missile inert weight. It is also very important that the nozzle half-angle should not be so great that flow separation occurs (i.e. a situation in which the expanding nozzle flow detaches from the nozzle wall with the formation of shock waves and uncontrollable, unpredictable, and variable thrust misalignment).

The purpose of all these design considerations is to produce a motor which provides thrust to propel the missile. Thrust is the force that the missile experiences as the result of the exhausting nozzle gases. It is actually the sum of two terms :-

(i) the momentum thrust which is the product of the mass flow rate and the exit velocity of nozzle effluent.

(ii) the pressure thrust, which is the pressure difference between the nozzle exit and ambient pressures operating over the nozzle exit area.

The impulse (often called total impulse) of a motor is the integral of the thrust over the operating duration. The specific impulse (Isp) is the total impulse divided by the weight of propellant. Specific impulse is also a propellant parameter that can be defined thermochemically. Specific impulse of a propellant is the thrust that the propellant can provide at unit weight flow rate. The specific impulse of any propellant is a function of the chamber pressure at which combustion occurs, and the nozzle exit pressure. In the United States, for tactical propellants, these parameters are usually given for 1,000 psia (6.89 MPa) chamber pressure and 14.7 psia (0.101325 MPa) exit pressure, unless stated otherwise.

3.1.2 Solid Propellant Ingredients and Other Factors Related to Plume Signature

Specific impulse is usually considered to be the single most important propellant property related to performance, and this certainly is true for weight-limited rocket motors. However, for volume limited systems, propellant density is also important, and the density may be traded against specific impulse in propellant selection to improve performance, although not on a one-to-one basis. When propellants with reduced exhaust plume signature effects are selected for operational use, the specific impulse invariably suffers.

3.1.2.1 Solid Propellant Ingredients

To provide the necessary energy for missile propulsion, a rocket motor must contain fuel and oxidizer ingredients that combust to produce the high velocity nozzle gas and other effluents that propel the missile. In a solid rocket motor the fuel and oxidizer are bound closely together in an elastomeric binder matrix that provides the necessary structural properties over a wide range of required performance and storage temperatures (as broad as 219K to 344K). The binder is typically a fuel, although, in some propellant types, the binder may also have some oxidizer molecules. There is increasing interest in polymeric energetic binders which definitely have oxidizing capabilities ; however, these do not generally contribute to increased plume signature.

Two basic types of propellant are in wide use today, double-base propellants and composite propellants. Although the molecules in these propellants differ widely, both propellant types are based upon carbon, oxygen, hydrogen, and nitrogen atoms, and the exhaust products that result from chamber combustion are close to equilibrium concentrations of the chemistry involved under nozzle exit conditions. (The chamber products that enter the nozzle throat are probably very close to equilibrium. Some non-equilibration occurs during the pressure drop of nozzle expansion, however, this has little effect on such major species like CO, CO_2, and H_2O, that strongly influence plume infrared signatures. Minor species like OH, H, H_2 and e^-, that influence ultraviolet and radio-frequency signatures, are more strongly affected and may diverge significantly from equilibrium.)

Double-base (DB) propellants are the oldest

type currently in use. The binder system is not dependent upon the curing of a polymer system, but on the capability of the nitropolymer (nitrocellulose (NC) is often used) to absorb and desensitize nitroglycerine (NG). Nitroplasticizers other than nitroglycerine may be used. They may also be used in combination with polymeric isocyanate curing systems with polyurethane or polyester polymers. Double-base propellant grains are manufactured both by extrusion methods and casting methods. Stabilizers are added to the propellant to prevent decomposition of the nitroglycerine. Ballistic modifiers (i.e. burning rate catalysts) are usually added to tailor double-base propellants to achieve desired motor performance. These catalysts are usually lead compounds, such as lead resorcilate, citrate, oxalate, carbonate, or others. A refractory, such as zirconium carbide may be added to control combustion instability. All metal-based additives will contribute to the exhaust primary smoke signature, although the small amounts used may not cause serious effects. Afterburning in the exhausts of double-base propellant rocket motors can be reduced or eliminated by the addition of certain additives (for example, potassium sulphate).

The need to improve performance of conventional propellants for tactical and strategic missiles (DB and composite propellants) has led to the development of advanced energetic-binder propellants such as composite modified double-base (CMDB). The CMDB family includes all propellants containing nitrate ester-based binder in which fillers (oxidizers and, if necessary, metallic fuels) are incorporated. Due to their composition, these propellants are intermediate between the DB propellant family (NC and NG or other liquid nitrate ester) and the composite propellant family (inert binder plus fillers). CMDB or elastomer modified cast double-base (EMCDB) propellants may contain in addition to NC and NG, solids such as ammonium perchlorate (AP), an oxidizer; aluminium (Al), a fuel; or nitramines, such as HMX or RDX. The last two tend to be fuel rich in rocket motor combustion, but are themselves capable of sustaining combustion and are, in fact, both detonable high explosive molecules. Two very different processes for manufacturing CMDB propellants can be used :-

(i) A casting solvent process which uses the manufacturing system for traditional cast double-base (CDB) propellants to produce composite modified cast double-base (CMCDB) propellants or elastomer modified cast double-base (EMCDB) propellants, if an isocyanate curable elastomer is included.

(ii) A slurry cast process similar to that used to produce composite propellants. These propellants are referred to as crosslinked double-base (XLDB) propellants or nitrate ester with polyether or polyester binder (NEPE) propellants for some specific high-energy grains. XLDB propellants consist of an energetic binder based on inert polymers such as polyesters - polyethers-polycaprolactone plasticized with a high level of liquid nitrate ester such as NG-BTTN-TMETN (nitroglycerine - butalanetrioltrinitrate-trimethylolethane trinitrate). High contents of fillers are introduced into these binders, for example, nitramines (RDX or HMX), nitramines and AP, or nitramines and AP and metallic fuel (aluminium).

Composite propellants, the other general class of propellants, support the oxidizer and the fuel as fine powders in a rubbery, cross-linked, isocyanate-cured matrix, called the binder. The oxidiser is usually AP and the fuel usually Al, although in propellants designed to produce reduced levels of primary smoke the binder serves as the fuel. The matrix may comprise as little as 9%, by weight, of the propellant. Burning rate tailoring can be accomplished, within limits, by adjusting the particle size distribution of the AP. To achieve highest burning rates, iron, copper, or chromium containing additives are used, however, these additives increase the hazard sensitivity of the propellants. AP combustion releases HCl into the exhausts of composite and CMDB motors. This increases the propensity to form secondary smoke. The chlorine present in composite propellant combustion gases spoils the action of afterburning-suppression additives; thus exhaust afterburning of AP containing propellants cannot be suppressed by additives (such as potassium sulphate) in the propellant or motor combustion chamber. The combustion of aluminium or other metals results in fine oxide particles in the exhaust, creating primary smoke in close proportion to the amount of metal in the propellant.

Other particulate oxidizers that might be used in solid motors include potassium perchlorate (KP) and ammonium nitrate (AN). Requirements for insensitive munitions may lead to future use of these oxidizers for special applications. Iodine pentoxide and lead nitrate have also shown potential as oxidizers in high density propellants;

however, the former is a scarce and expensive material and is degraded to a very corrosive acid by small amounts of water, and the latter is increasingly prohibited by environmental protection laws in the United States. Fluorine based oxidizers have also been used in development systems, and some fluorocarbon binders were successfully employed years ago. The use of KP in propellants will greatly increase ionization in the plume, and may prohibit its use in certain applications. KP is less energetic than AP and there are problems in trying to obtain useful burning rates with KP oxidized propellants unless some AP is added. From a plume signature standpoint, KP has more disadvantages than AP. AN has no disadvantages from a plume signature standpoint, but nickel or potassium stabilizers (which must be added to prevent undesirable phase transitions) can result in plume signature difficulties.

A wide variety of particulate metallic fuels might be used in solid propellants, depending upon the application; zirconium hydride has applications in high density propellants; boron and boron hydrides are also potential fuels. Insensitive munitions requirements may lead to the use of these fuels to maintain high motor total impulse at reduced sensitivity, by increasing propellant density. Boron is used as a ramjet fuel. Other fuels based on lithium or beryllium were considered in the past, but are unlikely to be used; lithium because it is very hydroscopic and beryllium because it is extremely toxic.

Composite propellants, which produce only small amounts of primary smoke and no secondary smoke over a wide range of atmospheric conditions, can be made by eliminating AP and aluminum, and by using particles of AN, and/or nitramines (HMX, RDX, and, perhaps in the future, other high-energy explosive molecules). Ingredients, added for phase stabilization or combustion stability, or derived from the combustion of metal-based ballistic modifiers, will contribute metal oxides to exhaust smoke or increase ionization of the plume.

Future use of increasing amounts of energetic binders and plasticizers in solid rocket propellants is anticipated. This should not quantitatively change exhaust-plume considerations. The effects of additional nitrogen that such binders contain may result in somewhat cooler plumes. The reduced solid content possible in propellants with energetic binders may result in qualitative differences in plume signatures and other effects.

3.1.2.2 Other Factors

Nozzle, liner, insulator, and inhibitor materials may contribute to the motor exhaust. Liners for internally perforated motor grains are often the rubbery binder matrix material of the propellant. When they burn (being fuel rich) during motor tailoff, significant quantities of soot may be exhausted. Liners, inhibitors, and insulators may have fibrous inorganic materials added to improve insulating behaviour and leave a charred insulating layer even after organic constituents burn away. Asbestos (hydrated magnesium silicate) has been a common constituent, however, laws preventing its use because of carcinogenic behaviour, are forcing a search for replacement materials. Silicones and bulk aramids are being considered for use in insulators. Inhibitors and liners (often the same material) may contain a variety of metal based oxides (for example, calcium silicate [Wollastonite], antimony oxide, aluminium oxide hydrate, titanium dioxide, etc.) or carbon black. All of these ingredients can contribute to the exhaust signature, although the contribution will depend upon how well the components do their job. If char layers form, as is desired, very little contribution to the motor effluent will come from these ingredients. Nozzles are increasingly fitted with graphite inserts which contribute little to the exhaust signature.

Igniter combustion products will contribute momentarily to plume effects at the launch location. Common igniter ingredients (including potassium nitrate, sulphur, charcoal, boron, KP, and Al) will contribute to exhaust smoke, flash, and ionization. Recently developed "smokeless" igniters have been designed specifically to reduce or eliminate signature effects.

In summary, the factors that must be controlled in solid rocket motor design, development, and production include performance (range, velocity, miss distance), signature, service life (aging, material compatibility), safety (transportation, storage, insensitive munitions), producibility, and cost. Some of these factors are synergistic in their influence. This report is concerned primarily with only one of those factors, signature, and how it is influenced by all the other factors.

3.2 Plume Properties in Different Flowfield Regions

In the following discussion the flow field is considered in four regions: combustion chamber,

nozzle expansion, base region, and exhaust plume. These regions have been selected because of the unique contributions each makes to exhaust plume phenomena. Figure 1-4 shows the latter three of these regions, although only the last, the exhaust plume region, is shown in any detail, and that detail is fairly complete only in regard to shock structure.

3.2.1 Combustion Chamber

Propellant combustion in solid rocket motors creates a large number of different molecular species. In general, solid rocket propellants are fuel rich (to minimize the molecular weight of product gases and thus maximize the impulse) creating a surplus of oxidizable molecules following chamber combustion. These molecules may subsequently react with atmospheric oxygen in the exhaust plume to cause afterburning.

Hydrogen and oxygen are atomic constituents of all current solid propellants. Complete combustion of these two constituents forms water, which although a gas at the high chamber temperature, may condense to form droplets in the exhaust plume if ambient atmospheric conditions are propitious.

The chlorine present in the ammonium perchlorate of composite propellants reacts with hydrogen in the combustion chamber to form hydrogen chloride (HCl). This acidic molecule readily combines with water at lower temperatures, causing saturation vapour pressures well below those for water alone, and the consequent formation of droplets in the exhaust plume at higher ambient temperatures and lower ambient humidities.

Aluminium or other metals, added to some propellants to increase impulse, result in increased combustion temperature. Some of these metals form compounds which condense upon cooling to form the particles observed in the exhaust plume as primary smoke.

As might be expected at the high temperatures of chamber combustion, Ions (charged molecules) and free radicals (uncharged molecular fragments that are unstable at normal conditions because of the presence of an unpaired electron) are created in the motor combustion process. Those free radicals that survive subsequent nozzle expansion increase the reactivity of the exhaust plume since their reaction rates are higher than those of stable molecules. Free (unpaired) electrons are also created in the combustion chamber, and some of these survive nozzle expansion.

Solid rocket propellants contain a number of additives at low concentrations. Included are burning rate catalysts, anti-instability additives, and afterburning inhibitors. Some of the combustion products of these additives may condense in the exhaust plume to form particles, and some may be water soluble salts which have an effect on water similar to that of HCl. Additional particles in the plume may come from erosion of the propellant, liner, insulator, or nozzle during the combustion process.

In spite of attempts to stabilize rocket motor combustion and prevent oscillatory or uncontrolled excursions of chamber pressure during combustion, there is always some level of unsteadiness in the combustion pressure. This results in flow field fluctuations in the exhaust which may be the basis for some of the exhaust plume turbulence that is always observed.

Computational techniques for predicting equilibrium concentrations of chamber combustion products and resulting chamber temperatures and propulsive performance are available in all NATO countries [4]. Variations exist in the calculations used for propulsive performance ; the simplest calculations assume equilibrium expansion of effluent through the nozzle. More sophisticated techniques include non- equilibrium chemical effects and particle drag effects in the nozzle expansion computation and even generation of effluent particle size dis- tribution [5]. The results of such computations for predicting nozzle effluent temperatures pressures, species concentrations, and gas velocity can be used as the starting point for exhaust plume computations.

This has summarized the rocket motor combustion processes that are the starting point for exhaust plume properties and their effects.

3.2.2 Nozzle Expansion

Chamber combustion products are forced through the motor nozzle by the pressure in the chamber. The gases are accelerated as they are driven towards the nozzle throat where they reach sonic velocity and then expand as they flow through the expansion cone of the nozzle. Nozzles of tactical motors are usually fairly short, to reduce missile weight, and therefore the gases are often under-expanded (that is, at a pressure greater than atmospheric) when they emerge from

the nozzle into the atmosphere. The end of the nozzle is the beginning of the exhaust plume. The exhaust gases accelerate during the nozzle expansion and may reach velocities as high as Mach 3, which for some exhausts may be of the order of 3 kms^{-1}.

During nozzle expansion the pressure rapidly drops about two orders of magnitude from that in the chamber (of the order of 10^5Pa [100 Atm]) to approximately ambient atmospheric pressure. During the expansion there is a tendency for some chemical species concentrations to "freeze" rather than continuing the reaction process to their equilibrium concentrations. The departure from equilibrium is usually not very great for major species (such as H_2O, CO_2, CO, HCl, and H_2), however, for minor species, including free radicals (such as O, H, and OH) and ionic species the departure may be substantial, since equilibrium concentrations of these species drop very rapidly with decreasing temperature.

The nozzle expansion process may be computed, as part of the chamber and performance calculation as indicated in the previous subsection. It is also possible to use a confined flow model of the same general type subsequently used to model the plume free flow starting either in the sonic nozzle or in the chamber, upstream of the throat [6].

3.2.3 Base Region

In general, the exhaust plume of a rocket motor fired statically can be calculated without regard to the shape of the rocket motor itself. However, for missiles in flight, the shape of the missile, the angle of attack, the velocity, and altitude all interact and create a flow separation phenomenon that occurs in the base region of the missile referred to as "base flow." Base flow can have a profound effect on the downstream exhaust plume.

In the simplest cases of base flow effects on exhaust plumes, the effects are due purely to gasdynamics and result in modifications to the pressure field at the base of the missile. In more complex situations, the recirculation and mixing of exhaust and atmospheric gases in the base region results in ignition and combustion. This can drastically change the distribution of heat and all related properties in the exhaust plume from those values existing under static firing conditions, or even from very similar conditions without base combustion. The effect of base combustion on the exhaust plume is most significant in fairly cool exhausts that do not ignite unless there is some additional heat source or flame-holding action, such as that caused by base-flow mixing. The effect is dramatically apparent in optical emissions and in measured exhaust plume-microwave attenuation [7].

Base combustion will distort the downstream exhaust plume flow field from the geometry it would otherwise have. It also changes all local downstream plume properties [7-9]. The base ignition and combustion phenomena may be unsteady under some conditions, and result in very dramatic fluctuations in apparent plume size and all plume properties dependent on temperature. The base flow will be strongly affected by the angle between the missile velocity and the nozzle centre-line (angle-of-attack), also from bow shock and control surface wake effects.

These remarks on base flow are based on in-flight and wind tunnel observations. Computations of base flow with chemical reactions are difficult and very time consuming; however, functional computer programs have been developed and are operational in the United Kingdom and France (see references to BAFL and AJAX codes in Appendix 3 of this report). Equally, the U.S. has the capability to analyse the full base flow problem using both research and production codes. These programs are thought capable of accurately predicting measurable features of the base flow region, such as static pressure, as well as the effect on downstream plume properties. For practical purposes, the base flow region can be neglected for situations where :-

(i) the nozzle lip is very thin compared to the nozzle exit radius.

(ii) the missile velocity is very low compared to the nozzle flow velocity ($Vm<0.1Vn$).

(iii) no important chemistry occurs in the base region to modify the downstream flowfield or chemistry.

The foregoing considerations apply generally, although they are most easily visualized and computed for axisymmetric missiles and exhaust plumes.

3.2.4 Exhaust Plume

Previously in this section, the upstream contributions that influence the exhaust plume

have been introduced except for one, that of the atmospheric flowfield. Free-stream atmospheric flow interactions with the missile body influence the flowfield further downstream where atmospheric flow interacts in the missile base region and subsequently with the nozzle effluent.

Thus there are the following contributions to the exhaust plume :-

(i) the chamber combustion flow as it is ejected by the nozzle.

(ii) the interaction of the atmospheric flow field with the nozzle effluent in the base-region of the missile.

(iii) the interaction of the atmospheric flow field further downstream with the effluent of the base region and the exhaust jet. This last interaction occurs over the entire length of the exhaust plume.

These contributions to the exhaust plume must be considered with the earlier caveats of this section.

3.2.4.1 Computation of Steady-State Plume Flowfield Structure

Computer programs currently in use to predict plume properties and effects are based on the assumption that plume flowfields can be described by steady-state solutions of the Navier-Stokes equation [9-12]. Information on a number of these codes is given in Appendix 3 of this report. To accomplish this, the equation is solved by finite-difference methods with assumptions governing first; the introduction and effect of mixing between the effluent and atmospheric flow fields, and second; the paths along which finite-rate chemical reactions occur. The results of computations using these methods are often in reasonable agreement with measured data for a number of plume properties. For example, the total IR radiation from an exhaust plume can usually be predicted to an accuracy factor between 2 and 4, as can the average peak values of IR station radiation. Microwave attenuation can usually be predicted with an accuracy of ± 3 db (a factor of 2). Primary and secondary smoke spatial profiles and effects can often be predicted quite accurately on the basis of steady-state plume flow field assumptions. The codes do not model fine turbulent and temporal effects.

3.2.4.2 Weaknesses of Steady-State Plume Flowfield Calculations

The weaknesses of the steady-state assumptions first become apparent when one attempts to calculate plume properties or plume effects that depend upon time-dependent aspects of the exhaust plume flow field. For example, scattering of microwave radiation by fairly sharp gradients in the free-electron concentration seems to be responsible for observed levels of RF-noise and radar cross section (RCS) [13]. Computations of these phenomena cannot be made with the parameters generated by steady-state flow-field models. A turbulent, time-dependent structure must be superimposed upon the computed steady-state flow field. This can only be done with the current computer programs by artificially formulating the turbulence properties of the exhaust plume and superimposing them upon the steady-state profiles [14]. Measured real-time (rather than time-averaged) values of exhaust plume IR emissions tend to fluctuate by at least 50% around the localized spatial average values, a clear indication that time-dependent plume phenomena are real [15]. Temporal fluctuations will tend to be reduced for full-plume signatures because of spatial averaging.

If the time-dependent behaviour of the exhaust plume is real, and if it is based upon underlying turbulence, a number of questions emerge :-

(i) Does the turbulent fine-structure influence the mixing and chemical reactions occurring between the atmospheric flow field and the exhaust "source flow" in a manner more complex than steady-state formulations can solve?

(ii) Do the local heat and pressure fluctuations generated by the localized turbulent chemical reactions feed back to modify the instantaneous turbulent structure of the flow field?

(iii) How do the time-averaged exhaust plume properties and effects, based upon fluctuating phenomena, differ from the "average" values that are computed on the basis of steady-state flow-field assumptions? Are there important local differences in values? Averaged differences?

(iv) What experiments could be performed to determine the importance and nature of the time-dependent effects on exhaust plume properties?

(v) How could time-dependent exhaust plume computer programs be formulated so that they would give accurate results and be practical to use?

(vi) Is there important information in the fluctuating signatures of exhaust plumes that would be of military significance and would affect related work by NATO countries and this working group?

3.2.4.3 Exhaust Plume Contributions to Radiation Signature

What follows, in this section, to the extent it is based on the results of current steady-state exhaust-plume computer programs, should be treated cautiously; however, the information is probably qualitatively correct.

The contributions of exhaust products to IR emission and microwave interference increase with increasing exhaust plume temperature. Therefore, these contributions tend to be stronger in the presence of afterburning and behind strong shock waves. Since low-altitude shock waves are rather small, and the afterburning plume region (should one exist) is quite large, the latter is by far the major factor in tactical missile signatures. The increases in emissivity and free electrons are very sensitive to temperature increases (they tend to follow power or exponential relationships to temperature). Carbon dioxide (CO_2) is a major source of IR radiation in tactical exhaust plumes and, in spite of a strong atmospheric CO_2 absorption band, the major source of detectable IR signature in some important wavelength regimes. Combustion of carbon monoxide (CO) to form CO_2 is one of the major reactions contributing to exhaust plume afterburning (the other is the formation of water, H_2O, from various hydrogen and oxygen containing radicals) and the resulting increase in CO_2 concentration also increases the IR emission in and downstream of the afterburning region of the exhaust plume. Other molecular species, including H_2O, CO, and HCl also contribute measurably to the IR emission signature. Some self-absorption of radiation occurs within the exhaust plume as emissions from hot inner regions pass through cooler regions into the atmosphere. Additional signature losses occur as a result of absorption and scattering along the atmospheric path from the exhaust plume to any sensor.

Solid particles in the plume emit continuum radiation in approximate proportion to the particle concentration and the fourth power of their surface temperatures. Specific details of size distribution and optical properties of the particles significantly affect this emission. Plume particulates also scatter radiation, and promote an effect which may be observed as local anomalies in the intensity of IR emissions that depend on the spatial distribution of the plume's emitting sources. One of the more dramatic examples of this behaviour is the so-called "search-light effect," in which "black-body" radiation from the nozzle throat (i.e., from the combustion chamber) is scattered by particulates in the plume, and thus appears to originate from the plume.

IR radiation results from quantum effects. The emission of radiation from energy-releasing transitions in molecular rotation-vibration levels is responsible for molecular radiation, and thus should follow local gas temperature fluctuations. Particle radiation, obeying the Planck function (also a quantum effect) will tend to lag local gas temperatures because of thermal lag effects within the particles (the amount of lag is affected by particle size, and of course, any major exothermic or endothermic transitions that affect the particles). Particle scattering effects should be relatively independent of temperature, except to the extent that particle optical properties change with temperature and that the radiation being scattered fluctuates at its source.

Visible and ultraviolet (UV) radiation should follow local temperature fluctuations very closely since the former are generally due to changes in atomic electronic states, and the latter, generally, to radiation emitted during free radical reactions, which are part of the source of the afterburning temperature changes. There will also be some amounts of visible and UV radiation emitted by hot particles in the exhaust, and the hotter the particles, the greater the intensity of the radiation. Also the peak wavelength of particle radiation shifts toward shorter wavelengths (higher energy photons) as the particles get hotter, in accord with the Planck function.

More details on plume radiation are given in Section 3.3.1 and in Chapter 5 of this report.

3.2.4.4 Exhaust Plume Ionization

Free-electron production occurs as a result

of reactions, some of them multi-step, that accelerate at high temperatures and pressures. Free electrons will persist for some short time after they are formed, until recombination by collision with other species occurs (recombination will therefore be slower at higher altitudes). Therefore, one would expect some differences between the effects of turbulence on emission and its effects on RF-interference phenomena. More details are given in Section 3.3.2.2 and in Chapter 6 of this report.

3.2.4.5 Exhaust Plume Particles and Smoke

Downstream of the plume afterburning region, the emission and free electron effects decrease fairly rapidly, more rapidly at lower altitudes than at higher. In this downstream (wake) region, which may extend for many kilometres, primary and secondary smoke effects have their greatest importance. The particles, which in the aggregate, form primary smoke, are in general, the same particles that radiated and scattered in the afterburning region of the exhaust plume. Additional species of particles may also form by condensation at the lower temperatures that follow the afterburning region. Particle mass fractions as low as 0.01 (i.e., 1 %) of the nozzle effluent can affect plume visibility or transmission to a degree that may be of tactical or operational importance in some situations. Although the particles generally exist everywhere downstream of the nozzle, in practical terms they assume importance only because their spatial extent is so great that they can be perceived from long distances. Extreme attenuation of laser guidance beams can occur during transmission through these considerable lengths of exhaust plume smoke [16-18]. More details on primary smoke are given in Section 3.3.2.1 and in Chapter 3 of this report.

Secondary smoke, which is operationally important for the same reasons as primary smoke, forms only in regions of the exhaust plume where the local vapour pressure of the condensable species (usually water, water and HCl and/or HF, or water and some soluble salts) exceeds their saturation vapour pressure at the local temperature and pressure for the sizes of condensation nuclei (primary smoke particles) present [19-21].

Secondary smoke is comprised all or predominantly of water droplets. Secondary smoke in exhaust plumes that contain HCl and/or HF will start to form at higher temperatures and lower ambient moisture levels than for plumes without the acid vapours. At any given atmospheric conditions, secondary smoke will be thicker (larger droplets and perhaps more droplets) in the presence of acid vapours than in their absence.

Exhaust plume afterburning affects the formation of secondary smoke by producing additional water in the plume, which tends to enhance subsequent condensation and secondary smoke formation. By adding more heat to the plume, the afterburning delays condensation to locations further downstream and, in marginal situations, may prevent condensation altogether.

Because mixing and chemical reactions do not scale with plume size and missile velocity in the same way, afterburning may be significantly different for exhaust plumes of the same propellant fired under different conditions of these variables. Therefore care must be taken when extrapolating the results of condensation measurements on small motors, fired statically, to cases under flight conditions, even for a phenomenon as apparently simple and straight forward as secondary smoke formation.

When secondary smoke forms in plumes containing significant amounts of primary smoke the total effect on visibility and obscuration is roughly the sum of the individual effects until the optical density (optical depth) exceeds some value at which non-linear effects assume increasing importance [17-18]. More details on secondary smoke are given in Section 3.3.2.1 and in Chapter 4 of this report.

3.3 Plume Effects

This section is distinguished from the previous one by its more in-depth, although still cursory, treatment of the specific phenomena believed to be responsible for tactically important plume effects. The effects examined are :-

(i) Emitted (radiation) signature effects

- a. infrared
- b. visible
- c. ultraviolet

(ii) Interaction signature effects

- a. smoke signatures
- b. microwave interference

3.3.1 Emitted (Radiation) Signature Effects

Table 1.1 summarizes "state-of-the-art" of rocket exhaust plume radiation signatures.

3.3.1.1 Infrared

Infrared radiation emitted by the low altitude and medium altitude exhaust plumes of tactical missiles derives from two major sources; molecular emission and particle emission [22-24]. Molecular radiation originates with energy input to, or excitation of, a molecule. When the excited molecule returns to a lower energy state, a photon is emitted. Variations in the excitation process result in emitted energy that may be described as phosphorescence, fluorescence, chemiluminescence, X-rays, millimetre waves, radio-frequency waves, etc. The emitted photons are characterized by a wavelength or frequency, which is directly related to the energy of an individual photon by the Planck constant (h). Often the term "wavenumber," which is the reciprocal of wavelength in units of cm^{-1}, is used. Emitted and received spectra will typically be described by some measure of power (watts) vs. one of these three measures of the photon energy.

The infrared region of the electromagnetic spectrum can be characterized by wavelengths between approximately 0.7μm and 100μm (see Fig 1-5 for a survey of the entire electromagnetic spectrum). The emission of radiation in this spectral region is dominated by rotation-vibration transitions of molecules. However, the far-infrared (wavelengths longer than approximately 10μm) also includes radiation contributions from pure rotational transitions; some electronic transitions occur in the near-infrared.

When the energy state of a molecule undergoes a photon emitting transition, the change occurs between two very precisely defined states. The quantum theory accurately describes the energy states in which a molecule can exist and the rules for transitions between those states. The quantized energy differences between the rotational states are smaller than those between the vibrational states, and according to the quantum rules (fully verified by observation) some transitions between vibrational states are also accompanied by a transition between rotational states. Therefore, the molecular emission spectrum of any molecule is defined with absolute accuracy. The photons emitted in these transitions define a line spectrum. However, in practice, each spectral line is broadened about the central frequency corresponding to the transition by three processes : natural broadening caused by unavoidable uncertainty in energy levels, collision broadening due to perturbation of energy levels by molecular collisions, and Doppler broadening due to thermally caused motion of molecules relative to the observer. As a result of such broadening, the emission spectra of some molecules appear to be continuous (to some degree of resolution) over a "band" of the spectrum. Figure 1-6 illustrates plume infrared emission (and absorption) data over a fairly wide spectral range. Bands for H_2O, CO_2, and CO can be clearly seen. Line structure on these bands is apparent as well.

A line-by-line computation of all the molecular contributions to the infrared spectrum of an exhaust plume would clearly be difficult to set up and time consuming to perform. Band models have been developed to simplify the calculation of infrared spectra. Band models are commonly divided into three classes : the regular model, the statistical or random models, and the mixed models. The regular model considers absorption (or emission) by identical, equally spaced lines. This approximates the spectra of many diatomic molecules, such as HF or NO. Random models assume that all lines have the same line shape, but are randomly distributed with a specified line strength (or intensity) distribution. With proper choices of the intensity distribution function, the random models approximate features of polyatomic molecules such as H_2O, and CO_2. Mixed models interpolate between the limits of regularity and randomness of the other two models.

Considerable complexity can be incorporated into a band model, however, for most uses, when the line density is high, a band model that gives a smooth curve of absorption coefficient vs. wavelength is sufficient (Fig 1-7). A complete band model will include the general effect of temperature (shown for the 4.3μm CO_2 band in Fig 1-8). This permits band models to be used for both emission and absorption calculations, with the reservations described later.

Band models are also used to calculate atmospheric absorption of radiation by molecular transitions, for example, in the widely used LOWTRAN computer program [25]. Difficulties may occur if band models are used to calculate both source-emitted radiation and absorption along the propagation path. These difficulties occur because the band model is just a model, a curve fit, based on fitting scientific data, but not containing scientific fundamentals, and the failure of band models are due to their insensitivity to line-correlation phenomena. The band models are made by fitting discrete, though broadened, line spectra with a continuous curve. In actual emission-absorption situations, radiation will be absorbed by a molecule only if its photon energy (wavelength) corresponds exactly to an allowed energy transition of the molecule - that is, an

exact correlation. However, in the band model calculation, a specific resolution is selected (usually in wavenumber units, cm^{-1}, for example : 25, 5, 1, etc.) and that interval of the "absorption" band is activated for either emission or absorption, as appropriate to the problem at hand. This is not a bad assumption if either the emitter or absorber is quantized. However, if both are quantized, it is easy to see that wavelengths that are not exactly the same may be calculated to interact, while in practice they would not. This line-correlation problem may occur when calculating exhaust plume self-absorption as well as atmospheric absorption. The problem can occur for absorption due to the same species of molecule that emitted the radiation or for a different species.

TABLE 1.1

ROCKET EXHAUST PLUME EMITTED RADIATION STATE-OF-THE ART (Ref 22)

Wavelength (μm)	Phenomenological Understanding	Observational Base (Data)	Prediction Capability
Ultraviolet (UV) 0.2 to 0.4	⊗ Fair ⊗ Controversy over radiation mechanisms :- CO + O OH (A) particles	⊗ Fair and increasing ⊗ Small tactical missiles with data validity questions ⊗ Some large missiles	⊗ Poor ⊗ Errors up to a factor of 10^2
Visible (Vis) 0.04 to 0.8	⊗ Fair ⊗ Atomic transitions of minor species, Na, K (thermal vs chemi-luminescence issue) ⊗ Solar scattering from smoke ⊗ Search light effect	⊗ Fair ⊗ Largely photographic data ⊗ Some quantitative spectra	⊗ Probably poor but relatively untested ⊗ Errors up to a factor of 10^2 for trace species ⊗ Errors probably considerably less than a factor of 10 for smoke
Near Infrared (NIR) 0.8 to 2.0	⊗ Good ⊗ Atomic transitions with overtones of molecular vibration-rotation transition (N_2O) ⊗ Particulates ⊗ Blackbody peaks in NIR for most plumes	⊗ Poor ⊗ Some quantitative spectra	⊗ Probably fair but relatively untested
Short Wave Infrared (SWIR) 2.0 to 4.0	⊗ Very good ⊗ Molecular vibration-rotation bands (CO_2, H_2O, HF, HCl) ⊗ Particulates	⊗ Very good ⊗ Field and wind tunnel data giving spatial and spectral details :- 10 to 500,000 lb thrust, many propellants, ground-to-space conditions	⊗ Good ⊗ Molecular band predictions can be made with ± 30% errors - Errors of up to a factor of 3 occur for some altitudes and propellants ⊗ Particulate signatures are not reliably predicted
Middlewave Infrared (MWIR) 4.0 to 8.0	⊗ Very Good ⊗ Molecular vibration-rotation bands (CO_2 CO, NO, H_2O) ⊗ Particulates	⊗ Very Good Field and wind tunnel data giving spatial and spectral details :- 10 to 500,000 lb thrust., many propellants, groud-to-space conditions	⊗ Good Molecular band predictions can be made with ± 30% errors. Erros of up to a factor of 3 occur for some altitudes and propellants ⊗ Particulate signatures are not reliably predicted
Long Wave Infrared (LWIR) 8.0 to 100	⊗ Fair ⊗ Particulate thermal emission plus scattering of solar and earthshine ⊗ Molecular hybride rotation (HF, HCl, H_2O) ⊗ Molecular bending vibrations (CO_2, NH_3)	⊗ Fair ⊗ High altitude data base available in the 8 to 25μm region	⊗ Poor ⊗ Particulate and hydride molecular rotational systems predictions can be made to a factor of 5 ⊗ Moleculate vibrational predictions can be made up to a factor of 20

This kind of error can be avoided by calculating the contribution from each individual line. Such line-by-line calculations can be very cumbersome in spectral regions with many close or overlapping lines. However, when only a few lines are present, line-by-line calculations can be tractable, and in fact, this procedure is used to calculate HCl spectra in some exhaust plume computer programs.

All radiation sources emit more strongly at high rather than low temperatures. This is so because at high temperatures the higher quantum states are more heavily populated. This is even true of particulate radiation which follows the Planck function (shown as black-body radiation curves in Figures 1-9 for both wavelength and wavenumber units). The difficulties with calculating particulate radiation, absorption, and scattering in exhaust plumes are that we do not know the exact size distribution of the particles, the optical properties as functions of temperature and, even if we knew those two important parameters, we don't know the particle shapes. Particles in exhaust plumes are usually not pure substances, for example, aluminium oxide particles in exhaust plumes are contaminated sufficiently to make their absorption coefficient much different from that of the pure material. Therefore, even the most careful measurements of pure, finely divided substances would not provide the necessary optical property data for use in calculating plume particle emission, absorption, and scattering effects. Furthermore, the optical property data are needed over the entire temperature range of interest in the plume.

Approximations to particulate scattering can be based on adjusting the black-body radiation curve (Fig 1-9) for the emissivity of the radiating particles, for the particle size distribution (or effective particle size), and for the number density of the particles (particle-cloud density) [25]. In practice this can be complicated, although for the purposes of this overview it is clear that the result is continuum radiation with a spectral distribution that depends on the particle temperatures. One can judge, by examining Figures 1-9, that for a typical plume afterburning region at 2500K the continuum particle radiation (per μm) will peak at a wavelength about 1.1μm and will be an order of magnitude lower at 4μm and drop another order of magnitude by 7μm.

Determining the size distribution of plume particles is difficult, complicated by the problem of never being certain that all particles have been measured or that the distribution contains those important particles of interest. As an example, for radiation scattering, the important particle sizes are comparable to and larger than the irradiating wavelength. Therefore, in the visible, the important particle sizes are different from those in the infrared. Exhaust plume particle number densities (at least for aluminium oxide) tend to be higher for smaller particles and decrease with increasing particle radius. In general the largest 10% of the particles have 90% of the mass. Particle size distributions are often specified according to the reason for interest in them. Caution is necessary when using calculated particle size distributions (or sometimes, even distributions derived from measurements) for a purpose other than that for which they were intended. For example, in rocket motor performance calculations in which the effect of particles on delivered specific impulse is of interest, only the larger particles, with most of the mass and drag, are of interest. Consequently, models that give these are accurate enough [5], without regard to the many smaller particles that may be present. Such a distribution would be totally inaccurate for calculating UV or visible light scattering [16], and might be inadequate for accurate determinations of infrared scattering as well.

In summary, infrared emission in plumes is comprised of lines emitted by rotation-vibration transitions in molecules and continuum emission from particles. The particles can also scatter radiation incident upon them from other sources. These effects were discussed earlier. Infrared radiation is attenuated during propagation through the atmosphere. This attenuation can occur by continuum absorption and scattering by particles (for example, fog, clouds, or aerosols) or by molecular absorption by atmospheric species such as CO_2, H_2O, or pollutants.

3.3.1.2 Visible

Particle continuum radiation in the afterburning portion of a plume, will tend to dominate visible radiation, when particles are present. If the number density of particles is known, and temperatures of the particles can be estimated, an emissivity value between 0.05 and 0.2 may be used for typical plume afterburning temperatures.

Trace amounts of sodium atoms in the plume will produce atomic transition lines (yellow) at 0.589μm and 0.5896μm. Potassium lines at 0.7665μm and 0.7699μm will occur with trace amounts of that element, however, these lines are at the red end of the spectrum and

verge on the near-infrared, therefore they would not be particularly visible [26-28].

Frequently, exhaust plumes are judged to be not afterburning because of the absence of visible emission on film or video records. It should be clear that the exhaust plume of a propellant with a low particle content in the exhaust may well be invisible even when afterburning, because the emitted radiation is in wavelength bands other than those detectable by the medium used, or sometimes in fact, by the human eye.

Atmospheric propagation attenuates visible radiation by absorption and scattering. The atmospheric "daylight visibility range" may vary from 0.5km ($s = 8km^{-1}$) in moderate fog to 20 km ($s = 0.2km^{-1}$) in "clear" conditions to 50 km ($s = 0.08km^{-1}$) for "exceptionally clear" conditions. The Rayleigh scattering limit is 310 km ($s = 0.013km^{-1}$). These values for the attenuation coefficient (s) may be applied to Beer-Lambert transmission-attenuation equation calculations of atmospheric losses of visible plume radiation, both for emission and for smoke signatures discussed later [16].

3.3.1.3 Ultraviolet

In addition to continuum particulate radiation which predominates in heavily aluminized exhausts, ultraviolet emission also occurs due to some minor plume species. It is predicted by some that even in heavily aluminized plumes, CO + O chemiluminescence is dominant at the middle ultraviolet and shorter wavelengths. A spectral band from about 0.25μm to about 0.7μm seems to be emitted by the combination of these two radicals to form excited CO_2 and the subsequent de-excitation of the CO_2 molecule. For typical afterburning plume temperatures, the radiation peak is at about 0.35μm.

In hydrogen and hydrocarbon flames, studies have shown that a source of ultraviolet radiation is the electronically excited OH radicals produced in chemiluminescent reactions. Both of the following reactions are thought able to produce excited OH,

$$CH + O2 \rightarrow CO + OH^*$$
$$H + OH + OH \rightarrow H_2O + OH^*$$

however, the latter reaction is thought to be more likely in afterburning solid rocket exhaust plumes. The OH spectrum contains a large number of lines, which in all but the highest resolution spectra will blend together to form a continuous band. Therefore, OH radiation in the ultraviolet may be thought of as band radiation for some calculations. Some of the OH line centres are 0.2609μm, 0.2811μm, and 0.3064μm.

Ultraviolet radiation is very easily scattered by the atmosphere and absorbed by atmospheric ozone in the so-called "solar-blind" region of the spectrum which, between about 0.2μm and 0.3μm, peaks at about 0.25μm. Aerosol and molecular scattering of ultraviolet radiation severely limits the useful range of ultraviolet radiation detectors for locating and tracking exhaust plumes.

All radiation is scattered by fog or clouds. As might be expected, the shorter wavelengths are more strongly affected than the longer. It is all a matter of the relationship between the droplet sizes and the radiation wavelengths.

3.3.1.4 Millimetre Wavelengths

A number of workers have sought evidence of RF emissions from plumes. Many years ago, the author heard of "over the horizon" radar systems detecting large plumes, but it is not clear that these were plume emissions rather than bistatic scattering of "ambient radiation." Sume [29] reported comparisons of millimetre-wave emission measurements at 35 and 94 GHz which support the theory that the primary mechanism is based on free-free emission (bremsstrahlung), caused by collisions between free electrons and molecules in the plume. The results indicated no difference between the emissions from motor plumes containing aluminium oxide and those with no solid particles. Additional measurements of this phenomenon were under consideration in the United Kingdom (Royal Armament Research and Development Establishment) in the early 1990s. It is likely that other, unreported, investigations are or have been done in this area. Chapter 6 of this report contains additional details.

3.3.2 Interaction Signature Effects

The previous discussion in this section has dealt exclusively with radiation emitted by exhaust plumes. The following discussion covers interactions of plumes with radiation from other sources. The major interactions to be covered are the interactions of visible and infrared radiation with primary and secondary smoke particles, and the interactions of radio-frequency (RF) radiation, specifically microwaves, with free electrons and ions. The sources of the plume species was covered in a cursory manner in

Section 3.2 and will not be covered further in this Overview. The reader desiring more information should look at specific later chapters of this report or the extensive literature that is available [13].

One effect that will not be covered below is the scattering of radiation, particularly at laser wavelengths, by "clear gas" turbulence discontinuities of refractive index within the plume. This phenomenon has the effect of beam spreading the radiation (analogous to atmospheric turbulence effects) so that a small aperture detector may see apparent attenuation losses of up to 6 dB. There will also be "jitter" effects. Even the clear exhausts of liquid propellant rocket motors can cause this effect [13].

3.3.2.1 Smoke Signatures

Smoke particles in plumes can affect incident radiation by both scattering and absorption [16-21]. The magnitude of the effect of the interaction of radiation with a particle depends upon the real and imaginary terms in the particle refractive index, the particle size, and the particle shape. All of these effects combine to give scattering and extinction cross sections (or coefficients) for each particle/wavelength combination. The total plume effect is the combination of all the individual particle effects. When the optical depth of the plume is greater than about 0.5, multiple scattering effects become detectable. The importance of multiple scattering will depend upon the reason for concern about the smoke in the first place. The optical depth is the exponential term in the Beer-Lambert transmission-attenuation equation.

$$\text{Transmission} = 1 - e^{(-sd)}$$

where s is the attenuation coefficient of the medium
and d is the transmission path length in the medium

Multiple scattering occurs when enough photons are scattered more than once such that the effect cannot be ignored, and the single-scattering assumption fails.

In many solid propellants the predominant contributor to exhaust plume primary smoke is aluminium oxide (Al_2O_3) particles that result from the combustion of aluminium fuel. Other metals or refractory ingredients may also cause primary smoke; however, these sources will predominate only in propellants that are completely or relatively free of aluminium fuel. Primary smoke exists at all locations downstream of the motor nozzle, although its importance as "smoke" begins downstream of the afterburning region of the exhaust plume. Since a flying missile lays out a trail of these particles during the entire time that the rocket motor is burning, the smoke plume may be many kilometres in length. The smoke trail spreads with time. However, the amount of spread depends upon the missile velocity; the greater the velocity, the less the spread, but the longer the trail (for a given motor burn time). The smoke trail will be dissipated by wind. It may be visible from as far away as 100km, or more, depending on the amount of aluminium in the propellant, the thrust of the motor, the sun-plume-observer angle (scattering angle), and the atmospheric visibility conditions. At the lower extremes, as little as 0.5% aluminium in the propellant can cause visibility as great as 20km for certain scattering angles, although for most scattering angles (between 60 and 170 degrees) a visible range of 4km, or less, is predicted. Both of these visible ranges are based on "exceptionally clear" atmospheric transmission conditions. If the atmospheric conditions are "clear" to "very clear", the visible range of the plume will be halved. Figure 1-10 illustrates an example of the calculated scattering coefficients for exhaust-grade alumina particles over a wide range of sizes using Mie theory for visible light (0.55μm) [17].

If the sun is obscured, the visibility of the smoke trail is greatly reduced, and, since under these conditions the background is also cloudy sky, the plume will, in many cases appear slightly darker than the background. For all practical purposes, the smoke trail will not be visible, although it will have limited visibility with a dark earth background. In fact, even if the smoke trail is illuminated by the sun it will be practically invisible against a cloud background.

In addition to increased visibility, the scattering of ambient light by the smoke plume may interfere with optical detection systems that operate to wavelengths as great as 5μm. The degree of interference depends upon the wavelength of the detector, the optical depth of the smoke along the propagation path to the detector, the effective field-of-view of the detector, and, of course, the solar illumination of the plume smoke. In such a scenario, although radiation from the detector's target may pass through the plume and reach the detector, the radiation scattered to the detector by the plume may be so great that it has the effect of an overwhelming

background radiation.

Often, attenuation of radiation by the plume has a more important effect on detectors. In this situation an optical (laser) target illumination beam must pass through the missile smoke trail. If the scenario parameters are such that the beam must pass through a substantial length of the plume, attenuation losses of 2 to 3 orders of magnitude (20dB to 30dB) are possible, and may render the beam totally ineffective.

Composite propellants containing ammonium perchlorate (AP) but no metal fuel (often called "reduced smoke" propellants, incorporated into the terminology of Chapter 2 of this report as type *AB* or *AC* propellants under a new classification system) defeat some of the the problems of smoky plume trails. These propellants virtually eliminate primary smoke, down to the level of particulates necessary to maintain stable chamber combustion. However, the AP in these propellants causes HCl to form in the combustion process, which, as described earlier, can condense with plume and atmospheric water to form secondary smoke. It is generally considered that at typical atmospheric conditions, "reduced smoke" contrails will form above 6km altitude. These composite propellant exhausts will form secondary smoke contrails at sea-level over a fairly wide range of cold or humid climate conditions.

Propellants with neither metal fuel nor AP oxidizer (often called "minimum smoke" propellants, incorporated into the terminology of Chapter 2 of this report as type *AA* or *AB* propellants under a new classification system) eliminate this problem. However, even "minimum smoke" propellants can have a condensation plume or trail of secondary smoke when the climate is cold enough and a sufficient amount of water vapour is present. It is generally considered that at typical atmospheric conditions, "minimum smoke" contrails will form above 8km altitude. "Minimum smoke" contrails at sea-level will form only at the very coldest climate conditions, even with fairly high ambient humidity.

All the remarks above concerning visibility and transmissivity of primary smoke plumes apply also generally to secondary smoke plumes. The applicable caveat here is that secondary smoke particles (droplets) may be somewhat larger than those of primary smoke, although this will depend upon the number and size of the condensation nuclei and the amount of condensed water. In such a case the optical effects, when they occur, may be larger. If it were possible to get the water to condense on a very large number of very small condensation nuclei, of the order of $10^{14}m^{-3}$ in the condensation region of the plume, the ultimate droplet radii might be reduced to substantially less than $0.1\mu m$, and the optical effects would be substantially decreased. The Climate Model for defining appropriate conditions for determining secondary smoke formation is described in Appendix 4 of this report.

3.3.2.2 Microwave Effects

The free electrons produced in hot regions of exhaust plumes, primarily in the afterburning region, and less importantly, behind strong shock waves, can absorb energy from microwave radiation which they give up in collisions with molecular species in the plume. The two important parameters for calculating the microwave attenuation coefficient, unique to a given plume, are the electron density (or concentration, m^{-3}) and the collision frequency (s^{-1}), which is the number of collisions per second encountered by an average single electron, typically $\sim 2x10^{11}$ at sea-level ambient pressure. For radiation frequencies above 500 MHz, only the electrons need be considered. For lower frequency radiation, the ions present in the plume must be considered as well. Typically there are 1,000 to 10,000 ions, both positive and negative, for every free electron present, however because of their far greater mass the ions absorb much less microwave radiation.

If absorption is the only process encountered by radiation in the plume the simple calculation of the line-of-sight attenuation coefficient for each region of the plume is sufficient to give a reasonably accurate prediction of microwave attenuation. In general, this is not a bad first assumption for X-band radiation with composite-AP solid rocket propellants containing 5% aluminium or less.

However, for hotter propellants, with hotter afterburning, propagation through the plume is much more complicated. In general, the plume-microwave interference problem may be thought of in terms of the plume (a mathematical transfer function) modifying the electromagnetic field state. In other words, without the plume, a field exists in space; when the plume is interposed, the field is changed. This concept is illustrated in Figure 1-11. While simple in concept, this approach is difficult in practice. It has been solved fairly successfully using the Fresnel-Kirchoff-Huygens formulation of the wave equation [30]. Computer codes using this

formulation have been developed in the United States, France, and the UK.

It may be illustrative to describe the things that go on in the plume-microwave interaction in terms derived from elementary physics. We consider here a plume with arbitrarily large electron density (ED) values. The geometry we are considering involves a transmitting antenna on the missile body, and a receiving antenna at a location such that the line of sight is at a very slight angle to the plume axis. The microwave radiation (MR) penetrates through the outer plume layers where the ED is low without any interaction other than slight absorption. As the MR penetrates into higher ED regions the electron density gradient causes refraction of the MR along every path; attenuation per unit length increases. As the MR penetrates into the over-dense region of the plume (where the ED exceeds some critical value) attenuation losses are so high that for all practical purposes the MR is totally absorbed (actually attenuation losses of several hundred decibels are calculated to occur). While this is going on, MR propagating along the outer edges of the electrical plume behaves as though it were undergoing a combination of refraction and diffraction by the plume, and sets up an interference pattern very similar to optical diffraction. The MR that reaches the receiver displays local intensity structure characteristic of diffraction, modified by some refraction, and with some evidence of line-of-sight or refracted direct radiation, depending upon the locations of the antennas and the ED of the plume. Because of these paths of propagation, tactical missile microwave signal attenuation rarely exceeds 30dB, no matter how high the ED. For much larger space missile exhaust plumes at higher altitude, attenuation as high as 60dB to 70dB has been measured, however, this too is accounted for by the same propagation mechanisms. This effect can be modelled with fairly simple wave-diffraction assumptions [13,31].

But this is not all that is happening. Some of the MR that reaches the receiver shows evidence of frequency shifts, clear evidence that the radiation has been scattered by elements with a range of velocities. This can only be accounted for if the MR is scattered by refractive index gradients much sharper than those required to explain the absorption, refraction, and diffraction results. It seems clear that there is a fine structure, probably due to turbulence, that causes substantial scattering and with Doppler shifts corresponding, in general, to the mean flow velocities of the plume gases. Mathematical simulation of this concept of the process has given reasonable values of the spectrum and intensity of plume induced noise, including the frequency shifts seen. There also seems to be a strong surface type of scattering from the overdense boundary, when the exhaust plume ED is high enough for one to exist. The same approach has, at times, also given reasonable values of plume RCS, which is the same phenomenon, but with both transmitting and receiving antennas at the same location (monostatic) instead of at different locations (bistatic) [13,32-34].

4.0 DESIGN FACTORS

A systems approach to determining guidelines for missile-plume tailoring should follow the two check lists provided by Tables 1-2 and 1-3. The first of these tables lists the missile operational requirements and operational goals related to plume signature; to the extent possible these should be stated as quantified numerical values. The second list contains all available information relating to the plume of interest or similar plumes; this list should include propellant and rocket motor information and all measured and calculated plume data, not just those for the plume effects of concern for the current design.

For specific problems, the system designer will probably wish to expand on both of these lists. It is probably best to establish the final lists in a conference setting following review of initial drafts. Participation should include a broad spectrum of the design team and supporting technologists, not just people who are knowledgeable in plume technology. It is also appropriate to initiate the draft list of operational requirements in similar brainstorming sessions, if time allows.

Plume signature effects can often be reduced by appropriate tailoring of propellants or missile hardware designs. Since some approaches to tailoring are discussed elsewhere in this report the discussion in this overview will be brief. The factors that contribute to primary and secondary smoke signatures, adequately discussed in Chapters 2,3, and 4 are very fine particles and condensation contrails enhanced by acid vapours and other water soluble effluent.

Plume radiation and microwave effects are increased by high plume temperatures, thus approaches that reduce plume temperatures will reduce these effects. Suppression of afterburning can cause major reductions in the temperature of

verge on the near-infrared, therefore they would not be particularly visible [26-28].

Frequently, exhaust plumes are judged to be not afterburning because of the absence of visible emission on film or video records. It should be clear that the exhaust plume of a propellant with a low particle content in the exhaust may well be invisible even when afterburning, because the emitted radiation is in wavelength bands other than those detectable by the medium used, or sometimes in fact, by the human eye.

Atmospheric propagation attenuates visible radiation by absorption and scattering. The atmospheric "daylight visibility range" may vary from 0.5km ($s = 8km^{-1}$) in moderate fog to 20 km ($s = 0.2km^{-1}$) in "clear" conditions to 50 km ($s = 0.08km^{-1}$) for "exceptionally clear" conditions. The Rayleigh scattering limit is 310 km ($s = 0.013km^{-1}$). These values for the attenuation coefficient (s) may be applied to Beer-Lambert transmission-attenuation equation calculations of atmospheric losses of visible plume radiation, both for emission and for smoke signatures discussed later [16].

3.3.1.3 Ultraviolet

In addition to continuum particulate radiation which predominates in heavily aluminized exhausts, ultraviolet emission also occurs due to some minor plume species. It is predicted by some that even in heavily aluminized plumes, CO + O chemiluminescence is dominant at the middle ultraviolet and shorter wavelengths. A spectral band from about 0.25μm to about 0.7μm seems to be emitted by the combination of these two radicals to form excited CO_2 and the subsequent de-excitation of the CO_2 molecule. For typical afterburning plume temperatures, the radiation peak is at about 0.35μm.

In hydrogen and hydrocarbon flames, studies have shown that a source of ultraviolet radiation is the electronically excited OH radicals produced in chemiluminescent reactions. Both of the following reactions are thought able to produce excited OH,

$$CH + O2 \rightarrow CO + OH^*$$
$$H + OH + OH \rightarrow H_2O + OH^*$$

however, the latter reaction is thought to be more likely in afterburning solid rocket exhaust plumes. The OH spectrum contains a large number of lines, which in all but the highest resolution spectra will blend together to form a continuous band. Therefore, OH radiation in the ultraviolet may be thought of as band radiation for some calculations. Some of the OH line centres are 0.2609μm, 0.2811μm, and 0.3064μm.

Ultraviolet radiation is very easily scattered by the atmosphere and absorbed by atmospheric ozone in the so-called "solar-blind" region of the spectrum which, between about 0.2μm and 0.3μm, peaks at about 0.25μm. Aerosol and molecular scattering of ultraviolet radiation severely limits the useful range of ultraviolet radiation detectors for locating and tracking exhaust plumes.

All radiation is scattered by fog or clouds. As might be expected, the shorter wavelengths are more strongly affected than the longer. It is all a matter of the relationship between the droplet sizes and the radiation wavelengths.

3.3.1.4 Millimetre Wavelengths

A number of workers have sought evidence of RF emissions from plumes. Many years ago, the author heard of "over the horizon" radar systems detecting large plumes, but it is not clear that these were plume emissions rather than bistatic scattering of "ambient radiation." Sume [29] reported comparisons of millimetre-wave emission measurements at 35 and 94 GHz which support the theory that the primary mechanism is based on free-free emission (bremsstrahlung), caused by collisions between free electrons and molecules in the plume. The results indicated no difference between the emissions from motor plumes containing aluminium oxide and those with no solid particles. Additional measurements of this phenomenon were under consideration in the United Kingdom (Royal Armament Research and Development Establishment) in the early 1990s. It is likely that other, unreported, investigations are or have been done in this area. Chapter 6 of this report contains additional details.

3.3.2 Interaction Signature Effects

The previous discussion in this section has dealt exclusively with radiation emitted by exhaust plumes. The following discussion covers interactions of plumes with radiation from other sources. The major interactions to be covered are the interactions of visible and infrared radiation with primary and secondary smoke particles, and the interactions of radio-frequency (RF) radiation, specifically microwaves, with free electrons and ions. The sources of the plume species was covered in a cursory manner in

Section 3.2 and will not be covered further in this Overview. The reader desiring more information should look at specific later chapters of this report or the extensive literature that is available [13].

One effect that will not be covered below is the scattering of radiation, particularly at laser wavelengths, by "clear gas" turbulence discontinuities of refractive index within the plume. This phenomenon has the effect of beam spreading the radiation (analogous to atmospheric turbulence effects) so that a small aperture detector may see apparent attenuation losses of up to 6 dB. There will also be "jitter" effects. Even the clear exhausts of liquid propellant rocket motors can cause this effect [13].

3.3.2.1 Smoke Signatures

Smoke particles in plumes can affect incident radiation by both scattering and absorption [16-21]. The magnitude of the effect of the interaction of radiation with a particle depends upon the real and imaginary terms in the particle refractive index, the particle size, and the particle shape. All of these effects combine to give scattering and extinction cross sections (or coefficients) for each particle/wavelength combination. The total plume effect is the combination of all the individual particle effects. When the optical depth of the plume is greater than about 0.5, multiple scattering effects become detectable. The importance of multiple scattering will depend upon the reason for concern about the smoke in the first place. The optical depth is the exponential term in the Beer-Lambert transmission-attenuation equation.

$$\text{Transmission} = 1 - e^{(-sd)}$$

where s is the attenuation coefficient of the medium
and d is the transmission path length in the medium

Multiple scattering occurs when enough photons are scattered more than once such that the effect cannot be ignored, and the single-scattering assumption fails.

In many solid propellants the predominant contributor to exhaust plume primary smoke is aluminium oxide (Al_2O_3) particles that result from the combustion of aluminium fuel. Other metals or refractory ingredients may also cause primary smoke; however, these sources will predominate only in propellants that are completely or relatively free of aluminium fuel. Primary smoke exists at all locations downstream of the motor nozzle, although its importance as "smoke" begins downstream of the afterburning region of the exhaust plume. Since a flying missile lays out a trail of these particles during the entire time that the rocket motor is burning, the smoke plume may be many kilometres in length. The smoke trail spreads with time. However, the amount of spread depends upon the missile velocity; the greater the velocity, the less the spread, but the longer the trail (for a given motor burn time). The smoke trail will be dissipated by wind. It may be visible from as far away as 100km, or more, depending on the amount of aluminium in the propellant, the thrust of the motor, the sun-plume-observer angle (scattering angle), and the atmospheric visibility conditions. At the lower extremes, as little as 0.5% aluminium in the propellant can cause visibility as great as 20km for certain scattering angles, although for most scattering angles (between 60 and 170 degrees) a visible range of 4km, or less, is predicted. Both of these visible ranges are based on "exceptionally clear" atmospheric transmission conditions. If the atmospheric conditions are "clear" to "very clear", the visible range of the plume will be halved. Figure 1-10 illustrates an example of the calculated scattering coefficients for exhaust-grade alumina particles over a wide range of sizes using Mie theory for visible light (0.55μm) [17].

If the sun is obscured, the visibility of the smoke trail is greatly reduced, and, since under these conditions the background is also cloudy sky, the plume will, in many cases appear slightly darker than the background. For all practical purposes, the smoke trail will not be visible, although it will have limited visibility with a dark earth background. In fact, even if the smoke trail is illuminated by the sun it will be practically invisible against a cloud background.

In addition to increased visibility, the scattering of ambient light by the smoke plume may interfere with optical detection systems that operate to wavelengths as great as 5μm. The degree of interference depends upon the wavelength of the detector, the optical depth of the smoke along the propagation path to the detector, the effective field-of-view of the detector, and, of course, the solar illumination of the plume smoke. In such a scenario, although radiation from the detector's target may pass through the plume and reach the detector, the radiation scattered to the detector by the plume may be so great that it has the effect of an overwhelming

background radiation.

Often, attenuation of radiation by the plume has a more important effect on detectors. In this situation an optical (laser) target illumination beam must pass through the missile smoke trail. If the scenario parameters are such that the beam must pass through a substantial length of the plume, attenuation losses of 2 to 3 orders of magnitude (20dB to 30dB) are possible, and may render the beam totally ineffective.

Composite propellants containing ammonium perchlorate (AP) but no metal fuel (often called "reduced smoke" propellants, incorporated into the terminology of Chapter 2 of this report as type *AB* or *AC* propellants under a new classification system) defeat some of the the problems of smoky plume trails. These propellants virtually eliminate primary smoke, down to the level of particulates necessary to maintain stable chamber combustion. However, the AP in these propellants causes HCl to form in the combustion process, which, as described earlier, can condense with plume and atmospheric water to form secondary smoke. It is generally considered that at typical atmospheric conditions, "reduced smoke" contrails will form above 6km altitude. These composite propellant exhausts will form secondary smoke contrails at sea-level over a fairly wide range of cold or humid climate conditions.

Propellants with neither metal fuel nor AP oxidizer (often called "minimum smoke" propellants, incorporated into the terminology of Chapter 2 of this report as type *AA* or *AB* propellants under a new classification system) eliminate this problem. However, even "minimum smoke" propellants can have a condensation plume or trail of secondary smoke when the climate is cold enough and a sufficient amount of water vapour is present. It is generally considered that at typical atmospheric conditions, "minimum smoke" contrails will form above 8km altitude. "Minimum smoke" contrails at sea-level will form only at the very coldest climate conditions, even with fairly high ambient humidity.

All the remarks above concerning visibility and transmissivity of primary smoke plumes apply also generally to secondary smoke plumes. The applicable caveat here is that secondary smoke particles (droplets) may be somewhat larger than those of primary smoke, although this will depend upon the number and size of the condensation nuclei and the amount of condensed water. In such a case the optical effects, when they occur, may be larger. If it were possible to get the water to condense on a very large number of very small condensation nuclei, of the order of $10^{14}m^{-3}$ in the condensation region of the plume, the ultimate droplet radii might be reduced to substantially less than $0.1\mu m$, and the optical effects would be substantially decreased. The Climate Model for defining appropriate conditions for determining secondary smoke formation is described in Appendix 4 of this report.

3.3.2.2 Microwave Effects

The free electrons produced in hot regions of exhaust plumes, primarily in the afterburning region, and less importantly, behind strong shock waves, can absorb energy from microwave radiation which they give up in collisions with molecular species in the plume. The two important parameters for calculating the microwave attenuation coefficient, unique to a given plume, are the electron density (or concentration, m^{-3}) and the collision frequency (s^{-1}), which is the number of collisions per second encountered by an average single electron, typically $\sim 2x10^{11}$ at sea-level ambient pressure. For radiation frequencies above 500 MHz, only the electrons need to considered. For lower frequency radiation, the ions present in the plume must be considered as well. Typically there are 1,000 to 10,000 ions, both positive and negative, for every free electron present, however because of their far greater mass the ions absorb much less microwave radiation.

If absorption is the only process encountered by radiation in the plume the simple calculation of the line-of-sight attenuation coefficient for each region of the plume is sufficient to give a reasonably accurate prediction of microwave attenuation. In general, this is not a bad first assumption for X-band radiation with composite-AP solid rocket propellants containing 5% aluminium or less.

However, for hotter propellants, with hotter afterburning, propagation through the plume is much more complicated. In general, the plume-microwave interference problem may be thought of in terms of the plume (a mathematical transfer function) modifying the electromagnetic field state. In other words, without the plume, a field exists in space; when the plume is interposed, the field is changed. This concept is illustrated in Figure 1-11. While simple in concept, this approach is difficult in practice. It has been solved fairly successfully using the Fresnel-Kirchoff-Huygens formulation of the wave equation [30]. Computer codes using this

formulation have been developed in the United States, France, and the UK.

It may be illustrative to describe the things that go on in the plume-microwave interaction in terms derived from elementary physics. We consider here a plume with arbitrarily large electron density (ED) values. The geometry we are considering involves a transmitting antenna on the missile body, and a receiving antenna at a location such that the line of sight is at a very slight angle to the plume axis. The microwave radiation (MR) penetrates through the outer plume layers where the ED is low without any interaction other than slight absorption. As the MR penetrates into higher ED regions the electron density gradient causes refraction of the MR along every path; attenuation per unit length increases. As the MR penetrates into the over-dense region of the plume (where the ED exceeds some critical value) attenuation losses are so high that for all practical purposes the MR is totally absorbed (actually attenuation losses of several hundred decibels are calculated to occur). While this is going on, MR propagating along the outer edges of the electrical plume behaves as though it were undergoing a combination of refraction and diffraction by the plume, and sets up an interference pattern very similar to optical diffraction. The MR that reaches the receiver displays local intensity structure characteristic of diffraction, modified by some refraction, and with some evidence of line-of-sight or refracted direct radiation, depending upon the locations of the antennas and the ED of the plume. Because of these paths of propagation, tactical missile microwave signal attenuation rarely exceeds 30dB, no matter how high the ED. For much larger space missile exhaust plumes at higher altitude, attenuation as high as 60dB to 70dB has been measured, however, this too is accounted for by the same propagation mechanisms. This effect can be modelled with fairly simple wave-diffraction assumptions [13,31].

But this is not all that is happening. Some of the MR that reaches the receiver shows evidence of frequency shifts, clear evidence that the radiation has been scattered by elements with a range of velocities. This can only be accounted for if the MR is scattered by refractive index gradients much sharper than those required to explain the absorption, refraction, and diffraction results. It seems clear that there is a fine structure, probably due to turbulence, that causes substantial scattering and with Doppler shifts corresponding, in general, to the mean flow velocities of the plume gases. Mathematical simulation of this concept of the process has given reasonable values of the spectrum and intensity of plume induced noise, including the frequency shifts seen. There also seems to be a strong surface type of scattering from the overdense boundary, when the exhaust plume ED is high enough for one to exist. The same approach has, at times, also given reasonable values of plume RCS, which is the same phenomenon, but with both transmitting and receiving antennas at the same location (monostatic) instead of at different locations (bistatic) [13,32-34].

4.0 DESIGN FACTORS

A systems approach to determining guidelines for missile-plume tailoring should follow the two check lists provided by Tables 1-2 and 1-3. The first of these tables lists the missile operational requirements and operational goals related to plume signature; to the extent possible these should be stated as quantified numerical values. The second list contains all available information relating to the plume of interest or similar plumes; this list should include propellant and rocket motor information and all measured and calculated plume data, not just those for the plume effects of concern for the current design.

For specific problems, the system designer will probably wish to expand on both of these lists. It is probably best to establish the final lists in a conference setting following review of initial drafts. Participation should include a broad spectrum of the design team and supporting technologists, not just people who are knowledgeable in plume technology. It is also appropriate to initiate the draft list of operational requirements in similar brainstorming sessions, if time allows.

Plume signature effects can often be reduced by appropriate tailoring of propellants or missile hardware designs. Since some approaches to tailoring are discussed elsewhere in this report the discussion in this overview will be brief. The factors that contribute to primary and secondary smoke signatures, adequately discussed in Chapters 2,3, and 4 are very fine particles and condensation contrails enhanced by acid vapours and other water soluble effluent.

Plume radiation and microwave effects are increased by high plume temperatures; thus approaches that reduce plume temperatures will reduce these effects. Suppression of afterburning can cause major reductions in the temperature of

many tactical missile plumes. Chemical approaches to afterburning suppression involve adding chemicals that remove free radical species, such as OH, O, and H that are necessary to sustain afterburning. The alkali metals (usually potassium is used) are incorporated either into a propellant or in some other way that will produce gaseous products in the exhaust. These chemical additives do not work when present in combination with Cl species produced in AP-composite propellant exhausts. When potassium or other alkali species are used for flame suppression serious microwave effects due to plume species ionization can result if exhaust concentrations of the alkali drop below levels necessary to completely suppress afterburning.

There has also been some success in the reduction of microwave effects by the suppresison of free electron concentrations in plumes resulting from the additon of molybdenum trioxide (MoO_3). It has also been noted (see Chapter 6) that plume free electron concentrations in composite propellant plumes can be reduced by decreasing the concentration of H radicals in the exhaust.

Elimination of regions in the aft end of a missile that may cause separated flow and recirculation (base flow) will eliminate a source that ignites afterburning in otherwise cool plumes of missiles in flight. This approach will only marginally affect hot plumes for which it may reduce slightly the maximum altitude at which afterburning occurs in flight. Other hardware methods for reducing plume temperature involve modifying plume turbulent mixing such that it cools the plume to temperatures below those that ignite afterburning, i.e. before free radical concentrations can reach levels necessary to sustain combustion. This can be accomplished by reducing the length of the flowfield, for example by using multiple nozzles instead of a single, larger nozzle. Noncircular nozzles may also enhance plume cooling because of the larger surface-to-volume ratio of their plumes. In the plumes of missiles in flight at non-zero angles of attack, the tendency to create seperated flow regions increases and stronger steps to reduce afterburning may be necessary than those found successful for strictly axisymmetric situations.

The objective of the design effort is to determine, quantitatively, the available trade-offs between all the various requirements and goals, and to optimize them for the missile system under consideration.

5.0 CONCLUSION

This overview has presented a brief semi-technical narrative of the plume technology areas covered by AGARD PEP Working Group-21. The reader is cautioned that the information presented here has been greatly simplified for the sake of brevity. Only trends are presented, hopefully with little loss of correctness. There are a number of phenomena associated with plumes at higher altitudes that were not even touched on in this overview. While this report is concerned with tactical missile exhaust plumes, which generally occur at low to medium altitudes, there are instances where higher altitude plume phenomena may emerge even in the tactical regime. Anyone desiring to explore this field more deeply will find an extensive literature helpful to understanding the phenomena and the theory, and useful for solving specific practical problems.

TABLE 1.2

OPERATIONAL CONDITIONS CHECKLIST

1. Missile design
   - Design requirements
     - Design goals
     - body signatures
     - plume signatures
   - Rocket Motor
     - Thrust/time
     - Propellant
       - trace elements (K,Na, etc.)
       - signature suppression
     - Nonpropellant contribution
     - Chamber Conditions
       - pressure/time
       - chemical species
     - Nozzle
       - design for signature control
   - Missile flight conditions
     - External air flow
       - velocity
       - altitude
       - angle of attack
     - Body geometry/base signature control

2. Operational Conditions
   - Guidance mode(s)
   - Targets
   - Range
   - Velocity
   - Altitude
   - Manoeuvre capability
   - Countermeasures
   - Climate/atmospheric conditions
   - Threat conditions
     - Density
     - Range capability vs missile capability
   - Guidance
     - Detectors Active/Passive
     - range
     - detection
     - identification
     - track
     - terminal

TABLE 1.3

PLUME DATA CHECKLIST

1. Rocket Motor
   - Thrust/time
   - Propellant
     - trace elements (K,Na, etc.)
     - signature suppression
   - Nonpropellant contribution
   - Chamber Conditions
     - pressure/time
     - chemical species
   - Nozzle
     - design for signature control
2. Data test conditions
   - External air flow
     - velocity
     - altitude
     - angle of attack
   - Body geometry/base signature control
3. Plume conditions
   - Internal plume flow
     - chemical species
     - reaction kinetics
     - temperatures
     - pressures
     - velocities
     - ionization
     - turbulent mixing
     - unsteady flow
     - afterburn ignition
     - shock structure
     - particle flow
   - Flowfield calculations
     - Signature calculations
       - correlation with data
       - extrapolation to missile conditions
         - uncertainties
4. Visible Signature
   - Radiation/Flash
   - Smoke
   - Visibility
   - Guidance Interference
5. Passive Sensor Detected Radiation
   - Infrared Signature
   - Ultraviolet Signature
   - Millimeter Wave
6. Radio-Frequency Interactions
   - Guidance Attenuation
   - Guidance Noise
   - Radar Cross Section

6.0 REFERENCES

1. Brown, A.S., "Stealth Comes of Age," Aerospace America, Vol. 28, No. 3, pg. 116, March 1990.

2. Piesik, E.T., "A Method to Define Low-Altitude Rocket Exhaust Characteristics and Impingement Effects, *Journal of Spacecraft and Rockets*, Vol. 7, No. 4, pp. 446-451, Apr. 1970.

3. Piesik, E.T., "A Semi-Empirical Method Defining Low-Altitude Exhaust Flow Fields - Updated and With Data Comparisons, 14th JANNAF Plume Technology Subcommittee Meeting, Naval Weapons Center, China Lake, California, CPIA Publication 384, Vol. I, 1983.

4. Cruise, D.R., "Notes on the Rapid Computation of Chemical Equilibria," *Journal of Physical Chemistry*, Vol. 68, pp. 3797-3802, Dec. 1964.

5. AGARD Advisory Report No. 230 Propulsion and Energetics Panel Working Group 17 on Performance of Rocket Motors with Metallized Propellants, AGARD-AR-230, September 1986.

6. Victor, A.C., *Guide to Computer Techniques for Calculating Exhaust Plume Properties at the Naval Weapons Center*, NWC TM 3900, Naval Weapons Center, China Lake, California, September 1980.

7. Victor, A.C., "Calculations of Rocket Plume Afterburning Coupled to Reacting Base Recirculation Regions," *Journal of Spacecraft and Rockets*, Vol.14, No. 9, pp. 534-538, Sept. 1977.

8. Chemical Propulsion Information Agency, *JANNAF Handbook, Rocket Exhaust Plume Technology, Chapter 5, Base Flow*, CPIA Publication 263, July 1981.

9. Dash, S.M., "Analysis of Exhaust Plumes and Their Interactions with Missile Airframes," *Tactical Missile Aerodynamics, Progress in Astronautics and Aeronautics, Volume 104*, AIAA, New York, New York, (1986)

10. Mikatarian, R.R., Kan, C.J., and Pergament, H.S., "A Fast Computer Program for Non-Equilibrium Plume Predictions," AFRPL-TR-72-94, Air Force Rocket Propulsion Laboratory, Edwards AFB, California, Aug. 1972.

11. Jensen, D.E., Spalding, D.B., Tatchell, D.G., and Wilson, A.S. , "Computation of Structures of Flames with Recirculating Flow and Radial Pressure Gradients," *Combustion and Flame*, Vol. 34, pp. 309-326, 1979.

12. Chemical Propulsion Information Agency, *JANNAF Handbook, Rocket Exhaust Plume Technology, Chapter 2, Fluid Dynamic Flow Models*, CPIA Publication 263, May 1975.

13. Chemical Propulsion Information Agency, *JANNAF Handbook, Rocket Exhaust Plume Technology, Chapter 4, Plume Electromagnetic Interactions*, CPIA Publication 263, April 1977.

14. Cousins, J.M. and Jensen, D.E., "On the Computation of Ionization Levels in Rocket Exhaust Flames," *Combustion and Flame*, Vol. 52, pp. 111-125, 1983.

15. Guernsey, C.S. and Luchik, T.S., "Analysis of High Frequency Image Data of Rocket Exhaust Plumes," 17th JANNAF Exhaust Plume Technology Meeting, CPIA Publication 487, Vol. 1, pp. 1-8, April 1988.

16. Victor, A.C., and Breil, S.H., "A Simple Method for Predicting Rocket Exhaust Plume Smoke Visibility, J. Spacecraft and Rockets, Vol. 14, No. 9, pp. 526-533, Sept. 1977.

17. Victor, A.C., "Effects of Multiple Scattering on Rocket Exhaust Plume Smoke Visibility," J. Spacecraft and Rockets, Vol. 26, No. 4, pp. 274-278, July-Aug, 1989.

18. Miller, E., "Prediction of the Visible Signature of Solid Rocket Plumes," J. Spacecraft and Rockets, Vol. 27, No. 1, pp. 82-84, Jan-Feb, 1990.

19. Victor, A.C., "Prediction of Rocket Exhaust Smoke Formation in Free Jets and Smoke Chambers," 1978 JANNAF Propulsion Meeting, CPIA Publication 293, (1978)

20. Hoshizaki, H., et al, *Plume Visibility Detection Study*, AFRPL-TR-78-32, Lockheed (Nov 1978). See also :- Meyer, J.W., "Kinetic Model for Aerosol Formation in Rocket Contrails," AIAA Journal, Vol 17, No.2., pp. 135-144 (1979)

21. Miller, E., "Smokeless Propellants", *Fundamentals of Solid-Propellant Combustion, AIAA Progress in Astronautics and Aeronautics*, Volume 90, pp. 841-884 (1986)

22. Chemical Propulsion Information Agency, *JANNAF Handbook, Rocket Exhaust Plume Technology, Chapter 3, Rocket Exhaust Plume Radiation*, CPIA Publication 263, May 1980.

23. Ludwig, C.B., Malkmus, W., Freeman, G.N., Slack, M., and Reed, R., "A Theoretical Model for Absorbing, Emitting, and Scattering Plume Radiation," *Spacecraft Radiative Transfer and Temperature Control, AIAA Progress in Astronautics and Aeronautics, Volume 83* , pp. 111-127, 1982.

24. Spiro, I. J. and Schlessinger, M., *Infrared Technology Fundamentals*, Marcel Dekker, Inc., New York, 1989.

25. Kneizys, F.X., *Atmospheric Transmittance/Radiance :- Computer Code LOWTRAN 6*, AFGRL-TR-83-01187 (Air Force Geophysics Laboratory, Hanscom AFB, Massachusetts (1983).

26. Edwards, D.K., Bobco, R.P., "Effect of Particle Size Distribution on the Radiosity of Solid-Propellant Rocket Motor Plumes," *Spacecraft Radiative Transfer and Temperature Control, AIAA Progress in Astronautics and Aeronautics, Volume 83*, pp. 169-188, 1982.

27. Lyons, R.B., Wormhoudt, J., and Kolb, C.E., "Calculation of Visible Radiation From Missile Plumes," *Spacecraft Radiative Transfer and Temperature Control, AIAA Progress in Astronautics and Aeronautics, Volume 83*, pp. 128-148, 1982.

28. Jones, G.A., *Application of the Improved Rocket Exhaust Plume Program REP3-82 to Some Plume Chemistry Problems :- New Predictions for Plume Characteristic Visible Emissions and Combustions Suppression*, RARDE, UK Ministry of Defence, Report 12/85, 1985.

29. Sume, A., "Millimeter Wavelength Emission from Solid Propellant Rocket Motor Plumes," Forsvarets Forskningsanstalt, FOA rapport, Sept 1982

30. Senol, A.J., and Romine, G.L., "Three-Dimensional Refraction/Diffraction of Electromagnetic Waves Through Rocket Exhaust Plumes," *Journal of Spacecraft and Rockets*, Vol. 23 No. 1, pp. 39-46, Jan-Feb. 1986.

31. Golden, K.E., Taylor, E.C., and Vicente, F.A., "Diffraction by Rocket Exhausts," *IEEE Transactions, Antennas and Propagation*, pg. 614, Sept, 1968.

32. Draper, J.S., Jarvinen, P.O., and Conley, T.D., "Analysis of Radar Return from Turbulent High-Altitude Rocket Exhaust Plumes," *AIAA Journal*, Vol. 8, No. 9, pp. 1568-1573, Sept. 1970.

33. Rickman, J.D., et al, *Plume Attenuated Radar Cross Section Code - Users Manual*, Aerodyne Research, Inc., Billerica, Massachusetts, AFRPL-TR-76-14, June 1976.

34. Guthart, H. and Graf, K.A., "Scattering from a Turbulent Plasma," Radio Science, Vol. 7, No. 7, pp. 1099-1118, 1970.

FIGURES

TABLE OF CONTENTS

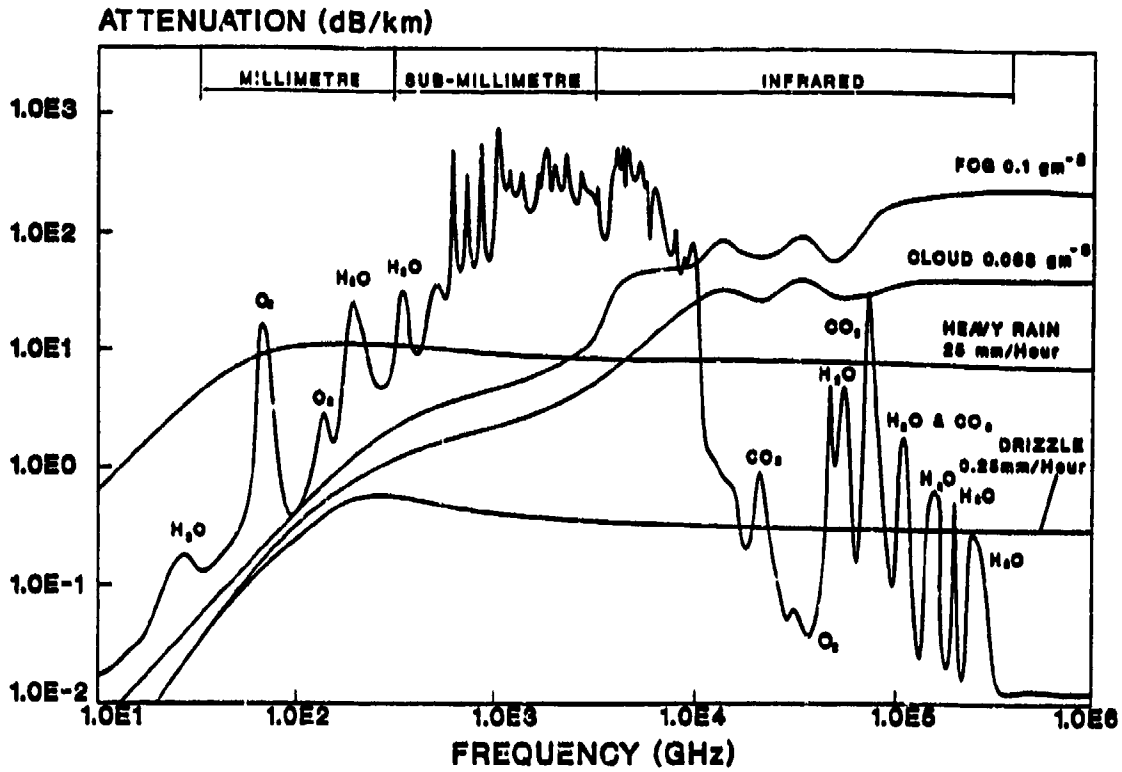

Fig. 1-1 Atmospheric Attenuation

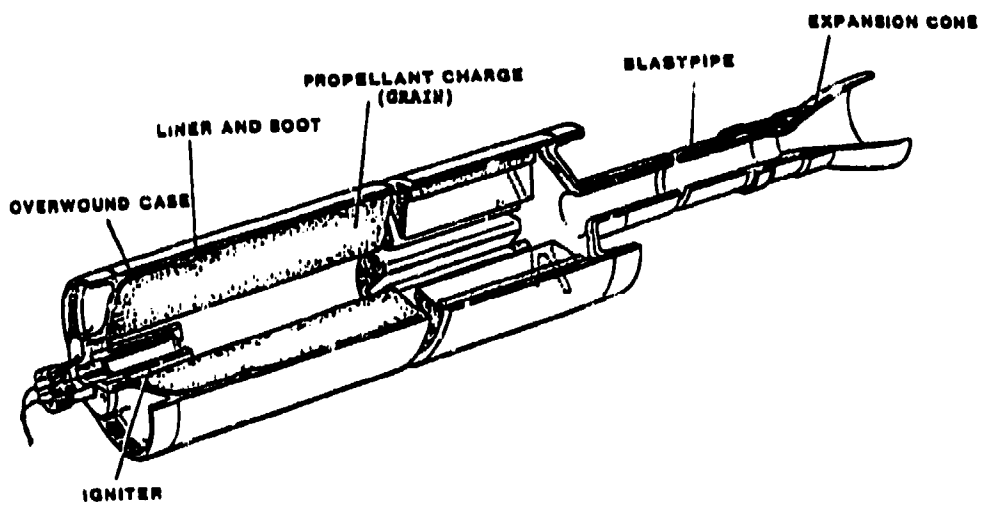

Fig. 1-2 Solid Propellant Rocket Motor

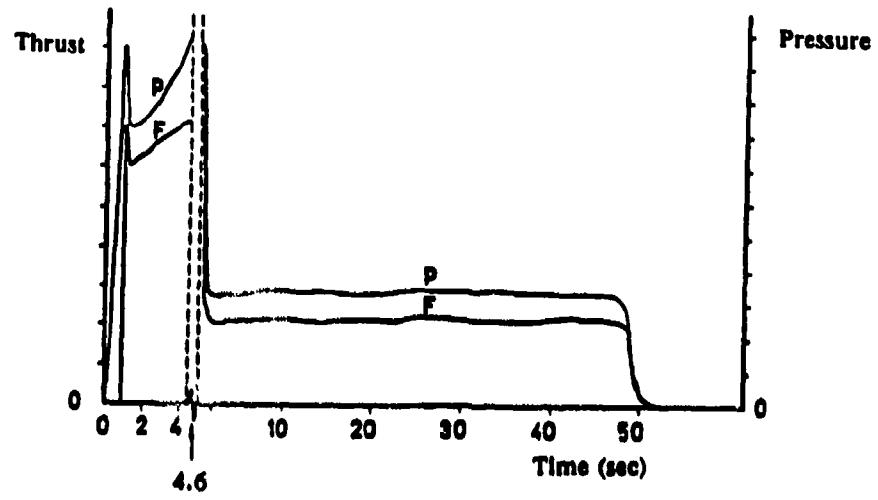

Fig. 1-3 Typical Thrust-Time and Pressure Curves for a Boost-Sustain Rocket Motor

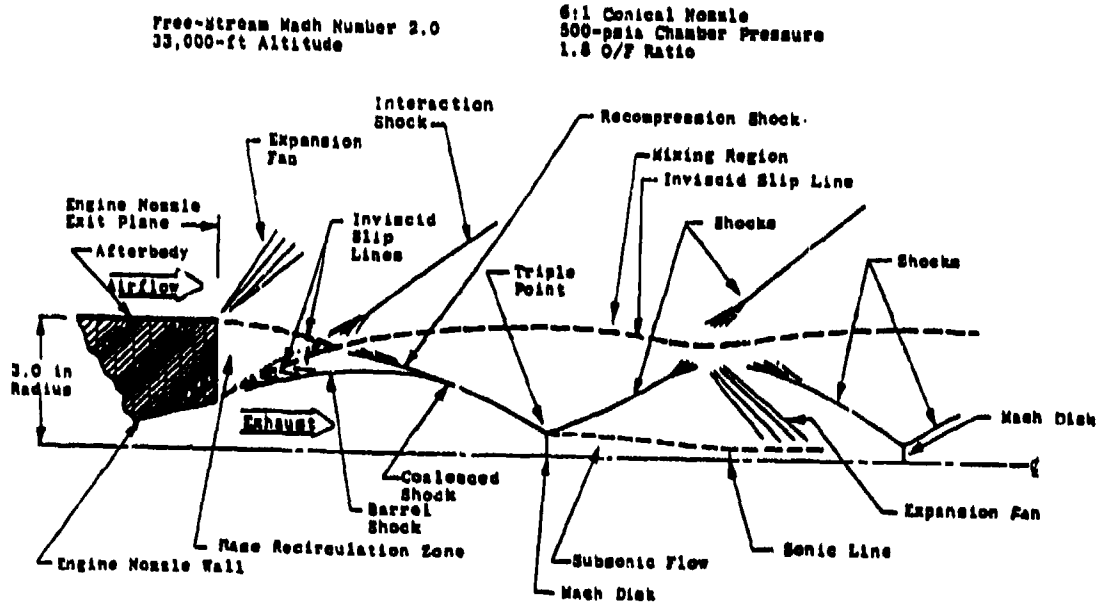

Fig. 1-4 Sketch of a Rocket Exhaust Plume Flowfield

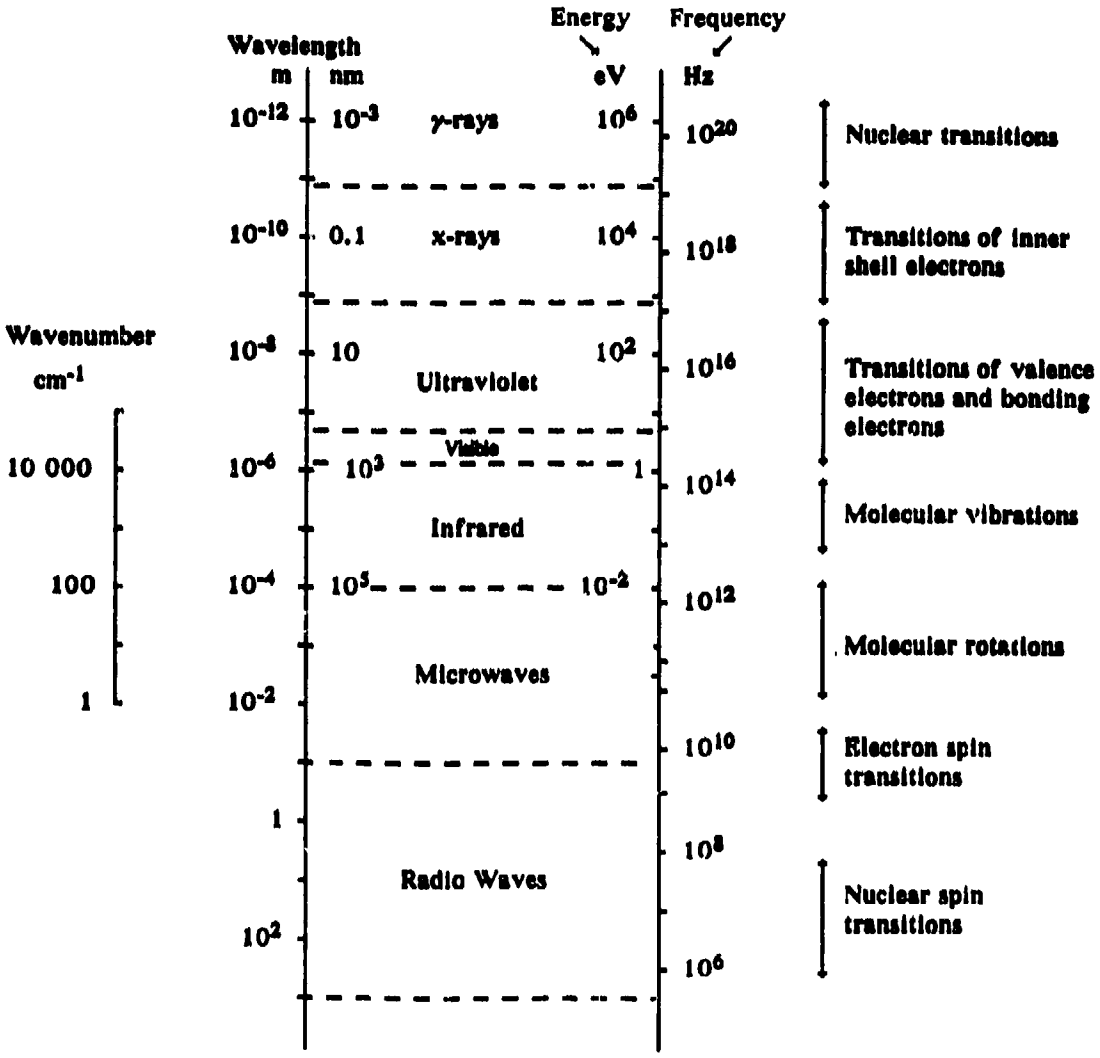

Fig. 1-5 Survey of the Electromagnetic Spectrum

3.0 PRIMARY SMOKE

3.1 Background

For each of the propellants, shifting equilibrium calculations were performed with a chamber pressure of 70 atm (7.07 MPa) and a nozzle exit pressure of 1 atm (0.1013 MPa). From these data the mass percentage of condensibles at the nozzle exit were tabulated as shown in Table 1.

In an attempt to provide a relatively simple method for the primary smoke classification it was decided to base it upon the equation for the transmittance through a cloud of polydispersed particles [1].

$$Tr = \exp [- 3 \dot{Q} C_v L/2 D_{32}] \qquad (1)$$

where

- Tr = Transmittance = I/I_o
- $\dot{Q}$ = Mean Extinction Coefficient = fn (wavelength of incident light, complex refractive index of the particle relative to the surrounding medium, particle size distribution)
- D_{32} = Sauter (volume-to-surface) Mean Diameter
- C_v = Volume Concentration of Particles (volume of particles/volum of mixture)
- L = Path length which contains particles
- I = Intensity of Transmitted Light
- I_o = Intensity of Incident Light

In order to not require detailed Mie calculations for an assumed particle size distribution and assumed particle properties, it was decided to attempt to base the primary smoke classification on C_v and an optical properties constant N.

C_v can also be written

$$C_v = C_m/\text{density of the particle} \qquad (2)$$

where

C_m = mass concentration of particles (mass of particles/volume of mixture)

The density of the particle is proportional to the specific gravity of the particle (SG). Thus,

$$Tr = \exp (- C_m N/SG) \qquad (3)$$

where N contains all of the terms in equation (1) which cannot be specified in this simplified formulation. (For the same path length L, $N \sim \dot{Q}/D_{32}$). For the present purpose of classification, N = 1.0

Now C_m can be written $M_p/M_{mix}\ (RT/M_{mix}P)$

where

- M_p = Mass
- R = Universal Gas Constant
- T = Mixture Temperature
- M_{mix} = Molecular Weight of Mixture
- P = Pressure of the Mixture

Since the primary smoke signature is most important in the far-plume region where mixing is essentially complete, P and T were taken to be the local ambient values. Variations in M_{mix} were also neglected. M_p/M_{mix} is the mass fraction of condensibles in the exhaust. Thus, for a mixture of condensibles in the exhaust,

$$Tr = \exp [- \textstyle\sum_i (\% M_{pi} N_i/SG_i)] \qquad (4)$$

where $\% M_{pi}$ = Mass percentage of condensible species i.

The obscuration is defined as (1 − Tr). Thus, an AGARD primary smoke classification number is defined as follows :-

$$\text{AGARDP} = 1 - \exp [- \textstyle\sum_i (\% M_{pi} N_i/SG_i)] \qquad (5)$$

This formulation results in a classification scheme for primary smoke in which the calculated number will lie between zero and unity.

Using Equation (5), the detailed data (totals summarised in Table 1) for the exhaust compositions were used to determine values for AGARDP. These are presented in the following classification together with the estimates for the primary smoke classifications provided by the various AGARD countries. The encircled symbols represent exhaust products which contain large amounts of potassium compounds. These compounds generally result from the inclusion of flash suppressants in the propellant formulations. The triangular symbols are for condensed products which contain only carbon. Potassium and carbon smokes generally consist of very small particles and can; therefore, result in Rayleigh scattering of visible light.

PRIMARY SMOKE CLASSIFICATION	AGARDP NUMBER
A	0 → 0.35
B	>0.35→ 0.9
C	>0.9

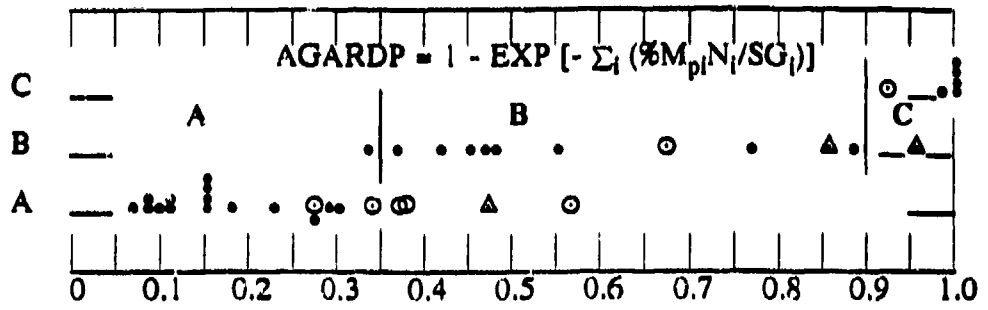

AGARDP
Primary Smoke Classification

The above classification scheme for primary smokes is currently recommended

3.2 Limitations

Primary smoke measurements reveal that the AGARDP values are somewhat high for potassium salts and low for aluminium additives. This deficiency may be attributed to failure of the classification procedure to account for the differences in optical properties of these additives. The optical property constant N (currently taken as 1.0) may vary considerably for certain materials due to different refractive indices and particle sizes which are present in the plume. When sufficient data become available in the future, substitution of the actual values for N_i should permit AGARDP to better fit smoke observations for additives such as potassium and aluminium. Inadequate knowledge of primary smoke material properties emphasizes that AGARDP should not be substituted for actual measurements when smoke specification is critical to system performance.

3.3 Assumptions

(i) Complete mixing of exhaust products with atmosphere at standard conditions

(ii) Primary smoke can be classified using the percentage of condensible metallics at the nozzle exit for the reference conditions of 70 atm (7.09 MPa) chamber pressure and 1 atm (0.1013 MPa) exit pressure, with shifting equilibrium, adiabatic flow.

3.4 Problem Statement

Given the propellant ingredients and their heats of formation, determine the AGARD primary smoke classification.

3.5 Classification Procedure

(i) Input propellant ingredients into a chemical equilibrium, adiabatic combustion code with a specification chamber pressure of 70 atm (7.09 MPa) and an exit pressure of 1 atm (0.1013 MPa)

(ii) For shifting equilibrium nozzle exit conditions record the mass percentages of each of the condensible metallics.

(iii) Calculate AGARDP

$$= 1 - \exp\left[- \sum_i \{\%M_{pi} N_i / SG_i\} \right]$$

where $\%M_{pi}$ and SG_i and N_i are the mass percentage, specific gravity and optical property constant (currently taken as 1.0) of species i, respectively.

(iv) If AGARDP $\leq$ 0.35
= A Classification
If 0.35 < AGARDP $\leq$ 0.9
= B Classification
If AGARDP > 0.9
= C Classification

4.0 SECONDARY SMOKE

4.1 Background

The following method is a theoretical classification method for secondary smokes based on the condensation of water vapour and/or water/acid vapour by exhaust gases in the presence of ambient humidity. Mole fractions of condensible gases, ie HCl, HF, KOH and H_2O, are determined using any one of the thermochemical codes which are used to predict rocket exhaust products assuming equilibrium, adiabatic flow. The calculation for propellant secondary smoke classification is performed at a selected standard condition (0.1013MPa pressure and 273.15K temperature) with the assumption of a fully expanded, chemically and thermally stable equilibrium exhaust mixture diluted with atmospheric air to produce $1/1000^{th}$ of the original concentration where pressure is expressed in mbars. Isenthalpic mixing was not considered because of the necessity of using the heat contents of the different individual propellants. Although the following procedure is greatly simplified by neglecting important effects, it is considered adequate as a tool for classification purposes. It has been shown [2] that potassium compounds will produce secondary smoke in propellants that normally have only primary smoke. Several researchers have identified KOH vapour as the key inhibiting species in proposed flame suppression mechanisms [3]. The existence of KOH which is predicted by thermochemical codes to be in suppressed plumes is known to reduce the vapour pressure of water in solution as do many other salts [4,5]. However, no detailed data have been collected and correlated to permit calculations for KOH similar to those currently made for HCl and HF. The following discussion is for HCl and HF, but it should be noted that the effects of KOH on secondary smoke may have increased importance in the future.

4.2 Assumptions

(i) Isothermal mixing of the exhaust with the atmospheric air to produce $1/1000^{th}$ of the original concentration.

(ii) Ambient conditions of 0°C or 273.15K and 1 atm (0.1013MPa).

4.3 Problem Statement

Determine the ambient relative humidity necessary for the onset of condensation, given the mole fraction of condensible species (ie, HCl, HF and H_2O) in the exhaust products.

Calculation Procedure :

The condition for saturation may be written as :-

$$P_{H_2O\ amb} + P_{exhaust\ condensibles} = P_{saturation} \qquad (6)$$

where P is the partial pressure of the gas.

From Dalton's Law :-

P = Mole Fraction (f) x Total Pressure

with dilution (6) then becomes :-

$$P_{H_2O\ amb} = P_{sat} - \qquad (7)$$

$$1.01325\ (f_{H_2O} + f_{HCl} + f_{HF})$$

From Oliver [6], the normal saturation pressure of water is depressed by a factor K that depends upon the concentrations of HCl and/or HF. The saturation pressure for water at 273.15K is 6.1078 mb (610.78 Pa). Thus,

$$P_{sat} = K \times 6.1078\ mb \qquad (8)$$

where K = partial pressure of water over acid/normal saturation pressure of water

Substitution of (8) into (7) yields :-

$$P_{H_2O\ amb} = 6.1078 \times K - \qquad (9)$$

$$1.01325(f_{H_2O} + f_{HCl} + f_{HF})$$

Dividing (9) by 6.1078 and multiplying by 100 yields :-

$$RH_{amb} = (P_{H_2O_{amb}}/6.1078) \times 100 \quad (10)$$
$$= 100 \times (K - f_{total} \times 0.16589)$$

Equation (10) may be evaluated by reference to the Oliver data in Reference 7 or Figure 2-1 which gives values of $K = P/P_0$ as a function of the partial pressure of the diluted concentration for HCl or HF at 273.15K.

Equation (10) was used to calculate the ambient relative humidity required to saturate the exhausts of AGARD propellants given the mole fractions of H_2O, HCl and HF (Fig. 2-2). The saturation relative humidity at the stated standard conditions may be used as a figure of merit, e.g. AGARDS = 52.5% Sat RH, which uniquely determinates the secondary smoke classification for a given propellant.

Figure 2-3 shows the recommended AGARD secondary smoke classification for actual propellants which were submitted by the various AGARD countries. The classification is based upon the results of thermochemical codes run by the individual AGARD countries.

4.4 Classification Procedure

Curve Fit Approximation

(i) Determine the H_2O, HCl and HF contents (in mole fraction) of the propellant exhaust products from a thermochemical prediction with shifting equilibrium nozzle flow.

(ii) Referring to Figure 2-2, determine the curve which best corresponds to the total halogen exhaust gas mole fraction and select a point on the line whose abscissa corresponds to the H_2O mole fraction of the exhaust.

(iii) The ordinate of the selected point is the ambient relative humidity required for saturation, ie secondary smoke formation. The point also defines the AGARD A, B or C secondary smoke classification for the propellant.

5.0 SAMPLE CALCULATION

To implement the AGARD smoke classification procedure one must first perform a thermochemical calculation assuming shifting equilibrium flow to determine the exhaust content of the desired propellant formulation. The appropriate conditions are 70 atm (7.09 MPa) for the chamber pressure and 1 atm (0.1013 MPa) for the exhaust pressure. Table 2 presents a typical output.

TABLE 2.2

EXAMPLE OF EXHAUST CHEMICAL COMPOSITION

MASS FRACTION		MOLAR FRACTION	
N_2	.1023	N_2	.0944
CO_2	.2368	CO_2	.1391
CO	.1161	CO	.1071
H_2O	.2488	H_2O	.3569
H_2	.0088	H_2	.1130
HCl	.2577	HCl	.1826
$FeCl_2$	.0106	$FeCl_2$	.0022
$Al_2O_3(s)$	.0189	$Al_2O_3(s)$	.0048

The condensible species in the exhaust are $Al_2O_3(s)$ (with a mass percentage of 1.89 and an SG of 3.97) and $FeCl_2$ (with a mass percentage of 1.06 and an SG of 3.16). Thus, from equation (5) :-

$$AGARDP = 1 - \exp\{-[(1.89 \times 1.0/3.97) + (1.06 \times 1.0/3.16)]\}$$
$$= 0.56$$

From the primary smoke classification diagram this will be classified B.

Table 2.2 also shows that the exhaust gases contain both H_2O and HCl with mole fractions of 0.3569 and 0.1826, respectively (with a total mole fraction of 0.5395). To determine the secondary smoke classification, Equation (10) must be used together with Figure 2-2. To evaluate Equation (10) the value of the HCl depression factor (K) must be determined from Figure 2-1, which expresses K as a function of the HCl partial pressure in millibars. The assumption is made that the exhaust is in equilibrium with ambient air at 273.15K and diluted with atmospheric air to produce $1/1000^{th}$ of the original concentration. Thus, the diluted partial pressure of HCl is :-

$P_{HCl} = (1013.25/1000)\ 0.1826 = 0.185$ mbar

From Figure 2-1 the value for K is 0.48. Substitution of K = 0.48 into equation (10) gives :-

$RH_{amb} = 100\ [0.48 - 0.5395\ (0.16589)] = 39\%$

From Figure 2-2 with "Saturation RH" = 39 and "Exhaust H_2O Content" = 0.3569 the secondary smoke classification is C.

Therefore, the AGARD smoke classification for the propellant with exhaust products given in Table 2 is BC.

6.0 REFERENCES

1 Dobbins, R.A., Crocco, L. and Glassman, I., "Measurement of Mean Particle Sizes of Sprays from Diffractively Scattered Light", AIAA J, Vol 1, No 8, Aug 1963, pp 1882-1886

2 Greer, C.L. Jr., Thorn, L.B. and Wharton, W.W., "Signature Suppression and Evaluation in Static Motors", JANNAF Propulsion Meeting, San Diego, CA, April 1985

3 Cox, J., Grillo, A., Slack, M., Ambrusco, R. and Bakos, R., "Flame Inhibition by Potassium Salts", Gruman Corporation, Bethpage, New York 11714-35807

4 Gmelins Handbuch, Der Anorganischen Chemie, System-Number 22, 1938, pp 218-224

5 Harned, H.S. and Cook, M.A., "The Thermodynamics of Potassium Hydroxide Solutions from Electromotive Force Measurements", J Am Chem Soc, Vol 59, 1937, pp 496-500

6 Oliver, R.C., "Smokeless Solid Propellants: An Overview", Institute for Defense Analysis, Alexandria, VA, Research Paper No P-472, pp 46-47, March 1979

7 List, R.J., Smithsonian Institution, Smithsonian Meterological Tables, 6th Revised Edition, Publication 4014, Washington, DC., 1963

FIGURES

TABLE OF CONTENTS

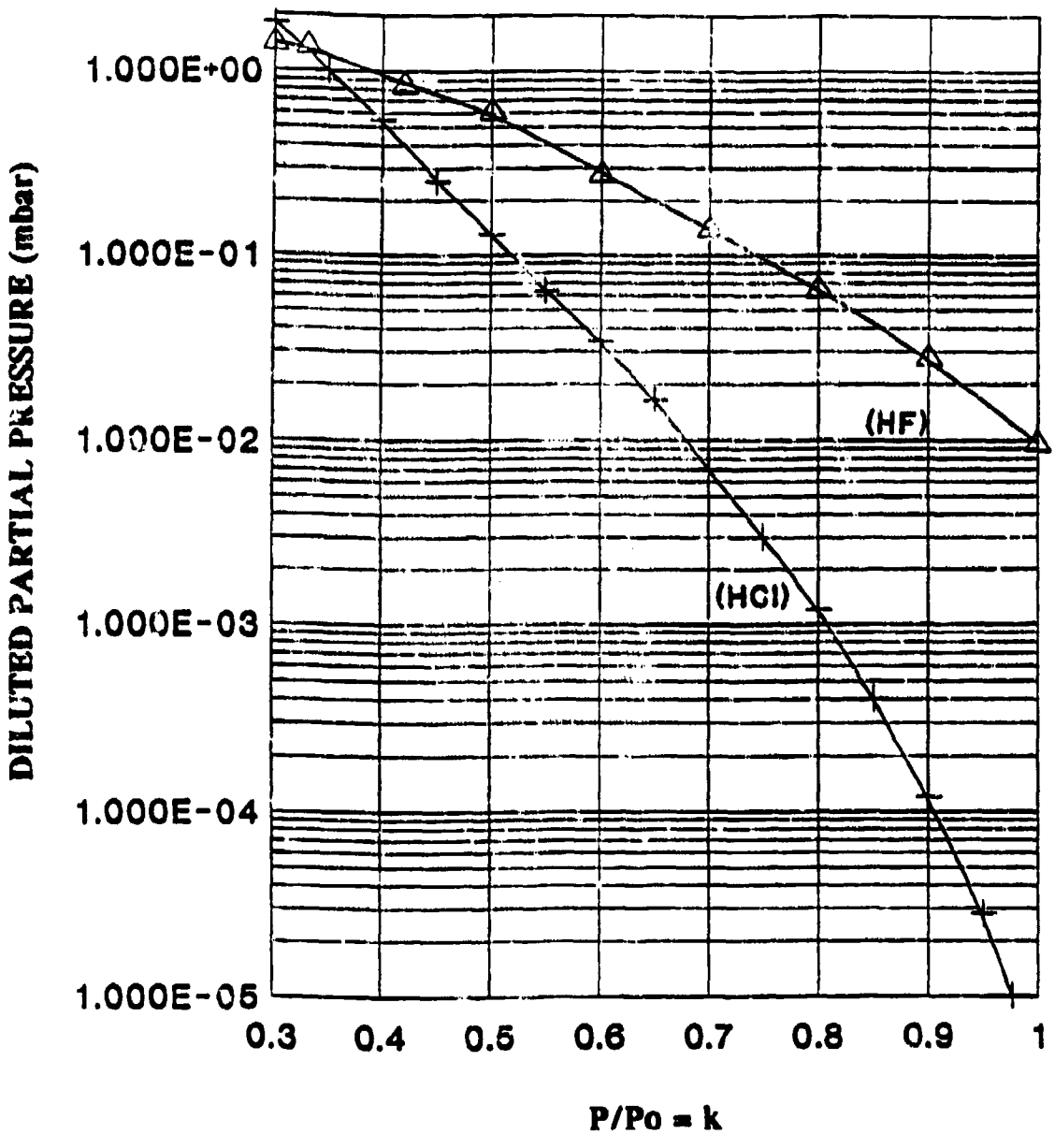

Fig. 2-1 Oliver Depression Factor for Acid/Water Vapour Equilibria at 0°C

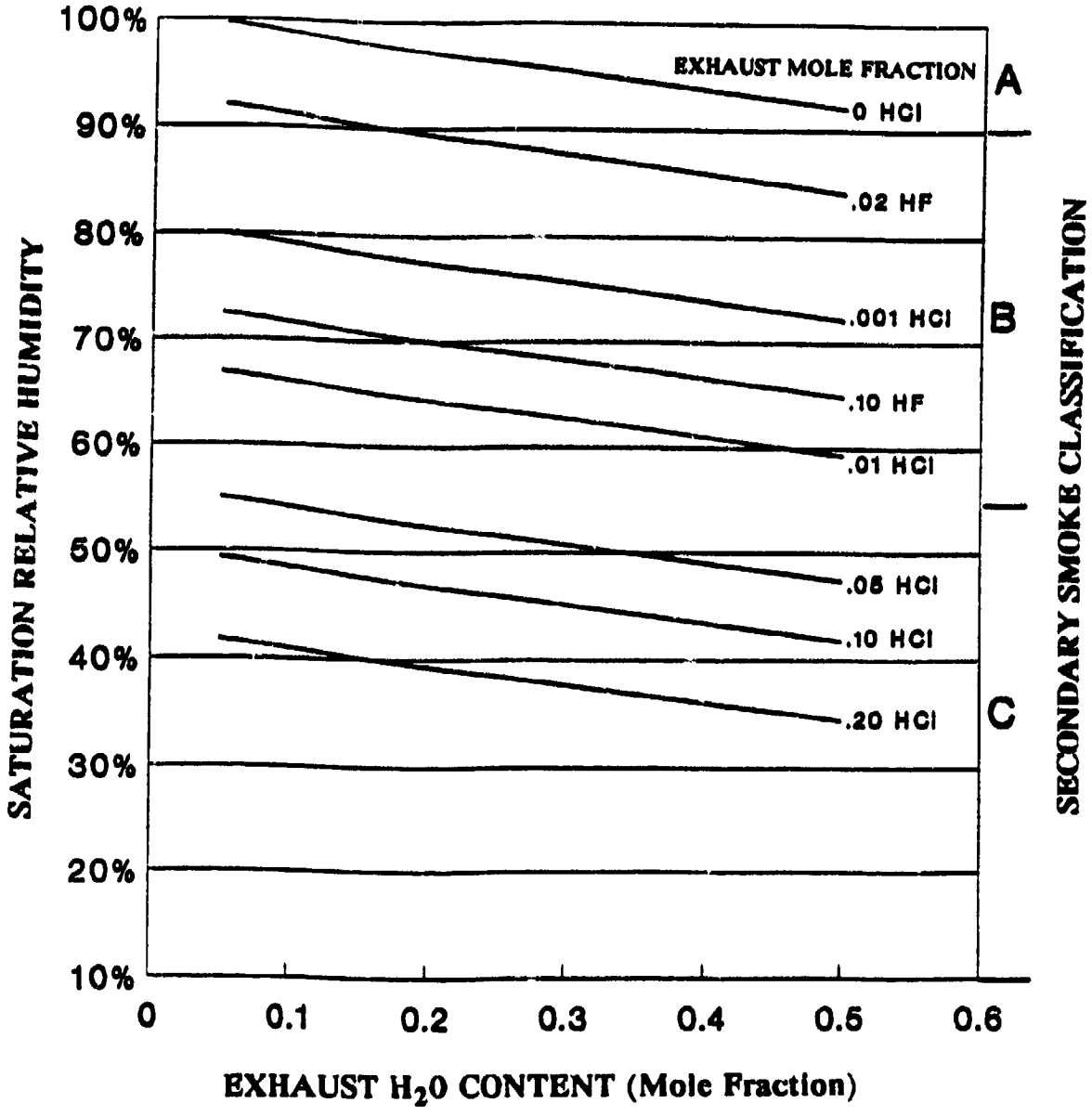

Fig. 2-2 Saturation Relative Humidity for AGARD Secondary Smoke Classification at 0°C, 1 atm., 1000 Dilution

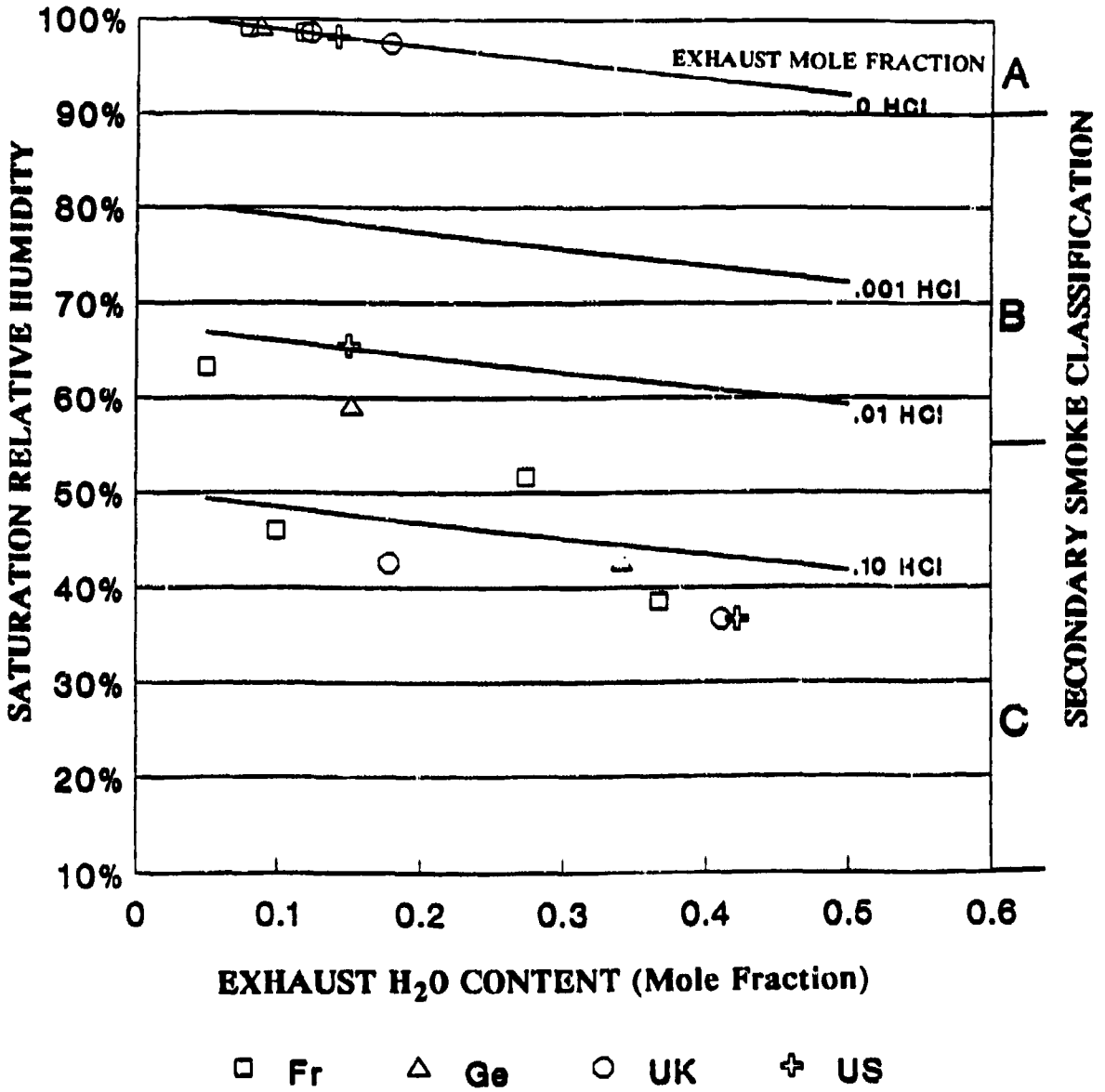

Fig. 2-3 AGARD Secondary Smoke Classification for NATO Propellants

CHAPTER 3

Plume Primary Smoke

CHAPTER 3

Plume Primary Smoke

TABLE OF CONTENTS

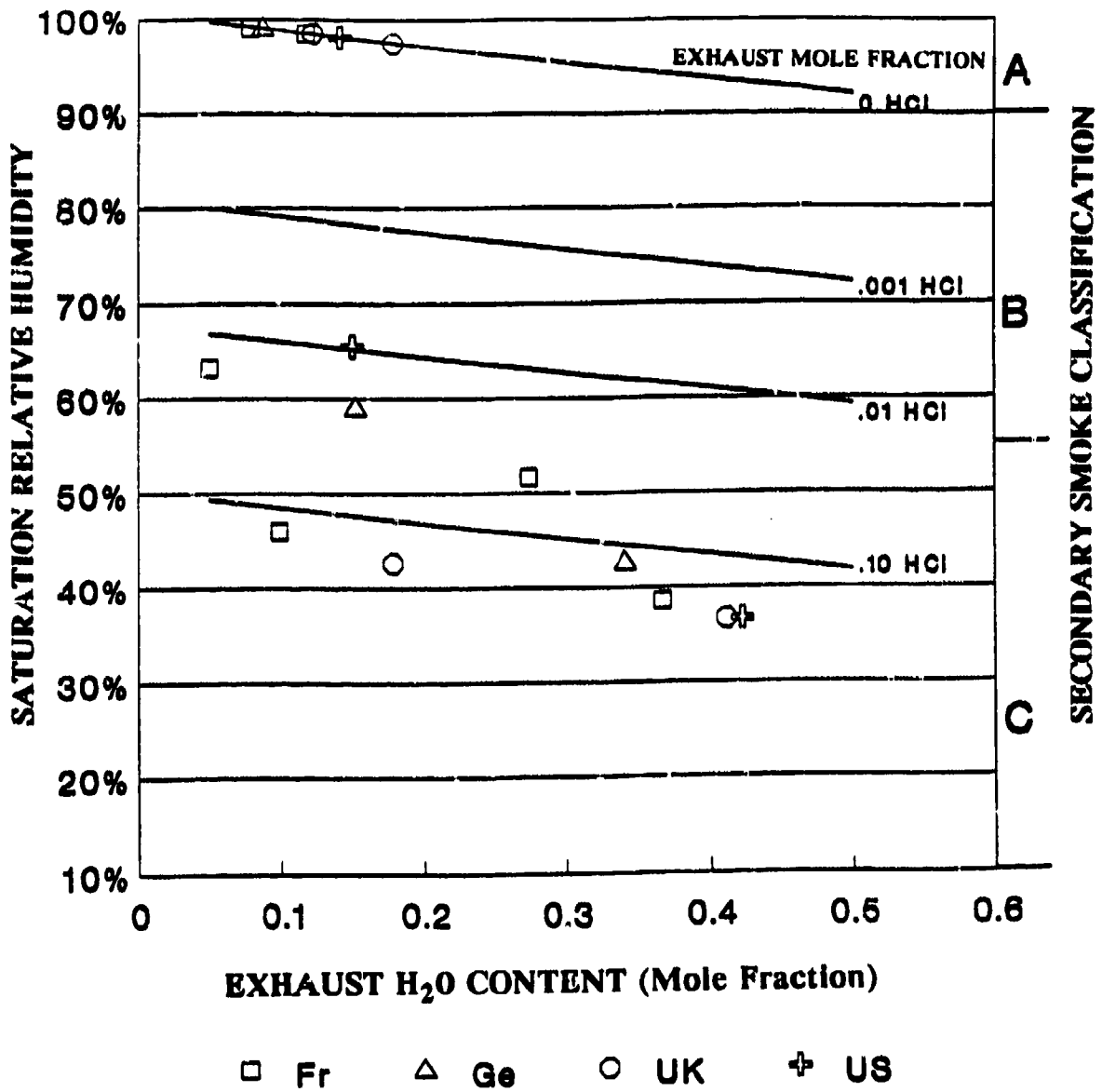

Fig. 2-3 AGARD Secondary Smoke Classification for NATO Propellants

CHAPTER 3

Plume Primary Smoke

CHAPTER 3

Plume Primary Smoke

TABLE OF CONTENTS

1.0 INTRODUCTION

1.1. Definition of "Primary Smoke"

The exhaust from a solid propellant rocket usually contains some solid material in addition to the main gaseous combustion products thereby resulting in the formation of a particle cloud in the atmosphere downstream from the nozzle: the so called "primary smoke" cloud.

1.2. Origin of Primary Smoke

Particulates have a variety of origins. Propellant formulation is only one and among propellant ingredients the main contributors to primary smoke are :-

(i) Burning rate catalysts, e.g. ferrocene compounds (catocene), lead oxides, lead salts (lead resorcinate), copper salts (copper chromate), iron oxides ...

(ii) Anti-instability additives, e.g. zirconium carbide, zirconium oxide, silicon carbide ...

(iii) Aluminium or other metals (e.g. beryllium, zirconium ...) added to increase the thermodynamic performance.

(iv) Afterburning suppressant, e.g. potassium salts (K2SO4).

This list is not exhaustive.

Thermodynamic computations have shown that these products, mostly metal compounds, are to be found in exhausts as metal atoms (e.g. Cu), hydroxides (e.g. KOH) or more often as oxides, chlorides or fluorides. Some refractory materials (mostly anti-instability additives) do not decompose in the combustion chamber and are discharged as particles into the exhaust.

Other than the propellant all motor parts which are exposed to flame may pyrolise or ablate and generate smoke: eg liner, inhibitor, thermal insulation, nozzle, etc. Their contribution can be significant, typically in the form of carbon (soot), silica, and iron oxide, especially during and after burnout of the motor. Finally, the igniter may also play a significant role in the generation of primary smoke.

1.3 Optical effects of Primary Smokes

Particle clouds interact with light in two ways, scattering and absorption. Scattering of the ambient light can make smoke highly visible and a major contributor to missile signature in the visible spectral range. Attenuation by smoke can interfere with a guidance system should optical communication be used between the launching platform and the missile or its target.

1.3.1 Attenuation

Attenuation depends upon various factors :-

(i) The structure of particles defining their complex optical index. Their shape, size and distribution, aspect ratio, surface angularity and roughness are all dominant parameters. Since it is difficult to describe arbitrary shaped particles in calculations, they are often considered to be spherical

(ii) The optical wavelength

(iii) Particle concentrations which are directly dependant upon motor parameters and flight conditions

(iv) The optical path across the cloud. Note: The wavelength (λ) and the particle size (r_p) are strongly related through the dependence of attenuation on the dimensionless size parameter $\nu = 2\pi\, r_p/\lambda$

The last two parameters are connected with motor performance and particularly the mass flow rate.

The radiation intensity loss due to primary smoke is the consequence of the scattering and absorption by particles and can be expressed according to the Beer-Lambert-Bouguer law for monodispersion :-

$$\frac{dI}{I} = -n\,\pi\, r_p^2\, Q_{ext}\, d\ell$$

or with a constant exponent coefficient

$$\frac{I}{I_o} = \exp(-\gamma_{ext}\,\ell)$$

where

$$\gamma_{ext} = n\,\pi\, r_p^2\, Q_{ext}$$

ℓ is optical path length and Q_{ext} the extinction coefficient.

$$\tau = \exp\left(-\frac{3}{4}\,\frac{Q_{ext}}{r_p}\,.\,C_v\,.\,\ell\right)$$
$$= \exp\left(-\frac{\gamma}{V_p}\,\frac{C_v \ell}{n}\right)$$

where τ is the transmittance

C_v is the particle concentration by volume

V_p is the individual particle volume

Calculation of a plume flowfield permits the transmittance to interface with motor parameters such as mass flow rate or chamber pressure by substitution of parameters C_v and ℓ in the formula.

Since the monochromatic beam crossing the plume scatters from particles of varying number density and size, the equation must be modified as :-

$$\ln \frac{I}{I_o} = -\int_0^t \int_0^\infty n\,(r_p)\,\pi\,r_p^2\,Q_{ext}\,(r_p)\,dr_p\,dt$$

The extinction coefficient can be predicted by Rayleigh or Mie theory for spherical particles of a given refractive index and monochromatic light of wavelength λ [1] [2] [3]. The light scattering theory allows calculation of different values of Q_{ext} over each of the following ranges :-

(i) When the particle diameter is far smaller than the wavelength, the scattering is called Rayleigh scattering. Scattering of this type varies directly as the second power of the particle volume and inversely as the fourth power of the wavelength. Equal amounts of flux are scattered into the forward and back hemispheres (Fig. 3-1a)

(ii) When the particle diameter is greater than about one-tenth of the wavelength, the greater overall scattering and pattern complexity (Fig 3-1b and c) requires that the theory developed by Mie be used. Although this theory is confined solely to isotropic spheres, it is customary to employ it even when particles may be somewhat irregular in shape such as those issuing from propellants.

(iii) When the particle diameter is very large with respect to the wavelength, it is necessary to apply the laws of geometrical optics.

The particles collected in rocket exhaust plumes with various mass flow rates show that equivalent diameters of non aggregate particles lay between 0.1μm to 30.0μm (Fig. 3-2). A large number of small particles with diameters probably in the range 0.01μm to 0.1μm also exist, these are difficult to quantify, but their size precludes important scattering over the visible region of the electromagnetic spectrum. In the visible, near or middle infrared, the important scattering is generally described by Mie theory.

Following this theory, when a particle of complex index $m = n - ik$ is illuminated by unpolarized light, represented by two electric vectors perpendicular and parallel to the plane of observation (Fig. 3-3) but having no coherent relationship, the scattered light consists of two incoherent components (indexed 1 and 2) such that the total angular intensity is :-

$$I(\theta) = \frac{1}{2}\,(i_1(\theta) + i_2(\theta))$$
$$= \frac{\lambda^2}{4\pi^2}\,.E.\,\left(\frac{i_1 + i_2}{2}\right)$$

E is the irradiance of the particle and i_1 and i_2 are the Mie functions, expressed by a product of Racecati-Bessel functions (f', f'') and Legendre polynomials (g, g') which are tabulated in mathematical literature, giving

$$i_1 = f'(\alpha, m)\,.\,g(\lambda) \text{ and } i_2 = f''(\alpha, m)\,.\,g'(\lambda)$$

Figure 3-4 gives variations of log I_1 and log I_2 versus θ for particles of Al_2O_3 and C (soot) when $\psi = 45°$ (Defined in Fig. 3-2). ($i_1 = i_2$ for $\theta = 0$), $r_p = 1\mu m$ and $\lambda = 0.7\mu m$ [5].

The Mie coefficient Q_{sc} which can be expressed by a ratio of the total scattering cross-section of a particle to its geometric section (independent of θ) is given :-

$$Q_{sc} = \left(\frac{\lambda}{2\pi r_p}\right)^2 \int_0^\pi (i_1 + i_2)\,\sin\theta\,d\theta$$

The difference between the total flux removed from the incident beam (Q_{ext}) and that scattered (Q_{sc}) must be the flux attributed to absorption by the particle, which occurs when the refractive index is complex. Since the extinction effects of scattering and absorption are additive, we have :-

$$Q_{ext} = Q_{sc} + Q_{abs}$$

Q_{ext} and Q_{sc} are given by the former equations solving for the total complex index or its real part respectively. Q_{abs} is obtained from the difference.

Typical variations of Q_{ext} are given in Figure 3-5 (a, b) [6]. An example of the influence of the imaginery part of the index on the scattering and extinction coefficients is given in Figure 3-5c.

In a real rocket motor exhaust with a large range of particle sizes the scattering is more isotropic than suggested by Figure 3-4.

A direct measurement is often preferred to a numerical computation which depends upon a large number of ill defined parameters. This is particularly the case for optical indices found in the literature for pure compounds at room temperature. This data applied to particles present in the rocket exhaust is highly questionable. Nevertheless, Mie scattering calculations are useful for interpreting results of measurements and applying them to propellant optimization and other aspects of rocket motor design.

Figure 3-6 shows the nature of particles in an original way. Two graphs, representing different wavelengths, show the particle mass fraction inducing a transmission factor (T) of 95% across a given particle cloud (optical path = 1 m, dilution = 5×10^{-2}) as a function of particle size. The condensed mass fraction in the plume of a given propellant and in a section of equivalent dilution must keep under the curves in order to obtain the specified transmission level.

Such representation (Figs 3-6 and 3-7) make it appear that :-

(i) Carbon or soots are very absorbing, whatever the wavelength.

(ii) When the particle radius is not too large, transmission is better in the infrared than in the visible region of the electromagnetic spectrum.

(iii) Copper and lead have similar scattering features (but with respect to only the volumetric fraction, lead is more transparent than copper).

1.3.2 Effects of Smoke Visibility

The visibility of smoke issuing from a burning rocket motor has two distinct adverse effects, it allows the missile in flight to be detected or the launch platform located. Equally, smoke can obscure a target or missile from an optical guidance operator (case of visual target designation guidance).

It is therefore necessary to establish the existence of these important effects since they are likely to prove more difficult to overcome than the effect of attenuation on guidance.

1.3.2.1 Smoke Visibility in the Sky

The term visibility is generally used to describe the possibility of detection by an observer without the aid of any auxiliary device. Quantitatively, visibility is expressed as a probability of detection for a given contrast between the object (the plume) and its background, in this case the sky. Ignoring chromaticity factors as being less important than luminance contrast, the plume-background inherent contrast C_o is defined by :-

$$C_o = \frac{L_p - L_b}{L_b}$$

where L_p and L_b are the luminances of the plume and the background with respect to a given observation point in a given wavelength band. The contrast tends to -1 for an ideal black object and may have a large positive value if $L_p \gg L_b$.

Calculation of contrast involves a detailed knowledge of all radiation sources and transport functions (sunlight, diffuse skylight, diffuse light from ground, ...). The plume optical transmittance T appears in the contrast equation. For a given sunlight, making a hypothetical angle of π with the direction of observation (i.e. setting sun in the back of observer, plume near the horizon), the transmittance appears for example, in the plume luminance expression (assuming single scattering) :-

$$L_{p_{SUN}} = \frac{E_o \gamma_{sc}(\pi)}{2 \gamma_{ext}} (1 - T^2)$$

T being exp ($-\gamma_{ext}$.ℓ), with ℓ the plume dimension in the direction of observation and E_o the irradiance [5].

Moreover transmission through the atmosphere affects the plume background contrast because of the angular scattering of environmental light towards the observer within his cone of vision (Fig. 3-8).

Considering a horizontal line of sight, the apparent contrast plume-horizon at a distance R becomes :-

$$C_R = C_o \exp(-\gamma_{sc} R)$$

The values of γ_{sc} (hyp. $\gamma_{abs} = 0$) are presented in Table 1 for standard configurations. [9]

stability or energetic performance. Accepting this point, loose specifications such as "primary smoke should be minimized" can often result in unacceptable exhaust smoke levels and should be avoided.

The missile designer would like to specify a maximum level of smoke compatible with the operational needs of the missile and then be able to check that this specification is met by the solid rocket motor proposed by the propulsion engineer.

Methods of primary smoke assessment should therefore include (a) experimental procedures to rank propellants, other motor components and finally the assembled motors with respect to primary smokes and (b) computational methods to predict primary smokes and translate

TABLE 3.1

INTERNATIONAL VISIBILITY CODE, METEOROLOGICAL RANGE, AND SCATTERING COEFFICIENT

Code No	Weather condition	Meteorological range R_m (metric)	Scattering coefficient γ_{sc} (km^{-1})
0	Dense fog	<50 m	>78.2
1	Thick fog	50 m	78.2
		200 m	19.6
2	Moderate fog	200 m	19.6
		500 m	7.82
3	Light fog	500 m	7.82
		1000 m	3.91
4	Thin fog	1 km	3.91
		2 km	1.96
5	Haze	2 km	1.96
		4 km	0.954
6	Light Haze	4 km	0.954
		10 km	0.391
7	Clear	10 km	0.391
		20 km	0.196
8	Very clear	20 km	0.196
		50 km	0.078
9	Exceptionally clear	>50 km	0.078
-	Pure air	277 km	0.0141

1.4 Goal of this Work

It is obvious that primary smoke is undesirable but most of the time unavoidable. Although some control of the smoke producing properties of different components in a solid rocket motor is possible a very low level of primary smoke is usually achieved only at the expense of other more desired qualities such as operational requirements into motor specifications that could be checked by established experimental procedures.

2.0 DESCRIPTIONS OF VARIOUS METHODS OF PRIMARY SMOKE ASSESSMENT USED IN NATO COUNTRIES

2.1 Visibility of Primary Smoke

From an operational viewpoint, specifications for primary smoke visibility should be defined in terms of whether or not a missile will be visible to an enemy observer. Because this factor is sensitive to the operational environment, one of a limited number of typical" or "worst-case" environmental conditions should be defined for the missile, specifying the solar flux, the background, the atmospheric conditions or any parameter likely to affect the visibility.

Following the US Army methodology, visibility can be defined in terms of the probability of missile detection by unaided human eye. The major physical factors determining visibility are the size and shape of the plume, its contrast with the background and transmissivity of the atmosphere; they can be derived from modelling plume flow and scattering of solar flux. Detection probability is related to natural variations in human eye response between individuals.

Many well, and less well supported assumptions have to be made in the process. The main weakness is thought to be the determination of the optical properties of particles.

The theory of interactions between light and particles is approached in Section 1.3. It solves the Maxwell equations for the interaction between a monochromatic plane wave and a spherical particle and was first written by Mie at the beginning of the century. It addresses both scattering and absorption by particles, but requires the knowledge of little known parameters such as the particle size and its optical index. Furthermore the assumption of a spherical particle shape has to be made.

An experimental approach has been attempted in the U.K., with various methods of measurement. These include measuring the intensity of the reflected component from high intensity light sources impinging on a smoke cloud and photographs of contrast scenes through the cloud, either at the time of firing or from cine or video records. All of these methods can provide useful information and differing smoke levels can be detected. However no one system can provide all of the required information. More complete information can be found elsewhere [10] [11].

Smoke visibility is an area where the development of measuring techniques is required. It may suffice here to emphasize that a complete and accurate assessment methodology is unfortunately not available but could be developed using present state of the art techniques.

2.2 Opacity of Primary Smoke

Plume opacity assessment is a much less difficult task than plume visibility. Opacity is a physical parameter that can be directly measured and is independent of the optical environment.

Accurate and validated models for opacity prediction are still unavailable, but experimental techniques have been developed and used for years. From an engineer's viewpoint, transmission measurement is the only available way to assess primary smoke.

2.2.1 Transmission Measurements in Static Tests

The U.S., the U.K., France, Germany and Italy are performing plume transmission measurements on static tests, with the implicit assumption that the result of a comparison between two motors on a ground static test should be qualitatively unchanged in flight. An improvement in ground testing transparency results is interpreted as an improvement of transparency properties in flight. The methodology to translate transmission measurements from static tests into quantitative flight predictions is not yet available, but, as for primary smoke visibility, it could be developed with existing techniques.

Therefore, the practical application of plume transparency measurements on static firings is the comparison of propellants or motors, one with another. In some cases, the purpose of these measurements is limited to a specific study - like the improvement of a motor with respect to primary smokes, or the assessment of new ingredients in a propellant formulation; the experimental procedure can be defined on a case by case basis. For more general purposes, such as having a quantitative method for comparing the smoke properties of a broad range of solid rocket propellant formulations, a widely accepted, standardised procedure is required.

In the following paragraphs more details will be given on the instrumentation, experimental procedures and interpretation of measurements used in France, the U.S.A., and the U.K. for the assessment of primary smoke transparency.

2.2.2 French Methodology

2.2.2.1 Transmissometers

The transmissometers used in France (SNPE) are of three kinds :-

(i) The first kind and oldest were commercially available apparatus (brand name : SICK) and are used in the facilities described in the next section. The source is a wide spectrum lamp, with a beam chopper, and the detector is a silicon cell.

The two other types were custom built :-

(ii) The source is a wide spectrum lamp emitting a large beam in the visible and IR range. The detector is a radiometer equipped with a telescope. The desired optical response can be adjusted with a spectral filter between 0.4μm and 1.1μm. 100% and 0% transmission levels are recorded before the firing,

(iii) The source is a HE-NE laser (0.63μm). The detector is a silicon cell equipped with a narrow band filter. Calibration is performed before each firing by intercepting the laser beam with a range of neutral density filters. Optical alignment is used to ensure that the transmissometer axis crosses the motor axis (Fig. 3-9). More details can be found in Appendix A.

The wavelengths of interest are in the 0.4μm to 14μm region, the most studied being 10.6μm, and those in the visible range (human eye response). Transmission at 0.63μm is considered a good estimate of transmission in the visible range.

2.2.2.2 Experimental Facilities and Procedures

Experimental procedures for primary smoke measurements vary from facility to facility. However, measurements made at different facilities on identical motors have shown good agreement with each other.

Firing facilities for the specific purpose of smoke assessment are used :-

(i) The "fumimètre" which is a kind of wind tunnel housing a fan (Fig. 3-10)

(ii) The "banc opacimetrique", an open firing facility (Fig. 3-11).

However, most smoke trials are performed on firing locations which have not been optimized for transmission measurements thereby suffering adverse changes in environmental conditions (wind, rain, etc ...). Transmissometers are mounted just before a test run and dismounted after.

Transmission measurements are not used to identify propellants for classification, but are limited to the task of studying specific propulsion systems. The foregoing firing facilities ("fumimetre" and "banc opacimetrique") function primarily for the assessment of smoke produced by inhibitors. For such work motors with end burning grains (diameter 90 mm) of identical propellant formulation are fired. The other test facilities are used to compare different propellant formulations and to assess the effect of including additives [12]. These firings employ motors with radial burning grains with a constant burning surface and identical inhibitor; the motor thrust is typically between 2500N and 5000N.

The transmissometer locations in the specific firing facilities are indicated in Figures 3-10 and 3-11. For other tests, the transmissometer beam makes a $\pi/2$ rad angle with the motor axis and is located 3m to 4m downstream of the nozzle exit or beyond the afterburning flame if it is longer than 3m. Transmission is measured after completing one traverse through the smoke plume.

The detailed procedure for transmission measurements in a free jet with a 0.63μm laser transmissometer is given in Appendix A.

2.2.2.3 Presentation and Interpretation of Transmission Measurement

Results of plume transmission measurements are analysed case by case except for those transverse measurements on standard motors for which a standard procedure exists.

Measurements are time averaged having beforehand eliminated the unsteady part of the record at ignition and at the end of firing. That remaining usually maintains a steady mean level making the averaged value representative of existing smoke conditions (Fig. 3-12).

To compare the smoke properties of two propellants it is essential that the test motors are the same in all respects other than the propellants and that the test environmental conditions are identical for each firing. If this is not the case then only a qualitative comparison is possible. No reliable quantitative corrections are applied.

There is no methodology to extrapolate transmission measurements from reduced scale tests to those of full-scale, consequently, a quantitative assessment of the primary smoke of a given motor requires a full scale firing. For large motors this is especially costly and difficult since the firing facilities for these motors are rarely suitable for transmission measurements.

Atmospheric conditions have little influence upon transverse transmission but are believed to be a major cause of non reproducibility in axial transmission measurements. The latter are mainly used qualitatively to observe the evolution of the plume during and after the firing or to compare low smoke motors which cannot be separately distinguished by transverse transmission measurements.

2.2.3 U.S. Methodology [13]

Transmission measurements are only conducted on a regular basis at MICOM in the Army Signature Characterisation Facility (SCF). This facility is designed for simultaneous assessment of primary and secondary smokes, but climatic conditions can be set to prevent secondary smoke formation thereby allowing primary smoke assessment only.

2.2.3.1 Transmissometers

Chopped emissions from a 200W (50Hz) tungsten-halogen lamp are measured after passing through a distance of 5.3m by filtered silicon diode detectors. Two detectors approximate photopic response with peaks at 0.55μm. Others have narrow band (0.01μm) interference filters peaked at 0.52μm, 0.63μm, 0.85μm, 0.95μm and 1.06μm respectively. Objective lenses (34mm diameter and 66mm focal length) are used with field stops to limit the angular field to less than 0.17rad (10°). This reduces the collected radiation scattered from angles other than the forward direction.

Signal intensity data are sampled at a rate of 600Hz. They are ratioed to the 100% pre-test value recorded immediately before the firing and average transmission values are obtained for 1s intervals.

A recent acquisition is the Series 7000 Nicolet Fourier Transform Interferometer System (FTIS) which extends the spectral range and capability of the SCF. The system which incorporates two interferometer spectrometers interfaces with the climatic chamber as illustrated by Figure 3-13. A transmission/absorption spectrometer, using the chamber as a sample cell, modulates and projects the beam energy to a remote detector positioned diagonally across the chamber. A second interferometer spectrometer employs a mirror to collect emitted energy from the motor plume. The design permits measurement of the afterburning plume emission as well as transmission through the smoke produced by the motor. Optics and detectors are available for the FTIS which access the spectrum from 0.5μm to 25μm, with varying degrees of sensitivity. Portions of the visible and IR may be scanned at variable rates up to $10s^{-1}$. The FTIS has a resolution capability of $0.06cm^{-1}$. A 4.5 million word dual-disk based data system permits great flexibility in selection of operational parameters (resolution, scan rates, gain, etc ...), as well as data analysis and presentation. Interferograms are generated by means of a Michelson interferometer with a HeNe laser operating as a reference at 0.63μm. The interferogram signals are converted by mathematical Fourier transformation from the time domain to the frequency domain.

Individual laser sources have also been occasionally used emitting at 1.06μm and 10.6μm.

2.2.3.2 Experimental Facilities and Procedures

The US Army MICOM Signature Characterization Facility (SCF), was developed to evaluate propellant smoke phenomena over a wide range of climatic conditions (Fig. 3-13). The smoke test chamber is a modified environmental room. It has dimensions of 5.96m x 1.58m x 2.08m, or $19.6m^3$ which gives an air to exhaust ratio of 380:1 (based on weight of dry air at STP) when firing a motor containing 70g of propellant. The temperature range is from 233K to 330K (-40°F to 140°F) and relative humidity can be varied from 20% to 100%. For primary smoke assessment, these parameters are chosen to prevent secondary smoke formation.

Structurally, the smoke test chamber is designed to withstand 2×10^4Pa internal dynamic overpressure. A spring loaded swing-out door at the chamber end opposite the motor is used to relieve the temporary overpressure caused by a motor firing. To reduce corrosion by exhaust gases, the stainless steel walls are coated with a black polyvinylacrylate paint. The exhaust gases and conditioned air are stirred at a rate of about $0.83m^3s^{-1}$ (gas velocity $0.3ms^{-1}$) by twelve-inch diameter fans mounted at each end of the chamber on opposing walls. A uniform mixture is verified by equivalent transmission analogues of different optical paths in the chamber.

The detectors are located at various points surrounding the motor and looking at the source 5.3m away at the opposite end of the chamber.

A 70g case bonded motor (50.8mm diameter x 50.8mm long, centre perforated, 6.4mm web) with a smokeless igniter and no inhibitor is used (Fig. 3-14). A typical smokeless pyrogen igniter contains one to three grains of N5 double base propellant. Tests have shown this amount to be undetectable in the SCF. In special cases an igniter may be developed using the test propellant as powder.

For testing inert motor components, a special motor is used (Fig. 3-15).

Procedures used in conducting the tests can best be considered as having three phases :-

(i) Facility preparation and conditioning,

(ii) Motor firing into stirred chamber with data recording

(iii) Post firing exhaust, clean up, and data analysis.

During the preparation period all instrumentation is set up and calibrated, and the chamber is conditioned by circulating air through the conditioning duct (containing the cooling coils, humidifier, and drier) and the test chamber. The air is first conditioned to the approximate test temperature, then the humidity, controlled by the humidifier and drier, is set to a true dew point. In all cases, only the air is conditioned allowing the insulated walls to come to some steady state temperature, depending upon the effectiveness of the insulation. This time period ranges from two hours to overnight, depending upon the severity of the conditions. Near the end of the conditioning period all instrumentation (calibration) is checked and the auxiliary equipment (particle size measuring devices, etc ...) set up and calibrated. The motor is prepared for firing and inserted into the end of the chamber through the closure. When the conditioning process is complete, the dry bulb and dew point temperatures are tracking within 1K. This provides an initial humidity control of $\pm$ 5% relative humidity.

The second phase, or test phase, is initiated by closing the damper to the conditioning equipment and firing the motor in the chamber. Data are recorded for six minutes as mixing continues, and the chamber reaches a quasi-steady state condition. By contrast with freejet measurements the transmission measurements are made in a uniform post firing cloud (stirred by fans) and not during the burn time of the motor.

All optical data channels are recorded on computer and analog magnetic tape together with motor pressure and the temperature-humidity history of the air/exhaust mixture. Other temperatures at various points in the chamber, both wall surface and air, are monitored using a thermocouple scanner that prints each channel at preset time intervals. The data is later digitized and processed using a computer code which averages the transmission and prints a data word for each 10s interval during the test. Selected channels may then be plotted for graphical display.

In the final phase the chamber is purged through the exit door and all conditioning equipment is shut down. While the chamber is being cleaned and prepared for another test, the data is processed for analysis.

2.2.3.3 Presentation and Interpretation of Transmission Measurements

Transmission results for each wavelength channel are tabulated as a function of time for the period of approximately 360s after the end of motor firing. The smoke transmission may then be plotted for one or more tests in the form shown of Figure 3-16 which shows the transmission properties of a minimum smoke propellant at several test conditions.

Transmission values at five minutes are typically reported as a figure of merit for the test item and have been found suitable for comparison between propellants. Figure 3-17 shows results of tests for various types of propellants at a single test condition. Figure 3-18 shows the results of testing various insulation materials.

Primary smoke transmittances are repeatable to within 5% over a wide range of moderate climatic conditions and are well within motor to motor variation.

2.2.3.4 Particle Sizing Instrumentation

Particle measurements are frequently obtained using a Climet 208 particle analyser and CI 210 counter-printer. The empirically calibrated particle analyser system works on the principle of forward angular scattering of a focused white light by isokinetically sampled particles in the range of a 0.3μm to greater than 10μm. These particles are counted and classified by size in 16 bins. Complete size distribution may be acquired as rapidly as one per 8.5s Smoke concentrations encountered usually require dilution to avoid optical saturation of the analyser.

2.2.4 U.K. Methodology

Transmission measurements carried out in the UK have concentrated on the use of two facilities.

For low thrust motors (up to 400N) a smoke tunnel is used, but firings of higher thrust motors are carried out on an open range. Each facility has its own specially built instrumentation.

2.2.4.1 Transmissometers [14]

For smoke tunnel firings a 0.9μm transmissometer is primarily used. The source is an IR emitting diode pulsed at 500Hz. The detector is equipped with a narrow band filter.

For standard tests on the open range facility a visible light system is used. The source is a quartz halogen lamp (emitting a continuous signal). The optical receiver is a modified SLR camera fitted with a photometric responding photodiode detector.

For other transmission measurements, a general purpose optical receiver has been designed. This instrument is readily adaptable for use on a variety of applications and can be used for simultaneous measurements in three wavebands. The construction permits quick changes of detectors, filters and lenses. Variable gain detector preamplifiers are installed, the output signal then passes to individual signal processing units. These demodulate the signal using phase-sensitive detection, the reference signal being supplied from the source, and produce a DC output proportional to the RMS signal within a narrow band centred at the modulation frequency.

This receiver is used with two sources. The first is based on a 50W quartz halogen lamp for visible and near IR wavelengths. The lamp output is collected by an ellipsoidal reflector, passes through a chopper disk and then through condensing and collimating lenses. The result is a low divergence 0.07rad (4°) beam with uniform intensity profile, modulated at 250Hz. The second source is a proprietary item, used as a broad-band IR source. It comprises an electrically heated ceramic tube, with refractory coating, positioned at the focus of a 50mm diameter parabolic reflector. The IR beam is chopped mechanically at 90Hz.

The spectral response of the receiver is defined by either optical filters or the detector response. Typical spectral regions of interest are the visible (photometric response) and the infrared between 8μm and 12μm, although a number of applications exist for measurements at other wavelengths, e.g. 0.9μm or 1.1μm.

2.2.4.2 Experimental Facilities and Procedures

Low thrust motors (up to 400N) can be fired in the Royal Ordnance (RO(S)) smoke tunnel. This consists of a cylindrical tube 1m diameter and 20m long, with the motor mounted on the centreline at the tunnel inlet. Smoke build up inside the tunnel is avoided by the use of fans at the exhaust end. Measurements are carried out both axially over the length of the tunnel and transversely at a position 2m downstream of the tunnel inlet, using a mirror to provide a double pass (Fig. 3-19).

Higher thrust motors are fired in an open range facility (Fig. 3-20). More details can be found in Appendix B.

To compare propellants within a range of very different burning rates, 1500N thrust motors of 8s burn time with pyrogen (smokeless) igniters are normally employed. The thrust is adjusted by varying the diameter for end-burning grains. Adjustment in grain length can similarly produce a constant burning time. However, this is considered less important provided that a reasonable burning time, say 5s, is exceeded.

For inhibition development and quality control work, a standard test charge is used. This is a 150mm cased SCB bi-propellant charge consisting of boost and sustain propellants having burning times of 6s and 20s respectively at thrust levels of the order of 1000N and 300N. This charge can be produced in the required inhibitor system and, when fired in an uninsulated heavyweight test motor, provides information on inhibitor smoke, at boost and sustain burning rates and at those of the transition from boost to sustain.

For propellant ingredient trials the test charge is produced in a "smokeless" inhibitor system. Using the range of propellant burning rates available at RO(S) this charge can have a burning time ranging from 4s to 80s at thrust levels of 3kN falling to some 150N using the lowest burning rate propellants.

2.2.4.3 Presentation and Interpretation of Transmission Measurements

Figure 3-21 shows typical results obtained for transverse and axial transmission.

For each firing a minimum and mean percentage transmission over the burning time is

given. The influence of climatic conditions on the experimental results is minimized by requiring that the firing be within a window of lighting, wind, and humidity conditions.

Comparison of two propellants can be done from transmission results of firings at the same thrust level. For very small differences, firings in rapid succession are necessary.

Visible (eye response) axial transmission measurement of 1500N thrust motors is used as a standard to classify propellants in the U.K. terminology: a minimum transmission value of 90% is required for the propellant to be classified as smokeless.

2.2.5 Review and Comparison of the Existing Methods

It would appear that three methods are currently used to determine the opacity of primary smoke during static test firings :-

(i) Firings in a closed chamber (U.S. Army S.C.F.)

(ii) Firings in a smoke tunnel U.K. Royal Ordnance Smoke Tunnel, French SNPE "Fumimetre")

(iii) Free jet firings. It seems to be the most widely used type of procedure in NATO (except the USA).

The three techniques do not share strictly common usage. Free jet transmission measurement is a technique adapted to evaluate the complete motor (propellant + inhibitor + etc...). With some caution it can also be used to rank propellant and inhibitor formulations. The same use applies to smoke tunnel tests but with more restrictions on the maximum thrust of the rocket motor. On the other hand, the SCF chamber is a facility which primarily assesses propellant formulation. Because of test duration and environmental control, this facility is better suited to carry out more sophisticated experiments on primary smoke than those of transmission measurements : e.g. transmission spectrum, particle sizing and maybe particle scattering characteristics.

It is assumed that most of the measurement procedures described herein have experimental repeatability, although, with the exception of the U.S. Army procedure, no supporting figures have been produced to support this assumption. One exception to this assumption must be the method adopted for axial transmission measurement in a free jet where repeatability very much depends upon atmospheric conditions. Furthermore, the existing procedures have not addressed the possibility of repeating experiments at different facilities to compare results, but have focused only on one location.

Another important characteristic is the sensitivity of the test. Propellants generating moderate or high levels of primary smokes (typically 2% Al_2O_3 or more in the exhausts) afford discrimination by transverse transmission measurements in freejet or smoke tunnel or by transmission measurements in the SCF facility. However, low smoke propellants have transverse transmission values typically in the 90% - 100% range that are not accurate enough to offer discrimination. This has not been a problem for measurements in the SCF chamber. For smoke tunnel firings, the problem is addressed by axial transmission measurements. For free jet firings, the latter are less satisfactory, because of their lack of reproducibility.

3.0 RECOMMENDATION OF METHODS FOR ASSESSING PRIMARY SMOKES

3.1 State of the Art

With respect to smoke visibility assessment, no reliable standard experimental or theoretical methods have yet emerged. Therefore the only recommendation that can be made is that more work on the subject is needed. A desirable first short term goal would be to develop an experimental procedure to rank propellants, putting the methodology for visibility and transparency assessment at the same level.

Indeed, transmission measurements during static tests, allowing ranking of propellants and motors is within present state-of-the-art knowledge. Moreover, it is the only industrial primary smoke assessment method available. Further effort is needed to establish a complete methodology which would allow quantitative extrapolation of ground test results to the flight case or, in reverse, translation of operational requirements in terms of minimum transmission level to be measured in static tests.

However, the only standardized method that can be recommended to date is that of transmission measurement in ground tests.

3.2 Procedure for Transmission in Free Jet

Detailed descriptions of two currently used test facilities are presented in Annex A and B. While it may be difficult to exactly reproduce either method, the principles of operation are very similar. A suggested procedure is shown in Figure

3-22 and is summarised in the following text.

3.2.1 Transmissometer

Source/Receiver

The transmissometer can have either an optical (0.63μm) laser source or a quartz halogen lamp with, in each case, a suitable receiver.

The system using the quartz halogen lamp may be preferable because it avoids the necessity for precise alignment between source and detector, thereby being less susceptible to vibrational disturbances during the motor firing. Current systems employ continuous sources but a chopped source is recommended to counteract interference from scattered ambient light falling on the receiver. The detector should have a high frequency response (like a silicon photodiode) which can record the rapid fluctuations of the smoke plume and a spectral response in the visible and near IR which spans the range of source wavelengths.

The energy recorded by the transmissometer involves both the direct flux and a small portion of forward-scattered flux. The latter comes from a spatial volume, usually of double-conical shape, which surrounds the source to receiver axis and is defined by the angular divergence of the source beam, the angular field of view of the receiver and the source to receiver distance. These factors, and the receiver aperture area determine the total scattered flux received. Typically receivers with a small angular field of view and apertures of a few centimeters are employed in measuring the nominally direct transmittance [15].

Calibration

To be carried out using neutral density filters the calibration of which should be traceable to international standards.

3.2.2 Measurement Paths

In general both transverse and axial measurements are performed, each of which has its associated advantages and disadvantages. Transverse measurements are particularly well suited to propellant ranking, inhibitor assessment or the study of additive effects. They are indeed reproducible, constant with time, providing the burning surface area doesn't vary during the firing period and tests conducted near the nozzle exit are not affected by secondary smoke. Furthermore, the limited volume of cloud viewed transversely gives an opportunity to undertake complementary optical measurements. Axial measurements, on the other hand, are realistic for smoke assessment in a missile guidance context and allow discrimination between similar products that produce near transparent smoke.

Transverse

These measurements are carried out at an angle of π/2rad to the motor axis. The transmissometer axis must cross the motor axis at a position downstream of the afterburning flame. This can be achieved using a constant distance for motors up to a certain thrust level (20kN) or by maintaining a set distance (2m) downstream of the afterburning flame.

Axial

These measurements are performed over a long path length with the transmissometer beam inclined at a shallow angle (typically 0.07rad $\equiv$ 4°) to the motor axis and intercepting the plume axis at a set distance downstream of the motor again beyond any possible afterburning flame and usually at the position of the transverse beam.

3.2.3 Motor Position

The height of the motor axis from the ground should be such that there is no interference between the smoke plume and the ground up to the position of the transverse transmissometer. Typical distances of 1.3 metres have been used.

3.2.4 Limitations

Firings should not be carried out in conditions of mist or rain or with crosswind speeds exceeding 3ms^{-1} for transverse measurements. Conditions of temperature and humidity should be such as to preclude the formation of secondary smoke.

The relatively short path length associated with transverse measurements will give transmissions of 90% - 100% with low thrust, low smoke, motors. At these smoke levels transmission measurements may not be sensitive enough to discriminate between motors. In such cases the path length can be increased by the use of front silvered mirrors but great care must be

taken to ensure that the mirror surfaces remain clean and that vibration of the mirrors is prevented during firings.

The much longer path length involved in axial measurements permits better discrimination between low smoke motors. However, as the path length increases so does the influence of atmospheric conditions. Recommended maximum crosswind speed is $1ms^{-1}$.

The results of smoke measurement trials performed on open ranges will always be influenced by atmospheric conditions. It is therefore recommended that control rounds of a known smoke level are included wherever possible and that successive motors are fired as quickly as possible to minimise any changes which may take place during the duration of the trial.

3.3 A Proposed Standard Procedure for Transmission Measurements in a Closed Chamber

The U.S. Army SCF components are cited as examples but are not necessarily recommended since technology has advanced beyond the SCF design which is retained to provide continuity of the data base. A copy of the procedure is shown in Figure 3-23.

3.3.1 Transmissometer

The following specifications for a smoke transmissometer are recommended:

(i) The transmissometer should be matched to the optical response of the human eye ie, the standard CIE daylight photopic response function. Photopic response requires that all components of the transmissometer be carefully selected so that the convolution of the individual spectral responses for the source, filters, and detector results in the desired photopic response. The SCF uses a 200W tungsten halogen lamp, and a Texas Instruments type LS-400 silicon transistor detector in combination with Corning filters Types 1-69 and 4-97 to approximate the eye response.

(ii) The field of view of the transmissometer detector should present a solid angle as narrow as possible to limit the measurement of scattered light. The constraints are the source intensity, detector sensitivity and the collector optical design. The SCF uses a simple telescope design with an f/2 collector lens and a field of view less than 0.018 rad (10°).

(iii) The source should be spectrally broadband to avoid preferential selectivity of the measurement to a given particle size distribution. Signal chopping is desired to discriminate between source energy and that from ambient light and rocket motor emission. Synchronous detection is desirable. The source beam should not be so narrow as to be steered by the intensity gradients of the exhaust plume.

The SCF source is a 50Hz chopped tungsten lamp with a total solid angle of projection of 0.35rad (20°).

(iv) All equipment which is used inside the test chamber should be sealed against moisture and corrosion of exhaust gases. Optical surfaces should be purged with dry air or nitrogen to prevent contamination and obscuration.

(v) A visible/near IR rapid scanning spectrometer is a valuable tool for smoke transmission and plume analysis. Photometric transmission and IR absorption measurements are easily obtained with modern Fourier Spectrometry and computer algorithms. The SCF uses an FTIR system routinely as an adjunct to the fixed band transmissometer. Such systems however demand considerable dedication of funds and personnel.

3.3.2 Description of the Chamber

The chamber shape and volume (5.96 x 1.58 x $2.08m^3$) are identical to MICOM's SCF (Fig. 3-13). Air in the chamber should be controlled to keep a moderate temperature and humidity in order to ensure that no secondary smoke will form. However, full climatic control as in the SCF is not a necessity. The chamber should be equipped with a device to mix the exhaust gases with the chamber air like the fan system used in the SCF chamber (see Section 2.2.3.2.). The homogeneity of the mixture should be verified by comparing transmission measurements for different positions and optical paths.

3.3.3 Transmissometer Position

The optical path for the transmissometer is 5.3m, with the detector near the motor and the source at the opposite end of the chamber.

3.3.4 Motor Description

The nominal weight of the propellant sample is 70g. If the sample weight is different, a correction should be applied to the transmission measurement in the following manner:-

$\text{Log } T_c = 70/m \text{ Log } T_r$

T_c is the corrected transmission
T_r is the uncorrected ("raw") transmission
m is the propellant sample in grams

This formula, based on the Beer-Lambert law, is an approximation that should be used with caution : it ignores, for instance, forward scattering effects.

The exact design of the motor is not specified here, since it may vary with the propellant manufacturing process. The SCF test motor described in Figure 3-14 is relevant to composite or XLDB propellant. Other motor types must be used for propellants which cannot be case-bonded. It is however essential that the level of smoke produced by the igniter, inhibitor or any other motor component besides the propellant is negligible.

3.3.5 Test Procedure and Interpretation of Transmission Measurements

Transmission measurements are carried out in the post firing cloud. Full mixing of the exhaust products and the air lasts for some time. When the mixture is homogeneous, a steady-state transmission measurement is obtained that shows on the transmission versus time plot as a plateau. The plateau value is interpreted as a characteristic of the primary smoke generated by the formulation.

To ensure a good estimation of this plateau value, transmission measurements should be recorded over a period of time significantly (typically 10 times) longer than the mixing time. In the SCF chamber, the mixing time is approximately 5s to 30s and measurements must be recorded over 300s.

3.3.6 Limitations

The measurements obtained from 70g propellant samples are easily adequate to discriminate between low smoke propellants in the 90%-100% transmission range. Typical measurements in the SCF show repeatability within plus or minus 1% transmission for equal propellant weights. Variations in the motor design : e.g. nozzle expansion ratio, propellant weight, igniter type and ballistic performance may limit the repeatability of transmission results.

Transmission measurement repeatability is affected by multiple scattering for propellants producing smoke transmission values below approximately 75%. Such values obtained in the SCF generally indicate undesirable smoke performance for a system using such a propellant.

3.4 Usage of the Standard Tests

Standard tests have been chosen to provide a flexible and relatively inexpensive method for obtaining quantitative results to characterise primary smoke. It is hoped that similar procedures to those described above will form a base that can be adopted as standard among NATO countries

The tests should reproduce results acceptable for the purpose of standardization. So far they have only been performed at the place of origin : U.S. Army MICOM for the chamber test and U.K. Wyre Forest for the free jet test. It is strongly argued that participants in smoke evaluation should aim for common measurement techniques to ensure reproduction of results and that an interchange of test programmes be organised to establish reproducibility.

REFERENCES

1 Kerker, M., The scattering of light and other Electromagnetic radiation
Academic Press, New York, 1963

2 Van Del Hulst, H., Light scattering by small particles
John Wiley and Sons, New York, 1957

3 D. Electromagnetic scattering on spherical polydispersions
American Elsevier Publishing Co, New York, 1959

4 Brumberger H., et al. Light scattering
Sciences Technology, November 1968, p 34-60

5 McCartney, E.J., Optics of the atmosphere, scattered by molecules and particles
J Wiley series, 1976

6 The new computer program "MIDI" for Mie diffusion theory calculations using the lentz algorithm
G Greman - Gouesbet
Internal Report TTI/GG/78/10/30
Laboratoire de thermodynamique, Faculte des sciences et techniques de Rouen 76/30 Mont-Saint-Aignan (FRANCE)

7 Hoshizaki, H., et al. Plume visibility screening study
AFRPL-TR-80-7, March 1980

8 Middleton, W.E.K., Vision through the atmosphere
University of Toronto Press, Toronto, 1952

9 Hulburt, E.C., Optics of atmosphere haze
J Opt Soc Am 31, 467-476, 1941

10 Victor, A.C., and Breil, S.H., A Simple Method for Predicting Rocket Exhaust Plume Visibility, J Spacecraft and Rockets, Vol 14, No 9, pp 526-533, Sep 1977

11 Victor, A.C., Effects of Multiple Scattering on Rocket Exhaust Plume Smoke Visibility
J Spacecraft and Rockets, Vol 26, No 4, pp 274-278, July-Aug 1989

12 Technologie des propergols solides
A Davenas - Ed Masson 1989

13 Thorn, L.B. and Pinkley, L.W., Propulsion Signature Characterization in the Army SCF, Technical Report RD-PR-86-1, US Army MICOM, December 1985

14 Ashton, R.M., and Taylor, F.L., Instrument Techniques for Measurements of Rocket Motor Plume Characteristics
Technical Note 88/58, Royal Ordnance plc, England

15 Hodkinson, J.R., The optical measurement of aerosols
Aerosol Science, C N Davies, ed Acadmic Press, New York, 1966

APPENDIX A

TRANSMISSION MEASUREMENTS IN FREE JET WITH A 0.63μm LASER TRANSMISSOMETER
(French procedure)

1 Transmissometer

Source:

He Ne laser (0.63μm) with power greater than 2mW.

Stability: ± 1% during one test (from calibration to end-of-firing)

Source is chopped at a frequency of 25Hz.

Detector :

Silicon cell equipped with a narrow-band filter at 0.63μm. To avoid possible detector saturation, an attenuating filter may be necessary. A field limiter reduces the field of view of the detector to less than 0.17rad (10°) (for instance an opaque cylinder : 13mm diameter x 75mm long).

Calibration:

Before each firing the transmissometer is calibrated using neutral density filters directly after the laser source. The delay between calibration and firing should be minimized. The calibrated transmission values are 0% (by intercepting the beams with an opaque material), 100% (no filter) and 8 intermediate values using 8 density filters : 10%, 20%, 25%, 40%, 50%, 63%, 71%, 79%.

2 Transmissometer Position

Distance from nozzle exit : 4m or 2m beyond the afterburning flame if it is longer than 2m.

The transmissometer axis must cross the motor axis at an angle of π/2rad. The optical alignment technique is shown in Figure 3-9 .

The detector must be at a distance of about 3m from the motor axis. The laser must be at a distance between 3m and 10m from the motor axis.

3 Motor Position

The distance between the motor axis and the ground or the surrounding wall must be greater than 1.30m.

4 Usage and Limitations

For high thrust motors (above 12kN) the procedure may have to be altered to adapt to the size of motor (e.g. transmissometer or position and height of motor axis).

The test may not be accurate enough to compare motors that would be in the 0 - 10% or 90% - 100% transmission range.

Transmission results at 0.63μm are believed to be representative of optical properties of primary smoke in the visible and near IR range (0.4μm to 1μm). Although transmission values will vary with respect to the wavelength (transmission is expected to increase with wavelength) it seems very unlikely that the ranking of motors would significantly change : it would imply a very "peaky" particle granulometry in the exhausts. The choice of 0.63μm as a standard wavelength is also justified by the availability and low cost of He-Ne lasers.

Typical repeatability of the measurement is ± 0.5%.

APPENDIX B

TRANSMISSION MEASUREMENTS IN FREE JET WITH A QUARTZ HALOGEN LAMP TRANSMISSOMETER (method employed at a UK open range facility)

1 Transmissometer

Source:

The source is a 24V 48W quartz halogen lamp fitted in a 150mm diameter parabolic reflector producing a uniform beam of light.

The lamp is powered by a regulated DC power supply. A cowling is fitted to the source to prevent reflected sunlight affecting the receiver.

Receiver :

For convenience, the receiver is based on a single lens reflex camera with a silicon photodiode detector fitted at the centre of the focal plane. This arrangement is to facilitate the visual alignment of source and receiver. The detector has a photometric response that conforms with the CIE photopic curve. A 400mm focal length lens is used with the receiver, the lens aperture being set as required.

An associated electronics unit provides signal amplification with independent offset and gain controls to optimise the output signal, followed by a 5Hz low pass filter.

The principle of operation is that the diverging angle of the source is much greater than the field of view of the detector so that precise alignment of source and detector is not critical.

Calibration:

Periodic Linearity Calibration

At regular intervals a laboratory calibration is performed to ensure the linearity of the measurement. This is accomplished with 5 neutral density filters, whose calibration is traceable to national standards, and have nominal transmittances of 5%, 25%, 50%, 65% and 75%. In addition, 0% (source blocked) and 100% (no filter) readings are recorded.

Site calibration:

Prior to a firing, the instrument output for 0% and 100% transmission levels are recorded in order that the data may be subsequently scaled during the analysis.

2 Measurement Paths

For motors up to 20kN thrust levels, two measurement paths through the smoke are considered :-

(i) transverse, at $\pi/2$rad to the motor axis and 15.7m from the nozzle

(ii)axial, at 0.07rad (4°) to the motor axis and intersecting the axis 15.7m from the nozzle (at the transverse position). The source is positioned forward of the motor and the receiver 67m from the source (Fig. 3-20).

3 Motor Position

The distance between the motor axis and the ground at the transverse position should be no less than 1.25m.

4 Limitations

The environmental constraints imposed on firing are that conditions should be free from mist or rain with cross wind speeds not exceeding $3ms^{-1}$. For primary smoke measurements conditions of temperature and relative humidity should be such as to preclude the formation of secondary smoke.

Transverse transmission measurements may not be sensitive enough to discriminate between low smoke motors where transmissions can be greater than 95%. For these motors the much longer path length associated with axial transmission will produce better results.

However as the path length increases so does the influence of atmospheric conditions in particular cross winds.

It is recommended that for precise axial measurements cross wind speeds greater than $1ms^{-1}$ should be avoided and that control rounds of established smoke level are used, the firings being comparative to these controls. Similarly it is required that when a phase is started, all motors within that phase are fired within the shortest possible time without interruption in an attempt to achieve similar atmospheric conditions for all rounds.

FIGURES

TABLE OF CONTENTS

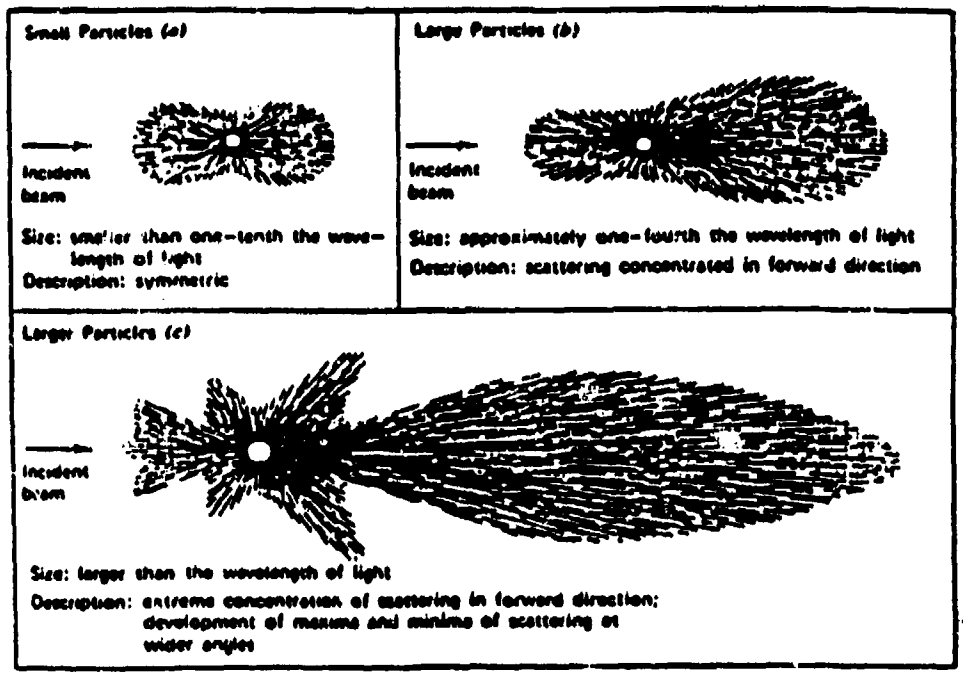

Fig. 3-1 Angular Patterns of Scattered Intensity from Particles of Three Sizes

(a) Small particles

(b) Large particles

(c) Larger particles [4]

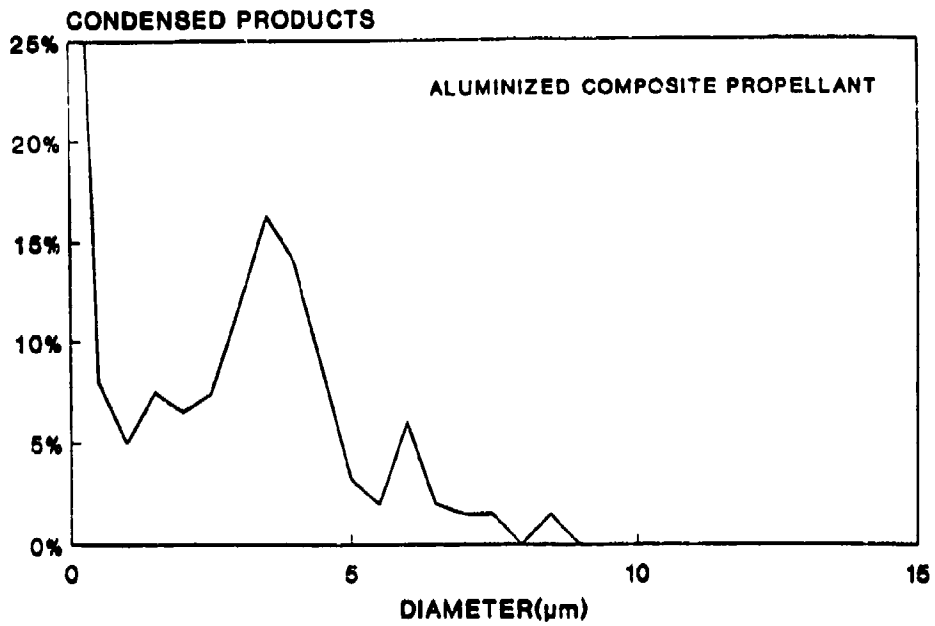

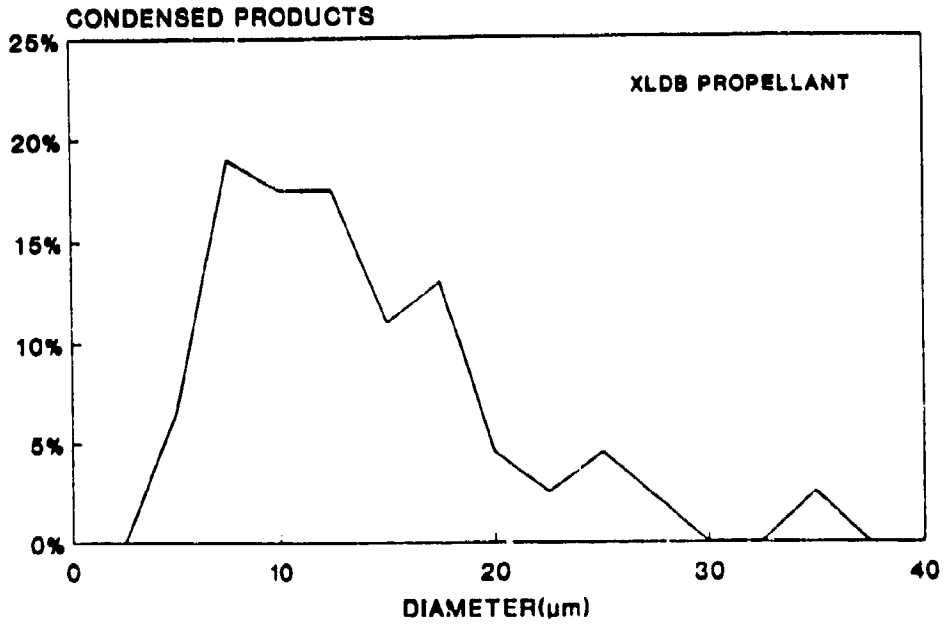

Fig. 3-2 Particle Size Distribution of the Condensed Products Collected in a Rocket Exhaust Plume. Analysed by an Electron Microscope with X-rays Diffraction System. (SNPE)

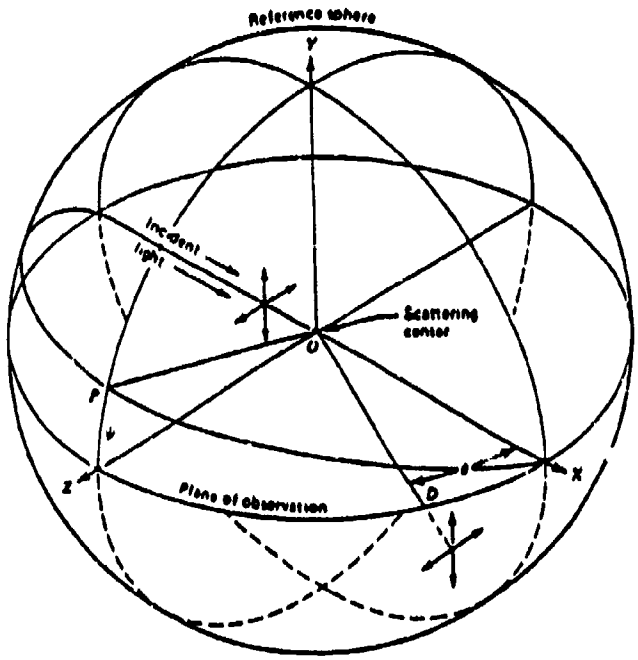

Fig. 3-3 **Geometry of Mie Scattering.** The two vectors correspond to incident unpolarized light. Line OD is the direction of observation and θ is the angle of observation. When the incident light is polarized, its electric vector is assumed to lie in plane POX, at angle ψ to the plane of observation [5]

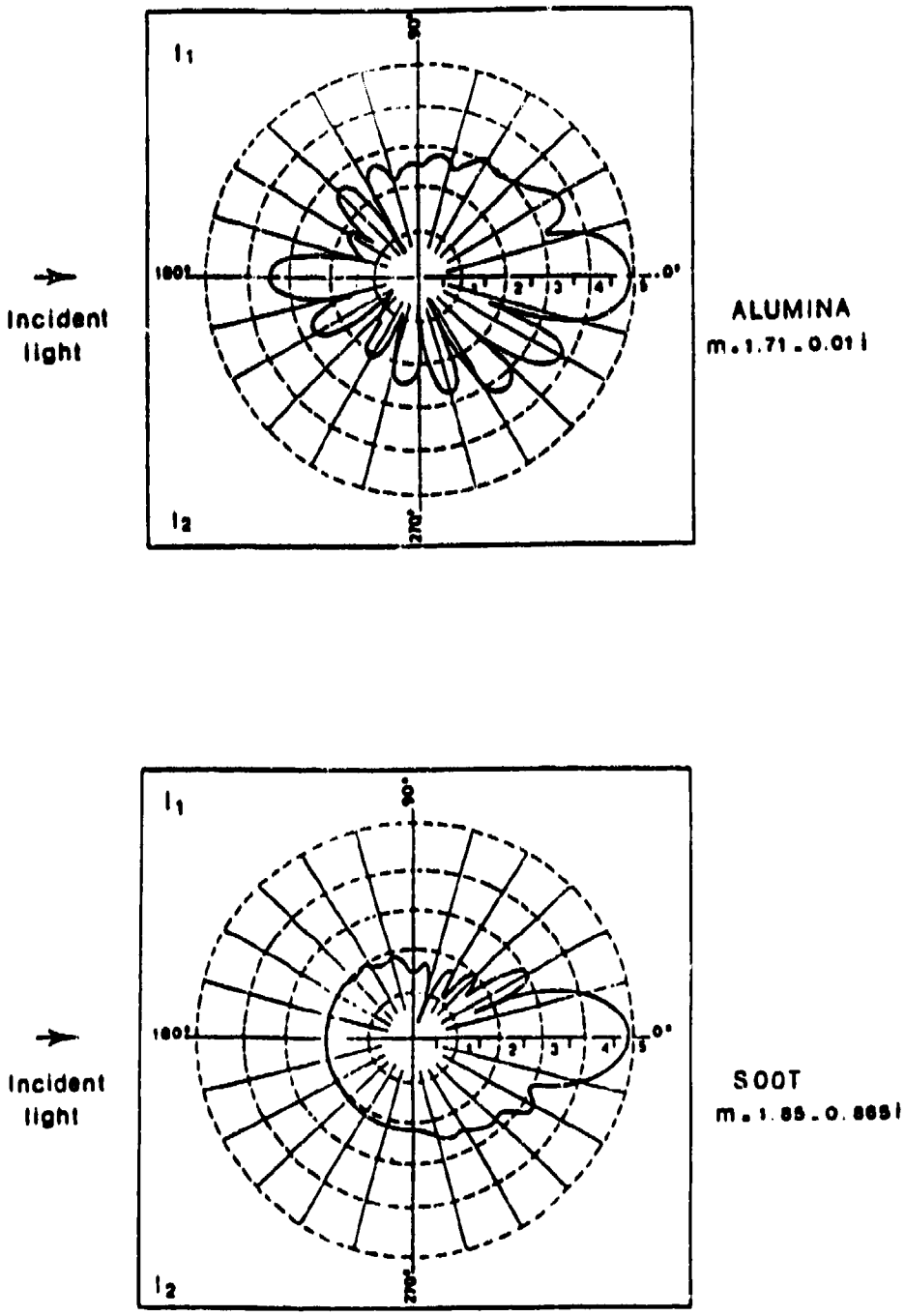

Fig. 3-4 Variations of log I_1 and log I_2 Versus θ for Particles of Al_2O_3 and C (Soot) when $\psi = 45°$ ($i_1 = i_2$ for $\theta = 0$), r = 1μm and λ = 0.7μm [5]

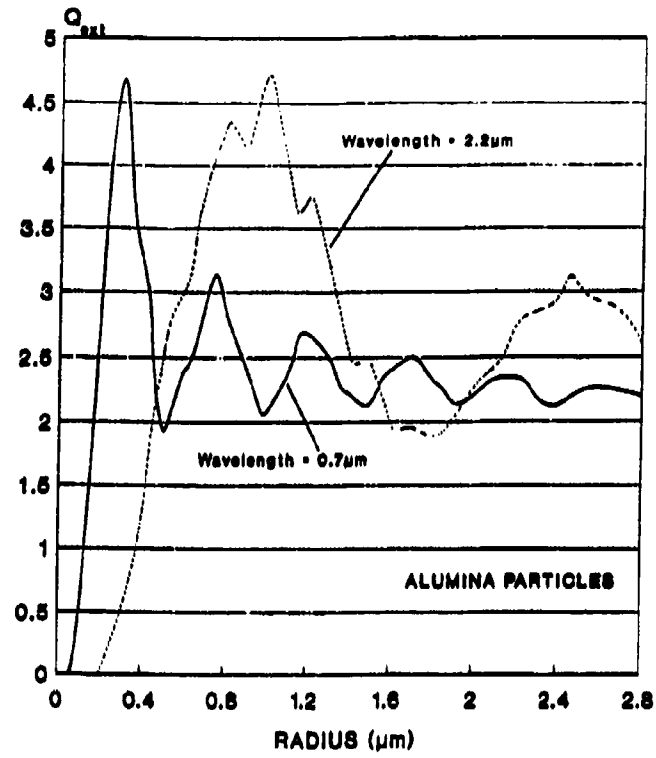

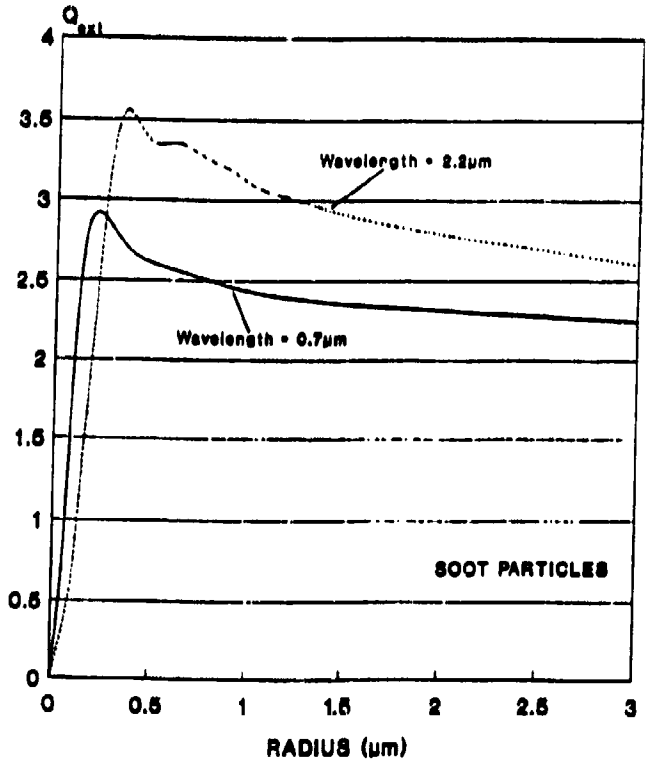

Fig. 3-5 Typical Variations of Q_{ext}

(a) Alumina particles
(b) Soot particles

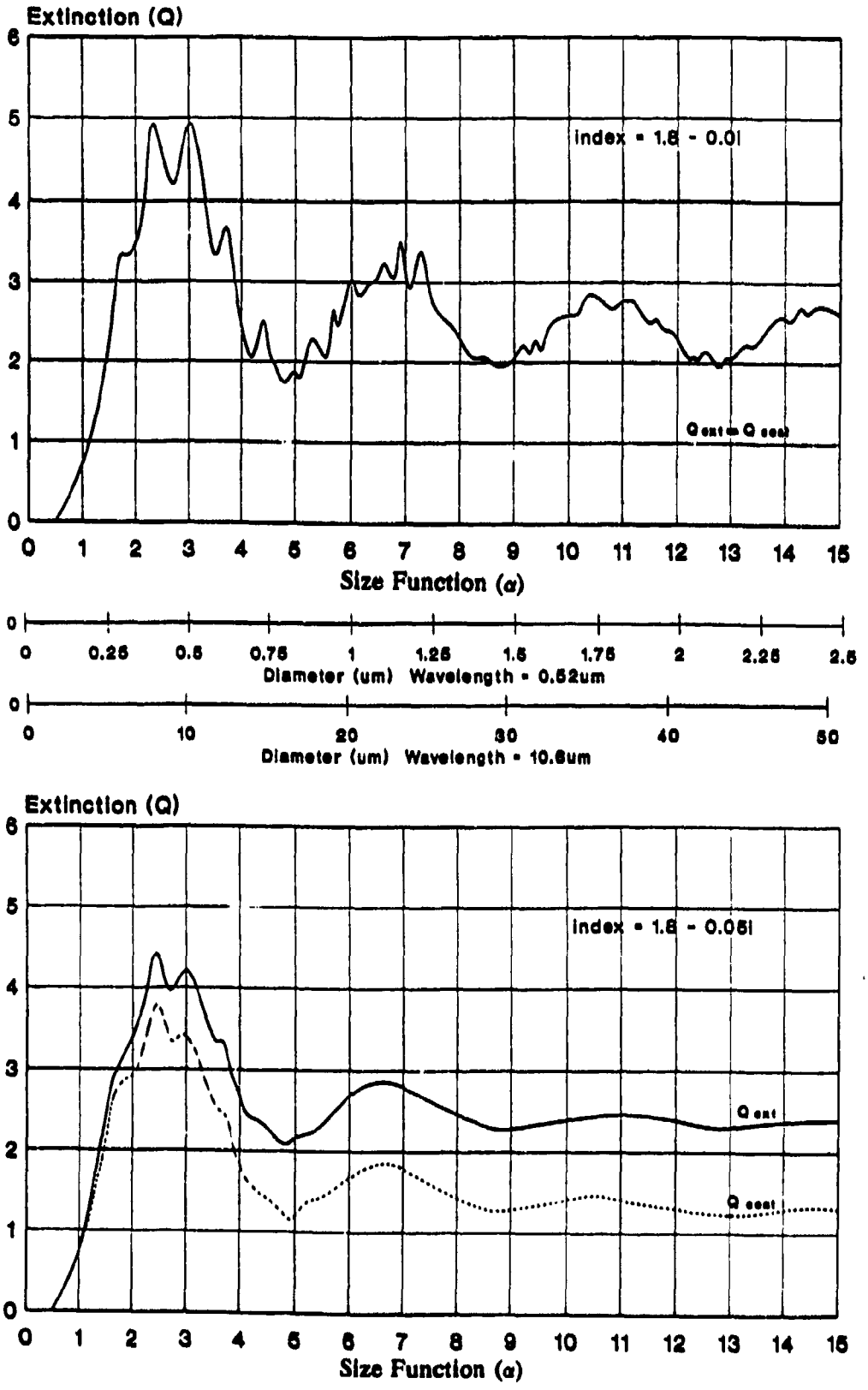

Fig. 3-3c Example of the Influence of the Imaginary Part of the Index on the Scattering and Extinction Coefficients. Size Function $\alpha = \pi D/\lambda$ (UK Royal Ordnance)

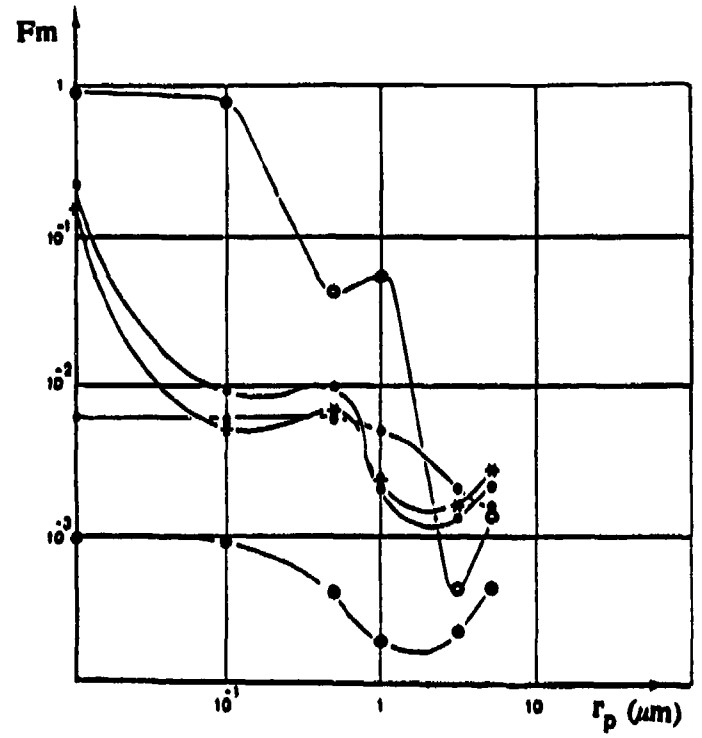

Smoke Cloud Diameter = 1m
Dilution = 5×10^{-2}
λ = 10.6μm
T = 95%

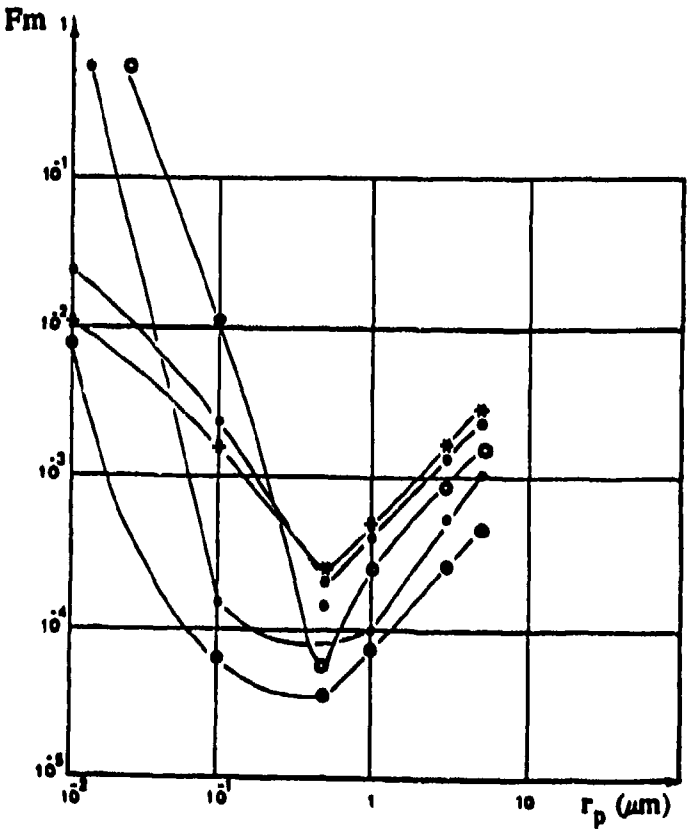

* Pb
* Cu
* Al_2O_3
O ZrO2
● C

Smoke Cloud Diameter = 1m
Dilution = 5×10^{-2}
λ = 2.2μm
T = 95%

Fig. 3-6 Mass Fraction (Fm) of Particle Inducing a Transmission Factor of 95% across a given Particle Cloud Versus the Particle Size

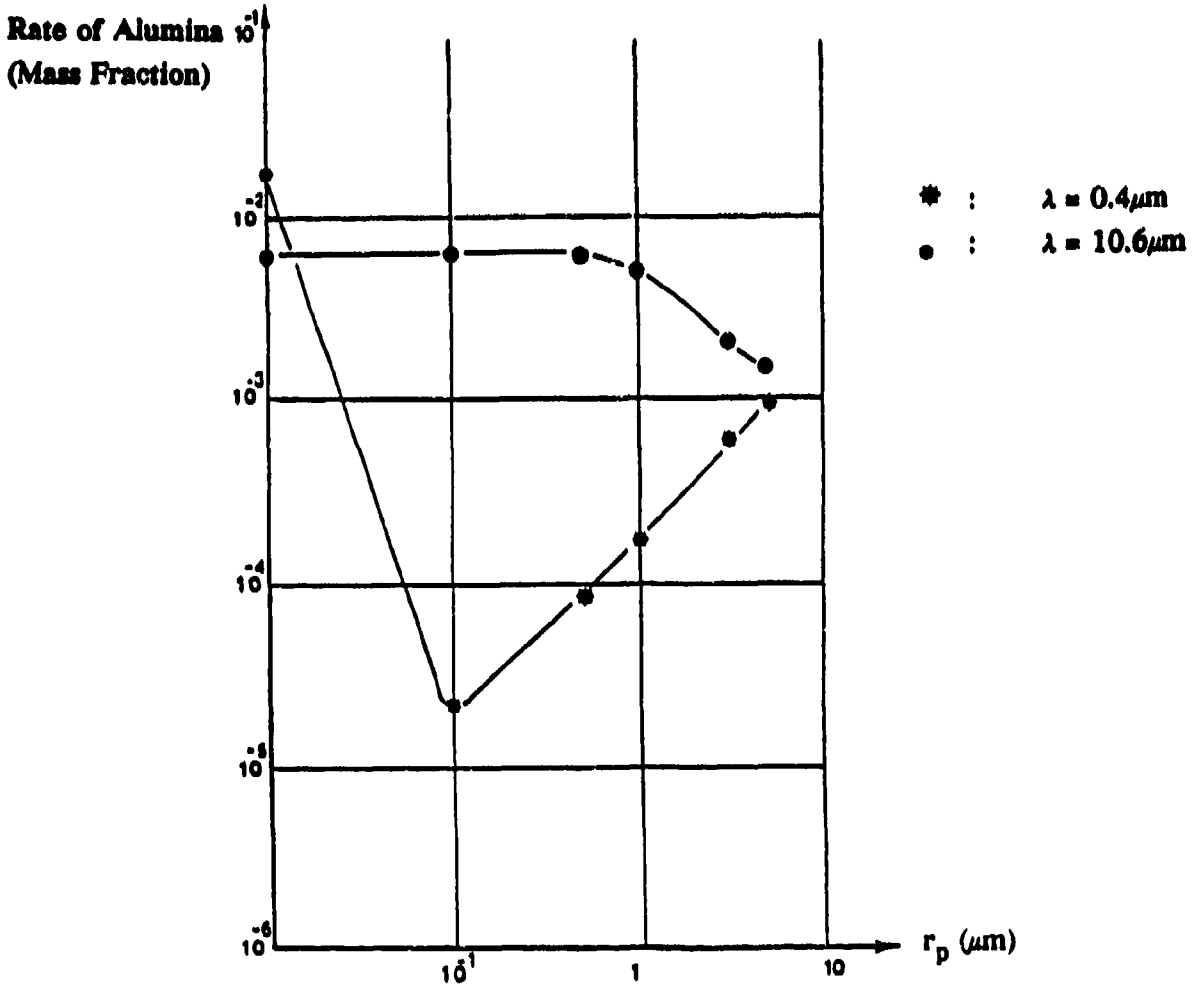

Fig. 3-7 Maximum Rate of Alumina (Mass Fraction) in Combustion Products for the Following Specification :

Smoke Cloud Diameter	:	1m
Dilution	:	0.05
Transmission	:	95%

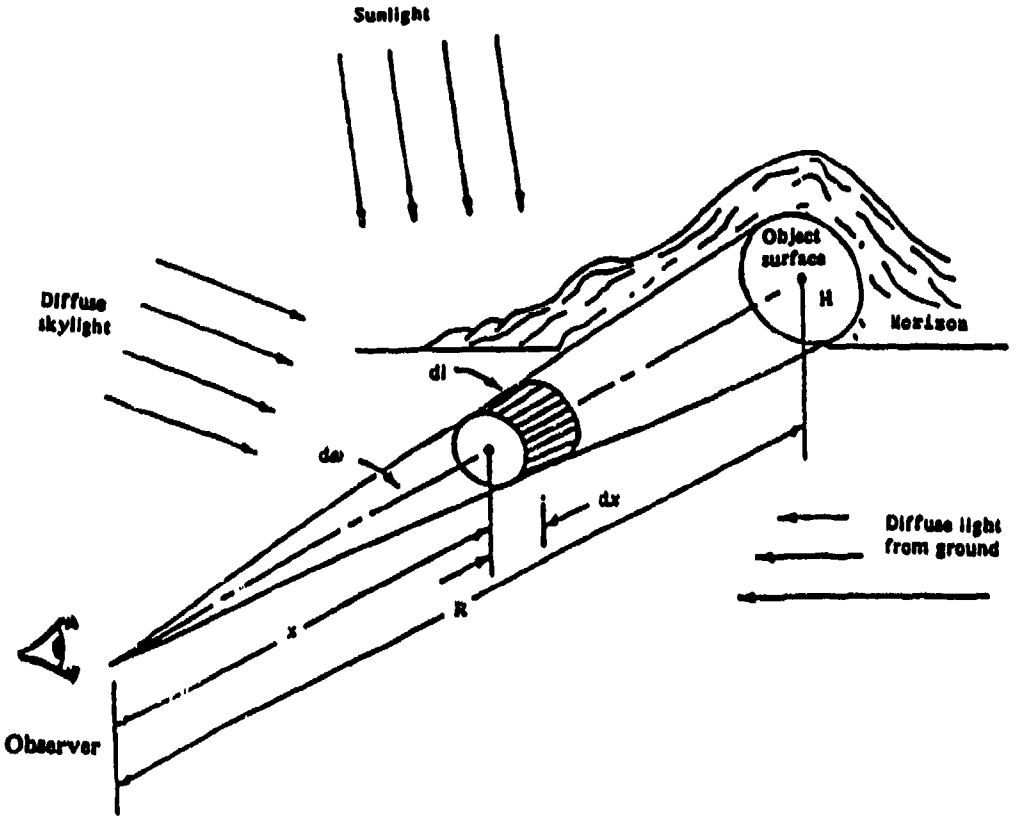

Fig. 3-8 Source of Air Light Between the Observer and an Object, and Apparent Luminance of an Object due to the Airlight [8]

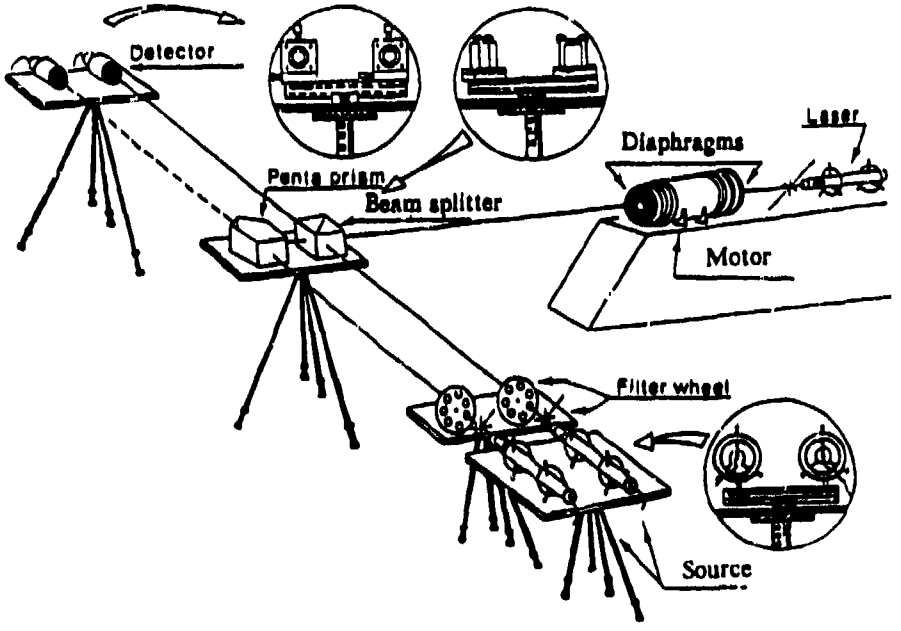

Fig. 3-9 Transmissometer at 0.6 μm

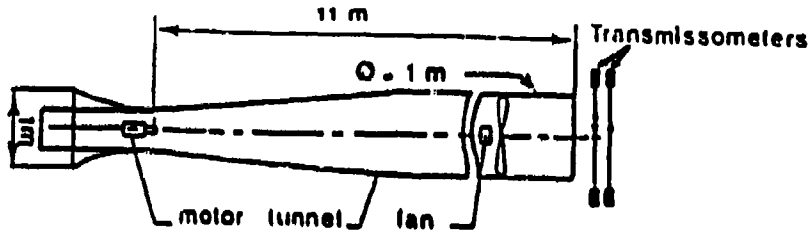

Fig. 3-10 "Fumimetre"

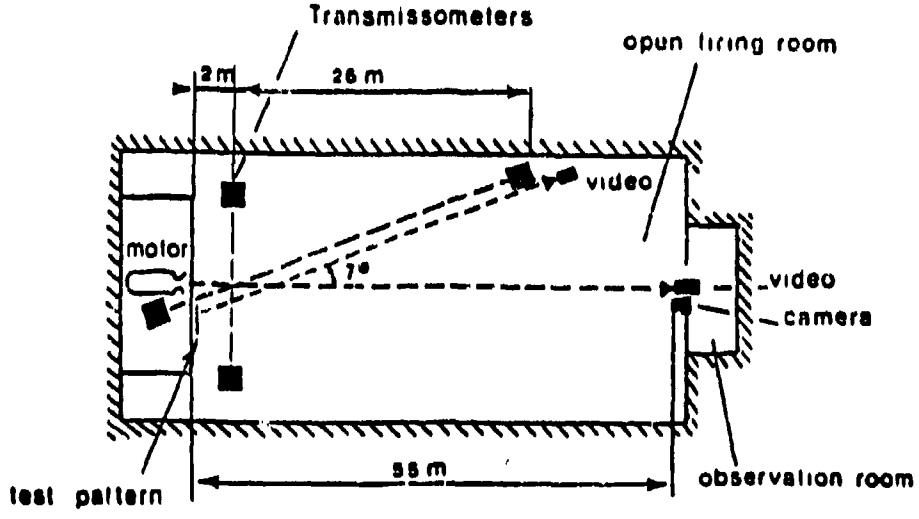

Fig. 3-11 "Banc Opacimetrique"

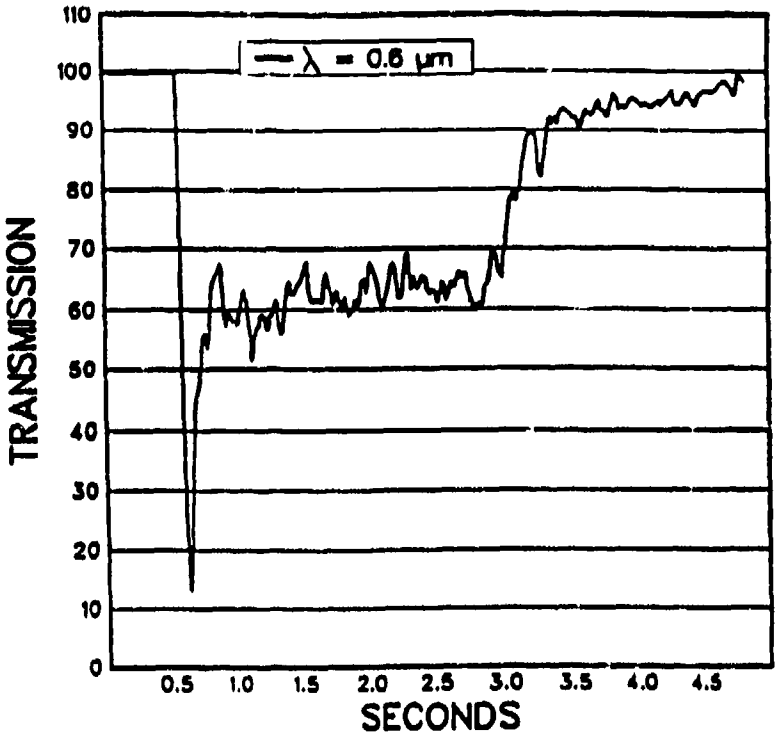

Fig. 3-12 Example of Transmission plot (λ = 0.63μm) Freejet Firing, Transverse Measurement

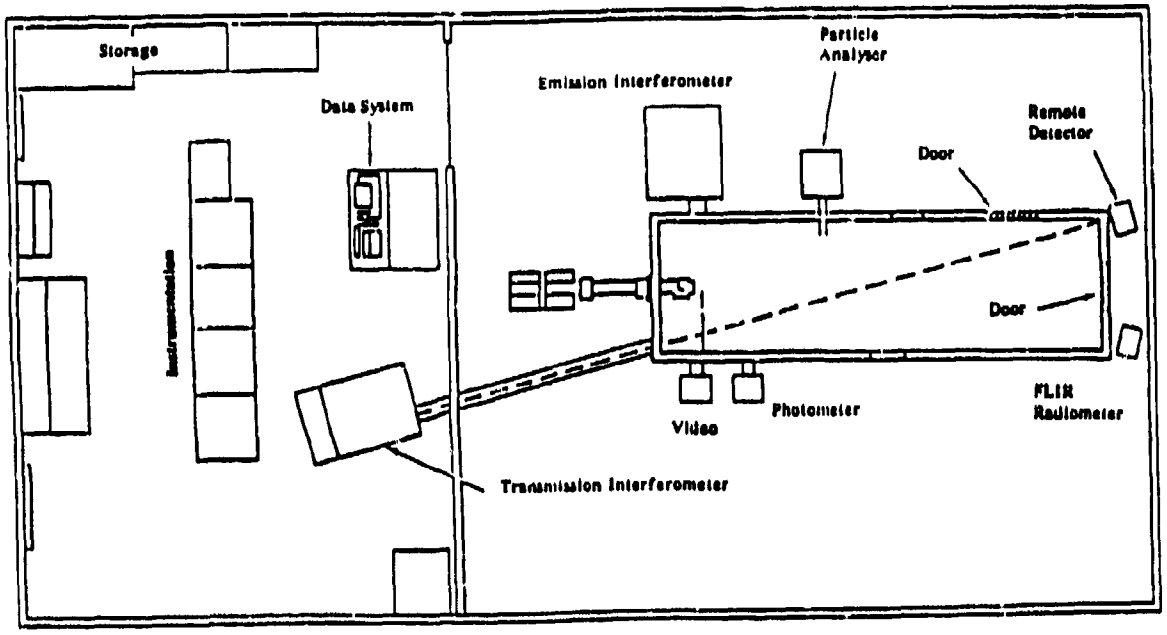

Fig. 3-13 US Army Signature Characterisation Facility

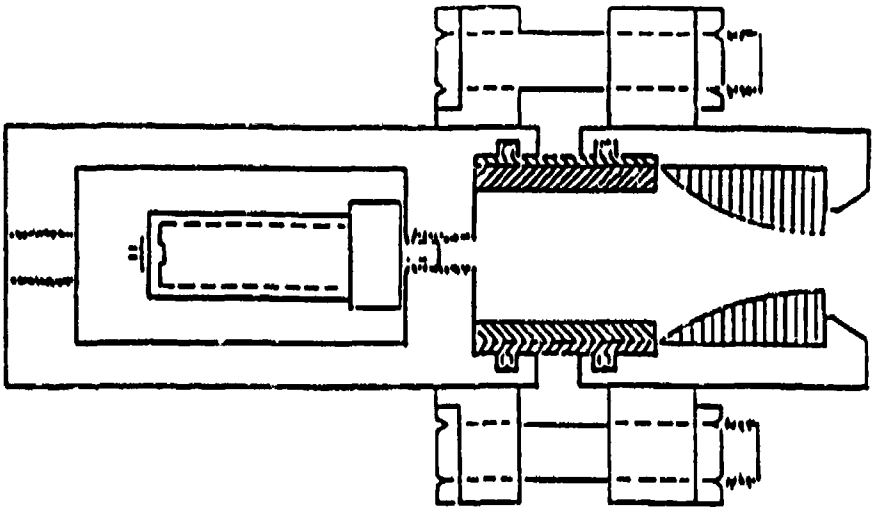

Fig. 3-14 SCF Test Motor

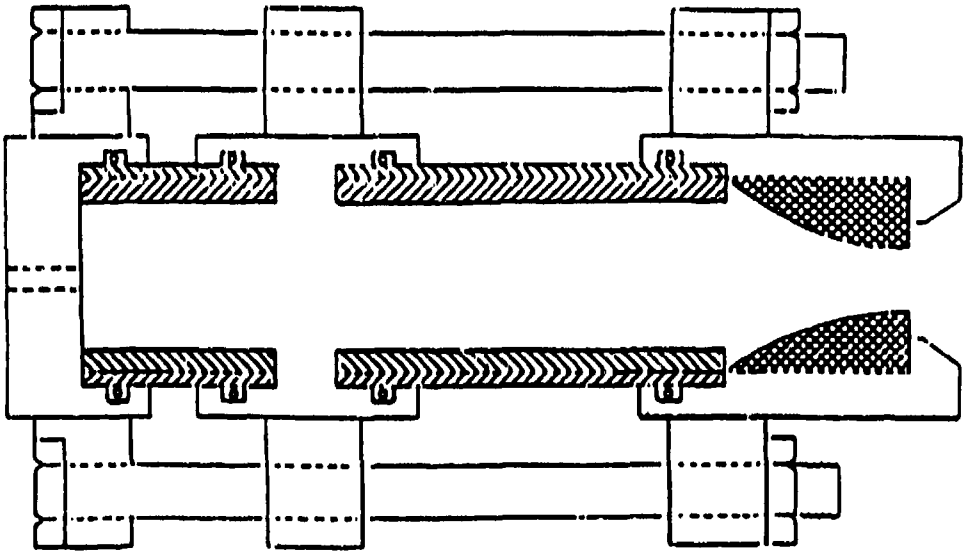

Fig. 3-15 Insulation Test Motor

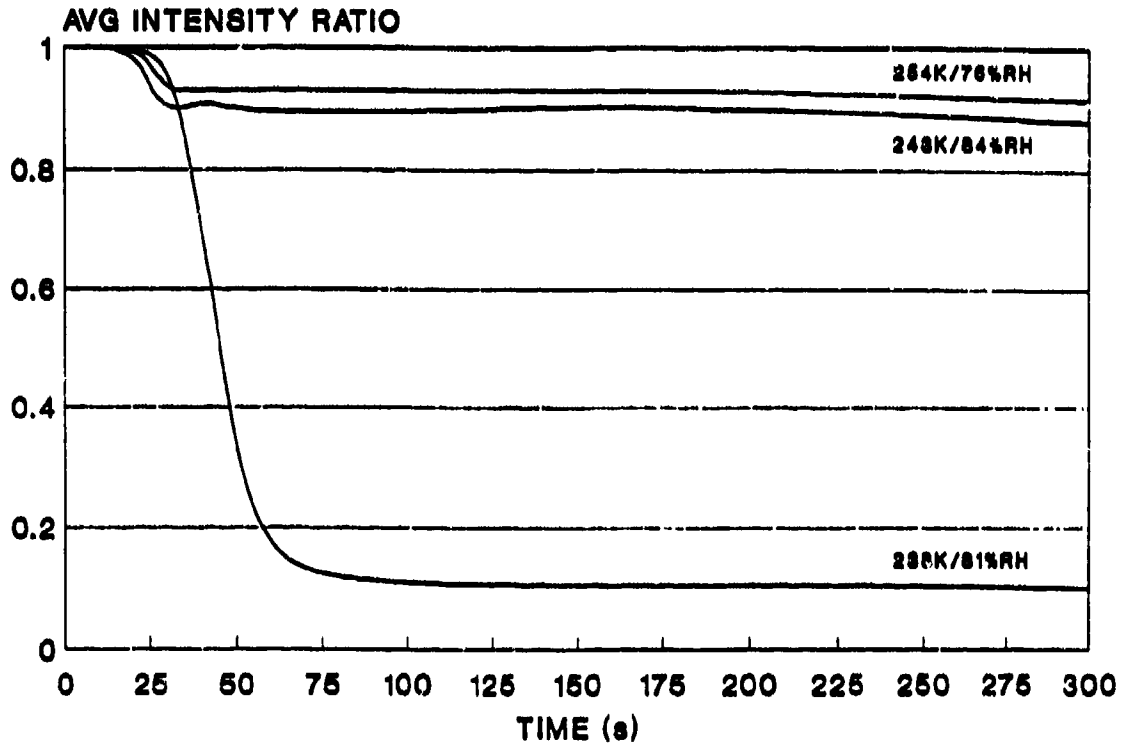

Fig. 3-16 FZZ Visible Transmittance

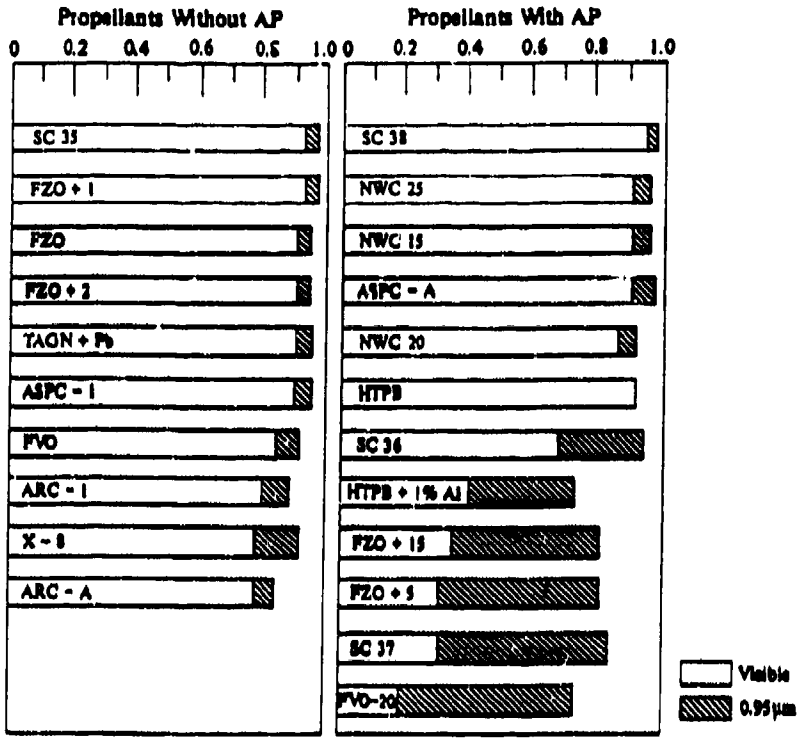

Fig. 3-17 Transmittance at 294K (21°C) and 60% H.R.

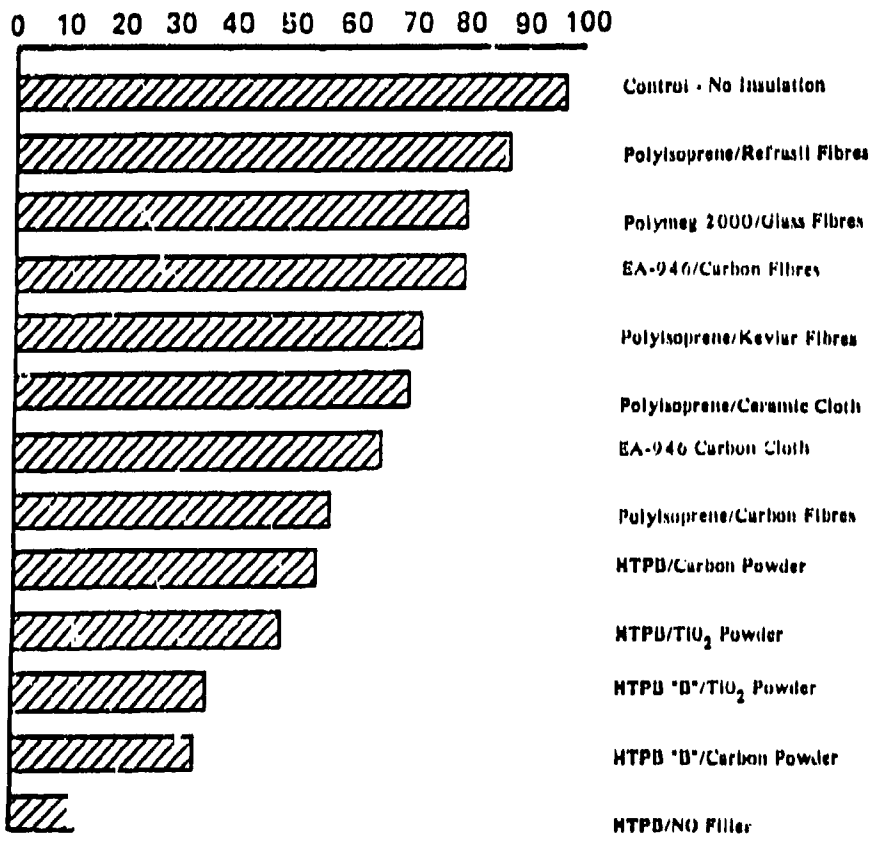

Fig. 3-18 SCF Photopic Transmission of Thiokol Insulated TP-7023 Motors

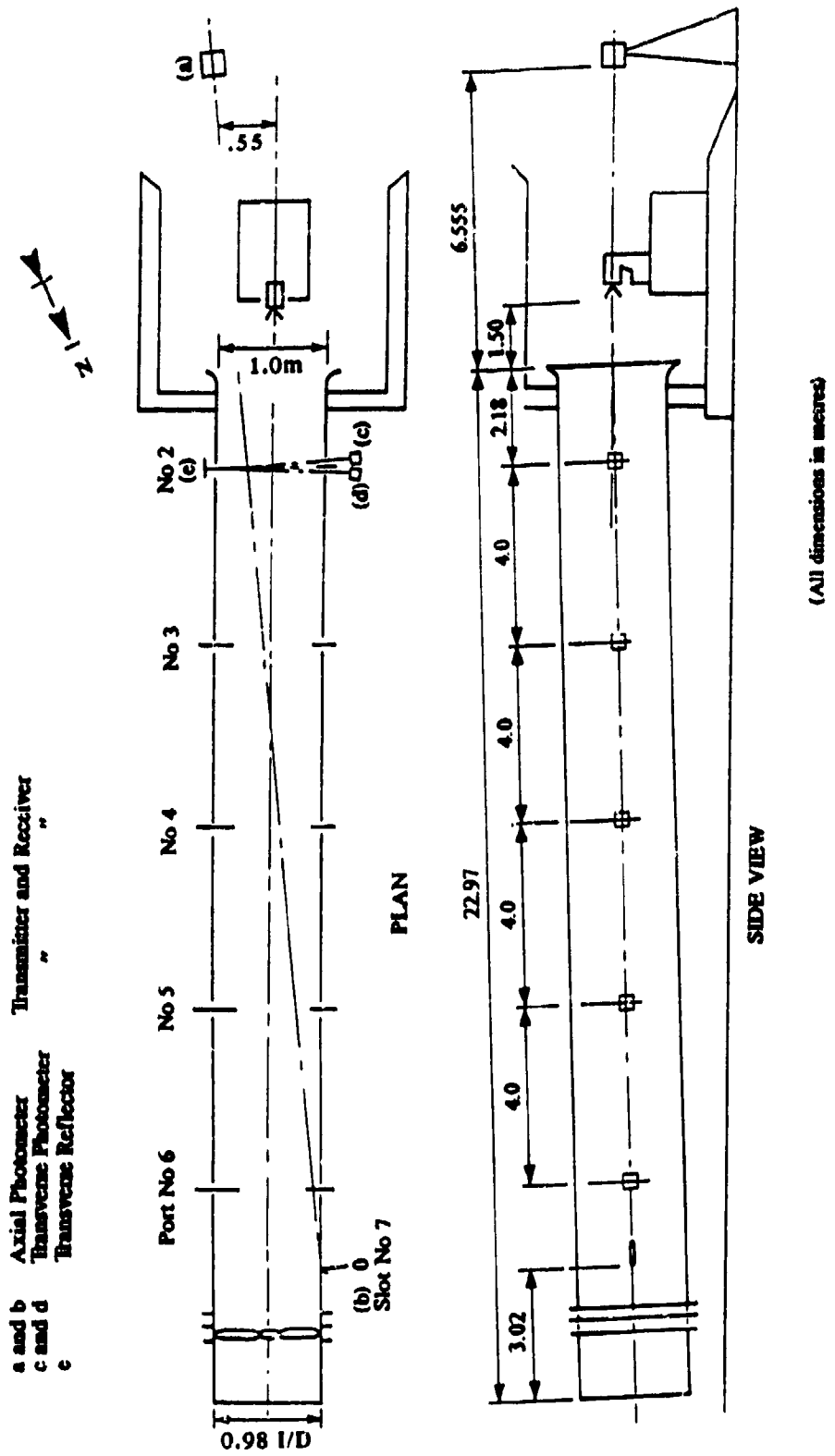

Fig 3-19 UK (RO) R7 Smoke Tunnel

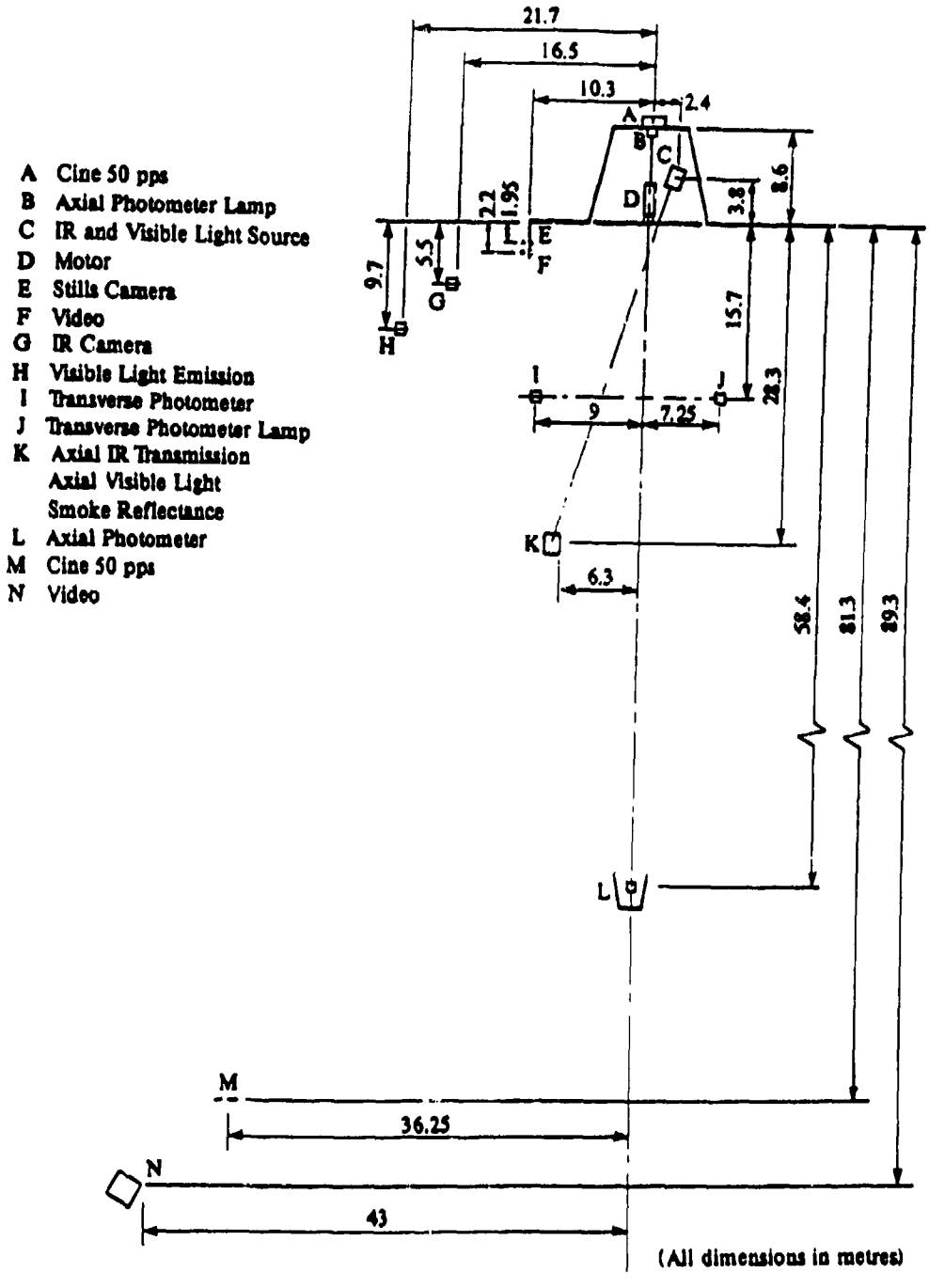

Fig. 3-20 Plume Instrumentation Wyre Forest

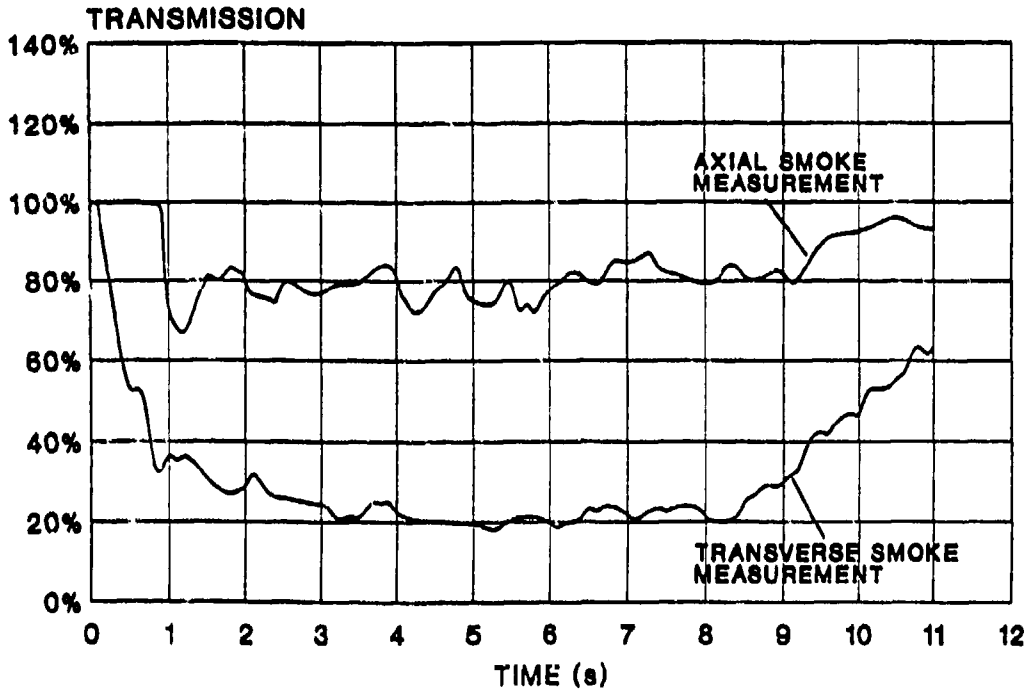

Fig. 3-21 Typical Results for Transverse and Axial Transmission (UK (RO) Smoke Tunnel)

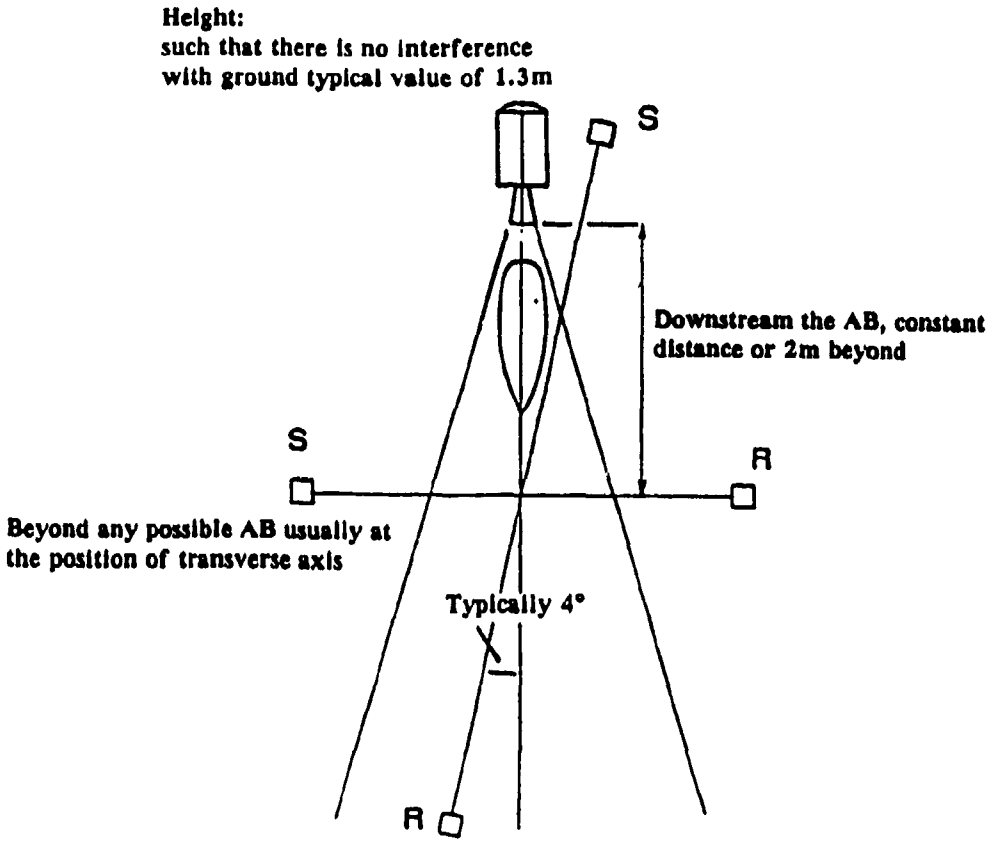

S : 0.63μm laser or a quartz halogen lamp (avoids a precise alignment and vibrational disturbances) chopped source

R : Suitable receiver, narrow f.o.v. (few degrees), few centimetres aperture area

Fig. 3-22 Procedure for Transmission in Free Jet

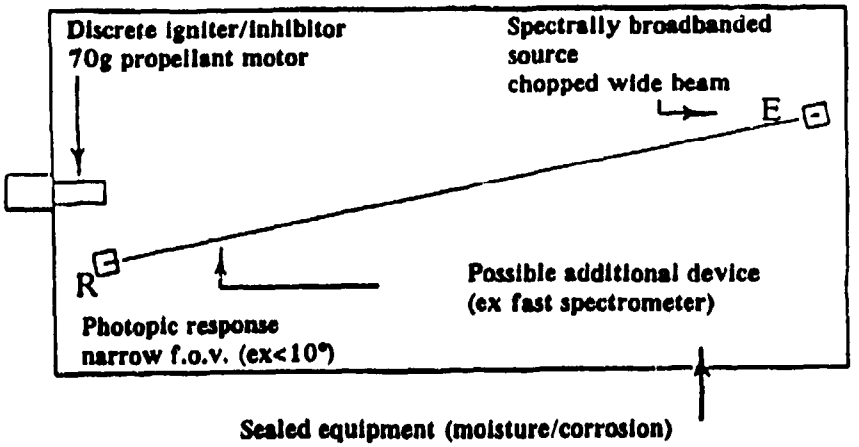

Chamber Volume 5.96*1.58*2.08 m^3
Air Controlled (Absence of Secondary Smoke)
Gases/Air Mixing Device (Ration 1/380)

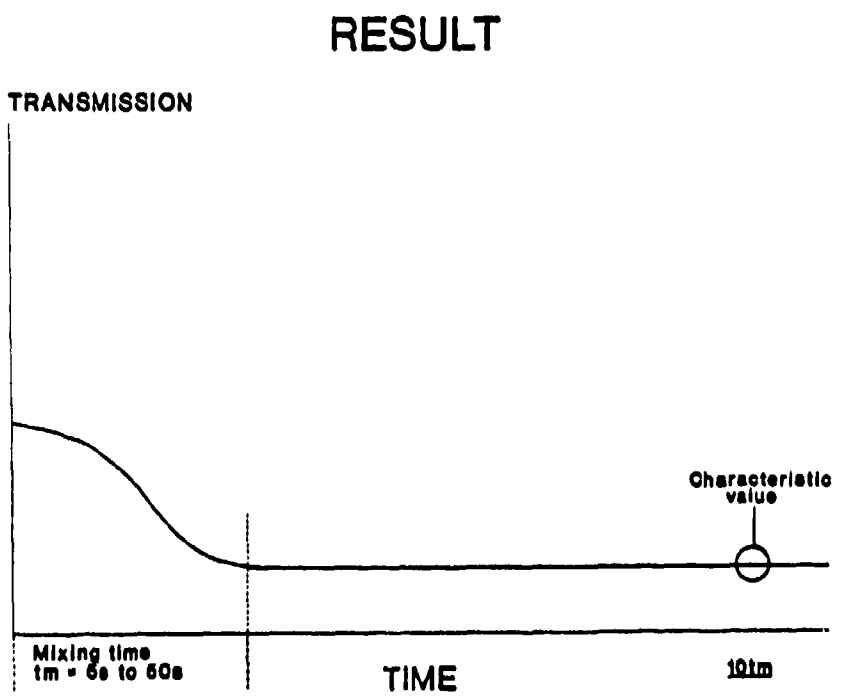

Fig.3-23 Procedure for Transmission in a Closed Chamber

CHAPTER 4

Plume Secondary Smoke

CHAPTER 4

Plume Secondary Smoke

TABLE OF CONTENTS

1.0 INTRODUCTION

1.1 Description of Secondary Smoke

Secondary smoke from rocket motors is formed as a result of interactions between the exhaust plume and the atmosphere. It typically forms after a delay of several seconds, during which the rocket motor exhaust mixes with the atmosphere. In this respect it differs fundamentally from primary smoke, which is the result of solid particles in the motor exhaust and is independent of ambient conditions.

Secondary smoke forms only in regions of the exhaust plume where the local vapour pressure of the condensable species (usually water, water and HCl, or water and some soluble salts) exceeds their saturation vapour pressure at the local temperature and pressure for the sizes of condensation nuclei present. Condensation nuclei are just primary smoke particles. Condensation will start preferentially at lower vapour pressures on larger particles and condense on smaller particles only as the vapour pressure reaches the saturation vapour pressure for the smaller size. Condensation will also start preferentially at lower vapour pressures on particles that contain soluble salts (the thermodynamics of solution are important here).

Secondary smoke is comprised all or predominantly of water droplets. From exhaust plumes that contain HCl and/or HF it will start to form at higher temperatures and lower ambient moisture levels than for plumes without the acid vapours. The optical properties of the acid-containing droplets will be somewhat different from those of pure-water droplets. Generally the effect of the particulate condensation nucleus is neglected in the calculation of droplet optical properties. At any given atmospheric conditions, secondary smoke will be thicker (larger, and perhaps more, droplets) in the presence of acid vapours than in their absence.

Exhaust plume afterburning affects the formation of secondary smoke in two ways :-

(i) Afterburning causes the formation of additional water in the plume, this tends to enhance subsequent condensation and the formation of secondary smoke.

(ii) Afterburning, by adding more heat to the plume, delays condensation to locations further downstream and, in marginal situations, may prevent condensation altogether.

Because mixing and chemical reactions do not scale with plume size and missile velocity in the same way, afterburning may be significantly different for exhaust plumes of the same propellant fired under different conditions of these variables. Therefore one must be careful when extrapolating the results of condensation measurements on small motors, fired statically, to flight conditions, even for a phenomenon as apparently simple and straight forward as secondary smoke formation.

Secondary smoke can form in plumes containing significant amounts of primary smoke. When this occurs, the total effect on visibility and obscuration is roughly the sum of the individual effects until the optical density (optical depth) exceeds some value at which non-linear effects assume increasing importance. One caveat here, the larger primary smoke particles, which are optically more important, would be the first, theoretically, on which condensation starts; this could have a major effect on changes to plume visibility and obscuration, compared to the simple summation of primary and secondary smoke effects. However, the larger particles cool more slowly than the smaller ones, and therefore condensation may start on the smaller particles, in which case summation of the two effects is a reasonable approximation. With current exhaust plume computer programs that treat non-equilibrium two-phase flow, these tradeoffs can be calculated, albeit somewhat tediously because of the great lengths of plume involved.

1.2 Occurrence of Secondary Smoke

From the above description, it is clear that the probability of secondary smoke formation is a function of :-

(i) the amount and type of condensable species in the motor exhaust. This is fixed by the propellant composition.

(ii) the concentration, size and type of solid products in the motor exhaust. Although these are not an intrinsic source of secondary smoke, they provide condensation nuclei which have a profound influence upon the size distribution of the condensed phase and its rate of formation.

(iii) the atmospheric conditions, in particular relative humidity and ambient temperature. As will be appreciated from the description of secondary smoke formation, low temperatures and high relative humidity are conducive to the occurrence of smoke.

1.3 Operational Implications

The signature of any rocket motor should be minimized. Since secondary smoke typically does not form for several seconds, the operational implications are somewhat different from those associated with primary smoke. The rate of formation of secondary smoke is dependent upon the rate of exhaust mixing with the surrounding air. If a flight mission is of a duration less than a few seconds then the operational implications may be minimal unless a post-firing cloud enhances detection of the launch platform or impairs its operational effectiveness

The exhaust signature has potential effects upon the guidance system, detectability of the missile and launch platform, and (possibly) the efficiency of the launch platform. Dealing first with guidance considerations, secondary smoke clouds may severely degrade the effectiveness of any missile guidance system which necessitates transmission of visible, near-visible, or infrared radiation through the plume. Examples would be Command-to-line-of-sight (CLOS) optically guided missile or a laser beam-rider; a secondary smoke plume between launch site and missile would likely render the system incapable of effective operation. Even if the plume is not very dense its characteristics need to be known before an assessment can be made of its effect upon the guidance system. Calculation of these effects is complex and involves accurate modelling of the smoke trail both spatially and in time (accounting for climatic conditions and the missile trajectory in typical operational scenarios), with an output which can only be expressed as a probability of interference with the guidance system. The secondary smoke trail may also enhance detectability of the missile. Since a finite time is required before a secondary smoke cloud forms the detectability of a missile with a short flight time will not be increased. However, for longer flight times, for example, long range and/or low velocity applications, the detection of a secondary smoke cloud will alert operators to the fact that a missile has been launched and will provide a rough indication of its position. This knowledge may allow effective countermeasures. The same smoke cloud effectively pinpoints the launch site which, if static or slow-moving, is operationally undesirable. Detectability is usually framed in the context of the human eye, however, the increasing use of electro-optical detectors operating in the infrared and visible ranges required consideration of the response characteristics of the detector.

The effect of secondary smoke upon the effectiveness of a stationary or slow-moving launch platform is a matter of considerable importance. For missile systems where the command or tracking signals may be attenuated by the smoke, a second shot may have to be delayed until the cloud from the first missile has dissipated. Even if the missile system is not affected, obscuration of the launch platform by the smoke cloud generated by the missile will likely degrade the performance of optical or infrared sensors which may be mounted on the launch platform. This is likely to be of particular importance in a severe Electronic Countermeasure (ECM) environment where radar performance may be marginal. Full characterization of the plume is necessary before the importance of this effect can be quantitatively addressed.

Currently, user requirements are usually qualitative in nature, often amounting to simply specifying, usually very imprecisely, the type of propellant. The specification of meaningful requirements is crucially important, both from the point of view of the system designer, and to serve as a guide to experimental characterization and analytical prediction of the motor signature.

Operational implications are more fully explored in the overview of this report, and the reader is referred to that section for an in-depth discussion.

2.0 METHODS OF ASSESSMENT

2.1 Experimental Data on Secondary Smoke

2.1.1 General

The generation of experimental data is difficult because secondary smoke results from the interaction between the rocket motor exhaust and the atmosphere. The necessary inclusion of atmospheric effects increases the physical scale of any experimental work. To date, experimental data has been generated by three methods :-

(i) Motor firings in test chambers. The environment (temperature and relative humidity) within the chamber

can be measured accurately, and it is possible to characterize the motor signature through transmission measurements at various wavelengths.

(ii) Free jet tests, or static firings. Observations are predominantly visual, although the static nature of the test allows measurement of transmissibility.

(iii) Free flight tests, where observations are recorded of the signature of the motor in the operational environment. To date, such observations are predominantly "eyeball" records of smoke/no-smoke. Of necessity, the ambient environment cannot be closely defined.

2.1.2 Test Chamber Facilities

One facility is currently in use for studies on secondary smoke; the US Army SCF (Signature Characterization Facility). In France, the climatic chamber at ETBS, Bourges has been occasionally used. The characteristics of these two chambers are provided in Table 4.1 below.

2.1.3 Free Jet/Flight Test Facilities

In general, any regular static test facility or free-flight range can be used for secondary smoke measurement. It is necessary only to install instrumentation e.g. cameras, transmissometers, capable of making measurements on secondary smoke generation.

Free Jet/Flight Test Facilities have many measurement problems because of the nature of the test. Outdoor firings are subject to wind and terrain effects that introduce variable error into the results. Flight measurements have the additional uncertainty of the missile trajectory and orientation with respect to the measurement position.

2.1.4 Results of Experimental Studies

A sample of the available experimental data is given in Section 2.3 which compares experimental and theoretical results.

TABLE 4.1

TEST CHAMBER CHARACTERISTICS

Chamber		SCF	ETBS
Volume	(m^3)	19.6	600
Temperature Control		Yes	Yes
Humidity Control		Yes	Yes
Altitude Control		No	No
Motor Propellant Weight (gm)		67	
Common Instrumentation			
- Transmissonmeters		Yes	Yes
- Particle size/number		Yes	No
- Condensate mass		Yes	No
- Cameras		Yes	Yes

The instrumentation can readily be varied, and therefore specific details are not given in Table 4.1.

2.2 Predictive Methods

In the modelling of secondary smoke effects it is necessary to consider three primary aspects :-

(i) the species content and concentration of the exhaust at the nozzle exit. This is usually acquired through the use of the well known thermoequilibrium codes (eg the NASA/LEWIS code) and will not be considered further,

(ii) the formation of secondary smoke, which requires modelling the mixing of the exhaust with the atmosphere, and the mechanisms of droplet formation, and

(iii) the visibility of the resultant exhaust signature. This requires consideration of visual acuity, and of the background and lighting conditions.

2.2.1 Prediction of Secondary Smoke Formation/Visibility

2.2.1.1 Thermodynamics of Liquid/Vapour Equilibrium of Solutions

A variety of references are available for the thermodynamics of the water/hydrogen chloride and water/hydrogen fluoride/hydrogen chloride systems. Those in use in various NATO countries are given in Table 4.2, together with the techniques used to extrapolate beyond the temperature range of the references. Use of data for water/soluble salt systems is less common, but Reference 10 provides an illustration of the water/sodium chloride/hydrogen chloride system.

2.2.1.2 Methods of Predicting Secondary Smoke Formation

Modelling of secondary smoke formation requires prediction of the motor exhaust plume and the mixing with ambient air. Thermodynamic data per Section 2.2.1.1 and models for droplet growth are then used to determine the probability of condensation [10]. Accurate prediction of plume visibility or transmissivity requires knowledge of the size distribution and number density of the droplets. This necessitates prediction of the size distribution and number density of the condensation nuclei. Various techniques are used in different NATO countries to predict secondary smoke; these are given in Table 4.3.

TABLE 4.2

HCl/H_2O AND HF/H_2O LIQUID/VAPOUR EQUILIBRIUM

	Country	France	UK	USA (Army)	USA (Navy)	USA (AF)
1	**H_2O/HCl System**					
1.1	References	1	2,3,4,5	1,6,7	6,7,8	6,7
1.2	Temperature Range (K)	273-373	233-333	233-373	233-293	233-n.a
1.3	Extrapolation					
	Method	Under Study	Extrapolation	Graphical from smoothed data	Curve-fit technique	Graphical from smoothed data
	Temperature Limit (K)	n.a.	<233	218	n.a.	n.a
2	**H_2O/HF System**					
2.1	References	Note 1	Note 1	9	8	Note 2
2.2	Temperature Range (K)	-	-	-	258-293	-
	Method	-	-	-	n.a.	-
	Temperature Limit (K)	-	-	-	n.a.	-

Notes: 1 No work to date
2 References are not available

TABLE 4.3

PREDICTIVE METHODS FOR SECONDARY SMOKE

	Country	France	UK	USA (Army)	USA (Navy)	USA (AF)
1	Plume					
	- Computer code	AJAX, PLUME	REF	LAPP, SPF	SPF	SPF
	- Afterburning	Yes	Yes	Yes	Yes	Yes
	- Conservation of enthalpy	Yes	Yes	Yes	Yes	Yes
2	Mixing of Exhaust Products with Air					
	- Computer code	Note 1	No	Note 2	Note 6	n.a.
3	Secondary Smoke Formation					
	- Computer code	FUMAS + GOUTTE	SECSMOKE	DROP	Ref 10	n.a.
	- Condensation nuclei	Input variable	No	Yes	Yes	Yes
	- Droplet growth kinetics	Yes	No	Yes	Yes	Yes
4	Plume Opacity					
	- Computer code	No	No	OSA IFTA[5]	Note 3	Note 4

Notes: 1 A simplified analysis (similar to the Oliver Smoke Profile Program), assuming isenthalpic mixing, determines if smoke can form. Afterburning and the presence of condensation nuclei are not considered.

2 Oliver Smoke Profile Program

3 Computer Code not available, calculations are performed manually

4 Radiative transfer calculations

5 For light transmission through the plume under flight conditions

6 SPF in near field, Refs 14 and 19 in far field

2.2.1.3 Climatic Data Base

The prediction of secondary smoke formation per the methods of Section 2.2.1.2 requires input of the atmospheric conditions in terms of temperature, relative humidity, and pressure. For use in operational scenarios it is necessary to employ a climatic data base covering the range of environments which can be expected. At this time, different nations use different data bases, as shown in Table 4.4.

2.2.1.4 Methods of Predicting Plume Visibility

The prediction of plume visibility is difficult because of the extreme range of variables which must be considered. Table 4.5 presents an overview of the state of visibility prediction.

TABLE 4.4

CLIMATIC DATA BASES

Country	Data Base
France	Statistical climatic data bases are used according to the customer's requirements.
UK	A statistical data base is used.
USA - Army	Data is available from the US Army statistical climatic data library.
USA - Navy	Ref 12 for 40° and 50° North Latitude.
USA - Air Force	Statistical climatic data is generated using the Nichols Research ALMPDS code.

TABLE 4.5

PREDICTION OF PLUME VISIBILITY

Country	Method of Prediction
France	Panache code is used to calculate the smoke cloud transmittance from any ground observation point. It is assumed that plume visibility can be correlated with the transmittance for each line of sight
UK	Basic studies only per Ref 13. Typically, clouds are expected to be visible if the smoke concentration exceeds 2×10^{15} molecules/ml for tactical missiles in clear weather. Calculations of the visible contrast of the plume have been made using the CONTRAIL computer code.
USA - Army	MPLUME visibility code exists for specific systems.
USA - Navy	Plume visibility is studied using the method of Ref 14. This analysis includes the effects of plume dimensions, particle sizes, scattering of incident light, a visibility model and visibility criteria.
USA -Air Force	Plume visibility is studied by means of detailed radiative transfer calculations [15].
USA - Commercial	VISIG (Visual Signature) code for calculation of plume visibility [16]. Available through E Miller, USA, Tel (702) 831-0429 but is not considered to be thoroughly validated at this time.

2.2.1.5 Summary of Secondary Smoke Predictions

2.2.1.5.1 Smoke/No-Smoke Limits

The results of the varied prediction methods are most easily presented as plots of the temperature/relative humidity boundaries at which secondary smoke will form. An example is given in Figure 4-1 for sea level conditions, which shows :-

(i) The standard Oliver Curves commonly used in NATO for predicting the occurrence of secondary smoke.

(ii) A boundary curve for non-aluminised, AP composite propellant [17].

(iii) Two data points for 80% • ammonium perchlorate non-aluminised propellant [18].

The general trends of the three prediction methods are similar, however, temperature differences of up to 10K are apparent at a fixed value of relative humidity. The differences may be due to differing assumptions regarding propellant composition, nuclei size and mass density, the ratio of air to exhaust mass in the cloud, or the gas temperature at the point where condensation is occuring.

Figure 4-2 provides predictions for smoke formation from a non-aluminised, AP composite propellant as a function of altitude. Figure 4.3 illustrates smoke formation at an altitude of 8.23 km as a function of the amont of ammonium perchlorate and FEFO [(bis (Fluorodinitroethyl) formal)] in the propellant.

The reader is cautioned that the boundaries (Figs 4-1 to 4-3) should not be directly compared with those used as a basis for propellant classification in Chapter 2. The latter are computed at arbitrary values of temperature and dilution ratio and are intended to provide a simple method of classifying propellants, not to predict whether or not secondary smoke will form.

2.2.1.5.2 Other Predictive Aspects

The most sophisticated analytical codes produce data such as :-

(i) plume contours and temperature isotherms,
(ii) droplet size distribution as a function of time and spatial location,
(iii) attenuation of light passing through the plume, and
(iv) light scattering from the plume

The wealth of predictive data makes concise presentation of results impossible. Typical results are given in Figures 4-4 and 4-5. Figure 4-4 [19] provides predicted plume contours for a composite propellant containing 25% ammonium perchlorate. Figure 4-5 shows the dependence of the calculated transmission upon droplet radius, condensed mass, and particle number density [19].

2.3 Comparison of Experiment and Prediction

2.3.1 Qualitative Experimental Data

Motor open air static firings and flight tests usually produce qualitative data in the form of smoke/no-smoke observations. Atmospheric data is normally available, i.e. pressure, temperature, and relative humidity. These observations may then be compared with the theoretical predictions of the temperature/relative humidity boundaries beyond which secondary smoke forms. An example of this form of comparison is given in Figure 4.6 and Table 4.6 The predictions in both cases are from simple equilibrium models, and generally compare favourably with the experimental results. Additional data, including in-flight contrast measurements, are given in Reference 20.

TABLE 4.6

PREDICTED AND OBSERVED SECONDARY SMOKE FORMATION

Mission No and Firing No	Altitude (km)	Temperature (K)	Relative Humidity (%)	Smoke Formation Predicted	Smoke Formation Observed
M1 RS-1	8.23	243.6	51	Smoke	Smoke
M1 RS-2	7.26	251.9	37	No Smoke	Smoke
M2 RS-1	4.04	311.5	69	No Smoke	No Smoke
M3 RS-1	9.75	239.4	46	Smoke	Smoke
M3 RS-2	10.60	232.6	55	Smoke	Smoke
M4 RS-1	9.70	241.2	15	No Smoke	No Smoke
M5 RS-1	5.73	267.9	0	No Smoke	No Smoke
M5 RS-2	6.93	259.2	0	No Smoke	No Smoke

Note :-Data are from flight tests of Eglin AFB with a non-aluminised composite propellant containing ammonium perchlorate.

2.3.2 Quantitative Experimental Data

2.3.2.1 Test Chamber Results

Figures 4-7 and 4-8 compare calculated and measured light transmission across the chamber for small motors fired in the US Army SCF chamber (the SCF chamber, instrumentation and procedures are described in Chapter 3). Excellent agreement is obtained up to typically 150 seconds after the firing [19].

Table 4.7 provides limited data over a range of temperature and relative humidity for two different propellant formulations. Here the data is more qualitative, and the presence of smoke was determined from transmissometer measurements, cameras and visual observation. The experimental results are limited in precision, but do not disagree with the theoretical predictions [18].

TABLE 4.7

TEST CHAMBER RESULTS (Ref 18)

Propellant	Temperature (K)	Relative Humidity (RH) for Smoke Formation (%) Predicted	Observed
Composite reduced 80% AP	276.2	Smoke at RH>60	None at RH<59 Smoke at RH>65
	288.2	Smoke at RH>76	None at RH<63 Smoke at RH>76
Cross-linked 20% AP	276.2	Smoke at RH>74	None at RH<65 Smoke at RH>77

2.3.2.2 Flight Test Data

Limited experimental data are available from flight tests for the transmission of a 0.63μm laser beam through a missile flight plume. Figures 4-9 and 4-10 show these data, and compare them with theoretical predictions from the US Army IFTA code [21]. The transmission measurements were taken approximately perpendicular to the missile trajectory, and about 17m downrange. The agreement between theory and experiment is only fair and illustrates the dependency of the calculation on the beam position in the plume. The uncertainty of the fixed beam with respect to the missile flight trajectory is always a factor.

3.0 RECOMMENDATIONS

3.1 General

The results of secondary smoke measurements or predictions are necessary for analysis of operational usage. It is considered that there are three dominant factors :-

(i) The visibility of the plume, which affects the probability of detection of the missile and/or the launch platform

(ii) Transmission of radiation through the plume, which may be a factor influencing the capability of passing guidance commands to the missile. For optically-guided missiles, obscuration of the missile by the plume will results in loss of guidance capability.

(iii) Scaling and afterburning effects, particularly between flight and static conditions. Plume scaling is required in going from measurements on small test motors to operational motors, and can be grossly misleading if not coupled with adequate predictive methods. Afterburning can have a significant effect upon the temperature profile of the plume and the amount of water in the plume. In operational use afterburning is a function of afterbody geometry, flight velocity and altitude, missile angle of attack and propellant composition (see Chapter 1). If it occurs in flight but not on static test motors then no amount of static testing will adequately characterize the operational signature.

3.2 Experimental Methods

3.2.1 Firings in Test Chambers

Firings in test chambers are necessarily confined to small motors because of facility cost constraints. The US Army's Signature Characterization Facility (SCF) is typical of the type of facility required. Details of the SCF and the procedures used are given in Chapter 3.

3.2.1.1 Usage

Firings of small test motors in test chambers are recommended to :-

(i) Determine the secondary smoke characteristics of specific propellant formulations. The data from test firings are frequently used as an input to analytical codes to improve the predictive ability of the codes. It is worth noting that simple measurement of the plume transmissibility does not provide a significant improvement in predictive capability when compared to simple thermodynamic codes such as those described in Section 3.3.2.1. The data is also useful when the available thermodynamic data may not be adequate, e.g. propellants with a high level of flame suppressants.

(ii) Provide detailed experimental data for validation of analytical codes.

3.2.1.2 Facility Characteristics

The characteristics of the test chamber should conform to the following recommendations :-

(i) The dilution ratio, or mass of air within the test chamber divided by the propellant consumed, should exceed 300:1.

(ii) Means should be provided to allow conditioning of the test chamber atmosphere over the following ranges :-

Temperature 233 to 323K

Relative Humidity 10% to 90%

(iii) The test chamber should be equipped with fans to ensure mixing of the exhaust products and the atmosphere within the chamber.

(iv) Care should be taken to ensure the cleanliness of the chamber so as to minimize the number of potential condensation nuclei present in the chamber prior to motor firing.

3.2.1.3 Test Motor Characteristics

It is recommended that test motors conform to the following definition :-

(i) Approximately neutral burning characteristics, with expansion of the exhaust gas to atmospheric pressure.

(ii) Minimal (preferably no) usage of ablative materials.

(iii) A burn time of less than 2 seconds.

(iv) A smokeless igniter should be employed, typically using double base propellant as the pyrotechnic. Igniters using the same propellant as the main grain should also be considered. In cases where condensation nuclei are considered critical, replacement of the standard pyrotechnic initiator with a glow plug (hot wire) initiator should be considered. In any event, calibration firings with the igniter alone are recommended to ensure that the igniter does not contribute to the motor signature.

3.2.1.4 Experimental Procedures and Measurements

The following procedures and measurements are recommended :-

(i) The chamber conditions, the change in transmission and other optical properties should be carefully and continuously measured for a minimum of six minutes after motor firing because there is evidence (Figs 4-7 and 4-8) that droplet growth, as shown by the signature characteristics, occurs during this period.

(ii) The pressure, temperature and dew point of the atmosphere within the test chamber should be continuously measured. A fast response time of the instrumentation used to measure temperature is particularly important to assess the amount of afterburning. IR Radiometers are used in the SCF for this reason and are recommended. Dew point is measured in the SCF with a digital humidity analyser (Model 911 Dew-All, manufactured by EG and G Environmental Equipment, Burlington, Massachusetts, USA), equivalent equipment is recommended.

(iii) Cameras, transmissometers and view ports should be used to monitor the formation of secondary smoke. For transmissometers, the source and detector should generally be tailored to approximate the spectral response of the human eye. For specific wavelength measurements, dedicated sources and detectors are required. Detector aperture should be small to minimize the reception of forward scattered radiation.

(iv) Provisions should be made for the measurement of particle sizes and number density of nuclei and droplets. When measurements of the primary smoke particle size distribution are required for input to predictive codes which include heterogenous nucleation then particles as small as 10^{-3} to 10^{-2} should be included because of their large effect, even at low mass concentrations, upon the total number of condensation nuclei.

3.2.2 Free-Jet Firings

Free-jet firings (defined here as static motor tests with no restriction of the exhaust plume) are of limited utility in assessing rocket motor secondary smoke signature. They are not recommended for the acquisition of quantitative experimental data, since the environmental effects cannot be controlled or reproduced. The exhaust plume will inevitably be affected by wind

conditions, ground contours, and temperature and relative humidity. Thus the environmental control required for reproducible experimental results is lacking. Sand and dust entrained by the exhaust jet influence secondary smoke formation and represent an additional unknown factor. Location of the instrumentation is important in the case of an afterburning plume. It is imperative to avoid the afterburning region because of the sensitivity of secondary smoke formation to temperature.

At best, such firings reliably provide only a smoke/no-smoke assessment, and measurement of plume opacity and transmissibility is of limited utility.

3.2.3 Flight Tests

3.2.3.1 Usage

Flight tests, because of expense, are normally only performed as part of a missile development program. Usually, the purpose of the test is not primarily signature characterization, but even in this event the measures recommended in Section 3.2.3.2 will maximize their utility.

3.2.3.2 Experimental Procedures and Measurements

(i) If one of the purposes of the test is investigation of the secondary smoke characteristics then the test should be conducted in atmospheric conditions where smoke formation is expected.

(ii) Accurately record the locations and orientations of any transmissometers in relation to the launcher.

(iii) Record motor size, propellant composition, thrust, exit pressure, exit diameter, and burn time. Record trajectory data.

(iv) Record wind speed, ambient temperature and relative humidity, if possible at different altitudes.

(v) For visual and camera observations of smoke/no-smoke, record the background lighting conditions (e.g. cloud, clear sky), and the orientation of the sun.

3.3 Prediction Methods

3.3.1 Thermodynamic Data Base

3.3.1.1 HCl/Water System

The calculation procedure given below is used by SNPE and is based upon a curve fit of the data from Reference 1. It is recommended for temperatures above 240K.

(a) **NOMENCLATURE**

- PS_1 saturation pressure of pure water
- PS_2 saturation pressure of pure HCl
- P_0 reference pressure (P_0 = 101.3 kPa or 1 atm)
- T Temperature (in Kelvin) of both phases
- PP_1 saturation pressure of water on an HCl/H_2O mixture
- PP_2 saturation pressure of HCl on an HCl/H_2O mixture
- x_1 molar fraction of water in the liquid phase
- x_2 molar fraction of HCl in the liquid phase ($x_1 + x_2 = 1$)
- γ_1 activity coefficient of water in the liquid phase
- γ_2 activity coefficient of HCl in the liquid phase
- Ln(x) : Naperian (natural logarithm of x

(b) **BASIC EQUATIONS**

$$PP_1 = x_1 \gamma_1 PS_1$$
$$PP_2 = x_2 \gamma_2 PS_2$$

The activity coefficients γ_1 and γ_2 characterize the non ideal behaviour of the liquid phase.

(c) **CALCULATION OF PS_1**

$$\text{Ln}\frac{PS_1}{P_0} = a_{11}(1 - \text{Ln}\,T) - a_{12}\frac{T}{2} - a_{13}\frac{T^2}{6} - a_{14}\frac{T^3}{12} - a_{15}\frac{T^4}{20} + \frac{a_{16}}{T} - a_{17}$$

The a_{ij} coefficients are fitted on the JANNAF thermodynamic data for liquid and gaseous H_2O.

a_{11} = 4.593365
a_{12} = 1.1084499E-03
a_{13} = - 4.1521180E-06
a_{14} = 2.9637404E-09
a_{15} = - 8.0702101E-13
a_{16} = - 6687.164
a_{17} = - 40.65053

(d) CALCULATION OF PS_2

The origin of the data is the same and the expression identical after substituting PS_1 for PS_1 and a_{2j} for a_{1j}

a_{21} = 75.36436
a_{22} = - 0.6095065
a_{23} = 1.2167492E-03
a_{24} = - 2.0979720E-09
a_{25} = 9.8658191E-13
a_{26} = - 8099.362
a_{27} = -312.2104

(e) CALCULATION OF γ_1 AND γ_2

$$\text{Ln}\,\gamma_1 = x_2^2\left(\frac{A_1}{2} + \frac{B_1}{3}x_2 + \frac{C_1}{4}x_2^2 + \frac{D_1}{5}x_2^3\right)$$

$$\text{Ln}\,\gamma_2 = x_1^2\left(\frac{A_2}{2} - \frac{B_2}{3}x_1 + \frac{C_2}{4}x_1^2 - \frac{D_2}{5}x_1^3\right)$$

with

A_1 = 76.58848 + -39705.53/T
B_1 = -450.5769 + 109608.1/T
C_1 = 801.4499 + -109729.4/T
D_1 = -296.8485 + 31565.01/T

and

$A_2 = A_1 + B_1 + C_1 + D_1$
$B_2 = B_1 + 2C_1 + 3D_1$
$C_2 = C_1 + 3D_1$
$D_2 = D_1$

The A_1, B_1, C_1, D_1 coefficients were optimized to fit the Perry's Handbook data on HCl/H_2O binary equilibrium.

3.3.1.2 HF/HCl/Water System

The available data base is inadequate for systems involving fluorine. Reference 8 is recommended as an interim standard and, since Reference 8 is not generally available, the relevant data are given in Table 8.

3.3.1.3 KOH/W

Potassium salts are frequently used to suppress afterburning in exhausts of rocket motors containing double-base propellants. Potassium hydroxide (KOH) is the common exhaust product of these salts. KOH condenses to liquid and solid phases at temperatures of 1593K and 633K, respectively and thus will be in the form of solid particles long before any water condensation processes start in the plume. These particles will act as nuclei upon which water will condense when the appropriate temperature and vapour pressure conditions are reached. It is not clear to what extent the KOH will be either in the form of relatively pure particles, or will have condensed with, or upon, inert nuclei. However, KOH is very soluble in water and its presence in an exhaust will cause water condensation to begin considerably below the saturation vapour pressure. According to Reference 22 mixed nuclei of soluble and insoluble material behave like wholly soluble nuclei of equivalent size at relative humidities above about 70% (Ref 19, pp 7-9, section 9).

The saturation vapour pressure of water over KOH is given quite accurately by P_0A. Here P_0 is the saturation vapour pressure of water over inert particles, and A is given by

$$A = \exp(-2M\phi)$$

where

M is the molarity of KOH and

ϕ is the osmotic coefficient of KOH

The osmotic coefficient of KOH as a function of molarity of KOH [23] in water solution is given in Table 9.

At this time there is insufficient evidence to verify that real rocket motor exhausts behave in the ideal manner defined above. Further work is needed in this area.

TABLE 4.8

VAPOUR PRESSURE DATA OF HCl/HF/H_2O SOLUTIONS

Liquid phase composition (mole fraction)	Soln 79	Soln 24	Soln 60	Soln 82	Soln 85
HCl	.073	.093	.0637	.075	.075
HF	.163	.130	.1911	.175	.148
H_2O	.764	.777	.745	.750	.776
Gas Phase Composition at 273.15K (O°C) (mole fraction)					
HCl	.055	.148	.054	.112	.056
HF	.173	.152	.200	.208	.144
H_2O	.773	.701	.748	.679	.800
$\ln P = A + B/T$					
A (HCl)	19.22	18.57	18.99	19.89	18.104
B (HCl)	-5827	-5385	-5748	-5842	-5504
A (HF)	12.88	18.351	18.949	21.45	20.50
B (HF)	-3785	-5319	-5379	-6099	5901
A (H_2O)	14.53	19.07	18.821	20.15	18.15
B (H_2O)	-3824	-5097	-4985	-5421	-4791

Notes :- 1 Nomenclature as follows :- P = vapour pressure, torr T = absolute temperature, °K

TABLE 4.9

OSMOTIC COEFFICIENTS OF KOH

M	ϕ	M	ϕ	M	ϕ	M	ϕ	M	ϕ
.001	.988	.2	.930	.9	.989	5.0	1.533	10.0	2.229
.005	.976	.3	.934	1.2	1.023	5.5	1.604	12.0	2.480
.01	.968	.4	.940	1.6	1.072	6.0	1.675	14.0	2.700
.02	.958	.5	.948	2.0	1.123	7.0	1.817	16.0	2.880
.05	.944	.6	.957	3.0	1.256	8.0	1.957	18.0	3.009
.10	.934	.7	.967	4.0	1.393	9.0	2.095	20.0	3.079

3.3.2 Secondary Smoke Formation

3.3.2.1 Preliminary Determinations and Propellant Classification

For approximate determination of smoke/no-smoke limits as a function of atmospheric conditions, equilibrium calculations are satisfactory. Conservation of enthalpy should be assumed, it is not calculated. The propellant secondary smoke classification is also given by these calculations (see chapter on Terminology).

3.3.2.2 Complete Models

More complex modelling of secondary smoke formation should include (as a minimum) :-

(i) afterburning

(ii) mixing of the exhaust with ambient air

(iii) the effects of condensation nuclei, including soluble and insoluble material

(iv) the effects of droplet growth kinetics and droplet evaporation upon the size distribution of droplets and the resultant effects upon plume obscuration and visibility

The current analytical codes are not adequately verified, and further development is required. It is recommended that :-

(i) particle size distributions of condensation nuclei in the motor exhaust be measured for typical propellant formulations. This data should be used as input to the computer codes.

(ii) increased effort should be devoted to verification of the codes in free-jet conditions. This requires modelling of the exhaust plume as affected by, for example, ambient wind conditions. The IFTA code (see Table 3) incorporates such considerations. Suitably instrumented test firings will be required to verify the resultant predictions.

(iii) firings in test chambers should be continued to provide data for code development. Specific effort is required to validate droplet growth kinetics and evaporative mechanisms because of their effects upon the droplet size distribution.

3.3.3 Atmospheric Model

The recommended atmospheric model base is the AGARD Standard Climatic Data Base discussed more fully in Appendix 4. This is a statistical compilation of climatic conditions, eg temperature, relative humidity, as a function of altitude, time of year and geographical location.

3.3.4 Visibility

The visibility of a secondary smoke plume is dependent upon the plume characteristics, background illumination conditions, sun-plume-observer angle and atmospheric attenuation. These factors are not unique to the secondary smoke signature and are discussed in Chapter 1 which rightfully stresses the importance of, as far as possible, quantitatively defining the missile operational requirements and goals.

There is, however, one aspect in which secondary smoke signatures are unique. The formation of a secondary smoke plume is dependent upon the temperature and relative humidity of the ambient air. However, the parameters affecting plume visibility cannot be assumed to be independent of those governing the formation of secondary smoke. A low relative humidity, for example, is more likely to be coupled with "exceptionally clear" atmospheric transmission conditions and a clear sky than is a high relative humidity. This interrelationship is not quantified by existing climatic data bases (including the Climate Model described in Appendix 4).

The acquisition and compilation of the necessary statistical climatic data linking these parameters would represent a mammoth undertaking and cannot be recommended. It is therefore recommended that effort be devoted to the generation of algorithms which, at least for a specific operational scenario, provide a means of relating the factors governing plume formation to those affecting visibility. At the least, both users and system analysts should be aware of the potential for error if these inter-relationships are ignored.

4.0 REFERENCES

1 Perry, J.H., Chemical Engineer's Handbook, Physical and Chemical Data.

2 Fritz and Fuget; Vapor Pressure of Aqueous Hydrogen Solutions, Ind Eng Chem, 1956.

3 Zelsberg, Van Arsdel, Blake, Greenwald, Taylor; International ,and Critical Tables VM III, McGrauhiel, 1928, p 301.

4 Glasstone; Thermodynamics for Chemists, Van Nostrand, 1947.

5 Parker; Thermal Properties of Aqueous Uni-Univalent Electrolytes, NSRDS (National Bureau of Standards), No 2, 1965.

6 Miller, E., Vapor-Liquid Equilibria of Hydrogen Chloride-Water Solutions Below 0 degress C, J Chem Eng Data 28, 363 (1983).

7 Miller, E., Vapor-Liquid Equilibria of Hydrogen Chloride-Water-NaCl Solutions Below 0 degrees C, Ibid, October 1984.

8 Wilmot, G.B., Carpenter, G A., Measurement of the Saturated Vapor Pressure of HF/HCl/$H_2$0 Solutions, 1 October 1980-30 April 1981 Progress Report, Naval Surface Weapons Center, 30 April 1981 (Unpublished).

9 Oliver; Graphical Data, Unpublished.

10 Meyer, J.W., Kinetic Model for Aerosol Formation in Rocket Contrails, AIAA Journal, Vol 17, No 2, February 1979, pp 135 - 144.

11 Victor, A.C., Toward Guidelines for Rocket Exhaust Smoke Definition and Standardization, TM 3361, Naval Weapons Center, 7 April 1977.

12 Victor, A., A proposed Standard Climate for Evaluating Rocket Exhaust Smoke Formation and Visibility, Naval Weapons Center, TM 3638, 1978.

13 Jarman, R.R., de Turville, C.M., The Visibility and Length of Chimney Plumes, Atmospheric Environment, Vol, 3, pp 257 - 280, 1969

14 Victor, A.C., Briel, S.H., A Simple Method for Predicting Rocket Exhaust Smoke Visibility, J Spacecraft and Rockets, Vol 14, No 9, September 1977, pp 526-533.

15 Hoshizaki, H., et al, Plume Visibility Detection Study, Lockheed, AFRPL-TR-78-32, November 1978 (Limited Distribution).

16 Miller, E., Prediction of the Visible Signature of Solid Rocket Plumes, J Spacecraft, Vol 27, No 1, January - February 1990, pp 82 - 84.

17 Victor, A., Rocket Exhaust Smoke Signature (Unpublished).

18 Ajdari, E., Secondary Smoke Occurrence Comparison Between Prediction and Experiments in a Climatic Chamber, 1988 (Unpublished).

19 Victor, A.C., Computer Codes for Predicting the Formation of Rocket Exhaust Secondary Smoke in Free Jets and Smoke Chambers, TM 3361, Naval Weapons Center, February 1978.

20 Miller, E., Smokeless Propellants, Fundamentals of Solid Propellant Combustion, Progress in Astronautics and Aeronautics, Vol 90, pp 841-884, AIAA, New York, 1984.

21 Thorn, L.B., Chairman/editor, The Exhaust Plume Visual Signature Workshop, SR RD-82-1, US Army MICOM Redstone Arsenal, Alabama, 1-2 December 1981.

22 Mason, B.L., The Physics of Clouds, Oxford, 2nd edition, Clarendon Press, 1971

23 Hammer, W.J., Wu, Y.C., Osmotic Coefficients and Mean Activity Coefficients of Uni-univalent Electrolytes in Water at 25°C, J Phys Chem Ref Data, Vol 1, No 4, pp 1047 - 1099, 1972.

FIGURES

TABLE OF CONTENTS

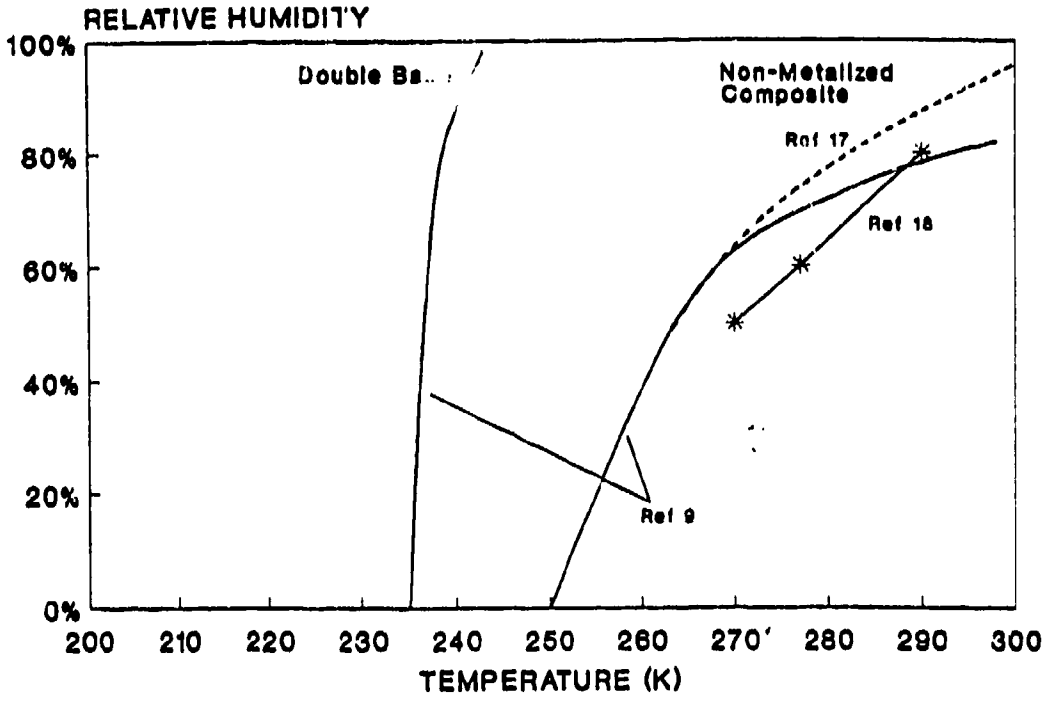

Fig. 4-1 Predicted Secondary Smoke Formation at Sea Level [9, 17, 18]

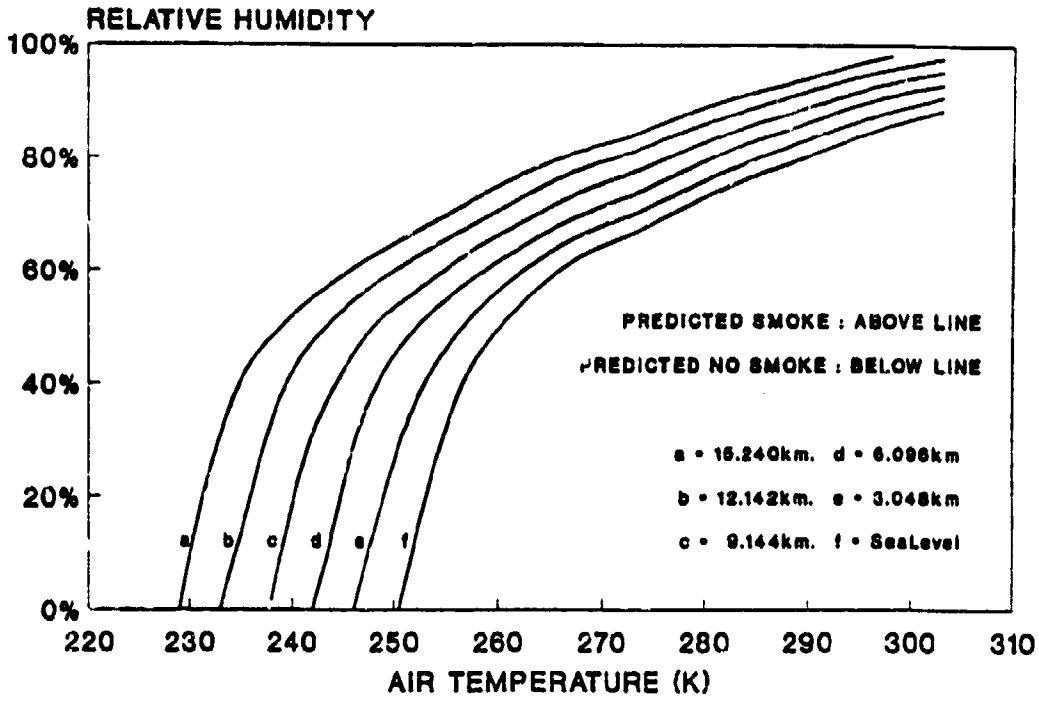

Fig. 4-2 Predicted Secondary Smoke Formation as a Function of Altitude Non-Metallic Composite Propellant (with AP)

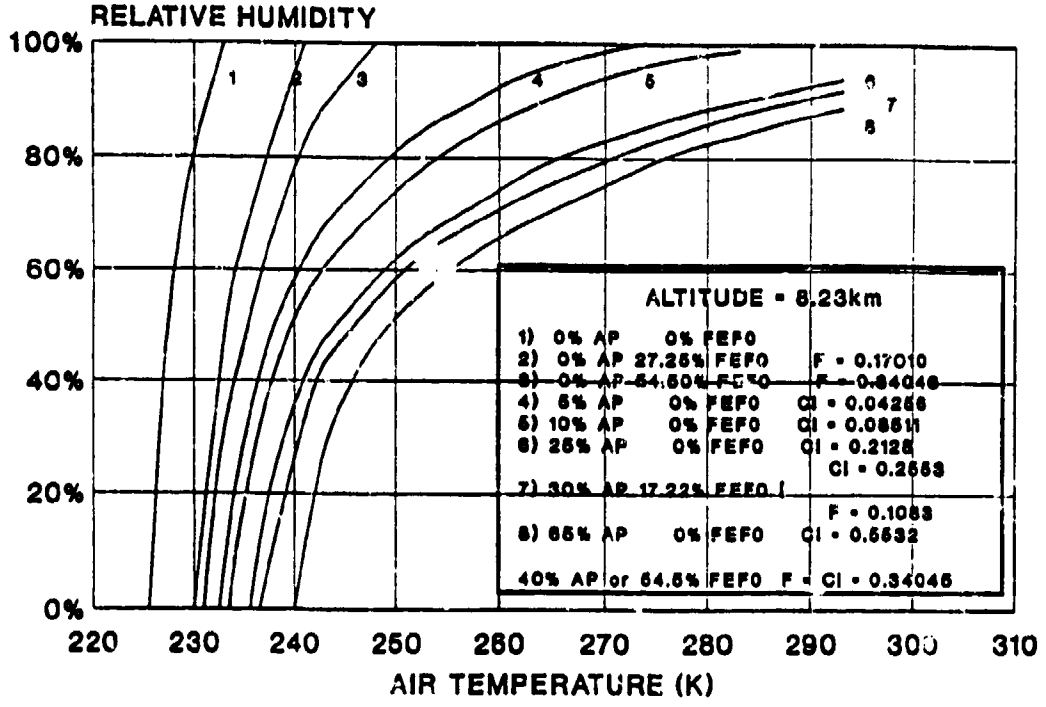

Fig. 4-3 Predicted Secondary Smoke Formation as a Function of Propellant Composition

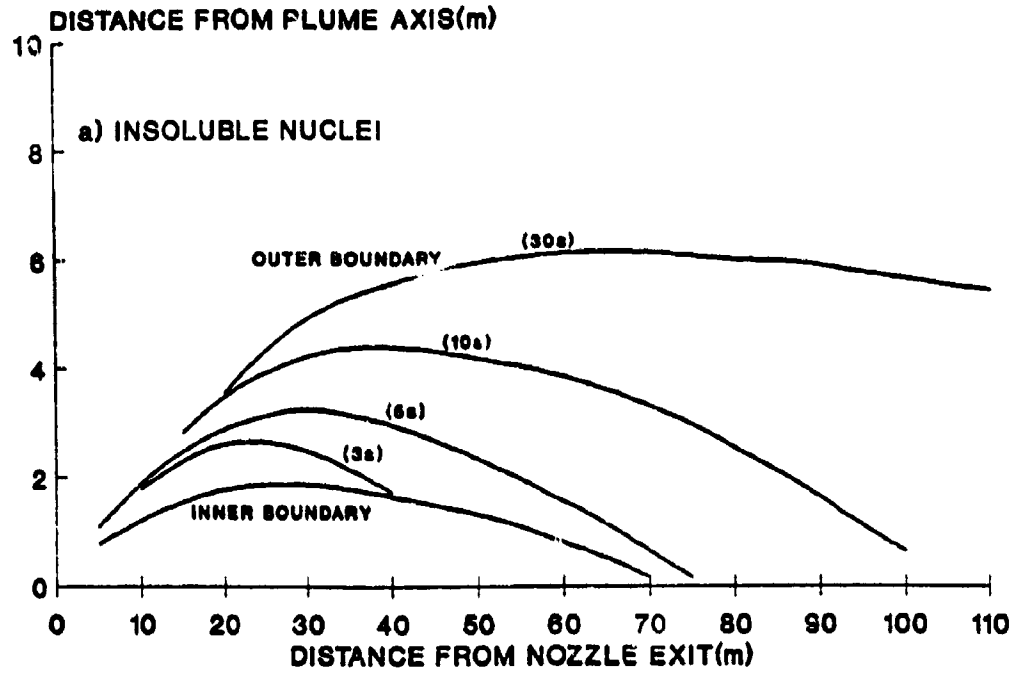

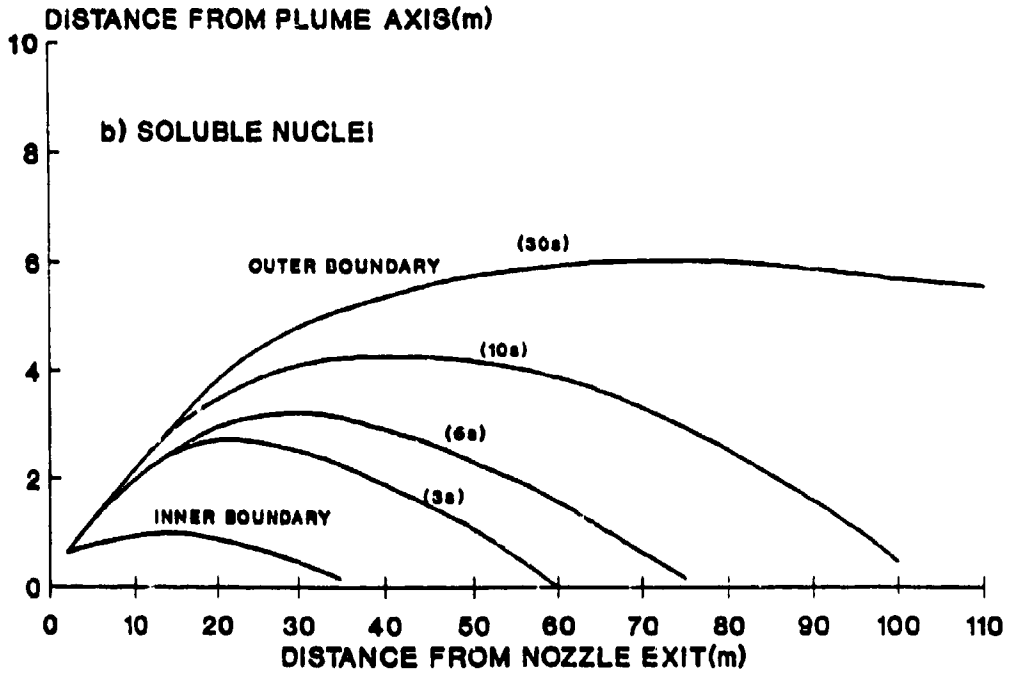

Fig. 4-4 **Predicted Plume Contours. Composite (25% AP) Propellant Sea Level**

(a) Insoluble nuclei
(b) Soluble nuclei

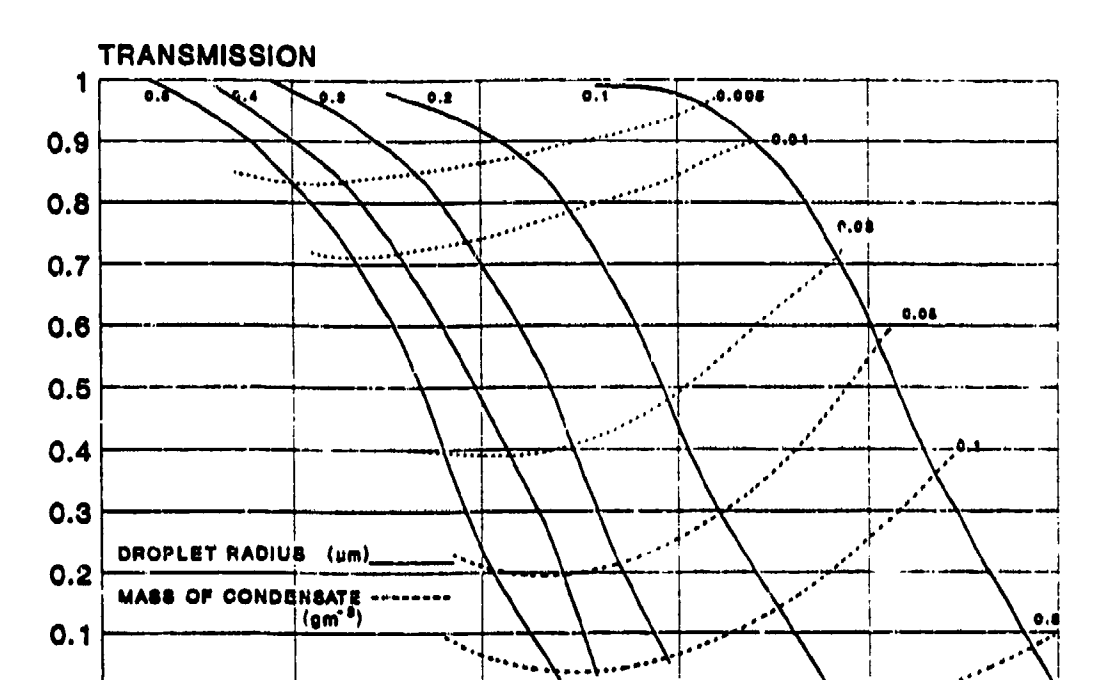

Fig. 4-5 Predicted Transmission as a Function of Plume Characteristics [19]

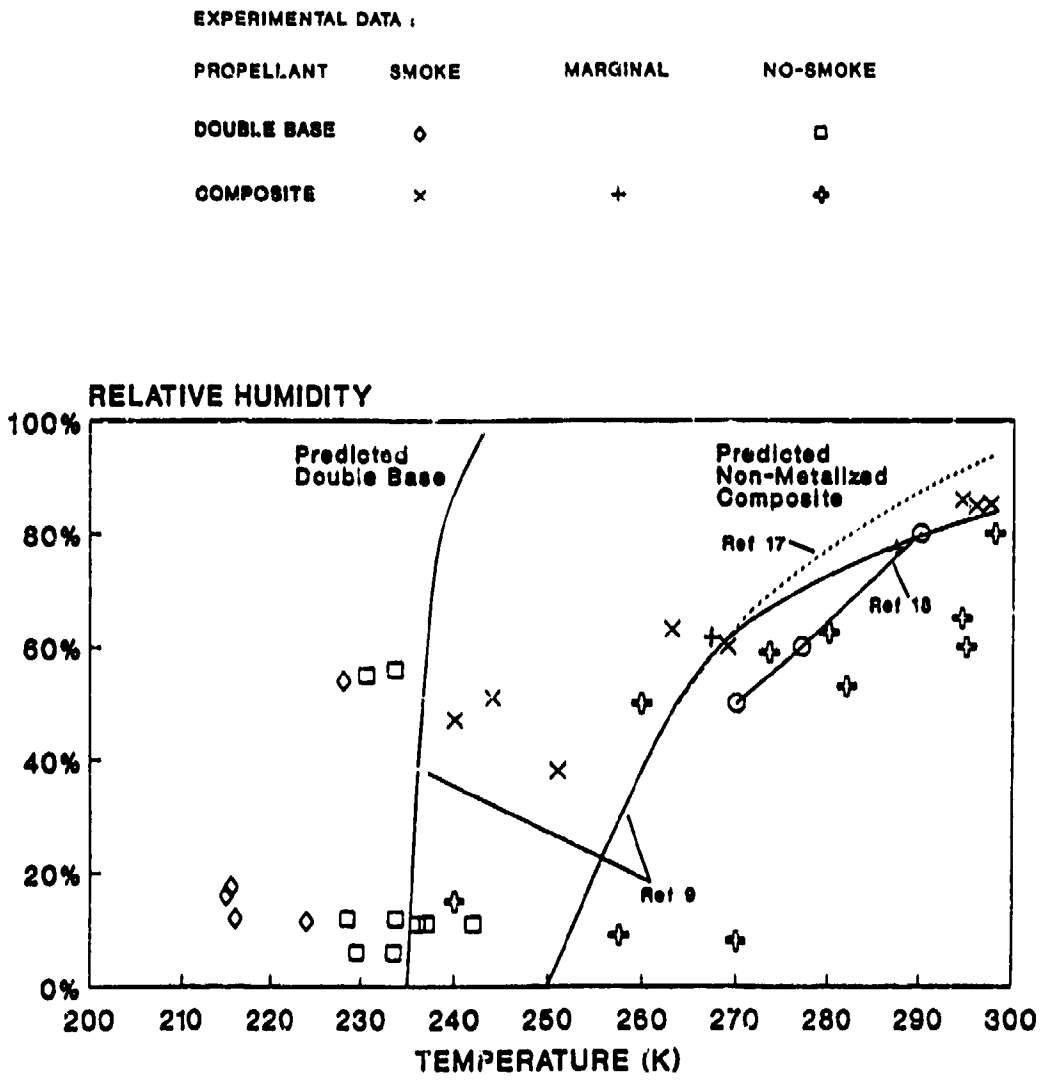

Fig. 4-6 Predicted and Measured Smoke/No-Smoke Boundaries [9, 17, 18, 21]

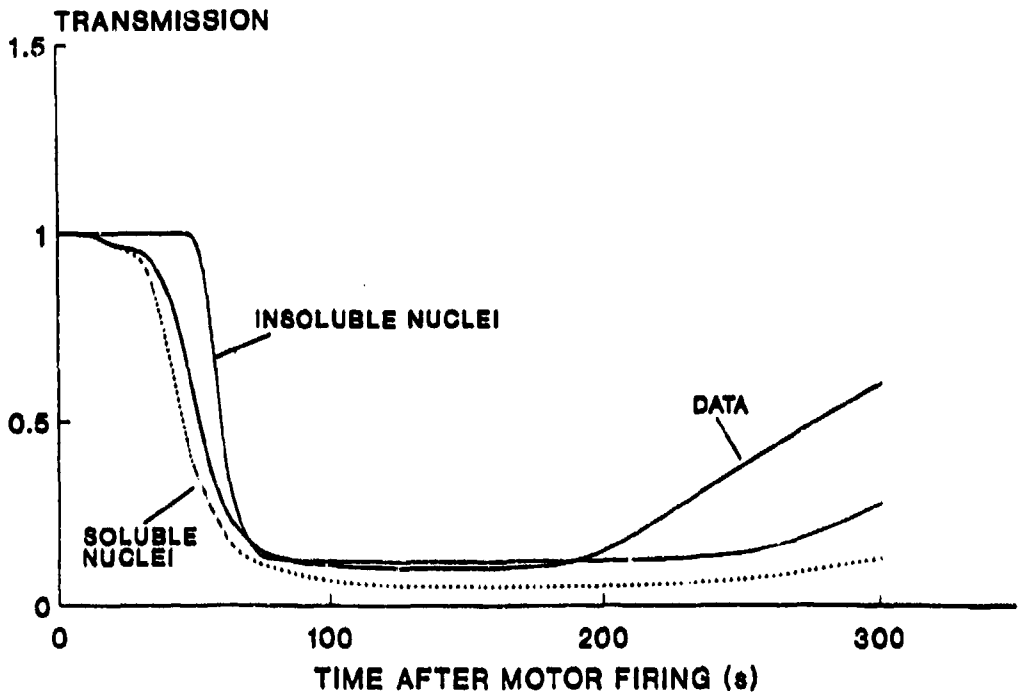

Fig. 4-7 Predicted and Measured Light Transmission - Test Chamber Data - HMX Composite with 25% AP, 256K, 73% RH Sea Level [19]

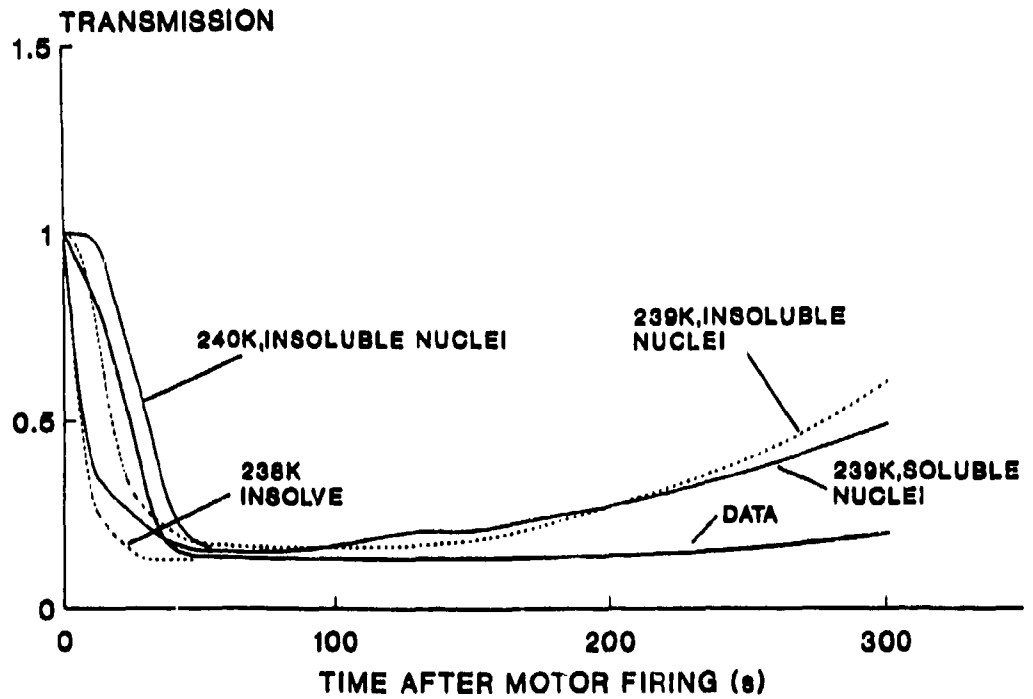

Fig. 4-8 Predicted and Measured Light Transmssion - Test Chamber Data - HMX Double-Base (no AP), 239K, 81% RH Sea Level [19]

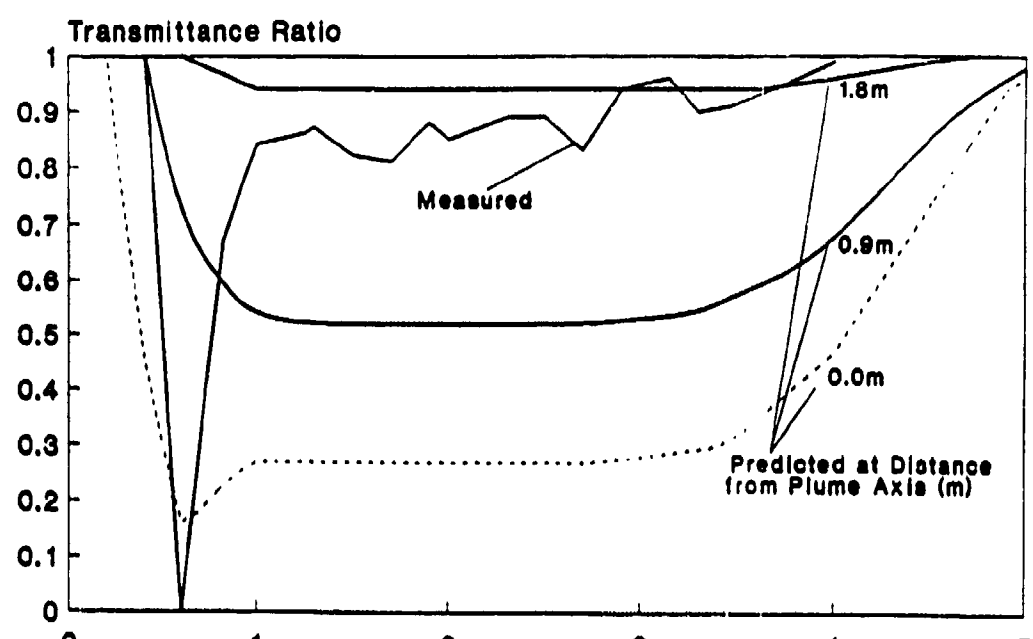

Fig. 4-9 Light Transmission Through Plume - Launch Phase - Test #1 [21]

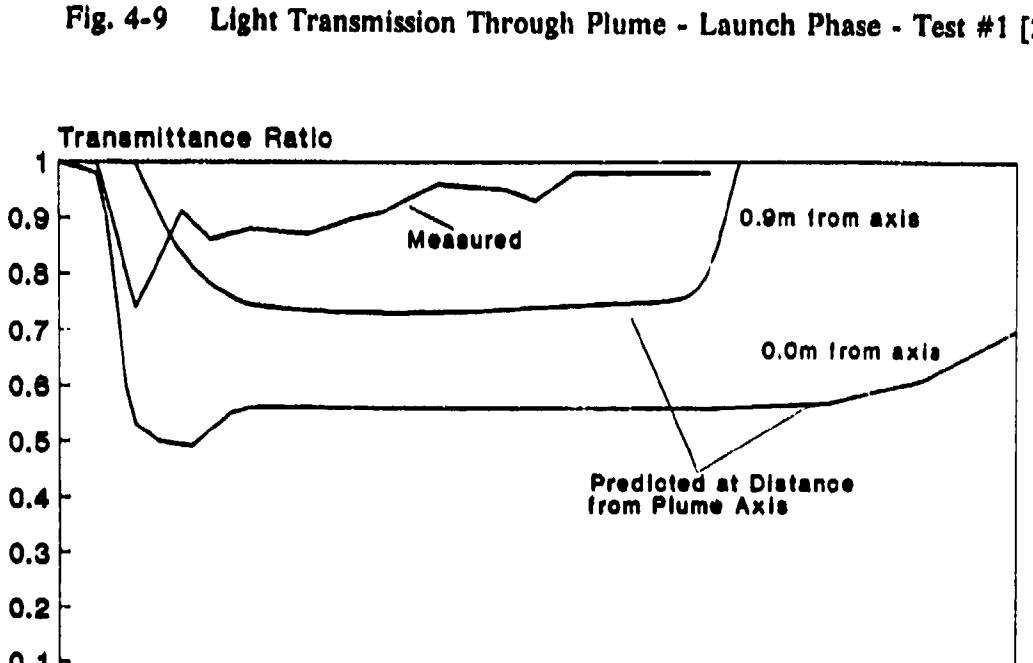

Fig. 4-10 Light Transmission Through Plume - Launch Phase - Test #2 [21]

CHAPTER 5

PLUME RADIATION

CHAPTER 5

PLUME RADIATION

TABLE OF CONTENTS

1. INTRODUCTION

Exhaust plumes of tactical missiles radiate energy over a broad spectral range producing signatures (finger prints) that may be used for detection, identification and targeting or for tracking and control. This phenomena very often poses two major conflicting requirements on system designers, one is for high ballistic performance and the other is for minimum signature. Good ballistic performance often requires the use of metal enriched propellants resulting in high temperature exhaust plumes laden with metallic oxide particles. Consequently the signature, composed of gaseous and continuum emission, is more intense. Design of the rocket motor nozzle and missile afterbody geometry can be tailored to reduce plume radiation by reducing or eliminating zones of recompression and high temperature thereby moderating or suppressing afterburning. Where dual stage propulsion is used, a method of reducing the intensity of radiation in the critical terminal phase of flight is to raise booster mass at the expense of sustainer mass.

To address signature problems it is necessary to have a thorough understanding of the mechanisms producing emissions in plumes. The classification of this emitted radiation into spectral regions, the operational role of the system which dictates spectral criteria, and the overall system design help in assessing comparative methods for rocket motor evaluation in terms of plume signature. From a designer's point of view the requirements are system dependent in practically every case and a simple grouping into two or three system based categories might be considered like :-

(i) small tactical missiles - short range (low altitude)

(ii) large missiles - long range (low and high flying, booster phase and sustainer phase).

The operational requirements concerned with obscuration, detectability, interference, guidance etc. are very system specific and in many cases classified. Because of this and the overall complexity of the problem it is natural that this "AGARD advisory report" can only give guidelines, general rules and baric recommendations for assessment methods such as :-

(i) theoretical calculation techniques

(ii) measurement procedures

(iii) presentation of results

(iv) standards

(v) units used

(vi) limitation of measurements and computer codes

The achievable prognostic results of plume radiation depend a lot on available measuring techniques and devices and on the effort and level of understanding that goes into the computation of radiation phenomena. Rocket plume flowfield calculations must provide sufficient information on the distribution of plume parameters such as temperature, pressure and species mole fractions throughout the plume. It is a continuous interplay between measured results, plume flowfield parameters and radiation calculation models.

2. CHARACTERIZATION OF ROCKET MOTOR PLUME RADIATION

2.1 General Description

The hot combustion products of a rocket propulsion system produce a highly turbulent exhaust plume as they expand through the nozzle into the surrounding atmosphere. These products consist of hot gases from the burning process, activated and deactivated molecules promoted by chemical reactions, accelerated particles of incompletely burnt fuel, soot, metal oxide condensates and other solid constituents. The plume is an extremely complicated chemical and thermodynamic entity whose properties very largely depend upon the type of propellant, motor

and nozzle design, gas dynamics and flight conditions. This chapter is mainly concerned with radiation from this complicated source which is scattered, reabsorbed and quenched during this emission process.

In a typical propulsion system, plume solid particles, the nozzle and other parts which operate at elevated temperatures fall into the thermal emitter category. Thermal emitters produce radiation which can be partially described by Planck's spectral distribution of emissive power. Considerable energy is produced in the infrared. The presence of this source of radiation is of importance in weapon systems where thermal seekers are used. Solid particles are evident in the far field plume region because they produce smoke but in this chapter we are concerned about the near field region, where several types of solids may be excited to emit radiation. Soot, for instance, exists predominately in rocket motors using carbon-hydrogen fuel with a C/H ratio of over 0.5. Metal oxides are formed from metallic additives such as Al, Mg, and Zr where concentrations between 5% and 20% are used in composite and composite-double base propellants. Boroxides are sometimes produced in solid ramjets where Boron is a content of the fuel.

Further flame emission comes from molecular reactions which can be divided into rotational spectra due to changes in the rotational energy of the molecule, vibrational spectra due to changes in the vibrational energy of the molecule, electronic spectra from changes in the energy of the molecule due to different electron arrangements, and to combinations such as vibrational-rotational transition spectra.

In these typically complicated processes there is rarely complete knowledge of the kinetics of the series and parallel chemical reactions occurring within the plume. Compounding the problem of source complexity is the fact that selective radiation from a flame does not correspond to a relatively simple spectral distribution as shown by a blackbody. The character of radiation from these sources is much more complex and difficult to treat than that from solid bodies and consequently more difficult to model. For the purposes of this article the different models describing the production mechanisms do not need to be presented. It is sufficient that molecules or atoms exist in discrete energy states and that the electromagnetic radiation emitted by an excited molecule appears only in discrete quanta of radiation.

2.2 Phenomenology

Rocket exhaust plumes are characterised by turbulent mixing and very often afterburning in a flow initially dominated by strong wave processes. The initially under-expanded exhaust equilibrates to ambient pressure via a sequence of expansion and compression waves. Mixing and afterburning processes commence and develop in the shear layer formed between the exhaust plume and ambient external flow.

The overall plume flowfield can be subdivided into the three regions as seen in Figure 5-1, namely :-

(i) the predominantly nearfield inviscid plume where wave strengths are strong and turbulent mixing processes are generally confined to thin layers.

(ii) a transitional region where the mixing layers engulf the entire plume and wave strengths diminish due to turbulent dissipation.

(iii) the farfield fully viscous plume where wave processes have totally diminished and a constant pressure, turbulent mixing environment prevails.

Given this complicated flow field regime, it is a challenging task to understand and predict its radiation properties. The objectives are to define plume signature mechanisms, quantify their temporal, spatial and spectral characteristics for various types of propellant and altitude regimes and list their importance for selected missile flight

tasks. To engage this problem one has to secure agreement on key definitions, on the recognition of crucial geophysical constraints and on the way the parameters are described. Such agreement would establish a common, uniform method of information gathering and would likely describe :-

(i) the mechanisms that create or produce plume radiation, with details of physical and chemical constraints

(ii) the intensities of electromagnetic radiation produced over a given wavelength band, the spectral distribution of energy within that band and how measured or predicted values relate to the source of emissions

(iii) how these radiation properties are influenced by

(a) motor design (performance optimization, propellant composition etc.)

(b) conditions independent of motor design e.g. flight regime, atmospheric extinction, plume background.

This type of characterization forms a parametric study, it allows for an understanding of plume radiation phenomena and the formation of a radiation prediction technique for applications in support of missile detection, guidance and tracking.

As rocket flight tests are extremely expensive and plume radiation in flight is difficult to measure it is very important to have accurate prediction codes.

In designing passive sensor systems, battle scene simulation codes are a vital aid. They must address all possible scenarios, a wide range of atmospheric conditions, variations in background structure, turbulence, short motor burn times etc. To distinguish a missile operating in such an inconstant environment its exhaust radiation must be characterised, emphasising unique spectral properties for positive identification.

2.3 Origin of Plume Radiation, System Aspects and their Operational Implications

Missile exhaust plumes radiate energy over wide regions of the electromagnetic spectrum. Radiation processes have their origins in the chemical reaction mechanisms of combustion that take place during the rocket firing. Emission spectra are governed by the excitation energy of atoms and molecules throughout the exhaust which, among others, is a function of local energy and thermodynamic conditions. If a local thermodynamic equilibrium (LTE) model is assumed, the excitation of molecular states can be described by a Boltzman distribution corresponding to a single temperature. If LTE is not guaranteed the development of such a radiation model is no longer valid. Gas phase radiating species present in the plume are, in major part, determined by the propellant composition and the reaction of its combustion products with the ambient air. Increasing the complexity of radiating species within the gas mixture creates a multitude of spectral lines with overlapping radiation properties so that a line-by-line model has to be replaced by a band model to describe the radiation characteristics. Table 5.1 denotes a number of possible plume radiation mechanisms.

Plume radiation can originate from :-

(i) chemical reactions in the burning process
- molecular and electronic excitations and transitions
- chemiluminescence, fluorescence
- exothermal, radiation producing reactions

(ii) thermal emission in the afterburning phase, plume/atmosphere mixing and shock heating in the afterburning region produced by liquid or solid particles.

TABLE 5.1

PLUME RADIATION MECHANISMS AND MAXIMUM EMISSION RATES

	Mechanism	Approximate Maximum Spectrum-Integrated Energy Supply Rates for an Exhaust With $\dot{W}$ = 350 kgs^{-1}(*)		Spectral Region
1	Core Radiation	2.30×10^3	Watts	IR
2	Afterburning Radiation	1.97×10^3	Watts ($h \leq 50$ km)	IR
3	Collisional Deceleration Radiation	11.8×10^3	Watts (h = 0 km)	IR/VIS/UV
		0	Watts ($60 \leq h \leq 90$ km)	
4	Internal Shock Radiation	32.8×10^3	Watts ($h \geq 200$ km)**	
5	Atmospheric Pumping Radiation	4×10^7	Watts/km ($90 \leq h \leq 130$ km)	IR
6	Atomic Oxygen Chemi luminescence			
7	High Altitude Molecular Association/Dissociation Radiation	3.0×10^3	Watts/km ($h \geq 130$ km)	IR/VIS/UV
8	Airglow from Rocket Vehicle Friction	6.70×10^3	Watts (h = 100 km)	IR/VIS/UV
9	Scattering of Chamber Radiation by Plume	6.73×10^3	Watts	IR
10	Solar Radiation Scattered by Solid Particles in Plume	2.2×10^4	Watts/km	VIS
11	Solar Radiation Scattered by Gaseous Species in Plume	0.39	Watts/km	VIS
12	Absorption of Solar UV by Plume Gases and Reemission in UV, VIS and IR	7.48×10^6	Watts/km	IR/VIS/IR
13	Plume-Reflected Earthshine	5.85×10^{-5}	Watts/km	IR

* The ascending rocket is assumed to follow a typical trajectory for near-earth orbit injection; h = altitude. Radiations given in watts/km refer to km of trail length with V_v = 3 kms^{-1}.

** This value is for $\dot{W}$ = 350 kgs^{-1}. Usually at this altitude, a second or third stage is burning and the radiation should be scaled down by a factor of 350/50 = 7.

The plume signature of a tactical missile is strongly enhanced by the burning of excess exhaust hydrogen and carbon monoxide in the atmospheric mixing region downstream of the nozzle. This afterburning elevates the continuum radiation from particles as well as that from gas emission.

Condensed species may be either solid or liquid and typically radiate in a broad continuum. Gas radiation is predominately molecular, with electronic transitions in the visible, ultraviolet and rotational-vibrational transitions in the infrared. Two key operational aspects of missile exhaust plume radiation arise, one is radiation interference with line-of-sight guidance systems where the guidance signal must pass through the plume and the other is the possibility of interrogation by early detection countermeasures.

Evasive manoeuvres and countermeasures assume a greater importance for longer range missiles where the response time available to an adversary is greater and where the final closing velocity of the missile at the end of a coast period can be quite slow. Another important consideration is simply the variation of the exhaust plume signature during the flight of the

missile. The launch typically begins with a bright burst of flame with some degree of plume impingement on the launcher which can act as a flame holder. Flight continues with marked changes in signature in going from boost to sustain and from the burn out to a coast period. Variations of altitude and velocity during flight also affect afterburning and modify the plume signature.

For the detection and tracking of tactical missiles, spectral regions of importance are those in which strong plume emissions occur in an atmospheric 'window', a spectral region where good long-range atmospheric transmission is possible. The atmospheric windows are restricted by the onset of strong UV absorption of water, oxygen, and nitrogen below about 250nm, by the strong 2.7μm and 6.3μm absorption bands of water, and by the strong 4.3μm and 15μm bands of CO_2. A special phenomenon exists in the ultraviolet zone near 300nm, commonly referred to as the solar blind region. In this spectral region the ozone layer of the earth's upper atmosphere blocks out nearly all sunlight, resulting in a virtual blackout with extremely low background levels, even during daylight hours. The intensity of plume emission from H_2O at 2.7μm and CO_2 at 4.3μm is strongly attenuated by atmospheric absorption. Nevertheless, the intensity of emission in the wings of these bands is high enough to make them historically the most important wavelengths for plume signatures. The detectability of this infrared radiation depends not only upon range, but also upon altitude, atmospheric conditions, and background.

From the foregoing radiation producing mechanisms we shall consider here in more detail only the chemistry of plumes, afterburning effects on plume radiation and particle radiation in the plume

2.3.1 Chemistry of Plumes

The variety of emitting species in the complex flow system of a rocket exhaust is a result of the radiation kinetics of collision processes in the gas phase. Contributions to the radiation stem from evaporation and condensation processes, particle-molecule reactions and reactive and inelastic collisions. A normal radiation producing chemical reaction (chemiluminescence) is written:-

$$A + B \rightarrow C + D^*$$

$$\text{or e.g.} \quad CH + O_2 \rightarrow CO + OH^*$$

where one of the products of the exothermal reaction is in an excited state (*) which is deactivated by the emission of radiation. The wavelength of this emitted radiation depends on the available energy so that emitted line spectra in the infrared, although broadened by the known effects of collision and doppler broadening, come from vibrational-rotational transitions, whereas UV and visible radiation between 100nm and 800nm have their origins in the more energetic electronic transition states. A listing, representing classes and examples of plume chemical reactions, is given in Table 5.2. Classes of reactive and inelastic collision processes are listed as well as their major effect on plume excited-state distribution. The first four reaction classes listed (A through D) represent bulk chemical rate processes where the reactants and products are assumed to have internal state distributions consistent with LTE, and all the energy consumed or released by the reactions is reflected in the local kinetic temperature. These four reaction classes, along with condensation, evaporation and heterogeneous reaction processes are sufficient to describe most chemical effects in low-altitude LTE exhaust plumes. If LTE is not guaranteed, the hypothesis involved in developing a radiation model is no longer valid, since the radiation is dependent upon the population of upper and lower states which are no longer related by a Boltzman distribution. Rather, the populations of the states must be calculated by codes that include finite rate kinetic processes along streamlines. This difficult type of calculation has been performed for the UV spectral range and yields values that range above those of the normal SPF species calculations.

TABLE 5.2

CLASSES AND EXAMPLES OF PLUME CHEMICAL REACTIONS

Reaction Class	Generalized Formula (MF Arbitrary Collision Partner)	Examples	Major Effect on Excited State Distribution
Reactions that release or Consume Heat			
A Exothermic Bimolecular Reactions	$A + B \rightarrow C + D + heat$	$OH + H_2 \rightarrow H_2O + H$ $CO + OH \rightarrow CO_2 + H$	Raises gas temperature
B Thermolecular Combinations	$A + B + M \rightarrow AB + M$	$H + H + M \rightarrow H_2 + M$ $OH + H + M \rightarrow H_2O + M$	Raises gas temperature
C Endothermic Bimolecular Reactions	$A + B + heat \rightarrow C + D$	$H_2O + O \rightarrow 2OH$ $CO_2 + O \rightarrow CO + O_2$	Lowers gas temperature
D Collisional Dissociations	$AB + M \rightarrow A + B + M$	$O_2 + M \rightarrow 2O + M$ $H_2O + M \rightarrow H + OH + M$	Lowers gas temperature
Reactions That Create, Destroy or Transmute Excited Internal States			
E Chemiluminescent Bimolecular Reactions	$A + B \rightarrow C^{*\dagger\perp} + D$	$CH + O_2 \rightarrow OH^{*} + CO$ $C_2O + O \rightarrow CO^{*} + CO$	Directly creates excited internal state
F Chemiluminescent Combination Reactions	$A + B + (M) \rightarrow AB^{*\dagger\perp} + (M)$	$CO + O + M \rightarrow CO_2^{*} + M$ $O + H + M \rightarrow OH^{*} + M$	Directly creates excited internal state
G Collisional Excitation	$A + B \rightarrow A^{*\dagger\perp} + B$	$CO_2 + CO_2 \rightarrow CO_2^{\dagger} + CO_2$ $O + H_2O \rightarrow H_2O^{\perp} + O$	Directly creates excited internal states
H Collisional Quenching	$A^{*\dagger\perp} + B \rightarrow A + B$	$OH^{*} + M \rightarrow OH + M$ $CO^{\perp} + M \rightarrow CO_2 + M$	Directly excited internal state to heat
I Reactive Quenching	$A^{*\dagger\perp} + B \rightarrow C + D$	$OH^{*} + O \rightarrow O_2 + H$ $HCl^{\dagger} + O \rightarrow OH + Cl$	Destroys excited internal state
J Excitation Transfer	$A^{*\dagger\perp} + B \rightarrow \begin{matrix} A + B^{*} \\ + C + D^{*} \end{matrix}$	$NO^{*} + O \rightarrow N_2 + O^{*}$ $H_2^{\dagger} + O \rightarrow OH^{\dagger} + H$	Transmutes excited internal state

* Excited electronic state
† Excited vibrational state
⊥ Excited rotational state

To a large extent, emission from molecular bands is concentrated in the infrared spectral region, with emitting molecules and band centres being documented in Table 5.3. When viewing plume radiation over long distances, atmospheric attenuation becomes important and detection is possible only in an atmospheric "window". Dominant IR-emission is that from CO, CO_2, and OH. If Boron is abundant emission from HBO_2 B_2O_3 can be obtained. Visible radiation originates predominantly from Alkaline metals such as Na (0.585μm), K(0.72μm) or oxides like BO_2 and AlO. Due to chemi-luminescence OH-intensities can be higher, as described by Planck's radiation laws. Examples of rate constants and spectra for CO + O chemiluminescent reactions are given in Figures 5-2 and 5-3. The reader is also directed towards Reference 18. A listing of important electronic chemiluminescent reaction mechanisms is given in Table 5.4.

TABLE 5.3

PRINCIPAL PLUME EXHAUST GASES NEAR-INFRARED EMISSION BANDS

Molecule	Band Centres (microns)
CO_2	1.96, 2.01, 2.06, 2.69, 2.77, 4.26, 4.68, 4.78, 4.82, 5.17, 15.0
CO	4.66, 2.34, 1.57
HCl	3.45, 1.76, 1.20
H_2O	0.94, 1.1, 1.38, 1.87, 2.66, 2.73, 3.2, 6.27
NO_2	4.50, 6.17, 15.4
N_2O	2.87, 3.90, 4.06, 4.54, 7.28, 8.57, 16.98
OH	1.00, 1.03, 1.08, 1.14, 1.21, 1.29, 1.38, 1.43, 1.50, 1.58, 1.67, 1.76, 1.87, 1.99
SO_2	4.0, 4.34, 5.34, 7.35, 8.69

TABLE 5.4

EXHAUST PLUME ELECTRONIC CHEMILUMINESCENT REACTION MECHANISMS

Emitting Species	Emitting State	CM^{-1}	$\lambda(\mu m)$	Possible Pumping Reaction
CO	$A'\Pi$ $d\ ^3\Delta$ $e\ ^3\Sigma^-$ $a'^3\Sigma^+$ $a\ ^3\pi$	65074.8 61120.1 90973 55901 48687	0.154 0.164 0.110 0.179 0.205	$C_2O + O \rightarrow CO^* + CO$ $CH\ (^4\Sigma^-) + O \rightarrow CO^* + H$ $CH\ (X^2\Pi) + O \rightarrow CO^* + H$
OH	$A^2\Sigma^+$	32684.1	0.306	$H + OH + OH \rightarrow OH(A) + H_2O$ $CH + O_2 \rightarrow OH(A) + CO$ $OH + N_2(A) \rightarrow OH(A) + N_2$
CH	$C^2\Sigma^+$ $B^2\Sigma^-$ $A^2\Delta$	31828 25949 23150	0.314 0.385 0.432	$C_2(^1\Sigma^+, {}^3\Pi_U) + OH \rightarrow CH^* + CO$
C_2	$d^3\Pi$	20022.5	0.499	$C_3 + O_2 \rightarrow C^* + CO_2$ $\rightarrow C_2^* + CO + O$
N_2	($A^3\Sigma^+$, Metastable)	50206	0.199	$N_2H_2 + O \rightarrow N_2^* + H_2O$
NH	$A^3\Pi$	29772.5	0.336	$N_2^*(A) + NH \rightarrow NH^* + N_2$
NH_2	$^2A_1$			Unknown
NO	$A^2\Sigma$	43965.7	0.227	$N_2^*(A) + N \rightarrow NO^* + N_2$
Na	2p	16973 or 56	0.589	$N_2^*(A) + Na \rightarrow Na^* + N_2$ $NaO + O \rightarrow Na^* + O_2$
CO_2	continuum ($^1B_2$)		0.28-0.45	$CO + O + M \rightarrow CO_2^* + M$
O_2	$A^3\Sigma^+$, $B\ ^3\Sigma^-$	36096 49802	0.277 0.201	$O + O + M \rightarrow O_2^* + M$
NO_2	continuum ($^2B_1$, $^2B_2$)		0.48-0.8	$O + NO + M \rightarrow NO_2^* + M$

2.3.2 Afterburning Effects on Plume Radiation

For applications keyed to missile detection, guidance, etc., (e.g., in IR-related applications) the overall plume structure and its radiation is of strong interest with attention generally focused on the far field solution. For such applications, the near field solution serves to provide starting conditions for a farfield, constant pressure mixing/afterburning calculation [14]. Both requirements and their interface present a challenge to mathematical modelling. The fuel rich products of combustion inherent in solid rocket motors, often combined with significant amounts of ignition residue, liner and inhibitor, mix and burn with the entrained air in the so called "Plume Mixing Layer" after leaving the nozzle (Fig. 5-4). A descriptive term for this secondary combustion is "afterburning". With energetic propellants this oxidation is very similar to the combustion that occurs in turbulent diffuse flames, except that it now occurs in a complex multi-phase expansion accompanied by strong shocks.

As in the case of ordinary combustion, afterburning is a free-radical chain reaction process requiring a moderate density of both oxidizer and fuel species to sustain the chain, a requirement that generally restricts this phenomena to low altitude LTE exhaust plumes. Afterburning can be suppressed at high missile velocities which tend to "blow off" the afterburning plume regions in much the same manner as the flames from a Bunsen burner can be extinguished by increasing the air/fuel flow rate above a critical value.

The chief impact that afterburning chemistry has on plume radiation signatures comes from the increase in plume temperatures through heat release. Most rocket exhausts produce H_2 and CO as the main gas phase species that fuel afterburning reactions with O_2 from the surrounding atmosphere to produce H_2O and CO_2. The energy transfer in the afterburning region producing excited vibrational, rotational and electronic states is rather complex and we refer here to the extensive available literature.

Predictions of exhaust plume temperature profiles for a typical tactical missile with a highly energetic propellant is exhibited in Figure 5-5. Particulates (16% aluminium in the propellant) were equilibrated with the gas phase in performing these calculations. The afterburning is quite rapid at sea level, with significant quantities of unburnt CO and H_2 in the exhaust being depleted within 100 radii of the nozzle exit. Non equilibrium gas/particle calculations for this system would exhibit substantial differences in the flow structure due to the high particle loading.

In flight, as missile altitude increases so the afterburning rate decreases due to a reduction in ambient pressure. Above 10-15km and/or for "cooler" double-base propellant systems (i.e., those with exhaust temperatures less than 1000K), the onset of afterburning is partially controlled by the conditions in the missile base region. The role of the base region as a flameholder has been noted during a number of studies and combustion that occurs at the base can induce afterburning in the downstream plume shear layer which would not otherwise be present. This is caused by higher initial temperatures in the plume shear layer and an increase in free radical concentrations.

2.3.3 Particle Radiation in the Plume

In general, particulate matter in the plume may influence the plume radiation signature in at least five ways:-

(i) by thermally interacting with plume gases
(ii) by chemically reacting with plume gases
(iii) by catalysing physical or chemical changes in plume gases
(iv) by emitting thermal radiation as a result of heating in the rocket combustion chamber or plume afterburning regions
(v) by scattering radiation, such as sunshine, earthshine or combustor radiation (searchlight effect)

It should be noted that measurements of plume radiation in the IR can be influenced by the hot nozzle exit which also emits in the IR.

The presence of hot particles in the exhaust plume generally leads to significant levels of radiation throughout the ultraviolet, visible, and infrared spectral regions. There are also other important particle effects such as the scattering of sunlight and the scattering of emissions from the combustion chamber and other hot parts of the motor known as the "searchlight effect". These scattering effects are considered in the "Secondary Smoke" chapter. The important particle parameters affecting plume signature are their size distribution, temperature, and concentration (Figures 5-6 and 5-7). For certain applications, such as scattering from laser beams, it is also necessary to know the particle shape. Temperature is, in general, dependent upon particle size (i.e. thermal lag), especially for small motors and high altitude plumes. In addition to the preceding flowfield particle parameters, the plume signature also depends upon certain optical parameters, specifically the variation of emissivity with particle size, temperature, and wavelength. The variation of emissivity with size can be computed using Mie theory, it provides the scattering and emitting properties of a spherical particle of known size and refractive index. The assumption of spherical shape is probably acceptable for emission, but it can lead to serious errors in certain scattering properties if the particles are actually non-spherical.

For plume calculations such information about particle properties is not generally available other than that for the more common materials of carbon and Al_2O_3. Values for the absorption coefficient of Aluminium Oxide (leucosapphire) can be three or more orders of magnitude underestimated as experiments with particles in flames have shown. Absorption coefficients and indices of refraction for temperatures up to 2950K are given in Reference 16.

Size of motor and, as indicated in Table 5.5, propellant formulation are two important factors in the computation of radiation from particles within a plume. The optical depth is the relevant non-dimensional parameter for determining the nature of the radiation transport and is the path integration (absorption + extinction) coefficient, or equivalently the ratio of pathlength to photon mean free path. If the motor is small and particles are present in small concentrations only as a stabilizer, the situation is one of low optical depth and the particle continuum and gas band radiation may simply be added together linearly. At higher optical depths the two contributions must be combined in a non-linear fashion. For "black" particles such as carbon, this is easy since the effects of scattering can be neglected. In such cases the plume signatures can be calculated using a simple, one-dimensional line of sight integration as used for gaseous emission. When scattering becomes important the signature calculation is considerably more difficult and must recognise the three-dimensional nature of the radiative transport process. Major interest lies in the detection of incoming tactical missiles and calls for viewing the plume at aspect angles close to the "nose on" direction. Plume obscuration by the missile body reduces the strength of signal available to the search receiver and to model such signature conditions presents a greater challenge than that for broadside viewing.

Common among important particle species in tactical missile plumes are carbon and metal oxides such as Al_2O_3, MgO, ZrO_2, and ZrC. The optical properties of these condensed species are considerably more complex than those of gaseous species such as H_2O and CO_2. Carbon usually occurs as a product of incomplete combustion and it is generally not possible to calculate the soot concentration in a plume a priori. Soot particle sizes tend to be strongly submicron and under certain conditions there is evidence of agglomeration, the building of smaller particles into longer chains. Carbon is a strong emitter over the entire ultraviolet, visible and infrared region. The optical properties are somewhat variable and depend, among other things, upon the hydrogen content. Al_2O_3 occurs either as a product of aluminised propellant combustion or as a stabiliser where it is added directly to the propellant in small quantities to suppress acoustic oscillations in

the motor chamber. The efficiency per gram of a stabilizer material is maximum for particles of micron size without absorbing energy, whereas larger particles have lower surface area per unit mass. Typical radiation mechanisms related to propellants and wavelength region are given in Table 5.5.

TABLE 5.5

RADIATION MECHANISMS/WAVELENGTH REGION

Propellant Type	Radiation Mechanism	Wavelength Region
Aluminised Solid Composites	Al_2O_3 Particle Thermoluminescence	Mid UV-Near UV
	OH, CO + O Chemiluminescence	Near UV
	Al_2O_3, Na D Line Thermoluminescence	Visible
	Al_2O_3, H_2O, CO_2, CO Thermoluminescence	IR
	Al_2O_3, H_2O, CO_2 Thermoluminescence	Far IR

Like the other metal oxides, Al_2O_3 is a large band gap semiconductor in the solid phase. The emissivity is high in the ultraviolet and far infrared but lower in the visible and mid-infrared (transparent regime). To a large extent emissivity in this regime depends upon the semiconductor contamination level. Al_2O_3 is generally liquid in the motor chamber and solidifies in the nozzle and external plume. There have been many attempts to model the formation of Al_2O_3 particles, but progress has been limited by lack of reliable size distribution measurements.

2.4 Classification of Rocket Motor Plume Signatures on Spectral Regions of Emitted Radiation

The design engineer must be aware of the spectral range of plume radiation whether it is his task to provide effective missile detection systems or, in the case of rocket motor design, a stealthy propulsion unit. Equally, he must recognise the spectral discrimination of atmospheric propagation and, in particular, that of the regime under which a given missile operates. Spectral information is important for design purposes since the required techniques for different parts of the electromagnetic spectrum can vary significantly. For instance, it is understood that ultraviolet emission can be dominated by minor constituents of the plume, whereas the infrared signature is generally dominated by the plume species of highest concentration. Theoretical models employ a range of application codes to cover the electromagnetic spectrum.

With a wide available choice of propellants, igniters and materials used for, or in contact with the combustion process it is important to remember that one spectral feature may uniquely identify a missile.

It is possible to classify plume radiation signatures by dividing plume emissions into four principal wavelength regions.

(i)	Ultraviolet:	100 - 400nm
(ii)	Visible:	400 - 700nm
(iii)	Infrared:	700nm - 14μm
(iv)	Microwave:	2 - 300 GHz

The ease with which detection can be achieved within each region will determine its operational importance. Many factors govern the choice such as missle flight altitude and attitude, type of propellant and motor, ways of sensing, and interactions with local environment and atmospheric propagation. Until recently the IR-region was the most studied sub-region in plume radiation investigations, but because of problematic background behaviour in the infrared newly developed sensing devices in the UV-region are gaining in importance. Figure 5-8 defines the IR, visible and UV wavelength regions of interest.

2.4.1 Ultraviolet-Radiation

The Ultraviolet (UV) region can further divide into the vacuum UV (VUV) (0.1μm to 0.2μm), the mid UV (0.2μm to 0.3μm), and the near UV (0.3μm to 0.4μm). At VUV wavelengths atmospheric attenuation limits transmission to extremely short ranges or longer ranges at very high altitudes. Test cell measurements can be made by operating in a vacuum and viewing through appropriate window materials. For tactical missiles the region is of no practical interest. In the mid UV, or solar blind region, atmospheric attenuation limits measurements to rather short ranges but the availability of extremely sensitive detectors and the absence of natural sources in this region make the mid UV an attractive region for the detection of tactical missile plumes. In the near UV atmospheric transmission permits measurements over long ranges, but solar scatter is prominent.

2.4.2 Visible Radiation

Visible radiation is easily detectable by the human eye. Its atmospheric propagation is constrained by water clouds. Very advanced detector technology is available using a range of silicon devices as well as high gain photo multiplier tubes. Principal interests are in the strong sodium (Na) and potassium (K) line emissions (Fig. 5-9 for Na). The emissivity is strong enough to detect impurities at levels of a few parts per million.

2.4.3 Infrared Radiation

The IR region can be further divided into the near IR (0.7μm to 2.5μm), the mid IR (2.5μm to 5μm), the far IR (5μm to 14μm), and the extreme IR (14μm to microwave). These regions have atmospheric transmission windows, with significant naturally occurring background radiation sources.

Species of major interest as sources of IR radiation are the molecular band radiators CO_2 and H_2O with possible additions CO, HCl, HF, N_2O and the condensed particles provided by inorganic oxides and soot etc., radiating as continuum emission. Particle radiation is broadband covering a wide range of the visible and IR regions whereas molecular band radiators tend towards discrete narrow wavebands which may characterise a particular propulsion system.

In the 8.0μm to 14.0μm infrared radiation band particle emission is a strong feature. In the 1.5μm to 5.0μm region narrow band molecular radiators will be found, 1.5μm to 3.0μm is dominated by H_2O while CO_2 and CO populate the region 3.0μm to 5.0μm together with other species depending upon propellant composition, Some continuum emission will also be present.

The near IR, especially 0.7μm to 1.1μm, is of significance due to the availability of inexpensive, uncooled silicon array detectors for imaging devices. Other uncooled detectors (e.g. pyroelectrics of Ge) are also used in this region.

2.5 Plume Flowfield Properties and Motor Design

The potential use of plume electromagnetic radiation to uniquely describe a missile for whatever purpose requires detailed knowledge of the exhaust flowfield properties that generate the chemi-physical emission mechanisms. Development of the flowfield is governed initially by conditions inside the combustion chamber starting with the propellant, its formulation and the conditions under which it burns, the acceleration of gases through the nozzle throat and their controlled expansion to meet the ambient conditions external to the motor at the nozzle exit. Fuel rich gases exiting the nozzle mix with oxygen from the surrounding air to promote secondary combustion (afterburning) creating an exhaust flowfield which is a fiercely burning, highly turbulent gas jet. Downstream of the nozzle exit the development of this flowfield is strongly influenced by the flight operating regime. Examples of such influences include pressure changes with altitude, missile forward velocity, base recirculation, flight attitude and whether or not plume combustion is supported throughout the whole of flight. These properties can affect

spatial radiation distributions and the quality of mixing in the afterburning region which, in turn, affects temporal radiation fluctuations.

From the foregoing it is clear that plume radiation signatures for a given motor can vary widely depending upon the conditions under which measurements are performed, ranging from those of static firings to those of flight tests. Comparison and assessment of missile plume radiation signatures should be made utilizing information from a variety of sources, using motor properties, flow field parameters and experimental test results. A listing to indicate the relevant data required would read :-

(i) Motor properties promoting the flowfield

- Propellant formulation including trace elements which might create non equilibrium phenomena producing highly excited states
- Thrust and massflow
- Combustion chamber properties
- Nozzle geometry and exit Mach number
- Presence of flame suppressants
- If a liquid engine, then fuel and oxidant composition and fuel ratio (F/O)

An example of a one dimensional kinetic analysis is shown in Table 5.6 and a calculation of Plume Radiance using the parameters of Table 5.6 in Figure 5-10.

(ii) Static firing radiation measurements

- Results of radiometric measurements
- Results of spectrographic measurements
- Measured motor parameters
- Viewing geometry and range
- Atmospheric conditions

(iii) Flight radiation measurements

- Results of radiometric measurements
- Results of spectrographic measurements
- Time history of flight to relate to measurements
- Atmospheric conditions

Time history of flight must recognise the missile altitude, velocity, roll rate, attitude, range and geometric relationship between the plume and measuring instrument for any instant during flight

(iv) Influences of environment

- Flight trajectory
- Altitude regime
- Constituents of surrounding air and mixing

TABLE 5.6

ROCKET ENGINE EXIT PLANE FLOWFIELD PARAMETERS/CHEMICAL COMPOSITION

Flowfield Parameters			Chemical Composition (Mole fraction, Xi)		
M	=	2.2	CO	=	164
PS	=	36.67 kN m^{-2}	CO_2	=	.2096
V	=	2036 ms^{-1}	H	=	.0416
T	=	2199 K	HO_2	=	.0000712
MW	=	26.14 lbm/lbm mole	H_2	=	.0324
Γ	=	1.23	H_2O	=	.2843
			O	=	.0458
			OH	=	.0514
			O_2	=	.1704

The plume shock structure of a rocket motor operating at simulated flight velocity of Mach 2 is shown in Figure 5-11 and is based on photographs and pressure measurements. The motor exhaust flow expands to an altitude static pressure and intersects with the supersonic free-stream airflow. The exhaust gases mix with the gases in the base recirculation zone which, in turn, mix with the free-stream airflow. At the point of intersection between the exhaust flow and the airflow, mixing continues directly between the two streams, and the mixing region increases in size downstream. At the intersection point, two shock waves are formed. The airflow-plume interaction shock diverges from the centre line whilst a barrel shock is formed from a series of compression waves generated by the turning of the exhaust flow. The barrel shock coalesces with the recompression shock to produce a strong shock which converges to the triple point where two more shock waves are formed. The shock wave normal to the axis of flow is called a Mach disk. The other shock diverges from the centre line to the plume boundary where another set of shock waves is formed. The converging shock wave, Mach disk, and diverging shock wave pattern is repeated downstream. The flow downstream of each Mach disk (normal shock wave) is subsonic and is reaccelerated to supersonic flow at the sonic line.

3 ASSESSMENT METHODS OF PLUME RADIATION - DETAILED DESCRIPTION

There are no generally accepted standards or methods in use to assess the radiation properties of rocket motor exhausts. If the radiation producing mechanisms are known to a certain degree of confidence then other aspects to be taken into account are :-

(i) the opacity of the plume with respect to its own emissions to determine the radiation exiting the plume. This will depend on the size and concentrations within the plume and the existence of any quenching molecules.

(ii) the opacity of the plume's immediate environment to the radiation released from the plume which would, for example, include smoke or any other form of local obscuration in the line-of-sight to the observer.

(iii) the complex and multiparametric problems of solar illumination, background radiation and atmospheric transmission where "windows" exist subject to various loss mechanisms such as Rayleigh and Mie scattering, molecular absorption and aerosol attenuation. Figure 5-12 shows atmospheric transmission windows.

3.1 Experimental Methods

The majority of experimental methods used to assess plume radiation employ one or more of three types of instrument

(i) radiometric devices which measure radiation intensity in a specific, broadband spectral region

(ii) spectrometric devices which measure the radiated plume intensity as a function of wavelength

(iii) imaging devices which record intensities and radiating plume geometries on a time scale given by the camera type

It is important to note that spectral measurements permit statements to be made about the chemical composition of a plume leading to the possibility of positive missile identification.

3.1.1 Radiation Essentials

As measurements depend to a large extent on "state of the art" instrumentation we shall avoid detailed descriptions of equipment. An

outline of how to proceed is given in Figures 5-13 to 5-15. Figure 5-13 is essentially a diagram of the radiative heat transfer equation, in Figure 5-14 detectors and artificial light sources over a broad spectral range are given and in Figure 5-15 a calibration procedure for a camera/radiometer is presented in a general graphical form.

3.1.2 Test Techniques

Backed by technical and financial feasibility, rocket motor plume radiation characteristics may be determined using a variety of techniques selected to focus upon the parameter of interest with the desired accuracy for the characterization.

Plume characterisation may be performed by computations, measurements during static, sea-level tests, simulation chamber tests, or flight tests. In principle, the flight test is superior in that it provides a real environment but the cost and measurement difficulties make it generally prohibitive. Testing under simulated conditions and simple static testing follow in order of reduced expense and complexity. The alternative, that of computer based theoretical modelling, is attractive but demands of confidence usually make validation by test firings necessary.

3.1.2.1 Static Testing

Open site, ground level, static testing of a solid propellant rocket provides access to the plume by radiometric instrumentation. It is the cheapest and easiest test to conduct. In terms of utility it is the least desirable since the rocket motor does not experience the conditions found in flight, consequently the static plume does not have burning characteristics identical to those in flight. Plume spectral and spatial radiation properties may be measured and used to validate predictive codes for the static condition. Recognising the limitations, the results of prediction and measurement combine to provide a strong indication of overall plume behaviour.

Atmospheric interference can affect measurements in this type of test, particularly over long ranges. It is necessary to adequately determine attendant atmospheric conditions to calculate signal losses. Normally atmospheric temperature, pressure, humidity, visibility, composition, and wind speed are recorded.

During a static test general motor performance is monitored. Dimensions, propellant formulations, and the like are predetermined but performance parameters such as thrust, chamber pressure, temperature, and body deformation can be measured.

Instrumentation deployment is relatively straightforward with fields of view and ranges stationary and easily determined. Limitations only exist where constraints produced by the test stand and terrain are encountered.

3.1.2.2 Altitude Chambers

Large vacuum chambers exist capable of testing full-scale models and subsystems up to simulated altitudes of 30km. Near field data (nominally one exit diameter) can be acquired which are useful for start conditions to code predictions. An example is given in Figure 5-16.

3.1.2.3 Simulated Flight Facilities

Testing a solid rocket motor under simulated flight conditions provides a more realistic plume than a static firing but often has restricted access to the plume by radiometric instrumentation. Flight simulation is more expensive than the static test although it is far easier and cheaper to conduct than a flight trial. In terms of utility it allows some parameter changes but still may not produce the true characteristics of the flight plume, especially when scaled models are used. Parameters considered for measurement in static tests apply equally to flight simulation and are increased in number by those introduced by simulation.

Test cells are available which can simulate flight conditions from sea level to altitudes of some 25km and from subsonic velocity to over M3.0. The capability exists for full operational speed manoeuvres. Facilities are flexible enough

to accommodate the complete propulsion system and during simulated flight tests, conditioned air flows past a stationary model and flight characteristics are measured. The airflow can be distorted to simulate conditions found in actual flight manoeuvres.

Simulated flight facilities can offer realistic flight environments for near and mid fields of the plume, however, the far field plume is generally perturbed by shocks and/or flow disturbances from the test section walls. Generally, the simulated flight facility is limited to small scale vehicles and reduced exhaust gas mass flows. Testing rocket systems and subsystems under simulated flight conditions permits early detection of hardware problems and, through recordings and analysis, a solution can be found before production begins. Equally, it allows the qualification of systems for flight and opportunities for diagnosis where problems exist with systems in operational use. (Fig. 5-17 and Fig. 5-18.)

The major advantage of testing tactical missiles under controlled simulated flight conditions is the ability to conduct extensive plume flowfield and radiometric measurements of a given phenomenon to acquire data to validate flowfield and radiative predictive codes. The major disadvantage is the inability to acquire far field data and perhaps that flight condition which identifies the onset or termination of afterburning.

3.1.2.4 Flight Tests

Flight tests offer true realism but they are expensive and present extreme experimental difficulties. Observations (measurements) may be from fixed or mobile sites. Instrumentation may be ground based with either fixed or tracking mounts, it may be mounted on mobile carriers (such as a tracking aircraft or missile), or it may be mounted on the test vehicle. Generally, limited instrumentation is available from observation platforms to assist in the full characterisation of the plume signature.

As with static measurements these tests suffer atmospheric effects which confuse measured quantities, consequently, a need exists to adequately monitor atmospheric conditions. Normally, atmospheric temperature, pressure, humidity, visibility, composition, and wind conditions are determined.

Trajectory and range are also of great importance both from the point of determining atmospheric effects as well as basic interpretation of results and must be adequately addressed.

3.2 Calculation Methods

Any attempt to model plume radiation from rocket motors must rely upon the construction of a theoretical plume in which flowfield properties are structured so as to interface with radiation application codes. Many such codes are split into :-

(i) a thermodynamic part (with input parameters such as propellant composition, pressure, temperature, expansion ratio etc.),

(ii) a flowfield part (with input parameters such as nozzle exit plane data, relevant motor design features, relevant chemical reactions with non-equilibrium chemistry solutions, turbulence model, atmospheric data, altitude and velocity, etc.),

(iii) a radiation part (with input parameters like output from flow field structure, emitting chemical species, molecular band model, gaseous and particle radiation, scattering, quenching, geometry, aspect angle, from which you can to a certain extent derive the plume radiation properties within a limited spectral and intensity range.

3.2.1 Plume Fluid Dynamics of Tactical Missiles

Calculation methods [14] [15] for plume

fluid dynamics have been established in various countries like the USA, Great Britain and France. They all have a similar approach to solving problems. Most of the advanced codes are classified. Here, as an example, we describe in more detail the American Standard Plume Flowfield (SPF) model. In Great Britain the code being used is called REP (Rocket Exhaust Plume).

A starting point for surveying the status of plume flowfield models prior to year 1964 is Chapter 2 of the Rocket Exhaust Plume Technology Handbook prepared for JANNAF (Joint Army, Navy, NASA, and Air Force agencies). At this time, the "standardized" US plume model was the Low Altitude Parabolic Plume (LAPP) code developed at the AeroChem Corporation. The LAPP code is a balanced pressure farfield plume model that contains a generalised, fully implicit, chemical kinetics package. Its use is restricted to engineering studies geared to predicting plume "observables", and simplistic procedures are used to "globally" represent the influence of the nearfield structure. During the period 1975-1976, an advanced plume model was developed at General Applied Science Laboratories (GASL) which solved the viscous/inviscid nearfield structure in detail using boundary layer type coupling concepts, and contained a two-equation, compressibility corrected turbulence model

Development of plume flowfield models is an evolutionary process to include additional physical phenomena and more efficient numerics. Physical processes are added as they are better understood and as dictated to improve the accuracy of the prediction model. Numerics are also changed to decrease computer run time when feasible.

A JANNAF program was initiated in 1978 to combine the features of the GASL and LAPP codes which is now known as JANNAF "Standardized Plume Flowfield" (SPF) model. The current version is SPFIII. It is the primary tool in the US to analyse tactical missiles exhaust plumes. The modular structure and computational techniques used in the basic SPF are given in the following Block Schematic.

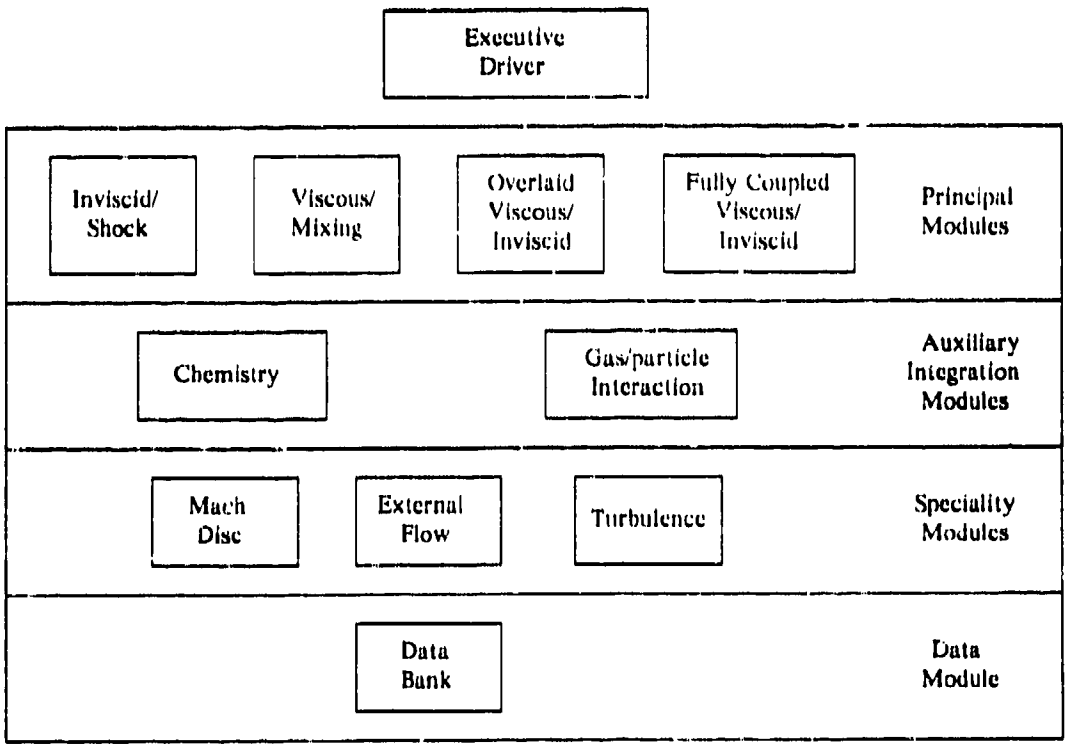

Block Schematic Modular Structure of JANNAF SPF

Versions of the JANNAF SPF

The JANNAF SPF is a computer code comprising a unified series of "modules" which provide for integrations of the flow equations in various flow regions, the inclusion of generalised chemical kinetics, two-phase flow interactions and various turbulence models, and the specialised procedures for interfacing with the external flow and treating embedded subsonic zones behind Mach discs.

SPF Models

The SPF model is built upon two principal components. One is a shock-capturing inviscid plume model (entitled SCIPPY) and the other, a turbulent mixing/afterburning model (entitled BOAT). In the plume nearfield, an overlaid procedure is utilized to couple the viscous shear layer and inviscid plume solutions; in the farfield, a constant pressure mixing solution is utilized. The Mach disc problem is treated inviscidly using a sting-approximation for small discs and the Abbett procedure for larger discs.

SPF is limited to the analysis of single phase exhausts but can treat two-phase exhausts in the equilibrated mixture limit.

Originally, SCIPPY and BOAT served as the principal components, extended to incorporate two-phase non-equilibrium effects. In particular, the two-phase flow version of SCIPPY uses numerical techniques, while the two-phase version of BOAT utilizes a particulate turbulence model formulation.

Subsequently, plume modification techniques were incorporated to solve the concurrent viscous/ inviscid processes occurring in streamline displacement effects on the pressure field. This approach is implemented within the confines of the two-step overlaid method via extensions to only the shock-capturing SCIPPY model which permits PNS spatial matching through this region (i.e., the extended version of SCIPPY calculates the inviscid nearfield structure and the coupled Mach disc mixing region in a one pass mode of operation). With this added capability, the "inviscid" flow map accounts for the strongly interactive effects of the Mach disc mixing region on the outer inviscid structure (i.e., the position of the inviscid plume slipstream is altered by the Mach disc mixing process, etc.). It also contains the detailed structure of the viscous/inviscid flow in the Mach disc mixing region, including the turbulence properties needed to properly merge the plume and Mach disc mixing layers.

The SPF analysis of a two-phase plume requires the stipulation of nozzle exit plane conditions to initialize the calculation, based on a comparable treatment of non-equilibrium processes in the nozzle. A standardized code to provide such a nozzle solution is currently not available. Modifications are being incorporated into the latest version of SPF that deal with the strongly interactive phenomena associated with plume/missile airframe interactions and the fully viscous transitional region of the plume. The formerly utilized overlaid coupling procedure thus becomes inadequate and parabolized Navier-Stokes methodology is required. The latest SPF model is being developed to provide these types of strongly interactive capabilities [17].

3.2.2 Listing of National Codes

Outline details of these codes can be found in Appendix 3.

3.2.3 Validation of Plume Radiation Calculations by Experiment

Validation exists for the infrared and visible regions, in many instances with sensible agreement taking into account the limitations of measurement conditions like altitude, range of motor size or simplified propellant constituents. In certain circumstances not enough parameters can be incorporated into the calculation methods to yield global emission characteristics.

The infrared region 1.5μm to 3μm is mainly concerned with water bands, these are strong emitters but radiation suffers from heavy absorption through the atmosphere and detection

ranges are short consequently little interest is shown in this waveband.

Much interest has focused on "CO_2 blue spike" radiation a common feature in rocket exhausts. It occurs in the very narrow spectral band of 4.17μm to 4.19μm, has good atmospheric transmission properties and lends itself to easy selection because of its narrow profile. Background and other spectral interference can be minimised by the use of narrow band optical filters. Line-by-line methods for modelling the blue spike have produced absolute spectral radiant intensities that agree to within about 20% of measured values.

Emissions in the 4.2μm to 5μm region come largely from CO_2 asymmetric stretch vibrations with contributions from CO and some N_2O. They form what is termed the "red wing". Because a great number of individual rotational lines contribute to the radiation, the theoretical concept is to divide the spectral base into a number of bands each overlaying a number of rotational lines. Each molecule in each band is given parameters describing effective strength and shape and these quantities go to form the emission spectrum. As might be expected this calculation method is known as a "band model" and can equally be applied to the 1.5μm to 3μm spectral region.

Band model predictions have been compared with experiments made over a wide range of circumstances resulting in a mixture of agreement. It has been argued that the uncertainty in absolute spectral radiant intensity given by predictions is typically a factor of 2 although this varies up or down with the complexity of modelling circumstances.

Propellant metal impurities such as sodium and potassium, catalyst metals, ballistic modifiers and others form a ready source of atoms from which visible radiation can take place. Line emissions from the first resonance doublet of sodium and potassium atoms are prominent in afterburning rocket exhausts. For these and other line emissions a line-by-line prediction model is adopted for the calculation of spectral radiant intensities. Lorentz and Doppler broadening occurs and a Voight profile is commonly used to describe line shapes. Although good agreement is sometimes achieved, it is considered that uncertainties in the plume flowfield structure and the radiation model, particularly collision broadening parameters, can justify no better uncertainty factor than 3 in absolute radiant intensity.

Theoretical plume flowfield models have not been directly validated due to the difficulties in measuring the relevant plume properties, i.e. spatial distributions of temperature, pressure and concentrations of chemical species etc. Laser diagnostic techniques are showing promise in this field of work, particularly since the laser beam does not disturb the medium under investigation. Some examples of validation of theory by experiment are given in Figures 5-19 and 5-20.

3.2.4 Limitations of Computer Codes

Limiting factors are :-

(i) lack of optical property data to adequately describe particles and radiating gases

(ii) lack of codes to handle base flow and a inadequacy showing the uncertainties of turbulent chemical interaction models

(iii) cessation of afterburning especially at high altitudes

(iv) incomplete treatment of particle multiple scattering

(v) the use of simplified assumptions such as steady state conditions only, simple geometries, no compression zones with perpendicular collisions.

3.3 Discussion of Plume Influencing Aspects

Afterburning is a major plume effect. The

nozzle area ratio is an important factor in the prevention of afterburning especially when considering radiation in the UV spectral region. Base flow recirculation affects afterburning, in many instances anchoring the flame to the base region. Contributions to plume radiation are strongly affected by propellant formulation, high metallic content produces a high continuum radiation in addition to gaseous emissions. Particle optical properties are very important, especially in areas where there are no molecular spectra. They also influence scattering losses and the "searchlight effect".

Uncoupling turbulence-chemistry interactions in steady-state plume models may have a significant effect on the predicted radiation observed from all angles of view, especially those far from broadside.

Free-free electron emission (Bremsstrahlung) is probably the dominant mechanism for millimetric emissions.

Flame suppression in the exhaust brings about a marked reduction in infrared emission, for instance, it has been found to reduce the Red Wing (4.4μm to 5.0μm) by more than an order of magnitude.

Conditions favouring flame suppression are :-

(i) Low exit plane temperatures

(ii) Low concentrations of plume particulates

(iii) Nozzle imperfections (any step or burr increasing turbulence)

(iv) Choice of propellant and suppressant

Plume suppression can be assisted by the introduction of additives into certain propellants to accelerate removal of flame radicals H and OH. An example of the affect of plume suppression is given for a double base propellant in Figures 5-21 to 5-23 where the main sources of IR radiation are molecular band radiation such as CO_2 and H_2 (CO is also important if the exhaust is suppressed). Figure 5-21 shows a dramatic fall in plume temperature for the flame suppressed case. This drop in temperature is accompanied by reduced levels of CO_2 and CO emissions as indicated in Figure 5-22 and again the presence of recirculation in Figure 5-23. Some continuum infrared radiation may arise from condensed particles such as ballistic modifiers or igniter products. The latter produce radiation over a wide range of both visible and infrared wavelengths while the former gives rise to characteristic emissions in specific wavebands. Band radiation from H_2O and CO_2 at wavelengths 1.5μm to 3.0μm and 4.0μm to 5.0μm are important in the context of detection.

Spatial distributions of broad-band infrared radiation have been computed by the so-called "nearly-weak/nearly-strong" band model for an exhaust plume in which recirculation was expected to be important. Figure 5-23 presents predicted and measured station radiations (obtained by integrating the radiation across a vertical diameter of the exhaust and referred to a specified axial increment) in the waveband 4.3 μm to 4.7 μm from CO_2 and CO. Calculated absolute spectral radiant intensities for a given exhaust, viewed as a whole, may have an uncertainty factor of about 2. The predictions underline the significance of including an analysis of base-recirculation in calculations when relevant.

4 RECOMMENDATIONS

4.1 General

Knowledge of rocket plume radiation properties is important in the context of guidance, tracking and detection. It is expensive and often difficult to measure these radiation properties and to determine their dependence on operational parameters like missile forward velocity, range, altitude and aspect angle. It is even more difficult to acquire this information about rocket motors of an adversary. To ensure guidance system integrity, to avoid interference with

friendly radiation sensors and to deny an adversary detection opportunities, the rocket plume and its properties must be regarded as an integral part of the missile system and, where possible "tailored" to meet operational needs.

Systems assessment teams may typically seek to know whether a flare need be attached to a missile as a tracking aid, or whether radiation from the exhausts of hostile missiles are likely to be of a magnitude permitting early detection, or whether emissions from the exhausts of a friendly missile will render it vulnerable to enemy countermeasures. Such questions can best be addressed by involvement in plume studies at the time of system feasibility and design, at a stage when accurate predictions are paramount and when validatory experimental rocket firings can be performed.

The countermeasures engineer, with a different viewpoint to that of the missile engineer, will nevertheless see the need for a similar approach in his efforts to combat an intruder. He will find it important to establish spatial and spectral distributions of radiated energy with instruments having good sensitivity and high spectral and spatial resolution to unambiguously identify missiles and minimise false alarm rates.

The following recommendations comprise a procedure for assessing rocket plume radiation that will enable uniform application of technology to :-

(i) set quantitative technical requirements on rocket motor signature.

(ii) compare rocket motors

(iii) recommend a terminology related to plume radiation based on quantitative criteria.

4.2 Recommended Test - Prediction Procedure

In trying to propose a standardised test technique for the assessment of plume radiation properties a general outline is given here. Its feasibility depends to a large extent on the availability of necessary measuring devices and instrumentation, rocket motors and prediction codes. The logic behind the assessment process is as follows :-

(i) Define the objective(s) and requirements.

(ii) Define the needed data base and the experimental approach to ensure that objectives are accomplished.

(iii) Set up and calibrate equipment.

(iv) Run most appropriate test to acquire data base.

(v) Run necessary/available plume and radiation codes to match acquired data base.

(vi) Use measured results for theoretical model validation.

(vii) Use validated plume and radiation codes to predict plume properties at conditions appropriate to the defined objective.

(viii) Present results, stating all assumptions and code modifications and using standard terminology and units.

The following eight steps enlarge on these concepts :-

Step 1 :- Clear definition of objectives and the requirements to meet those objectives may be the most difficult part of a programme to conduct successfully. The objectives might read :-

(i) detect, identify, track and destroy a target

(ii) detect, identify a missile threat and counter with evasive action

(iii) assess the feasibility of guidance and tracking methods

(iv) develop a threat countermeasure

(v) acquire phenomenology data for code validation

(vi) influence motor design with signature control proposal

At this stage it is important to define the system and the spectral regions in which it is to function. If, for instance, a detection system is called for, then specific details of sensor wavelength, bandwidth, resolution, limiting noise level and environmental details that affect signal transmission and distortion must be considered. There should be no compromise at this step, it is the least expensive to perform and study topics overlooked at this point may remain overlooked to the detriment of the system or be costly to introduce later in the programme. It is better and more cost effective to include tasks of potential value in the definition stage even if, for whatever reason, they subsequently become redundant.

Step 2 :- Defining the information needed for a project data base and the measurements required to obtain that information usually calls for a compromise dictated by available funding. Within financial constraints the objectives in Step 1 are assessed and the requirements and limits set. One obvious compromise comes in the choice between flight tests and those undertaken in dedicated ground facilities where it is possible to use scaled, heavyweight test motors with reusable hardware. Use of the wind tunnel, altitude chamber or static test site combined with standard measuring instrumentation will often satisfy most, if not all, of the data base requirements. Rocket motor experiments involve many technical staff and it is vital that test procedures are thoroughly documented and the staff cognizant of the data gathering process.

The prospect of meeting an objective is advanced by the prudent use of theoretical predictions and experiment. Theoretical studies may play a part in planning the course of an experimental programme. Before embarking on such a programme several questions are posed, not least among them is whether an experiment can be mounted that will directly or indirectly provide the data to satisfy the objective. The answer will depend upon the existence of test vehicles, test firing facilities and the correct diagnostic instrumentation. Test vehicles are generally available for ground or flight tests. However, should the missile of an adversary be under investigation then the supply of a test vehicle is improbable. In such a case calculations are made using whatever data is available and rare experimental firings would only be those to study the phenomena for prediction validation purposes. The choice of test facility, whether it be static, sea-level, an altitude chamber or wind tunnel depends upon the simulation desired. The advantages and disadvantages of each were considered in Section 3.1.2 "Test Techniques". Obviously a well conceived and controlled flight trial is preferable but the advantages are weighed down by costs which prohibit their use to other than final validation of the overall programme.

The selection of diagnostic instrumentation is governed by the radiation properties to be measured, focusing on spectral wavelength range, radiance level, spectral, spatial and temporal resolution and sensor sensitivity and speed. Flow charts are presented as guidelines in Figures 5-24 to 5-26. Types of optical detectors are shown in Figure 5-24. Radiometric measurements are presented in Figure 5-25 followed by a typical radiometric measurement system in Figure 5-26. To avoid later problems it is important to ensure that the instrumentation selected is well able to meet all the measurement demands and that it is backed by a full data analysis capability.

Step 3 :- The importance of accurate calibration, as indicated by Figure 5-27, cannot be overemphasised. Measurements can be complicated or invalidated by atmospheric absorption or extinction, obscuration by smoke, impractical or impossible sensor positioning and carelessness in ignoring background signature effects. It is a valuable exercise to rehearse the entire test

procedure to identify and eliminate any interference between instruments or power circuits that might cause a later test failure.

Step 4 :- The way in which the experiment is conducted (Section 3.1) is a critical factor in the acquisition of good data. Details of motor performance, its environmental test conditions such as Mach number, altitude and trajectory ; the deployment of instrumentation giving aspect angles, atmospheric transmission path, fields of view and the like, all contribute essential information for analysis and project assessment. Radiometric requirements were discussed in Section 3.1.1. Where similar instruments are used they should show a consistency of measurement and all instruments should have a specified accuracy. Error limits should be assigned to all data sets recorded and assumptions, where made, documented. If the preceding steps have been properly observed the measurement programme should be successful. To mitigate the effects of any equipment failure during a test firing it may be possible to duplicate some essential measurements. Instruments should be sited to guard against acoustic and ground-borne vibration, equally they should be protected from the possibility of rocket motor failure.

Step 5 :- The purpose of this step is to formulate techniques for calculating plume radiation signatures against test data obtained from the foregoing steps. To compare calculated levels of plume radiation with measured test results the parameters pertaining to the test conditions must be used as input data for calculations. The measure of agreement coming from these comparisons will determine the confidence placed on the calculations for use where measurements are not possible.

A plume flowfield should be calculated for the conditions under which the actual test took place, observing the precise propellant composition with trace metal impurities and motor design features affecting gas flow. Radiation codes should reflect sensor wavelengths together with their deployment positions and plume viewing aspect angles, the spatial and temporal nature of the radiation and the atmospheric signal attenuation. If measurements are made in a wind tunnel or on a missile plume in flight, the appropriate free-stream flow conditions must be known.

Predictions of rocket exhaust properties generally follow the stages indicated in Figure 5-28. First an equilibrium chemistry code is used to calculate chamber conditions and the temperature, pressure and equilibrium chemical species concentrations at the nozzle throat. Nozzle expansion flow calculations may be made in a number of ways ranging from one-dimensional chemical equilibrium, to three-dimensional multi-phase flow with chemical kinetics. The exhaust structure for static motor firings can usually be well simulated by a finite difference marching program (such as REP or SPF) which gives spatial distributions of non-equilibrium chemical species, temperature, velocity, pressure, and turbulent mixing based on limited assumptions. For wind tunnel and flight plumes, base recirculation or separated flow effects with non-equilibrium chemistry may have to be included to obtain more accurate calculations of plume structure. The appropriate applications code(s) are then applied to the calculated flowfield using the test geometry and applicable transmission path effects to obtain the results that may be compared with the measured data base.

Step 6 :- Comparison between calculated and measured values often yields discrepancies. In this step appropriate, judicious adjustments to the calculations are made within underlying scientific bounds to give closer agreement with measured values. For instance, if the near field radiation includes a searchlight effect, the measured plume continuum radiation will be larger than that predicted by a code ignoring such effects. The demands of prediction accuracy may require modification of the code to accommodate this feature. Alternatively, disagreement between data and prediction may be caused by different phenomena. An impurity in the propellant, such as sodium, may produce strong emissions in the visible spectrum that are not predicted by the

code. This may be the result of excluding sodium reactions from the plume flowfield calculations or an inability of the radiation code to predict these line emissions.

A prediction technique is strengthened if it can be confirmed against a range of conditions, including flight. Although these conditions may not completely match those for the systems of interest (e.g. a different motor) the validation process increases confidence in the calculation, putting it on a much broader base.

Step 7 :- This is the step where plume flowfield and application codes are run for the operational conditions of interest. Predicted values of plume signature and other effects yield information from which decisions about system design, tactics and other system-level parameters may be made. Depending upon the codes used for the specific test and operational conditions, improvements can be achieved when :-

(i) allowance is made for radial pressure gradients.

(ii) non-equilibrium two-phase flow (thermal and velocity lags of condensed particles) is included.

(iii) "base flow effects" are included, i.e. when a flight missile has a base diameter significantly greater than the nozzle exit diameter.

(iv) shock structure effects are treated

If, for instance, the missile has a large base diameter which could induce base flow recirculation and afterburning, a code without a baseflow model would not be applicable, equally, inappropriate choice of chemical mechanisms can produce false plume properties resulting in incorrect emission data. It is essential that the thermodynamic, chemical and physical attributes of the plume modelled by the code, the model limitations and the necessity for enlightened use of input data should be thoroughly understood if accurate analytical assessment is to be performed. After proper validation the code can be applied to meet the overall system objectives.

Step 8 :- With the continued advance of computer use in experiments and modelling the analysis of results becomes more "machine dependent" and the user faces the problems of incompatibility of operating systems for information exchange and languages used to describe the information.

Suggested data to characterise a plume signature are :-

(i) Spectral radiance vs wavelength (spectrometers) and versus time

(ii) In-band radiance vs time (radiometers)

(iii) Radiant intensity vs time

Other types of data presentation helpful in evaluating the signature are :-

(i) Video tapes from imaging sensors which provide a "false colour" image of in-band radiance versus position. Their use is for subsequent analysis of spatial fluctuations, spectral irradiance, shape and geometry of the radiating plume (isoradiance contours). In-band radiance plume radial and/or axial profiles within the image field allow the assessment of radial symmetry, axial decay etc. A properly calibrated video tape can be examined pixel by pixel to obtain information about the temporal and spatial distribution of "in-band" radiance from the plume.

(ii) Power spectral density plots which may be performed on the radiometric data to determine plume frequencies.

(iii) Radiant intensity vs time for variations in Mach numbers, alti-

tude, etc.

An experienced approach to data reduction is necessary to ensure that proper interpretations are made for code validation and the provision of sufficient information for their modification. Of primary importance is the correct data for atmospheric absorption as discussed in Section 3.

Documentation of records should be comprehensive such that there will be no need to repeat the work should future interest arise. Terminology should follow the accepted standards given in this report and universal SI-units, as defined in Table 5.7, should be used.

TABLE 5.7

TERMINOLOGY OF INFRARED SPECTROMETRY AND RADIOMETRY

Symbol	Term		Units
Φ	radiant power power	rate of transfer of radiant energy	W
$\Phi(\lambda)$	spectral radiant power	rate of transfer of radiant energy per unit wavelength interval centred at wavelength λ	$W\ \mu m^{-1}$
I	radiant intensity	radiant power emitted by a source into a unit solid angle	Wsr^{-1}
$I(\lambda)$	spectral radiant intensity	radiant intensity per unit wavelength interval centred at wavelength λ	$Wsr^{-1}\ \mu m^{-1}$
L	radiance	radiant power emitted by unit area of a source into a unit solid angle	$Wm^{-2}sr^{-1}$
$L(\lambda)$	spectral radiance	radiance per unit wavelength interval centred at wavelength λ	$Wm^{-2}sr^{-1}\mu m^{-1}$
E	irradiance	radiant power incident upon unit area of a	Wm^{-2}
$E(\lambda)$	spectral irradiance	irradiance per unit wavelength interval centred at wavelength λ	$Wm^{-2}\mu m^{-1}$
R_p	radiant power responsivity	the output of an instrument for unit radiant power input	instrument units W^{-1}
$R_p(\lambda)$	spectral radiant power responsivity	radiant power responsivity per unit interval centred at wavelength λ	instrument units $W^{-1}\mu m^{-1}$

Notes 1 The output signal of radiometers and spectrometers is the output voltage of the instrument detector/pre-amplifier combination modified by subsequent electronic and mathematical signal conditioning. When used in evaluating R_p and $R_p(\lambda)$ it is usually referred to as a standard gain configuration of any variable gain amplifiers.

5 REFERENCES

1 JANNAF Handbook
Rocket Exhaust Plume Technology
Chapter 3, Rocket Exhaust Plume Radiation
CPIA Publication 263, May 1980

2 Eerkens, J W et al
Rocket Radiation Handbook:

Volume I: Rocket Radiation Phenomenology and Theory (1974)
Volume II: Model Equations for Photo Emission Rates and Absorption Cross-Sections (1973)
Volume III: Fundamentals of Photonics
Volume IV: Gas Dynamics and Flow-Fields of Rocket Exhausts
Volume V: Atmospheric Properties and Optical Transmission
Volume VI: Radiation Sensing Systems Theory

US Department of Commerce, National Technical Information Service

3 Wolfe W L, Zissis G J ed,
The Infrared Handbook, Office of Naval Research, Dept of the Navy, Washington DC (1978)

4 Gaydon, A G
The Spectroscopy of Flames
John Wiley & Sons Inc, New York (1957)

5 Gaydon, A G and Wolfhard, H G
Flames: Their Structure, Radiation and Temperature
Chapman and Hall Ltd, London (1970)

6 Ludwig, C B, et al
Handbook of Infrared Radiation from Combustion Gases
NASA SP-3080 (1973)

7 Lyons, R B, Wormhoudt, J and Kolb, C E
Calculation of Visible Radiation from Missile Plumes
AIAA-81-1111 (1981)

8 Kolb, C E, Ryall, S B and Wormhoudt, J C
Proceedings of SPIE, Vol 932, 2, April 1988
The Chemical Physics of UV Rocket Plume Signatures

9 Rothschild, W J, Martin, C W
Experimental Results for Hydrocarbon Exhaust Infrared Model Verification
Air Force Armament Laboratory: AFATL-76-74 (1976)

10 Sukanek, P C, Davis, L P
An Assessment of the NASA Band Model Formulation for Calculating the Radiance and Transmission of Hot and Cool Gases
Air Force Rocket Propulsion Laboratory: AFRPL-76-9 (1976)

11 Jeffrew, W, et al
Rocket Engine Exhaust Plume Temperature Profile by Line Reversal Technique
Air Force Armament Laboratory: AFATL-TR-77-50 (1977)

12 Stephen, J Young
Inversion of Plume Radiance and Absorptance Data for Temperature and Concentration
Air Force Rocket Propulsion Laboratory AFRPL-TR-78-60 (1978)

13 Dennis, R, et al
Photographic Spectroscopic Measurement of Ultraviolet Solid Rocket Motor Plumes
The University of Tennessee Space Institute Tullahoma, Tennessee (1980)

14 Dash, S M
Analysis of Exhaust Plumes and Their Interaction with Missile Airframes, from Tactical Missile Aerodynamics, ed Hemsch, M J, Vol 104, AIAA. New York (1986)

15 Dash, S M, Wolf, D E, Beddini, R A and Pergamont, H S
Analysis of Two-Phase Flow Processes in Rocket Exhaust Plumes
J Spacecraft Vol 22, No 3 (1985)

16 Linghard Yu K, Petrov V A and Tikkonova, N A
Optical Properties of Leucosapphire at High Temperatures
Institute of High Temperatures, Academy of Sciences of the USSR
Translated from Teplofizka Vysokikh Temperature Vol 20, No 6 pp 1085-1092, Nov-Dec 1982

17 Dash, S M
Analysis of Tactical Missile External Plume Interaction Flow fields
Agard Symposium on Missile Aerodynamics
Friedrichsafen, FRG, April 23-26 1990

18 Slack, M and Gillow, A
High Temperature Rate Coefficient Measurement of CO + O Chemiluminescence
Combustion and Flame Vol 59 pp 186-196 1985

FIGURES

TABLE OF CONTENTS

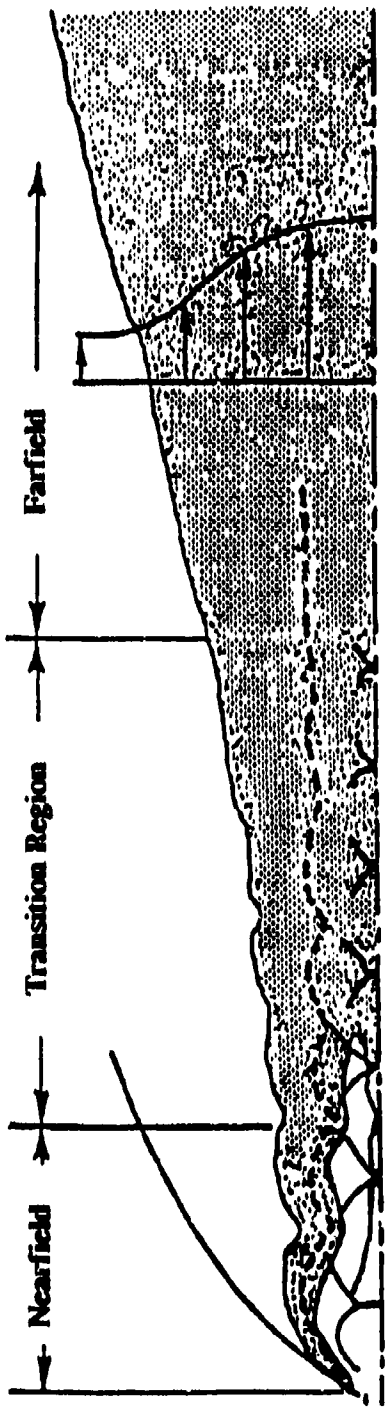

Fig. 5-1 Regional Division of Plume

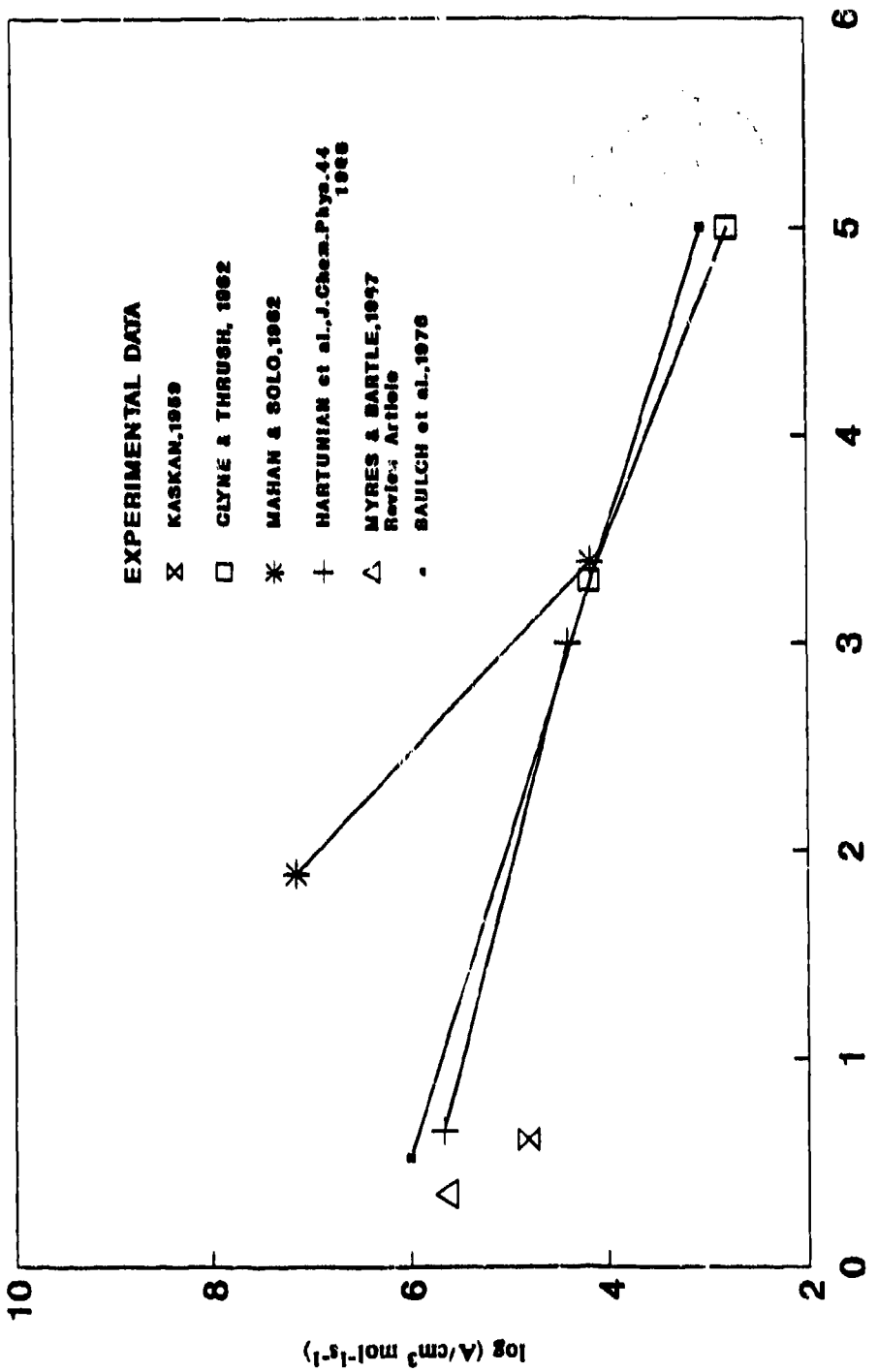

Fig 5-2. CO + O Chemiluminescence Rate Constant Data

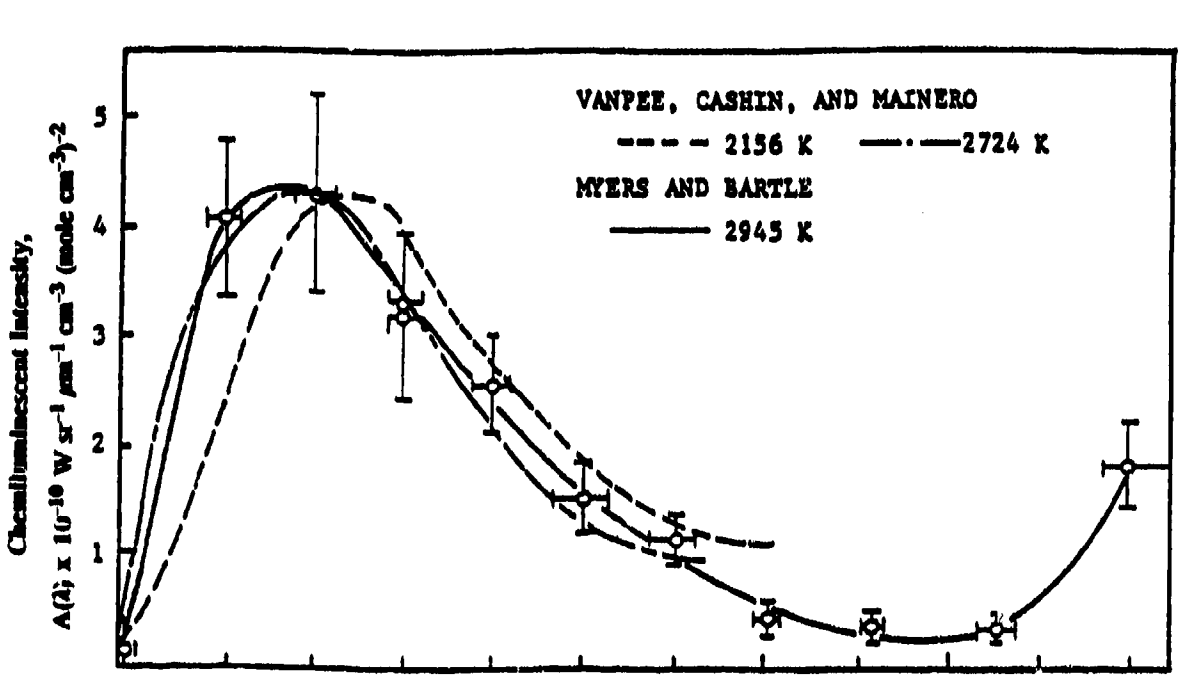

Fig. 5-3 CO + O Chemiluminescent Intensity Spectra

The points with indicated error bars as well as the solid line are the absolute intensity measurements of Myers and Bartle. The other two curves were normalized to the peak intensity of the Myers and Bartle curve.

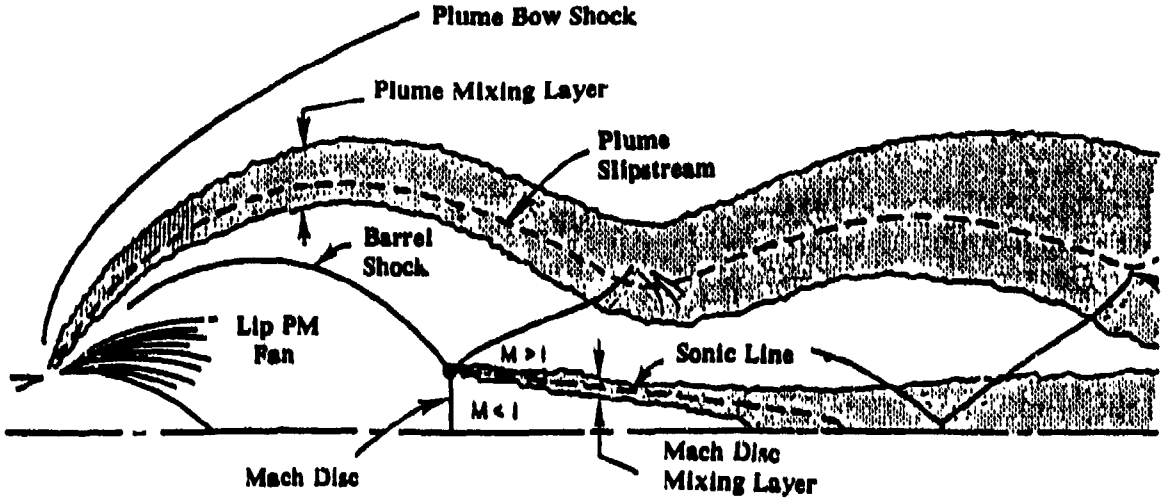

Fig. 5-4 Nearfield Viscous Inviscid Structure of Under Expanded Plume at Supersonic Flight Conditions

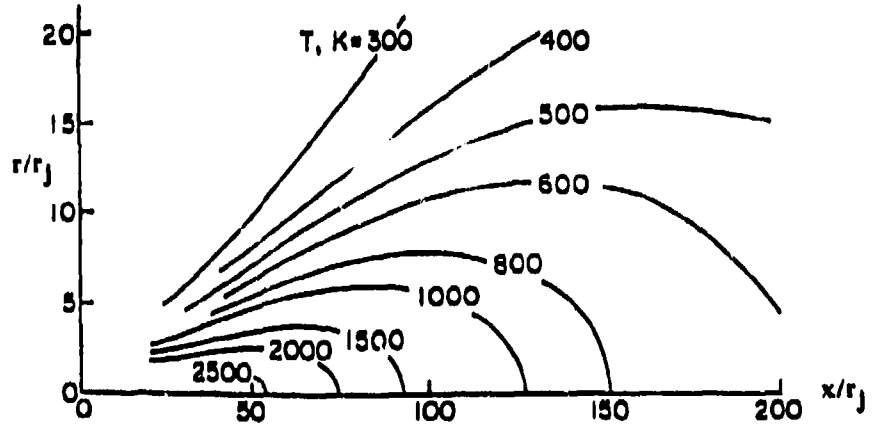

Fig. 5-5 Temperature Contours in Farfield of Energetic Tactical Missile Exhaust Plume

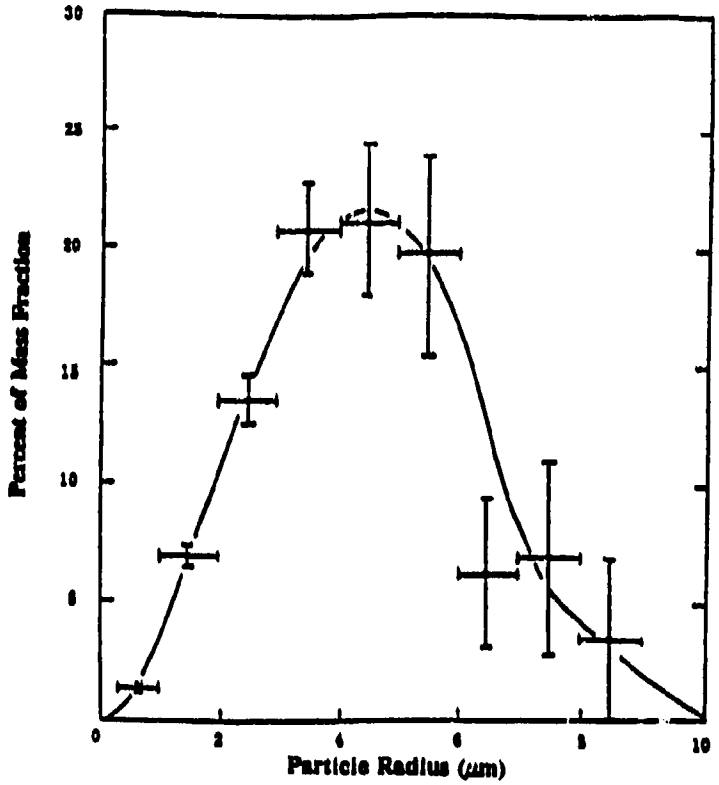

Fig. 5-6 Typical Measured Particle-Size Distribution

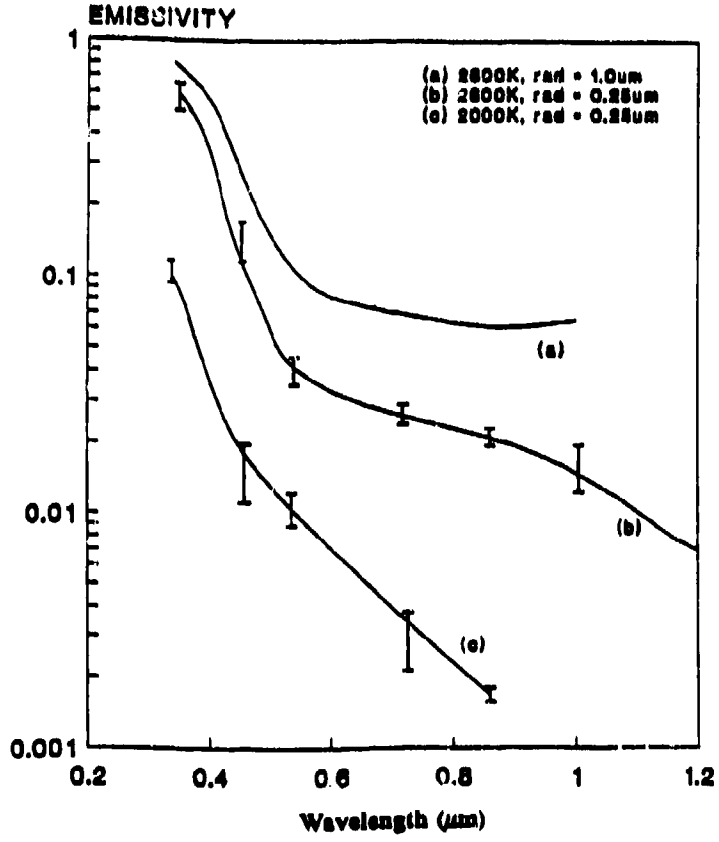

Fig. 5-7 Emissivity of Alumina Particles as a Function of Wavelength for Selected Values of Particle Radius and Temperature. Error Bars are for the Pure Alumina Measurements

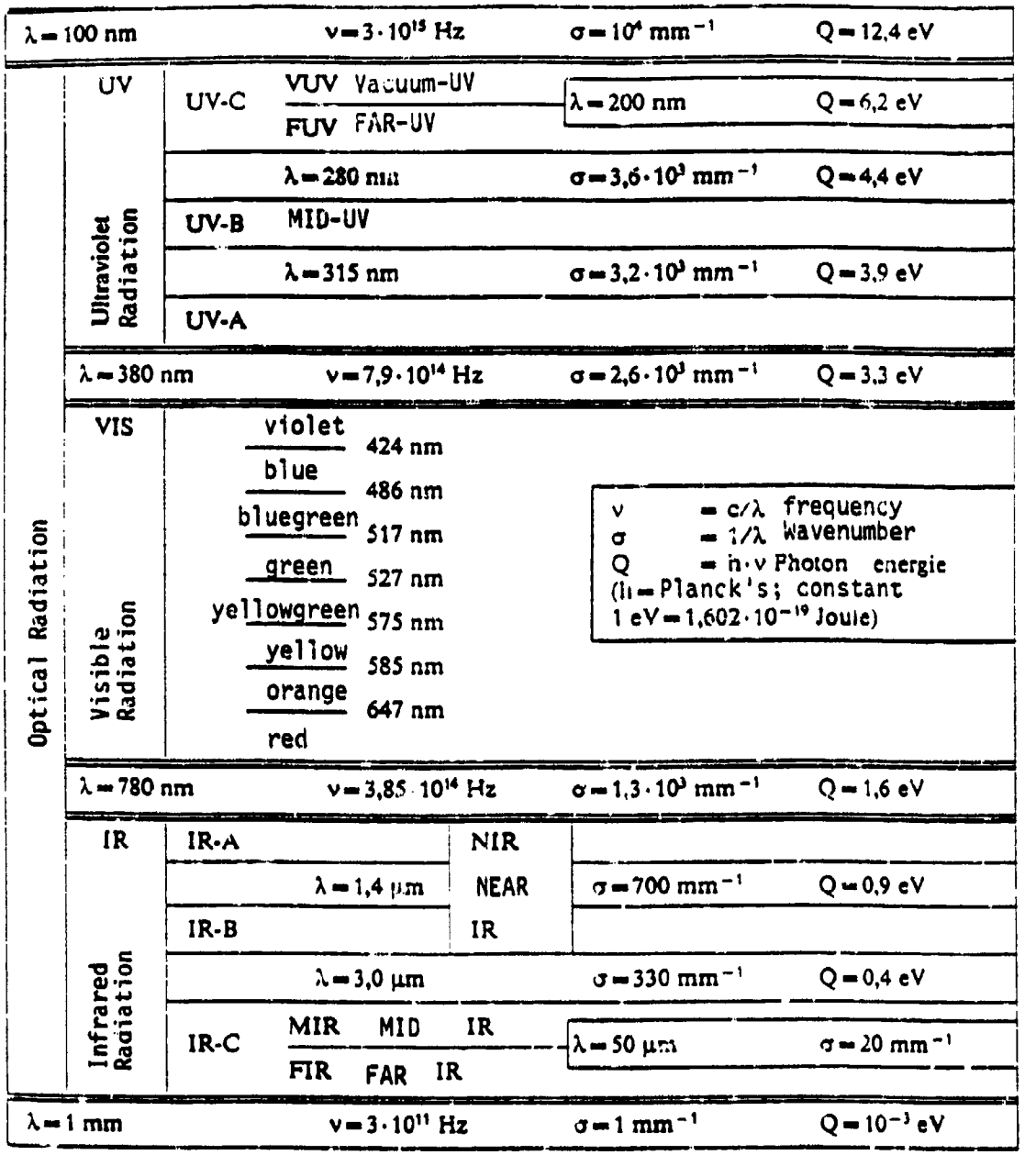

Fig. 5-8 Definition of Wavelength Regions of Interest

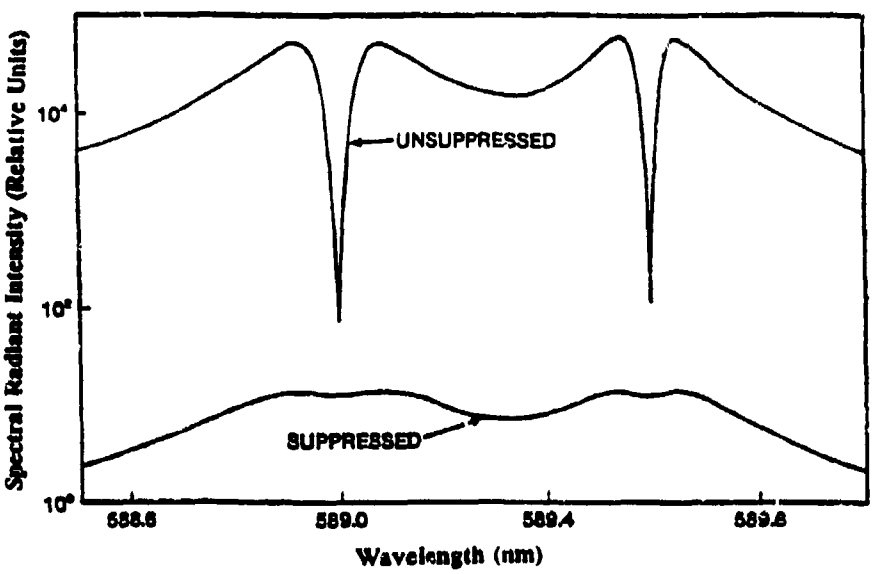

Fig. 5-9 Wavelength Distributions of Sodium Resonance-Line Emission Intensities for Unsuppressed and Suppressed Secondary Combustion Conditions

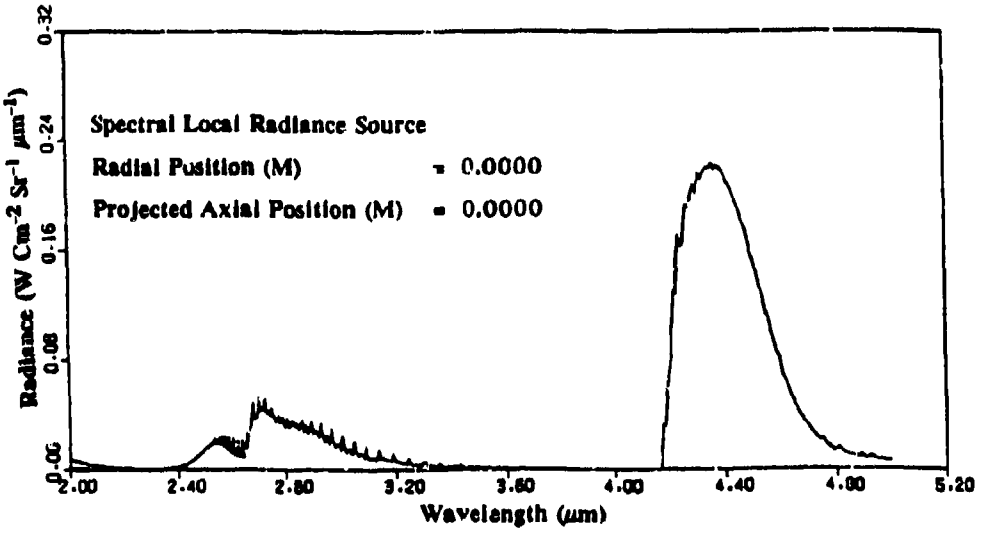

Fig. 5-10 Plume Radiance Calculation Performed with Parameters of Table 6

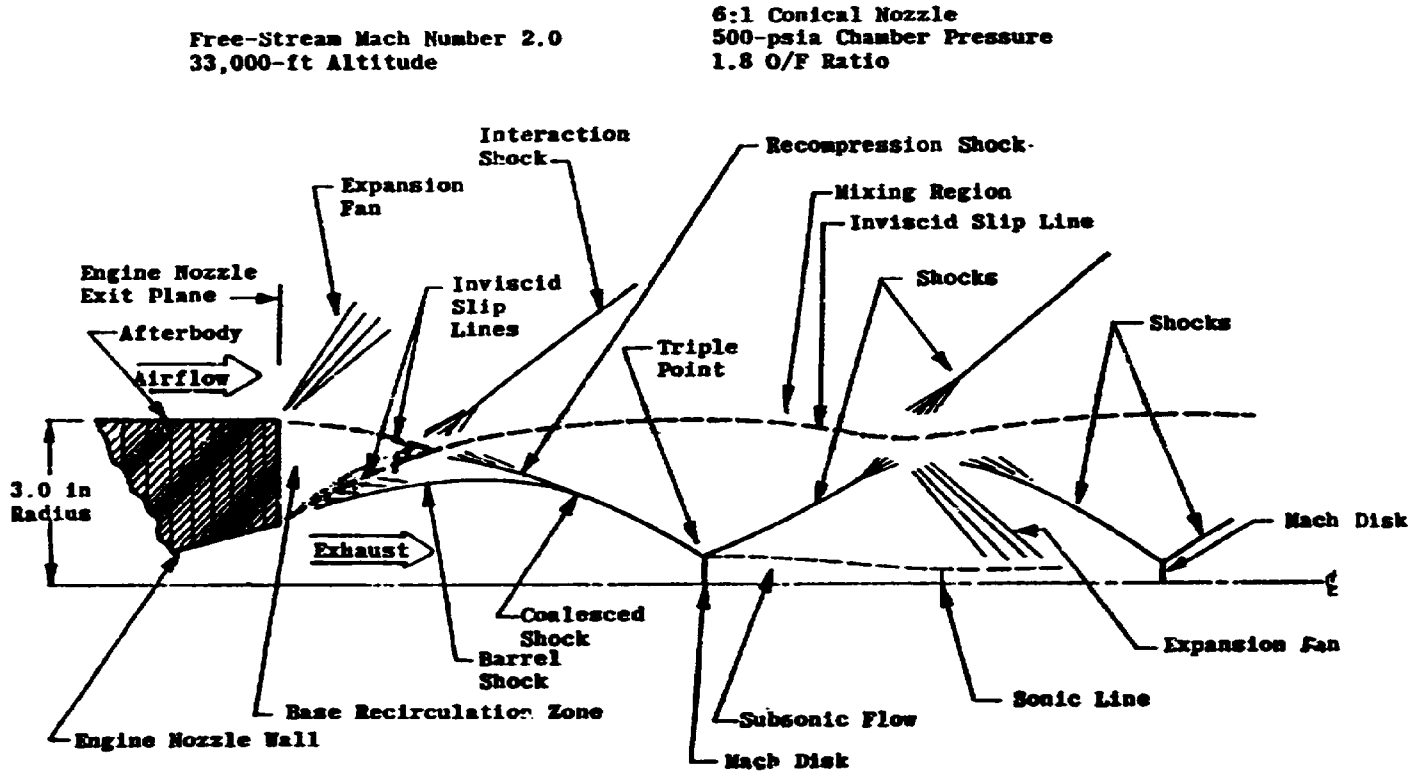

Fig. 5-11 Sketch of Plume Flowfield Shock Structure

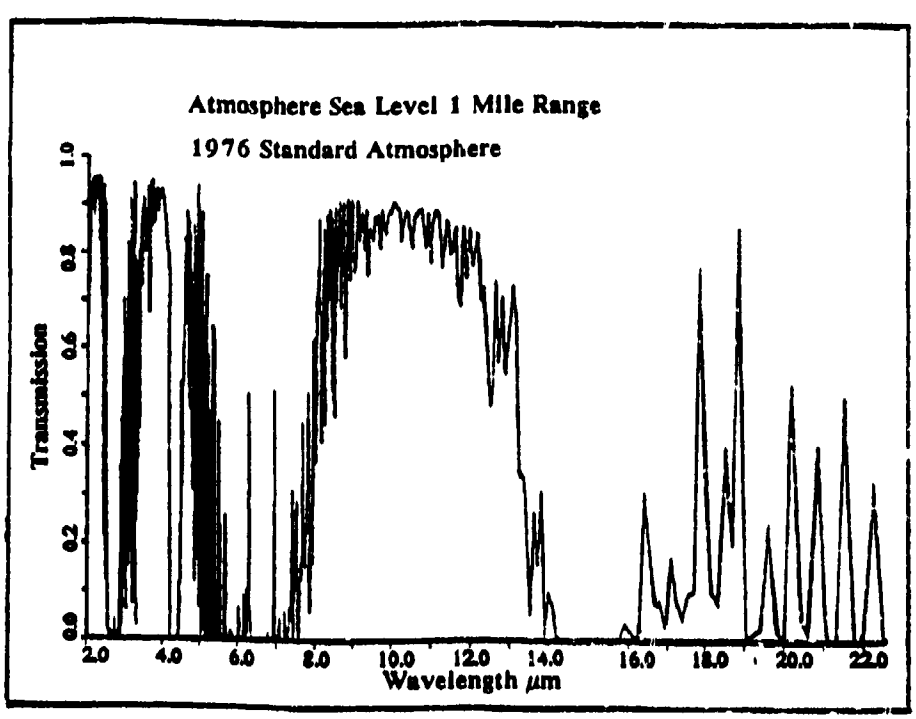

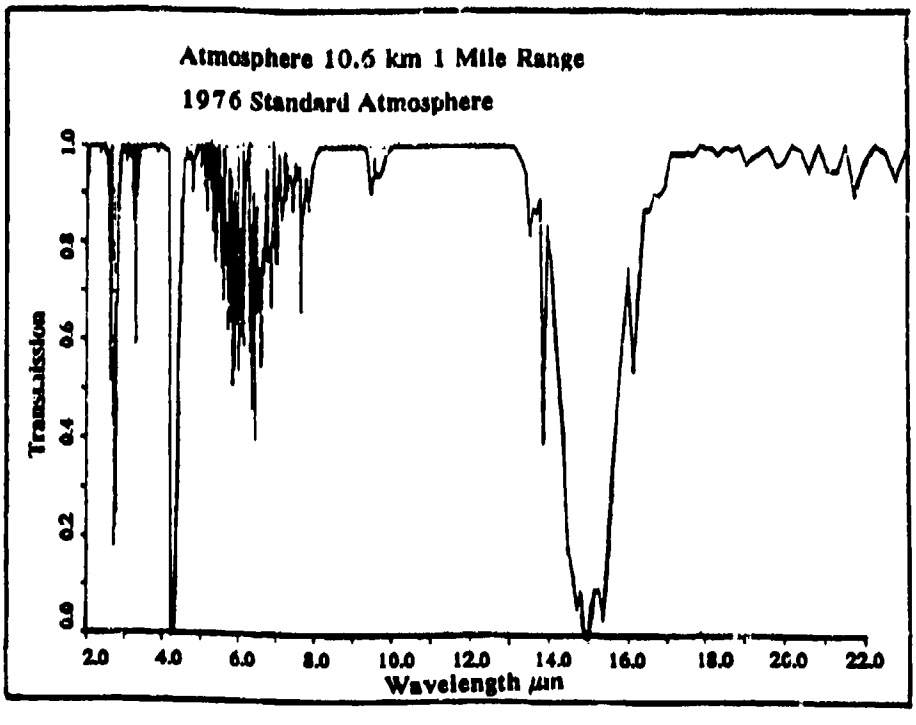

Fig. 5-12 Atmospheric Transmission (between 2.0μm and 22.0μm) at Sea Level and High Altitude

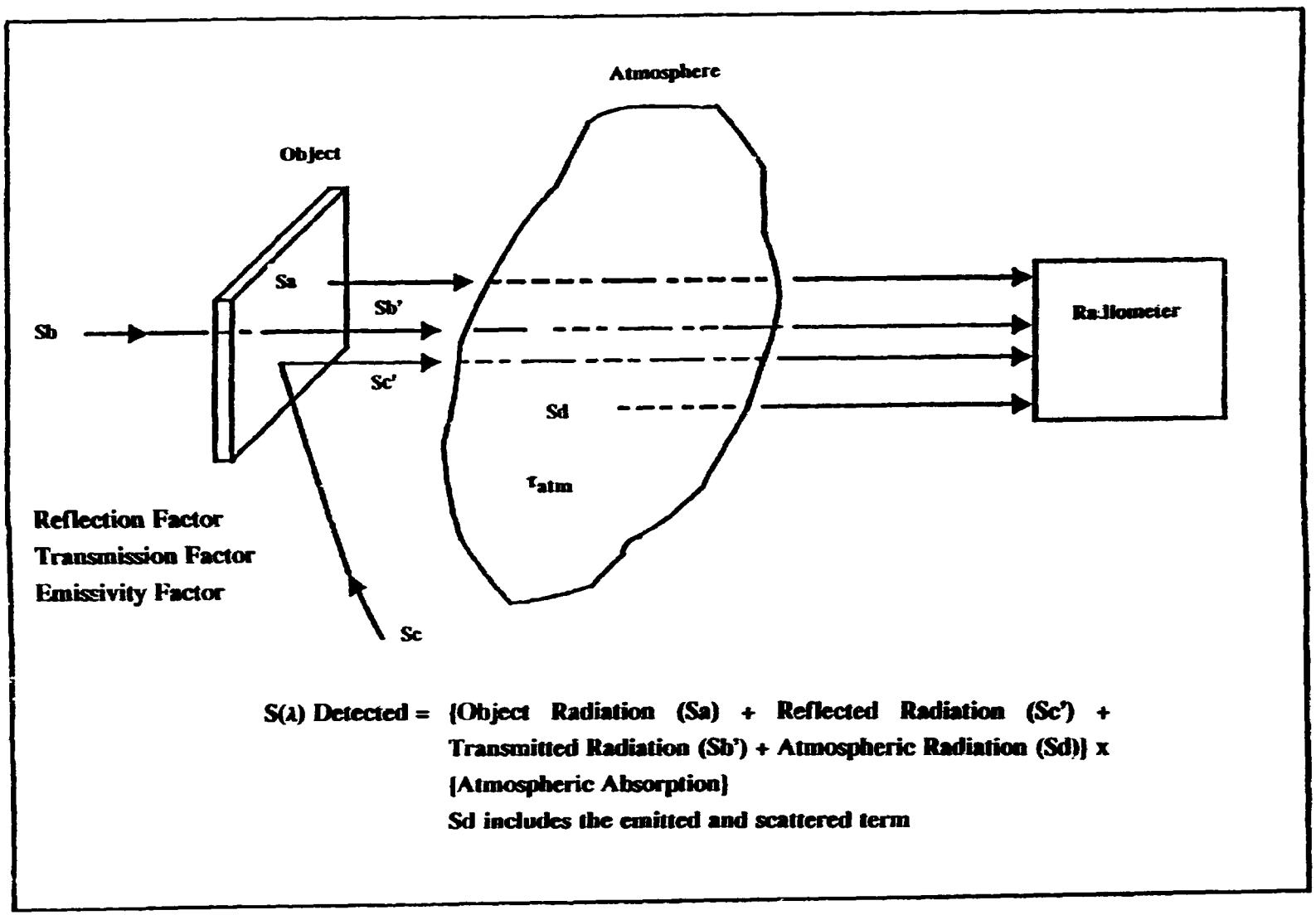

Fig. 5-13 Radiometric Essentials

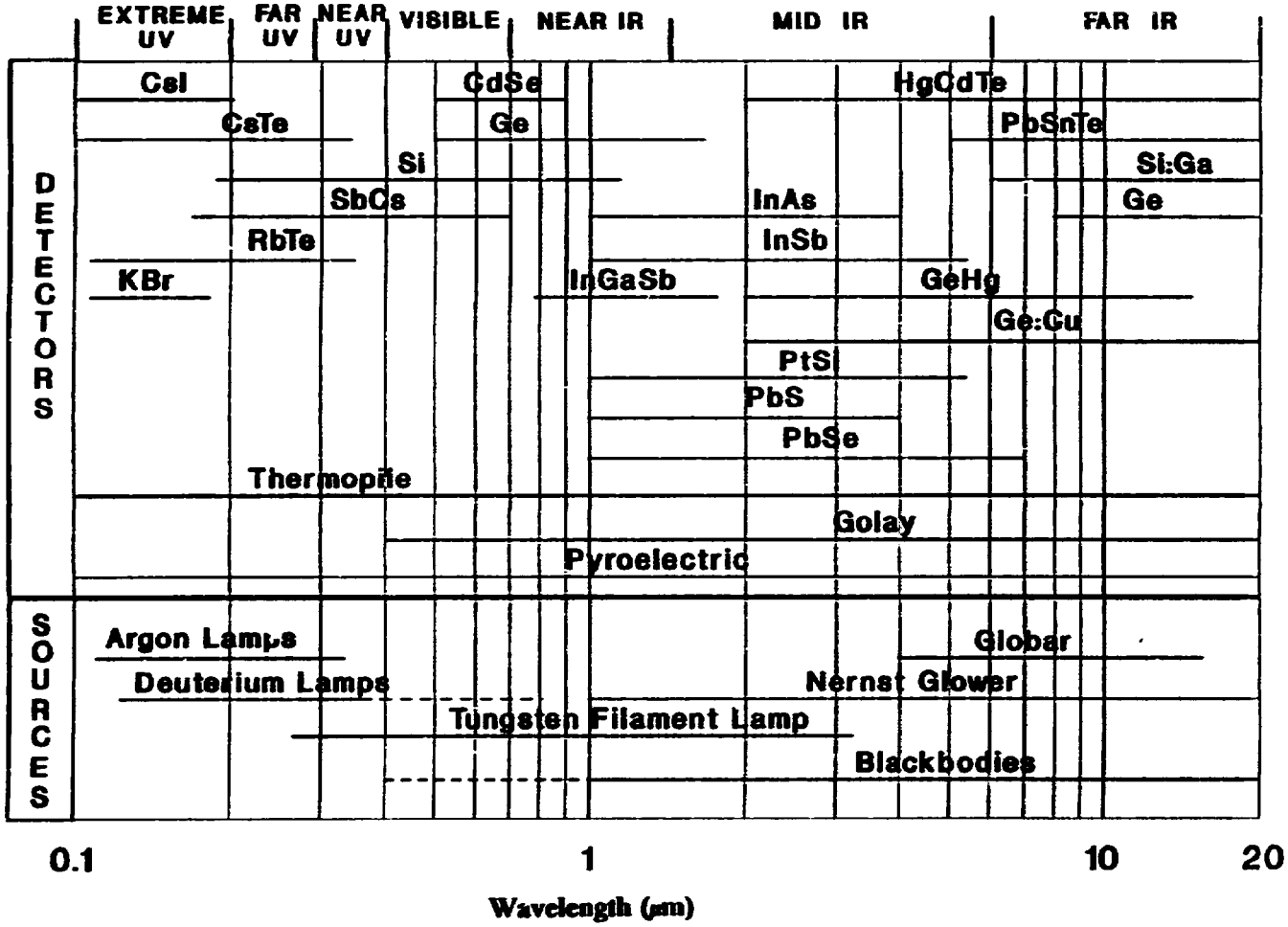

Fig. 5-14 Spectral Ranges of Applicability

$$L = \frac{\epsilon C_1}{\pi \lambda^5 \left(e^{\frac{C_2}{\lambda T}} - 1\right)}$$

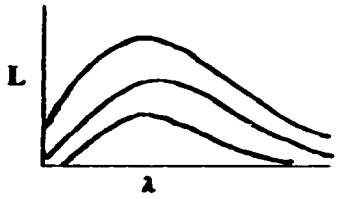

Calculate radiances of calibration sources use at least two sources.(e.g. different temperatures)

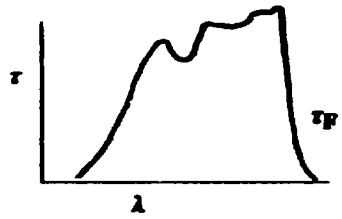

Find the transmission of filters being used. Include windows,etc.

Find the spectral response of the camera/radiometer

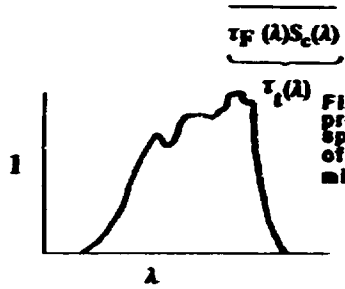

Find the normalized product of the spectral transmission of the filters,windows, mirrors,detectors,etc.

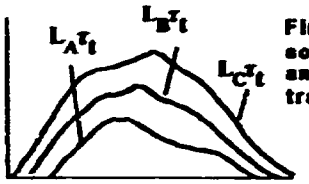

Find the product of source radiance and normalized transmission term

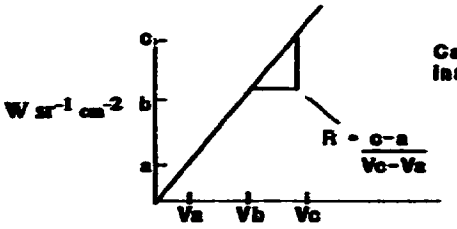

Calculate the instrument response

$\Sigma L_A \tau_f d\lambda = A\ (w/(Sr\ cm^2)) => V_A$

$\Sigma L_B \tau_f d\lambda = B\ (w/(Sr\ cm^2)) => V_B$

$\Sigma L_C \tau_f d\lambda = C\ (w/(Sr\ cm^2)) => V_C$

Integrate the calculated spectral radiance/transmission product and measure the corresponding camera/radiometer voltage (with overfilled FOV)

Valid for narrow bandpasses and greybody sources. No atmospheric effects have been considered

Fig. 5-15 Inband Radiance Calibration of Camera/Radiometer

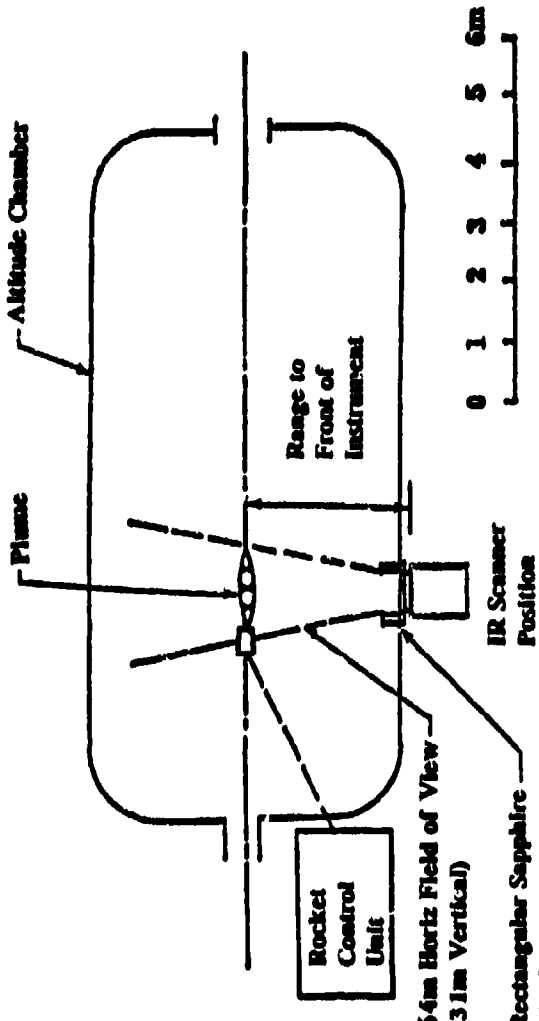

Fig. 5-16 Experimental Geometry for Infrared Scanner Plume Measurements

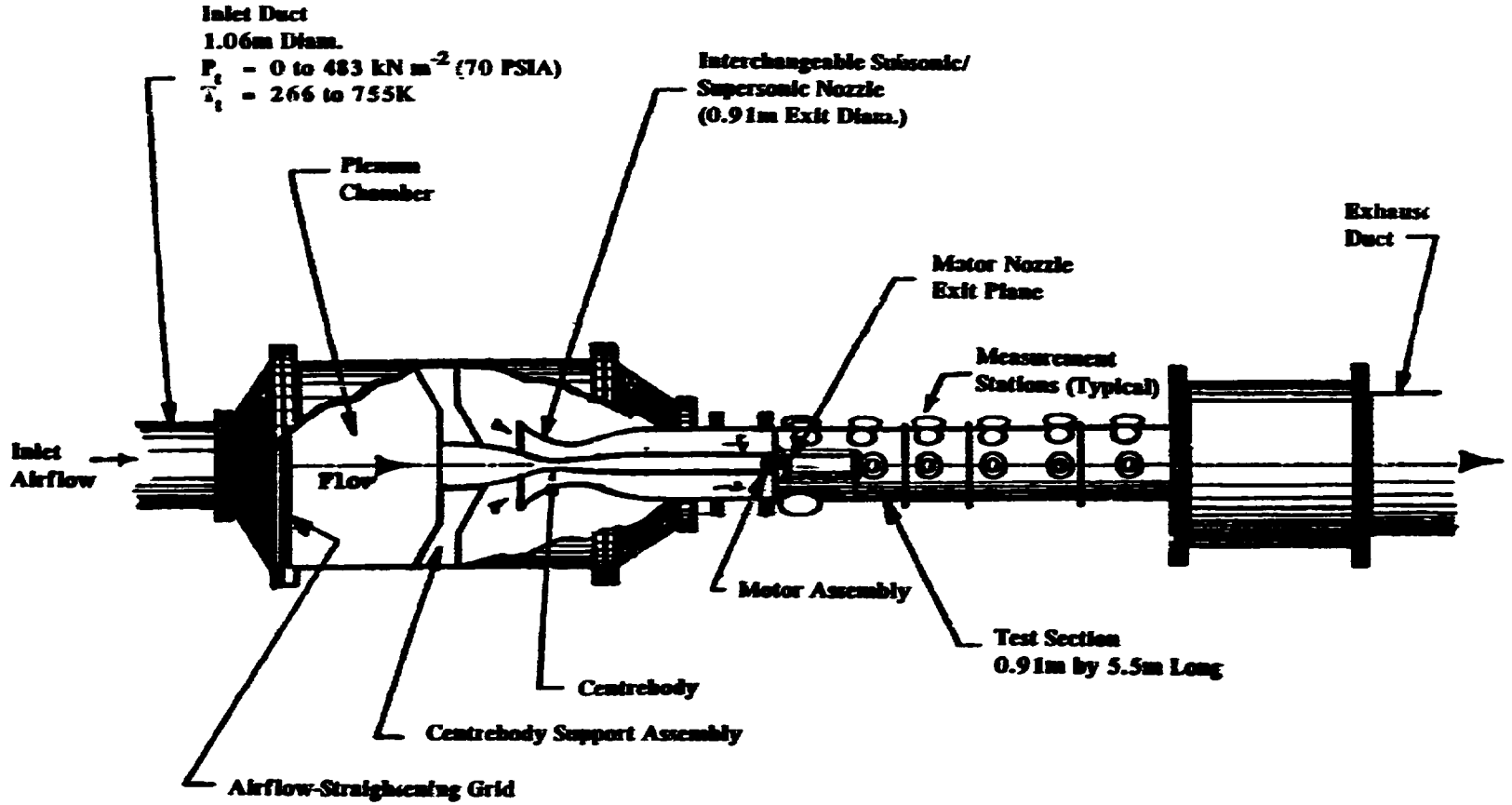

Fig. 5-17 Simulated Flight Test Facility Schematic

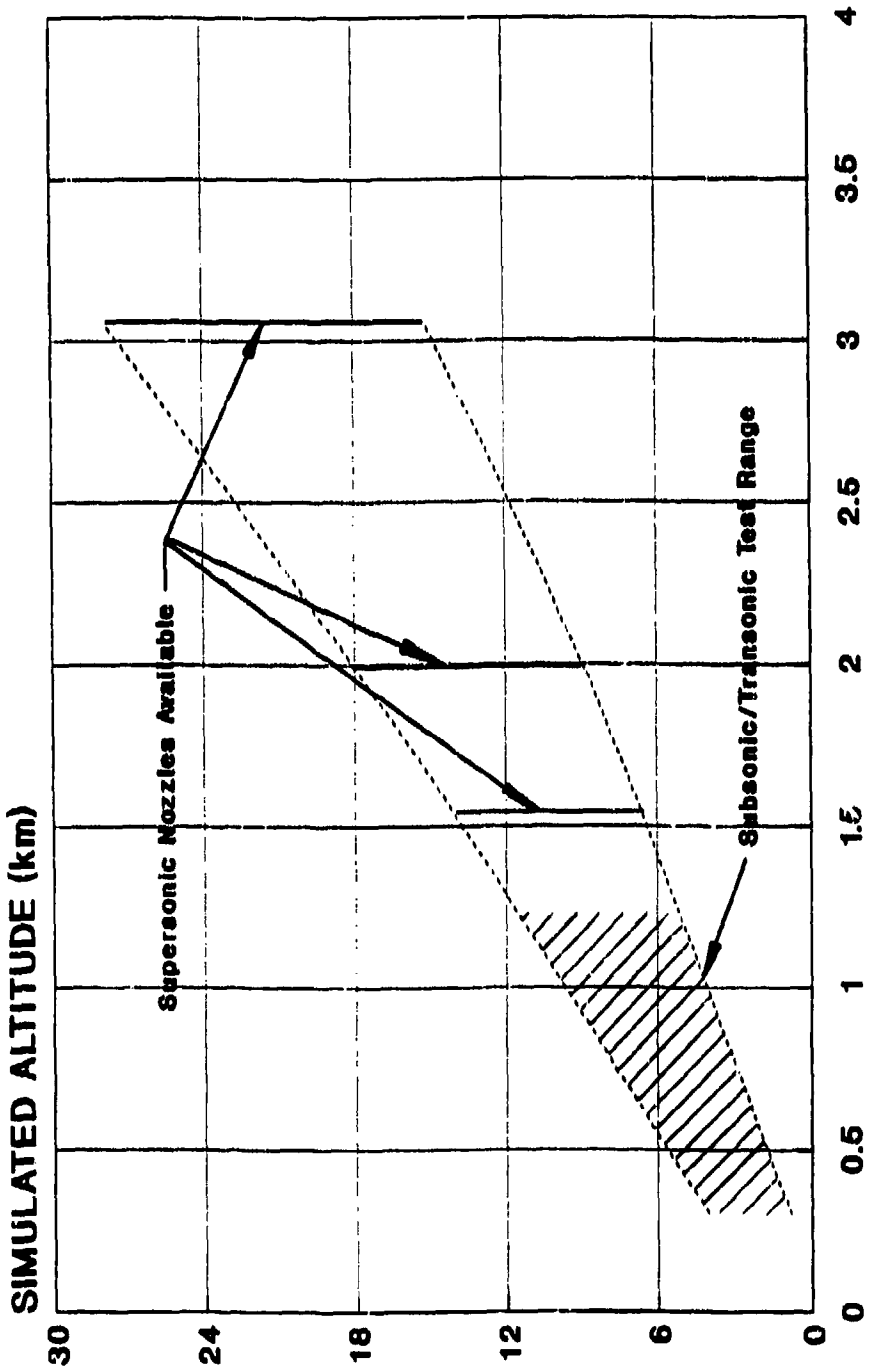

Fig. 5-18 Simulated Flight Facility Typical Aerodynamic Environmental Envelope

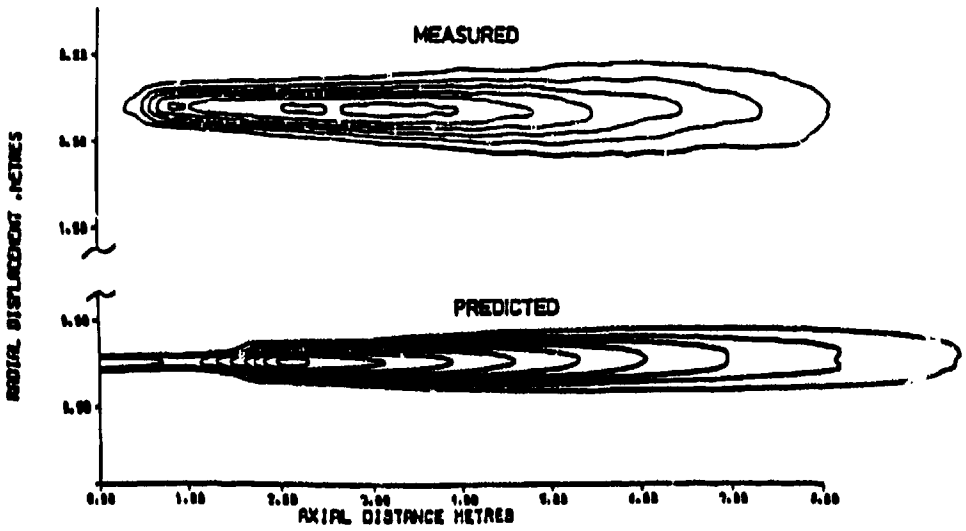

Fig. 5-19 ISO-Radiance Contours for a Composite Propellant Rocket Motor Exhaust

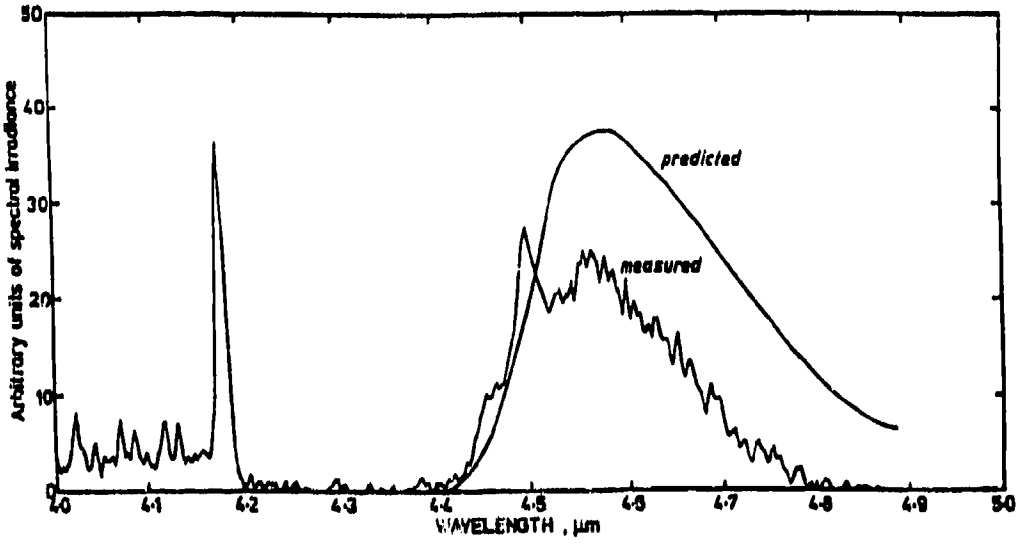

Fig. 5-20 Spectral Irradiance at 700m Range, 25° Aspect for a Composite Propellant Rocket Motor Exhaust

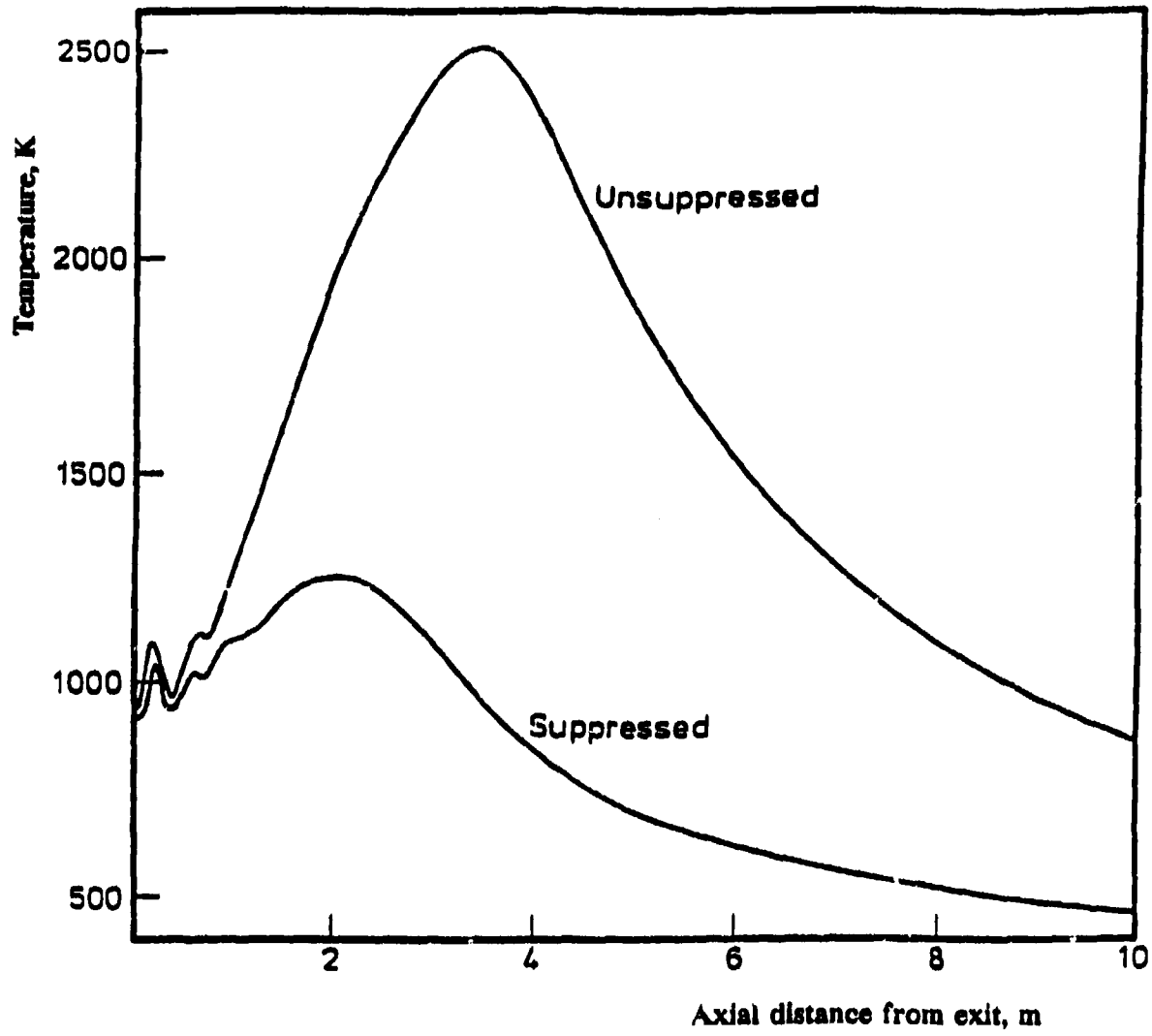

Fig. 5-21 Axial Temperature Profiles Predicted for Unsuppressed and Suppressed Secondary Combustion in Exhaust of Double Base Propellant Rocket Motor. Static Sea-Level Conditions

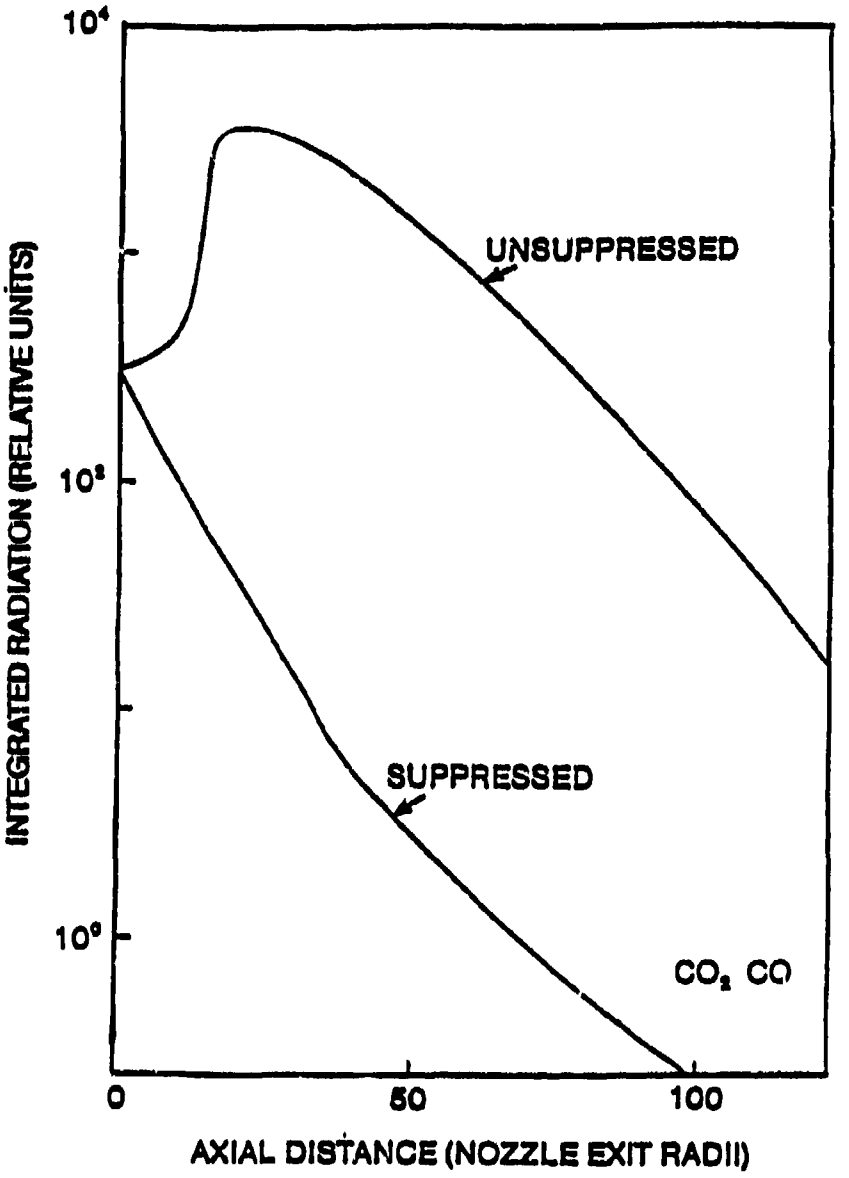

Fig. 5-22 Variation of Relative Radiation Emissions from CO in the Infrared Waveband 4.1μm to 4.9μm with Axial Distance for Unsuppressed and Suppressed Secondary Combustion Conditions

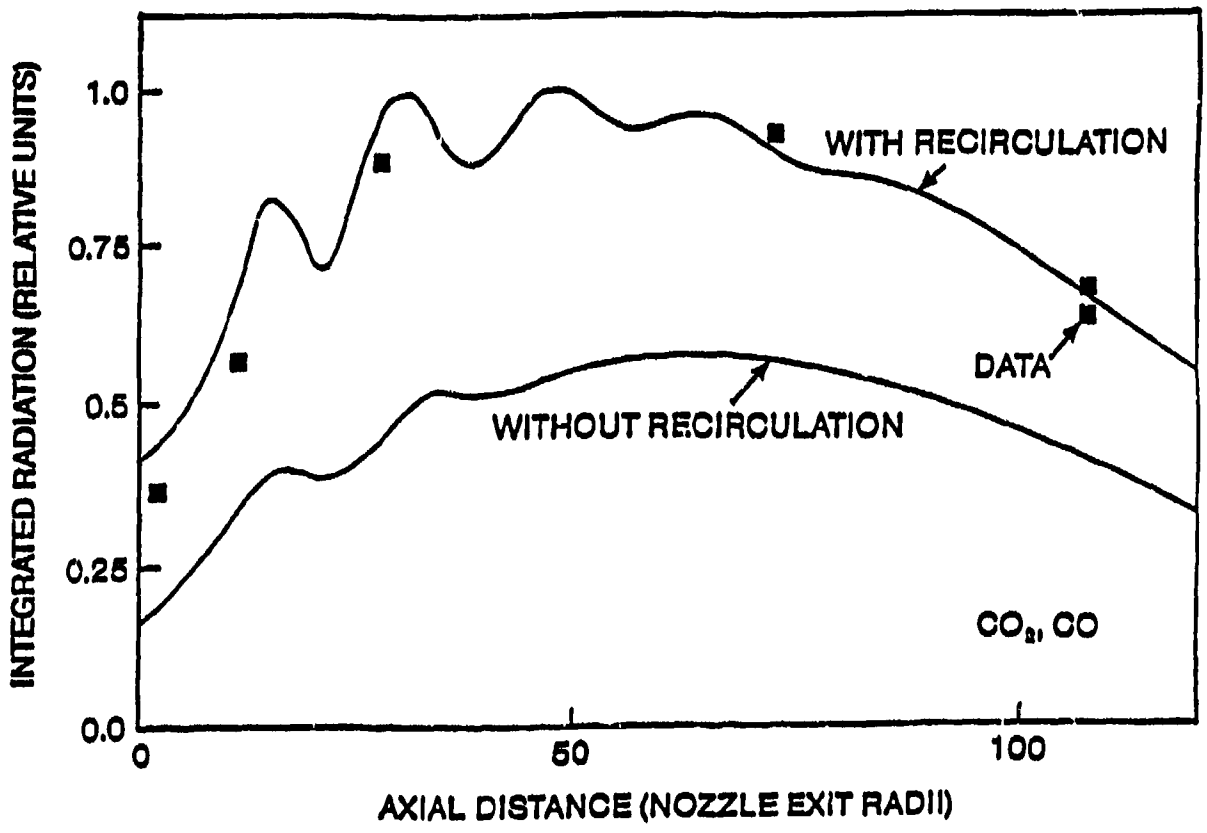

Fig. 5-23 **Infrared Station Radiation Distributions from CO_2 and CO in the Waveband 4.3μm to 4.7μm**
Comparisons between Predictions (with and without Recirculation included in Calculations) and Data

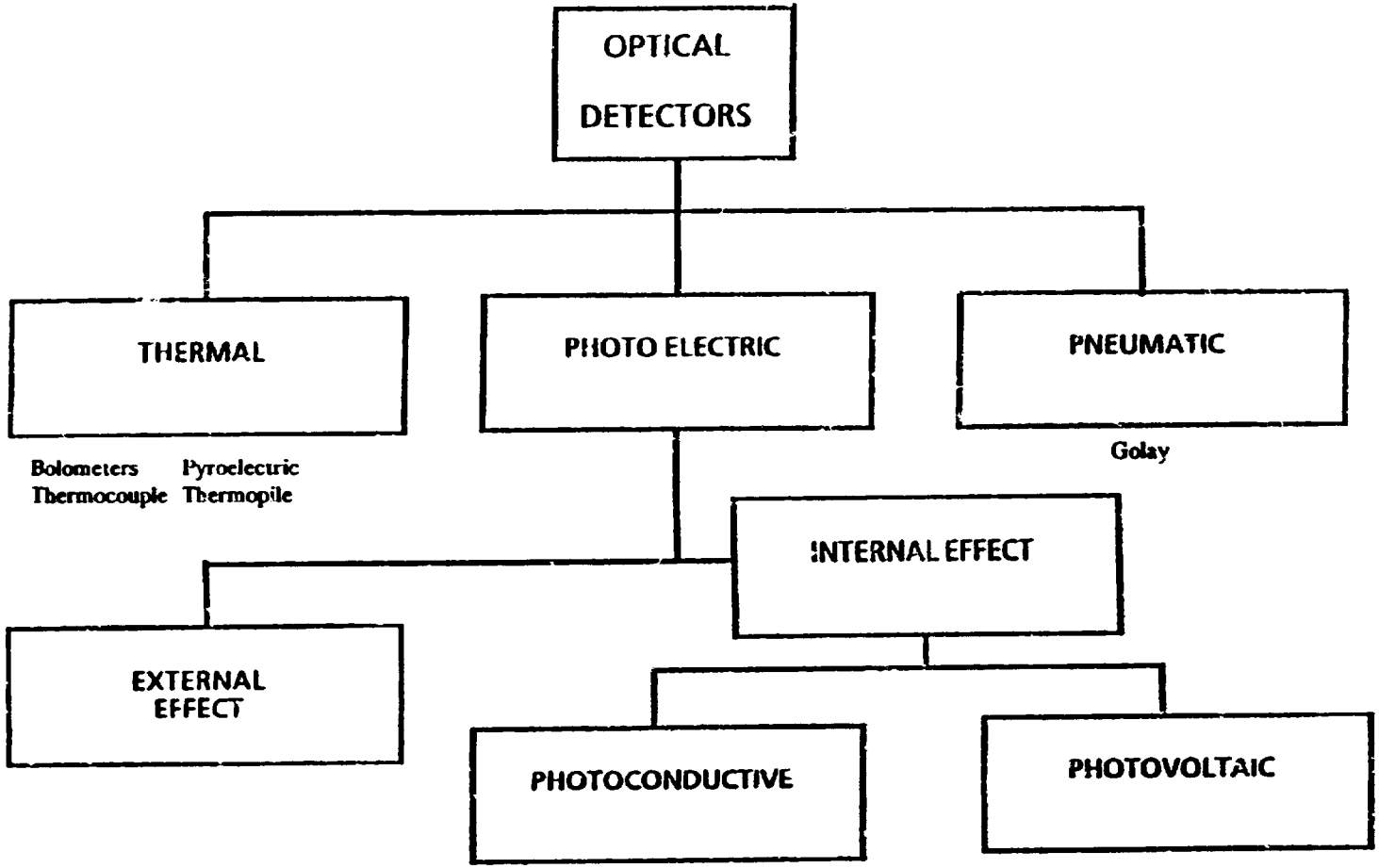

Fig. 5-24 Selection Guide for Optical Detectors

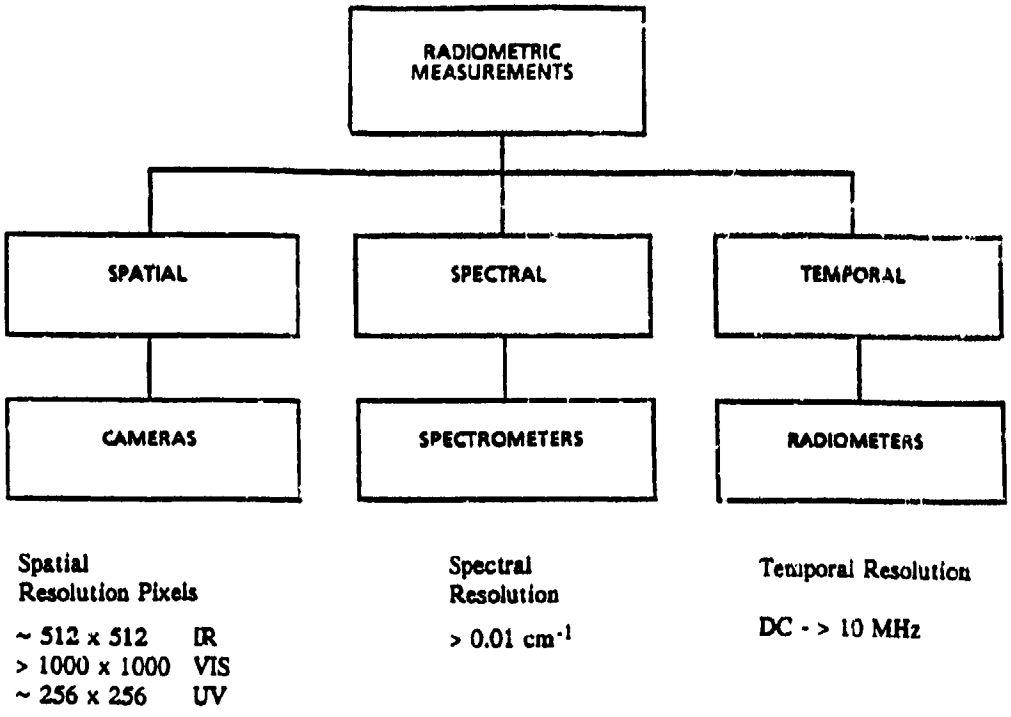

Fig. 5-25 Ways to Perform Radiometric Measurements

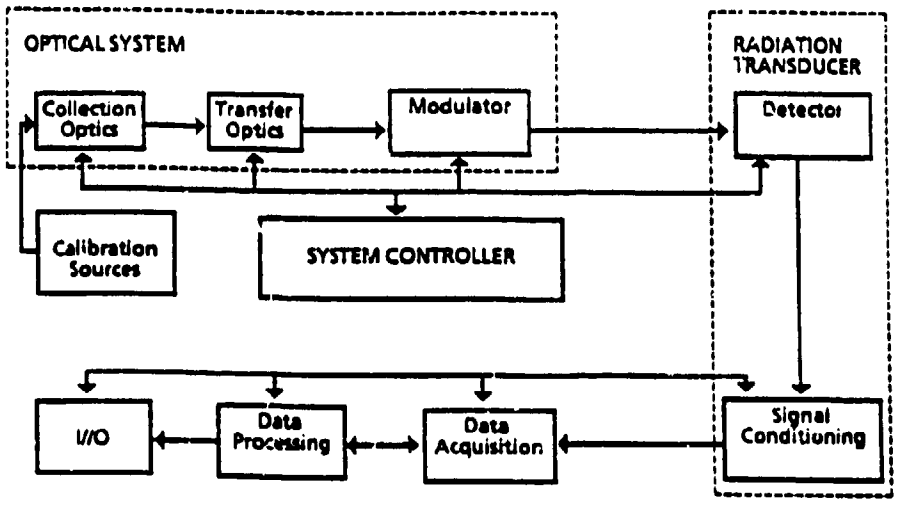

Fig. 5-26 Schematic Diagram for a Radiometric System

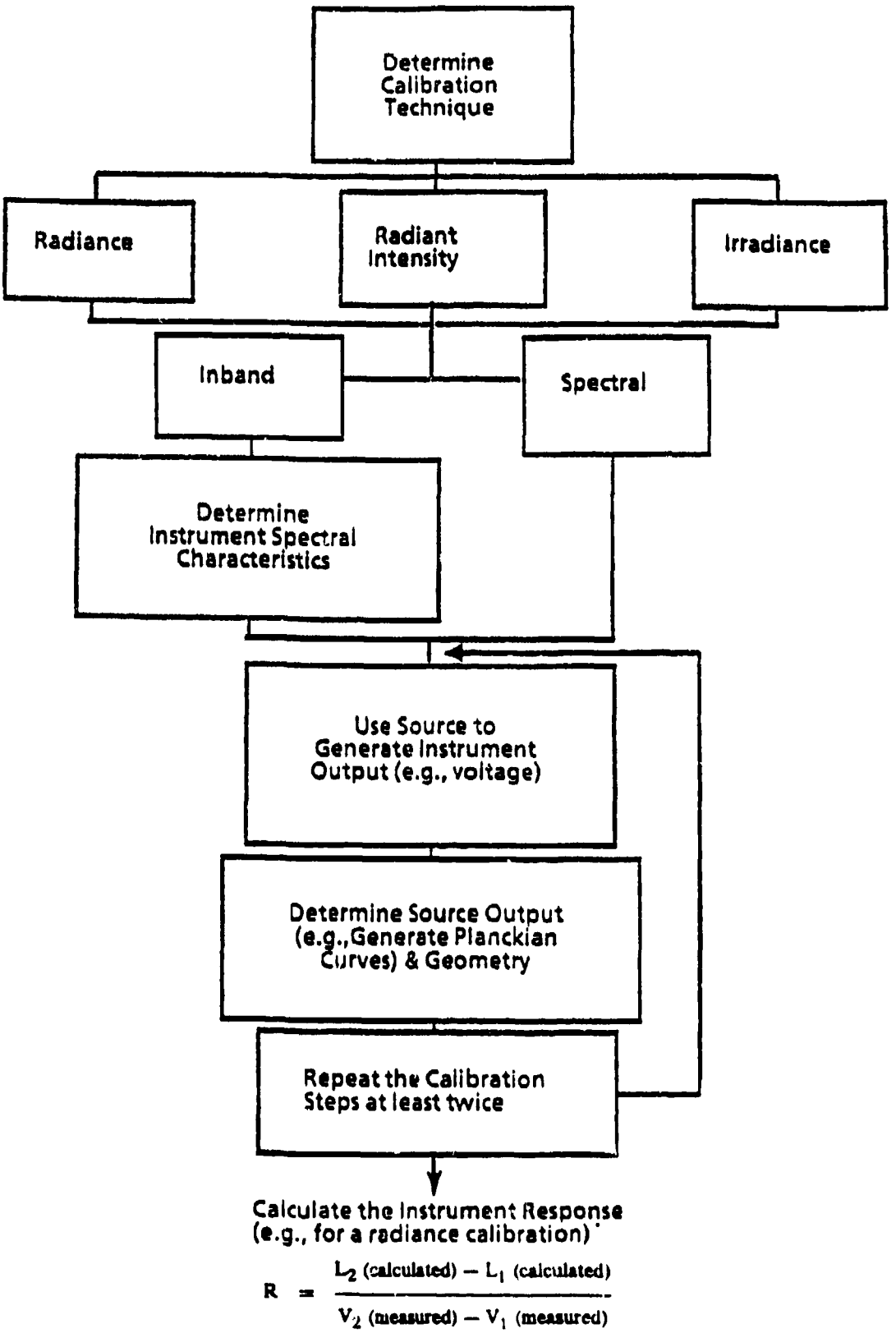

Fig. 5-27 Proposed Calibration Procedure

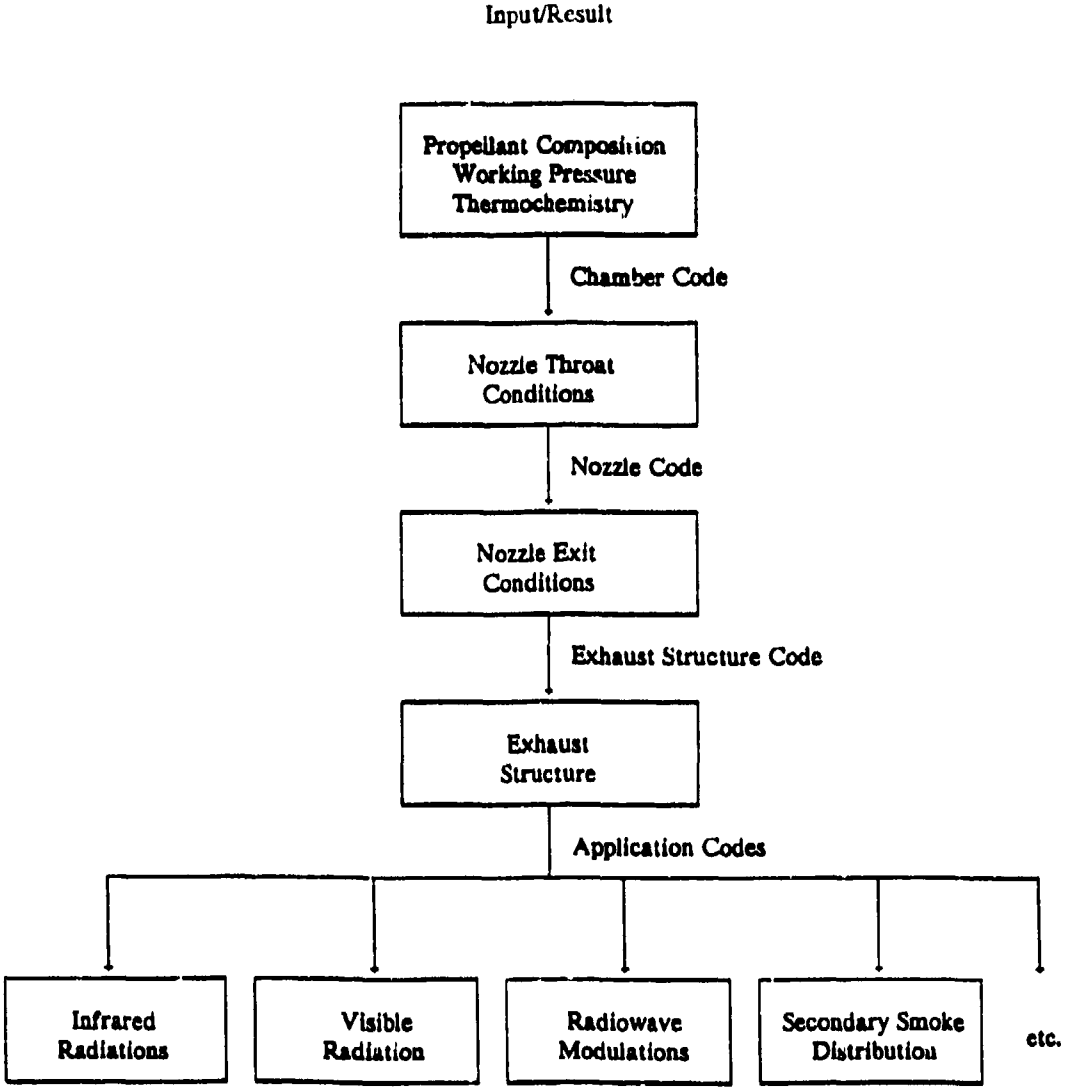

Sequence of Predictions of Rocket Exhaust Properties

Fig. 5-28 Typical Prediction Procedure

CHAPTER 6

Plume Microwave Properties

CHAPTER 6

Plume Microwave Properties

TABLE OF CONTENTS

1.0 INTRODUCTION

The rocket exhaust is a hot and highly turbulent gas jet. It possessses electrical properties that have serious implications for the missile design engineer employing microwave communication systems. Guidance and tracking can be heavily degraded as a result of interference from the plume while the scattering of radar signals and the emission of microwaves (particularly at millimetric wavelengths) may offer the opportunity of detection by an adversary.

"Microwave" is a generic term used broadly to describe the centimetric region of wavelengths, for the purpose of this chapter it will include that part of the millimetric range as outlined in the next paragraph.

As a guideline, operating frequencies of tactical missile systems typically fall in the range 3GHz to 120GHz. That is not to say that frequencies outside this range are excluded. Equipment that is small and light has obvious attractions for flight applications and where light vehicle and man-portable devices are used. Perhaps more important, the shorter wavelengths offer narrow, well defined beam properties and low side lobe intensity favouring good resolution, reduced interference and improved stealth.

2.0 PLUME MICROWAVE PROPERTIES

2.1 Attenuation (absorption)

High velocity, fuel rich gases ejected from the nozzle of a rocket motor mix with oxygen entrained from the surrounding atmosphere producing conditions that can cause the onset of exhaust combustion, often referred to as "secondary combustion" or "afterburning". Should this occur, a rapid rise in exhaust temperature promotes the ionisation of easily ionisable metals such as sodium and potassium which are found as intrinsic impurities within the propellant. The electric field of an incoming wavefront from a distant transmitter interacts with the free electrons of ionisation in the exhaust. Energy is taken from the field in the acceleration of electrons and is dissipated in collisions between these electrons and surrounding neutral molecules This results in a net loss of energy from the propagated wave. The loss and the integrated effect of such losses over the path through the exhaust to the "on board" receiver, is called line-of-sight attenuation or absorption. [1] Figure 6-1 presents the propagation geometry.

2.2 Forward Scatter (Amplitude and Phase Modulation)

A further mechanism [2-5] by which energy from the incoming wavefront arrives at the "on board" receiver is described by a scattering process. Turbulence induced eddies of fluctuating electron density populate large regions of the exhaust and become sources of incoherent scattering as they react with the wavefield. Each eddy, moving at local gas stream velocity, may be regarded as a source volume (dV) contributing energy to the overall received signal at a frequency changed from that of the incident wavefront by a Doppler shift imposed by source velocity with respect to the receiving and transmitting antenna.

The propagated wave along the path to the source volume and from it to the receiver suffers attenuation in the way indicated in Section 2.1.

The frequency spectra of all scattered energy at the receiver is recorded as sideband modulation both of amplitude and phase, limited in frequency range by the plume eddy velocities. Summation under the spectral curve gives the total energy from this mechanism.

2.3 Back Scatter (Radar Cross Section)

Forward scattering from the source volume described in Section 2.2 has its counterpart in energy scattered rearwards, back along the path travelled by the incident wavefront. Again, a frequency spectrum from all contributions is created and such energy is referred to as back scatter and forms the plume radar cross section (RCS). Its echo potential is usually several orders of magnitude below that of the missile body but increasing use of radar absorbing materials in stealth body design is reducing the gap between body and plume radar return.

2.4 Diffraction

Measured values of plume-microwave interference for highly-ionised plumes in longitudinal geometries show many of the characteristics of electromagnetic wave diffraction by solid objects. Simple diffraction models have been able to account quite accurately for the observed relationships between received signal strength and the angle between the plume axis and the line connecting transmitting and receiving antennas (aspect angle) for both static and flight plumes. The primary elements of diffraction involve the combination of surface waves

"skirting" most of the plume volume, multi-path refractions, and phase-interference of simultaneously received signals. In more sophisticated models recently developed the diffraction evolves from the mathematical solution of the propagation equations and demonstrates that the effect is real. Current model development in this area incorporates the combined effects of refraction, absorption, scattering, and diffraction.

2.5 Refraction

Variations of refractive index across the propagation path of microwave beams will cause distortion of the wavefront and deviated rays will promote a multipath effect in the farfield.

In a rocket exhaust plume two factors dominate in determining the spatial variation of local time averaged refractive index. One is the thermal inhomogeneity due to gradients of local plume static temperature, the other is the partially ionised nature of the plume gases caused by readily ionisable impurities in the propellant (e.g. sodium, potassium and calcium compounds). Local values of temperature, pressure and chemical composition, including concentrations of charged species (particularly free electrons) determine the plume refractive index field.

Calculations have estimated that for any given point in a plume changes in refractivity due to ionisation are at least an order of magnitude greater than those due to temperature gradients.

2.6 Exhaust Emission

In the ionised rocket exhaust the principal processes promoting millimetric wave emissions [6] are considered to be free-free electron emissions (Bremsstrahlung), molecular band emissions and free-bound electron emissions. Where aluminium fuels are present aluminium oxide particles may also emit thermal radiations.

Losses during free electron-neutral body collisions occurring naturally in the ionised exhaust form the so called Bremsstrahlung, or free-free emission, which is a continuum radiation. It is governed by the ionisation processes supported by high exhaust temperatures and alkali metal impurities in the propellant.

Electron concentrations of $10^{15}m^{-3}$ to $10^{18}m^{-3}$ and collision frequency of $10^{11}s^{-1}$ are typical at sea level.

Narrow band spectral emissions result from the change in energy state of atoms and of molecules. In the atomic case, free-bound emission takes place at electron/ion recombination when the acceptance of an electron releases transitional energy in radiation. If the electron enters an outer orbit at an excited energy level of high quantum number (n), it will either immediately drop to the ground state or cascade downwards through decreasing energy levels and, in so doing, release a series of photons at discrete frequencies. This process produces the spectral lines of recombination. Orbits associated with high quantum numbers have little difference in energy level and the transitions between them emit at millimetric wavelengths. Sume also observes that for high quantum levels (n = 24 at 300GHz, n = 60 at 30GHz) excited electron orbital radii become large making atomic nuclei resemble point charges. Consequently, recombination spectra can be similar, comparing one element with another and very much like that of the hydrogen atom. The molecular case involves a change in molecular rotational state with consequential release of energy. For molecules present in the exhaust, commonly H_2, H_2O, CO_2 CO and N_2, to contribute to molecular rotational emissions they must undergo a change in electric dipole moment. Of those mentioned, H_2, CO_2 and N_2 have molecular symmetry and for this reason do not contribute. CO and H_2O are asymmetric molecules where changes in dipole moment attend changes in rotational state and as such are of particular interest in line radiation within millimetric wavebands.

3.0 OPERATIONAL IMPLICATIONS

3.1 Guidance and Tracking [7]

Microwave radar has been a long established means of missile location, tracking and guidance. It is capable of providing an all weather function in a variety of roles and for successful operation the guidance and tracking communication links must be free of serious interference. It is clear from Sections 2.1 and 2.2 that the rocket exhaust is a potential source of such interference with serious system implications if the signal link passes through, or close to, the exhaust. This is particularly so if the rocket motor is required to burn unabated to maintain closing velocity in the terminal stage of an engagement and approaching maximum range. Figure 6.1 shows the general geometry of a situation where the wavefront of the transmitted wave illuminates the whole plume and the line-of-sight to the receiver passes through the plume. Quite clearly, attenuation by the

plume must be seen as an insertion loss within the microwave communication link. Furthermore, the sideband noise resulting from the scattering process of Section 2.2 and represented in principle by a single eddy (dV) in Figure 6.1 can be at frequencies that may interfere with semi-active homing systems.

3.1.1 Beam Rider

Beam riding missile systems can suffer from plume effects because the missile lies in the target tracking beam. For a successful interception the centre of the tracking beam must be maintained on the target and this requires very precise angular measurement by the tracking radar. Beam attenuation or distortion due to the rocket exhaust could degrade the target definition that is so crucial in the closing moments before impact. Guidance signals to the rear aerial of the missile can pass through highly attenuating regions of the plume.

3.1.2 Radar Command to Line-of-Sight

The beam riding missile requires only a simple guidance receiver which minimises the cost, weight and complexity of the guidance payload. This advantage is carried into the Radar Command to Line-of-Sight (RCLOS) guidance system where the tracker locks on to the target and, when the missile is airborne, continuously measures the angle between the missile and the target. It is a technique that allows a relaxation of beam centre to target accuracy, seen as a problem in the beam rider, but to some extent this accuracy is now transferred to the measurement of the missile to target angle. A separate command link, usually operating at a wavelength different from that of the tracker, guides the missile to reduce the angle to zero thereby maintaining a line-of-sight interception course. Rocket exhaust interference problems associated with the beam rider system apply equally to the "RCLOS" system. Refraction of the outgoing target tracking signal in the outer regions of an exhaust plume can introduce multipath effects at the target which cause returns at the tracker receiver to produce false positional information. This results in erratic manoeuvres by the missile as guidance commands respond to this false information.

3.1.3 Semi-Active Homing

The principle of semi-active homing systems is one where the target is illuminated and tracked by radar and the missile is launched on an interception course ahead of the target, anticipating its future position. A target seeker in the nose of the missile receives reflections from the target and determines its direction in space. Reference signals from a direct link between missile and tracker combine with the seeker output to establish target range and speed (Doppler) providing continuous guidance update until impact. The integrity of the system is again threatened by rocket exhaust interference in the form of attenuation of the rear reference and corruption of its information by sideband noise or as "spillover" noise into the missile forward receiver or as a contribution to "clutter", a commonly used term to describe unwanted echo signals from objects other than the target such as ground, sea, counter radar chaff and precipitation. To counter the effect of "clutter", natural or intended, tracking and seeker radars often employ "rangegates" and "speedgates". They are similar in concept. The "rangegate" discriminates against radar returns other than those within a prescribed distance frame from the transmitter while the "speedgate" acts similarly in discriminating against those radar returns that fall outside a prescribed "Doppler" frequency band which can be related to the velocity of the target. The signal to clutter ratio is significantly improved by their use.

In the context of semi-active homing, incoherent pulse radar systems, giving range information, would be sensitive to the amplitude of spurious signals that may appear as "clutter" in the rangegate. Continuous Wave Doppler and Coherent Pulse Doppler systems would be sensitive to signals having sideband frequencies that may affect the operation of the "speedgate" filter.

An indication of the "Doppler" frequencies encountered may be found in the simple relationship $f_D = 2V_t/\lambda$ where f_D is the "Doppler" frequency shift for a given radial target velocity (V_t) and stationary radar of wavelength "λ".

3.1.4 Active Radar Homing

In a semi-active homing missile the seeker is a tracking radar without the transmitter for target illumination. The active homing missile has the transmitter included making the missile fully autonomous when locked on to the target. The principle is that for semi-active homing but signal processing and computed course correction are done on board the missile. Only if the target falls outside the range of the illuminating radar is there a need for a remote signal link, this link gives mid-course guidance to the missile to

maintain it on course and bring it into radar contact with the target. During the autonomous stage of flight the rocket plume is unlikely to cause problems, in mid-course guidance the rear facing link could suffer plume attenuation and sideband noise interference.

3.2 Salvo Operation

Where two or possibly more missiles are fired in a salvo the exhaust of one may seriously interfere with target tracking or with the guidance of another. This can be complicated still further when the salvo is intended to engage multiple targets. The problems recounted in Sections 3.1.2 and 3.1.3 are valid for salvo operations but with the addition of inter-link interference.

3.3 Detection

Microwave radiation from the exhausts of tactical missiles can be a means of detection. Interest centres largely on the millimetric region of the spectrum where propagation windows exist in the earth's atmosphere that allow the passage of millimetric waves over relatively short distances. More details of the mechanisms of exhaust emission are given in Sections 2.6 and 4.2.7 and Figure 1-1 of the Overview shows the atmospheric spectral transmission range with windows at frequencies of approximately 35GHz, 94GHz and 140GHz.

Short range detection of exhaust millimetric radiation by passive sensors is possible and, with receivers having good spatial resolution, capable of providing accurate target bearings. The useful detection range of an incoming missile will be strongly influenced by the size and thermal ionisation characteristics of its exhaust. Much of the intense radiation may be obscured by the missile body when viewed at angles near to "head-on". Narrow angle reception would require rapid scan operation for surveillance purposes, the alternative of initial wide angle reception is likely to reduce detection sensitivity with increased background level, particularly at low elevations near the earth's surface. As a defence aid the detection of exhaust millimetric radiation may form part of a hybrid system to provide surveillance, detection and counter action.

3.4 Discussion

In trying to outline the problems associated with exhaust/microwave system interference no attempt has been made to offer solutions. Those available to the engineer depend on the operational role, but few overcome exhaust interference without recourse to expediency and some penalty.

Some solutions might be :-

(i) Flight path offset at critical periods of flight to avoid excessive signal losses. Penalty : Loss of optimum path.

(ii) Provide electronic discrimination against interference. Penalty : Increased electronic complexity, and cost.

(iii) Use of multiple antennae or reflectors attached to wing surfaces to remove propagation paths from highly attenuating regions of the plume. Penalty : Lowered aerodynamic efficiency.

(iv) Boost-Coast propulsion such that the exhaust is absent in terminal stage of useful flight. Penalty : Restricted terminal velocity (not always of importance).

(v) The reduction of free electron concentrations in the plume by chemical modification of propellant. Penalty : None; costs are in original propellant formulations. However, should it be a remedial change of propellant from the original then costs could be extremely high.

(vi) The use of an Active Homing System without mid-course guidance. Penalty : High cost, electronic complexity and weight.

While the broad principles of microwave homing, guidance, tracking and detection remain, sub-system technology has advanced to a remarkable degree. Reference 7 details some of these advances. Where past missile-borne systems have required large and heavy microwave and signal processing units, new generations of microwave equipment have become much smaller due to modern circuit design and fabrication. Signal processing, with the advent of monolithic integrated circuit technology, has led to miniaturization which has been carried into microwave technology with stripline techniques and microwave integrated circuits.

Millimetric waves offer the advantage of

small, lightweight systems having very narrow beamwidths with good spatial resolution, essential qualities for high accuracy and precise target definition. The physical size of microwave circuits are proportional to the inverse of the operating frequency and it is very noticeable in antenna design. Whereas at a frequency of 10GHz the antenna may have a diameter of 1.0m for a given beam width, at 95GHz, for the same beamwidth, the antenna diameter will be 0.1m.

This miniaturization process now makes it possible to have a complex homing system, such as that of active homing, within a missile of some 120mm diameter. One outcome of this reduction in size and payload is the opportunity to reduce the size and thrust required of a rocket motor for a given performance such that motors having combustion suppressed exhausts become the preferred option. This chapter will show that avoiding secondary combustion (afterburning) in the exhaust will prevent exhaust temperatures rising to cause ionisation and, without a large free electron population, exhaust emission will be dramatically reduced while attenuation and the generation of sideband noise will no longer be a problem.

4.0 ASSESSMENT METHODS

4.1 Measurement Techniques

The greater number of plume measurements have been made under static, sea-level conditions with both transverse and longitudinal propagation paths To a lesser extent wind tunnels and altitude chambers have provided information mainly with transverse, focused beam studies. Dedicated flight trials have been rare and propagation data obtained is difficult to accurately match with missile flight attitudes.

4.1.1 Static sea-level

4.1.1.1 Attenuation

Transverse measurements [8,9,10] of attenuation made with focused microwave beams over very short propagation paths through rocket exhausts offer the opportunity to spatially map the extent of the electrical plume by studying local properties at selected stations. Information gained in this way is especially valuable for the validation of theoretical models.

A system occasionally used in the UK operated with dual frequency channels, 14.5GHz and 35GHz. Separation between each transmitter and its receiver was 1.22m and matched conical horns with dielectric bi-convex lens formed the focused beams. The spatial resolution in the vicinity of the focus, midway between the horns, presented an Airy disc radius of 0.057m for 14.5GHz and 0.023m for 35GHz. Each microwave assembly was housed in a metal acoustic cabinet on anti-vibration mounts to minimise airborne and groundborne interference. These were then mounted on a frame which was raised and lowered by electrically driven jacks. System simplicity reduced the risk of false measurements, each transmitter consisted of a microwave generator, an isolator and a microwave feed to a lens corrected horn via calibration attenuators. Similarly, the receivers had lens corrected horns terminated by a crystal detector. Much the same equipment was used in the US through the early 1970s when measurements of this type were last made. A typical experimental facility is shown in Figure 6-2a with results from attenuation measurements using such a system compared with prediction in Figure 6-2b.

The concept of longitudinal measurements is one where propagation path geometries more nearly resemble those of a missile system. The receiving antenna is mounted on or near to the test motor, commonly in the nozzle exit plane, and the propagation path is to a transmitter in the far field at sufficient distance to allow illumination of the whole plume by a plane wave. The line of sight between the two antennae intercepts the plume axis at selected narrow aspect angles. Multipath interference by reflections from intruding objects in the propagation field should be avoided. A general geometry is shown in Figure 6-1. Rotation of a turntable mounted rocket during firing permits attenuation to be measured as a function of plume aspect (viewing) angle. Figures 6-3 shows examples of such measurements where attenuation was recorded for motors with propellant variants. The ratios, e.g. 88/20, refer to the solids/aluminium propellant loading. A plume induced multipath effect, showing enhancement of the signal at some negative aspect angles, is clearly seen. Further measurements compared with predictions are discussed in Section 4.2. Plume insertion loss and amplitude modulation have been measured for liquid and solid rocket motors at a variety of plume axis/wavefront interception angles in the frequency range 1.0GHz to 140GHz.

Equipment: A measuring system [11] typical in plume studies consists of a microwave bridge in which one arm is an air path subjected

to interference by the rocket exhaust and the second arm is a coaxial link providing an unmodulated reference (Fig 6-4). Propagation lies between two towers 31m apart and 9m high (UK). A 1.4w, 9.5GHz source supplies power to a "hoghorn" antenna on the transmitting tower and a lower power to the reference link between the towers. The receiving tower houses the rocket motor mounted on a rotating thrust stand with the receiving antenna attached to it adjacent to the nozzle. Both antennae are co-planar in the horizontal plane. Antenna polar patterns are shown in Figures 6-5 and 6-6 with the transmitter pattern, broad in the horizontal plane to illuminate the whole plume at any aspect angle and narrow in the vertical plane to prevent spurious ground reflections.

Received and reference signals are mixed with those from a local oscillator and the resulting intermediate frequencies (IF) are passed to the main processor housed in a control room 90m from the towers. Diode detection is used to extract the amplitude modulation, while received and reference IF signals are compared in a phase sensitive detector to obtain phase modulation.

Attenuation is measured by mixing part of the received IF signal with that from a crystal controlled oscillator to provide a low frequency output for direct recording. It is seen as a signal loss over a linear dynamic range of 40dB.

Typical Performance

Attenuation

Dynamic range -40 dB

System resolution (amplitude and phase modulation)

At 0 dB attenuation -100 dB to -120 dB
At 30 dB attenuation -99 dB to -103 dB

Cross talk

Signal AM to PM -27 dB
PM to Signal AM -30 dB
Ref AM to PM -10 dB

Polarisation

Can be vertical or horizontal. Occasional use of circular polarisation.

Analysis

Analogue and digital techniques are used.

4.1.1.2 Signal Scattering

Energy from an electromagnetic wave incident on the exhaust of a missile can be scattered forward into its "on-board" receiver where it is seen as amplitude and phase modulation presenting unwanted sideband noise to the system. This may distort or obscure vital communication signals rendering the missile less effective or causing mission failure. The geometries of Figure 6-1 clearly indicate that to observe the true scale of scattering by turbulent dielectric eddies the whole plume must be illuminated by the incoming wave. Scattered signal strength is measured with the equipment of Section 4.1.1.1 and analysed using a Fourier process where frequency components of noise form a spectrum as shown in Figure 6-7 with values referred to a received signal level (i.e. after attenuation) and quoted in a 1.0Hz bandwidth. The curves show amplitude and phase modulation spectra and are compared with the amplitude modulation spectrum (RPE) of an independent, similar equipment operating simultaneously at the same aspect angle. Phase modulation of a 9.5GHz incident wave has been recorded over a range of rocket motors and, for small amplitude signals such as those generated in the plume, has yielded phase spectra that are in agreement with simultaneously recorded amplitude spectra (UK).

To measure backscatter (radar cross section) from the plume the transmitter and receiver are in the same location (mono-static radar) with the receiver measuring signal returns echoed from the missile exhaust. These scattered returns can be expressed as an effective area compared with a known standard reflector and represent energy in the area under the spectral curve.

4.1.2 Wind Tunnel (Simulated Flight)

Wind tunnel dynamic plume tests, with a co-flowing free stream at altitude, provide the closest simulation of an in-flight missile, although there are often restrictions on antennae placement and undesirable shock reflection and wall effects to be avoided. Transverse attenuation measurements are best suited to these facilities and have been useful for analysing plume phenomena observed in flight.

Representing this type of work Figure 6-8a presents data for two composite motors with

different levels of aluminium fuel (10%, 12%) and compares these with essentially identical motors but with the inclusion of small quantities of molybdenum trioxide as an attenuation suppressant. The reduction in attenuation due to the additive is clearly demonstrated and the mechanism is further discussed in Section 5.1. In Figure 6-8b results are shown from a wind tunnel study used to assess the flight data of six propellants under simulated flight conditions. In all cases except E, peak attenuation occurred at maximum free stream velocity. Propellant E contained 3% K_2SO_4 and full afterburning did not occur. C, G and F had flames fully anchored to the nozzle.

4.1.3 Altitude Chamber

Transverse attenuation measurements of missile plumes generated in altitude chambers were made for a number of years at the US Naval Research Laboratory and to a lesser extent in the UK [12]. A similar capability now exists at SNPE in France. Results from such measurements are shown in Figure 6-9 where attenuation for two composite motors at simulated altitudes (~25/28kft and ~40/42kft) are compared with attenuation at sea-level. Such measurements have limited use since they neglect all dynamic aspects of flight, however, they make it possible to show the effects of reduced ambient pressure on certain chemical reactions occurring in the exhaust plume (particularly recombination reactions). Reference 13 also describes NRL facilities being used with co-flowing airstream for prediction validation at M2.2 and altitude 10.9km. Longitudinal measurements have dubious value when operating in confined spaces with chamber wall reflections and limited geometries.

4.1.4 Flight Testing

Figure 6-10 is an example of attenuation data gained from a well-instrumented flight test. Rotation of the missile during flight ($1rs^{-1}$) provided data from positive and negative aspect angles and from propagation paths not in the antenna/nozzle-axis plane. The variation of attenuation with altitude (Z) and missile velocity (V) is clearly seen, while the motor combustion chamber pressure (P_c) indicates the state and time of burning. Such information is helpful for the validation of longitudinal propagation models.

In-flight attenuation data (for positive aspect angles, i.e., "through the plume") for six propellants of Figure 6-8b are summarised in Figure 6-11. The order of attenuation is different between simulated and actual flight data. Propellants D and H had the lowest in both cases. Propellant E in the flight measurement gave high attenuation suggesting that the plume in this case was fully burning. Propellants C and D were identical apart from the additive ($P_bC_rO_4$) in D which was active as an attenuation suppressant. Missile/base diameter ratios were small indicating a large base with the likelihood that base recirculation and a critical combination of variables contributed to some of the differences observed.

4.1.5 Plume Emissions

To date emission data are sparse. One UK based experiment afforded the opportunity to undertake dual frequency measurements of emissions from double base and composite motors of 30kN and 10kN thrust, respectively. The frequencies of interest were nominally 35GHz and 90GHz and similarly constructed radiometers consisted of a dish antenna, radiometer head with a Dicke reference, a mixer with I.F. amplifier leading to a detector and band pass amplifier and finally coupled to a correlated detector. The antenna 3dB lobe widths were 1.3 degrees and 0.8 degrees for 35GHz and 90GHz, respectively. Data from the radiometer were analysed by a dedicated computer. Figure 6-12 shows the measured apparent brightness temperatures for the composite propellant motor and Figure 6-13 shows similar values for the double base motor.

4.2 Predictions and Comparisons

Microwave predictions rely, in the first instance, upon the construction of a theoretical exhaust structure in which the time averaged properties of combustion are quantified in an axisymmetric distribution of components spatially defined by axial and radial co-ordinates referenced to the axial point in the nozzle exit.

4.2.1 Plume Flowfield Model

Flowfield models [14-19] used for microwave predictions are those used for all other plume predictions but have five important additional properties that are particular to microwave interactions and must be included :-

(i) Ion/ion chemistry, especially that for alkali metal impurities. Other minor species that may interact with and affect the ionization processes.

(ii) Parameters that define the plume

turbulent structure which, as a minimum, include turbulent intensity related to electron density fluctuations and turbulent length scale

(iii) The electron collision frequency.

(iv) Free electron concentrations given by ionisation processes. [20]

All of these parameters will have specific values dictated by their spatial distribution throughout the plume as shown in Figure 6-14. Turbulence quantities must be appended to the values shown in Figure 6-14, these can be derived from turbulence kinetic energy values used to determine the shear layer mixing for the time-averaged flow. It is important [15] to consider the recirculation region established at the base of the missile in flight when the base diameter substantially exceeds the nozzle exit diameter. Recirculation affects the development of the downstream plume and may be critical to the onset of afterburning. Calculations [21,22] of this region are commonly based on iterative solutions over a fixed grid domain and, because the method is demanding of computer time and storage, computations are normally confined to structural information close to the nozzle exit where recirculation is significant.

4.2.2 Attenuation

Line-of-sight calculations are based on computing the absorption of a single RF ray as it passes through the plume. Along the ray path, the plume is assumed to absorb as a series of homogeneous plasma volumes normal to the ray.

The attenuation α (or energy absorbed) per unit path length (dBm^{-1}) is given by [1,15]

$$\alpha = 8.686 \left(\frac{\omega}{c}\right)\left[-\frac{(1-A)}{2} + \cdots\cdots\cdots\right.$$

$$\left.\frac{1}{2}\left\{(1-A)^2 + A^2\left(\frac{\nu}{\omega}\right)^2\right\}^{\frac{1}{2}}\right]^{\frac{1}{2}} \qquad (4.1)$$

$$\text{where } A = \omega_p^2 (\nu^2 + \omega^2)^{-1}$$

The phase shift coefficient β is given by

$$\beta = \frac{1}{\sqrt{2}} \frac{\omega}{c}\left[(1-A) + \cdots\cdots\cdots\right.$$

$$\left.\left\{(1-A)^2 + A^2\left(\frac{\nu}{\omega}\right)^2\right\}^{\frac{1}{2}}\right]^{\frac{1}{2}} \qquad (4.2)$$

The total phase shift θ through a length 'd' of homogeneous plasma is

$$\theta = (\beta - \beta_o)\, d$$

where $\beta_o = \frac{\omega}{c}$ and

c = velocity of light in vacuo

The terms α and β are the real and imaginary parts respectively of the complex propagation constant γ which defines the electric field of the propagating ray :-

$$\bar{E} = \bar{E}_o\, e^{-\gamma x}\, e^{-i\omega t}$$

$$= \bar{E}_o\, e^{-x(\alpha + i\beta)}\, e^{-i\omega t}$$

where $\gamma = \alpha + i\beta$

In certain cases the predicted line-of-sight attenuation is a reasonably good estimate of measurable values. These include focused-beam transverse attenuation where at the point of intersection between plume and beam axes, the half power radius of the beam does not exceed one forth of the plume radius. Equally, predictions of longitudinal (diagonal) attenuation by the line-of-sight method have shown reasonably good agreement with measured plume attenuation from composite propellants containing less than 5% aluminium [15]. Such plumes had a predicted maximum electron density of less than $10^{16} m^{-3}$ and showed a ratio of measured maximum longitudinal attenuation to measured maximum transverse attenuation that lay between 7 and 10. A range of composite propellant plume data that meet or fail these criteria are given in Figure 6-15a where measured values of the ratio fall between 0.7 and 10.

That diffraction may play a part in microwave propagation through highly ionised exhausts is indicated by combining results from transverse and longitudinal measurements and comparing them with predictions. Figure 6-15b compares longitudinal attenuation measurements for a given double base motor with predictions

from the line-of-sight code. At small plume interception angles from the axis, attenuations of 100dB or more are predicted. This is in marked contrast to the observed insertion loss which varies between -10dB and -30dB depending upon the location of the receiving antenna. Moreover, at these small angles the variation of measured insertion loss with frequency is not that to be expected should absorption be the dominant loss mechanism. Only at larger interception angles, where comparatively short path lengths close to the nozzle exist, is there reasonable agreement between prediction and measurement. This is further confirmed by Figure 6-2b, where transverse measurements at 35GHz, using a focused beam system, agree well with calculated values of attenuation for the same motor. It is clear however, that should attenuation measured over the relatively short diametric path at 3m be present over long paths through the length of the plume then attenuation in excess of 100dB would be expected. For exhaust jets where high electron densities exist, the insertion loss is not governed solely by absorption and other propagation mechanisms such as diffraction should be sought.

It is particularly interesting to examine the flight data analyses in Figure 6-10, the transverse wind-tunnel attenuation measurements of Figure 6-9 and calculations graphically summarised in Figures 6-16 and 6-17 in which base recirculating flow was coupled to the downstream flowfield [45]. All employ a common propellant; propellant 'C' which is non-metallised, consisting of 24% polyurethane and 75% ammonium perchlorate. In the wind-tunnel tests the results were very sensitive to free-stream Mach number. Below Mach 2.8 there was no afterburning, resulting in negligible attenuation. At Mach 2.8 and above, base burning induced combustion in the plume and attenuation reached a level comparable with those in Figure 6-16.

Figure 6-16a shows temperature calculations for propellant 'C' at 7.6km altitude, a velocity of M 2.2, with a 0.127m diameter missile base and 0.042m nozzle exit diameter (ϵ = 4.3, $p_c = 4 \times 10^6$ P_a). This Mach number was chosen because it corresponds to the onset of vigorous afterburning in flight tests using this propellant in a motor the size of that analysed in Figure 6-17. It is obvious that the calculations without a base effect show no afterburning at all, whereas the effect of the base is to cause significant afterburning, and, as seen in Figure 6-16b, a dramatic increase in electron density. Predicted sea level attenuation, wind-tunnel data, and predicted attenuation for simulated flight conditions are recorded in Figure 6-16c. The wind-tunnel data were obtained with a motor having a quarter of the thrust of that for which calculations were made. The base diameter was the same for both cases. The wind-tunnel data in Figure 6-16c have been adjusted by doubling the value on the abscissa which should partially compensate for the difference in thrust between the measured and calculated cases.

When the plume size is scaled up to that actually tested in flight (0.406m base diameter, 0.134m nozzle exit diameter), calculations indicate that the base effect is no longer critical to the initiation of in-flight afterburning or attenuation, although the base effect causes afterburning to start much closer to the nozzle exit. The same base diameter to nozzle exit diameter ratio is maintained in Figures 6-16 and 6-17. The results shown in Figure 6-17 are compatible with longitudinal microwave attenuation levels down to 20dB, which were measured in flight tests of propellant 'C'. The in-flight data have been reproduced fairly well by combining the results of Figure 6-17 with electromagnetic propagation calculations, which include the effects of refraction and diffraction.

Figure 6-18b compares measured and calculated longitudinal attenuation for a rocket motor having a composite propellant containing 5% aluminium. This did not produce a highly attenuating exhaust, and simple line-of-sight predictions were adequate.

4.2.3 Forward Scatter

Calculations of forward scattering [2,23,24, 25] of microwave radiation by exhaust plumes have been performed since the mid 1960s. In these calculations it is assumed that a receiving antenna is mounted at the rear of a rocket-propelled vehicle and is illuminated by a plane wave. The geometry of the problem is illustrated in Figure 6-1a, which also defines some of the variables. The incident plane wave illuminates the whole of the exhaust jet so that power is scattered from all parts of the jet into the receiving antenna. Turbulence-induced eddies of fluctuating electron density populate large regions of the exhaust and become sources of signal scattering, moving at local exhaust velocity. Each source volume (dV) contributes in some measure to the overall received signal strength, but at a frequency removed from that of the incident wave by a "Doppler shift" imposed as a result of local eddy gas velocity with respect to the receiver. Scattered energy received in this manner is related to the incident-received signal

by the equation :-

$$\frac{P_s}{P_i} = \frac{1}{4\pi G_{\beta_1}} \int_{Vol} \frac{G_{\beta_2} C_a}{r^2} \sigma \, dv \qquad (4.3)$$

where P_s/P_i is the ratio of the noise power to the signal power, G_{β_1} the receiving antenna gain in the direction of the transmitter and G_{β_2} that in the direction of the element dv. The distance between the receiver and the scattering element is denoted by r and σ is the volume scattering cross-section. The volume of integration includes the whole plume. C_a is the attenuation loss factor along the path through the plume to and from the element dv.

The volume scattering cross-section (σ) is a local property of the exhaust plume and may be shown to be :-

$$\sigma = \frac{0.63 \times 32\pi^4 r_e^2}{(1 + \nu^2/\omega^2)^2} \cdot \frac{n' \sin^2 \psi \, a^3}{B} \qquad (4.4)$$

where $n' = |n_e|^2 I^2$ the turbulent fluctuation of electron density [e⁻] and

$$B = (1 + 4a^2 k^2 \sin^2 (\alpha/2))^{11/6}$$

the Kolmogorov turbulence function.

In this equation r_e is the classical electron radius, ψ the angle between the direction of scattering and the incident electric vector and α the scattering angle. I is the local intensity of electron concentration fluctuations, n_e is the local mean electron density and 'a' the turbulent length scale. ν is the local electron-neutral body collision frequency, ω the angular frequency of the incident signal and k the wave number ($k = 2\pi/\lambda$).

In Equations 4.3 and 4.4 the angles ψ and α and the distance r may be determined geometrically; ω, k and the receiving antenna gain function are known characteristics of the microwave system. If n_e, ω, I and a are defined throughout the plume flowfield the scattered power may be calculated.

Flowfield calculations can provide local gas velocity, mean electron density and electron-neutral body collision frequency but considerable uncertainty surrounds the turbulence characteristics. The turbulent length scale (a) is commonly taken to be the correlation length for turbulent velocity fluctuations which may differ from the required length scale for fluctuations in electron concentration. It is calculated using a two-equation turbulence model in the plume structure program. The turbulent intensity (I) is often set to unity but can also be seen as a function of axial distance downstream of the nozzle exit and a corresponding radial distance. Both parameters are discussed in greater detail in Reference 20.

The "Doppler" frequency shift of the power entering the receiver from scattering elements dV is written :-

$$f_D = \frac{u}{\lambda} (\cos \beta_1 - \cos \beta_2) \qquad (4.4)$$

For a given element (dv), if the wavelength (λ) of the incident wave and the local gas velocity (u) are known the frequency of the scattered power for angles β_1 and β_2 of Figure 6-1 can be obtained from this equation. Summation of all scattered energy generated in this way throughout the plume forms the radio sideband spectra associated with rocket exhaust interference. Plume characteristics, which will change with altitude and forward velocity, govern the spectrum of the total received power. It may be dominated by line-of-sight or scattered energy or may contain significant contributions from both. Comparisons between prediction and experiment are shown in Figure 6-19.

4.2.4 Back Scatter

Back scatter of microwave radiation by a plume is calculated using the same scattering equations (4.3, 4.4 and 4.5) used for forward scatter. Some differences occur in the use of the equations for the two situations; for back-scatter the angle, α, is fixed at 180 degrees and the absorption function, C_a, is made of two parts that are generally the same on incidence and departure from a scattering element, dv. This contrasts with forward scattering where α assumes all values and C_a differs in value between that of incidence and departure.

Fundamental experimental work for determining plume backscatter has been conducted at the Stanford Research Institute (SRI) in the frequency bands 7GHz to 11.5GHz and 26.5GHz to 40GHz [26-30]. In this work the exhaust plume, which was studied at a reduced

ambient pressure of 800Nm^{-2}, was produced by burning ethylene and oxygen with KCl seeding to produce ions. Variables of the plume were studied including electron fluctuations and turbulence-scale length correlations. Variations of ambient pressure and the effects of a co-flowing stream were not studied. The SRI results offer some insight into the parameters 'n' and 'a' of the scattering equations.

An important flight trial, dedicated to the measurement of backscatter or, as it is often referred to, radar cross section (RCS) was made in the U.S. and the results were compared with calculations. In general, Doppler frequency shift relates to plume flowfield velocity components along the radar line-of-sight through the plume and can be associated with specific regions of a flowfield prediction that calculates the spatial distribution velocity. In the backscatter prediction code, specific RCS returns were associated with specific regions of the plume and hence, with specific velocities. These were then joined together to form the total theoretical radar cross section of the rocket plume. Figure 6-20a shows the total RCS Doppler spectrum measured in flight and was obtained by summing the Doppler spectra from nine individually resolved range "bins" in the RCS flight data. Doppler shift data from each of the range "bins" can also be plotted, each range "bin" corresponding to a 20.2m length of plume. This technique provided, in effect, a "diagnostic probe" with which to interpret data from the flight plume for comparison with spatially resolved plume calculations. Values from each of the nine "bins" are compared, calculation with experiment, in Figure 6.20b.

Past RCS measurements (RATSCAT) were made on firings of aluminized solid propellant motors and liquid motors seeded with controlled amounts of potassium to produce free electrons and thus modify the RCS [31]. The data collected was not taken with Doppler radar equipment but there is good total RCS data viewed from broadside and angles either side of broadside. The measurements were made by rotating the motors during firings. Early calculations [32] gave reasonably good agreement with data, more recent calculations in the U.S. are showing remarkably good agreement with the RATSCAT measurements [33]. A sample of RATSCAT data, from eight test firings, is shown without details in Figure 6.21. Six frequencies, between 0.15 and 5GHz were used in the experiments. All motors had thrust levels of about 8.96kN with two levels of aluminium 16% and 5%.

4.2.5 Diffraction

The transverse measurements described in Section 4.1.1.1 and 4.2.2 support the view that longitudinal received signal level is not determined solely by absorption and that significant amounts of energy can reach the receiver other than by the direct line of sight. An example suggesting a diffraction mechanism in operation is given by Figure 6-22a and b which presents plume attenuation at two wavelengths for a highly ionised exhaust plume. The measurements are compared with prediction at zero aspect angle and two plume intersecting aspect angles. The antenna displacement from the motor axis was changed for each firing.

Measured attenuation at K band (nominally 35GHz) shows good agreement with predictions at zero aspect angle suggesting conformity with the line-of-sight theory of Equation 4.1 in Section 4.2.2 which was used for the calculation. However as the increase in aspect angle directed the propagation path into regions of higher electron density so that conformity lessened. Even at zero aspect angle it is the steepness of the curve at 15dB which gives the appearance of agreement. The bracketed point pair shows the difference in attenuation for the same displacement. Accepting uncertainties associated with predictions, experiment and theory are not in great disarray, particularly below the 10dB attenuation level.

I band (nominally 10GHz) does not show the same degree of agreement and with the reduced slope of the experimental curves it is evident that they will cross those of K band. Beyond the intersection, in increasing attenuation, there will be a reversal of exhaust penetrative powers between K and I bands, which is contrary to Equation 3.1. Slight differences in aspect angle do not invalidate these observations since the family of curves allows reasonable interpolation. Further substantiation of a diffraction mechanism is given by the very close agreement between plume attenuation measured for a 0.2% potassium seeded, 20% aluminised rocket motor and the diffraction pattern of an aluminium cylinder (Fig 6-20). Lower potassium and/or aluminium loadings of the rocket propellant result in similar radiation patterns, but with reduced signal loss. The apparent discrepancy between the two straight lines shown in Figure 6-16 is explained by a diffraction calculation.

A good theoretical description of the diffraction process has yet to evolve, it is a complex subject [15,34,35]. Simple computer programs for modelling diffraction of microwaves by an afterburning rocket plume have met with some success and reproduce experimental longitudinal attenuation data quite well. (Figs 6-23, 6-24 and 6-25). One such model is based on the theory of line source diffraction by semi-infinite wedges and strips and has been consistently successful. (Fig 6-25). This and other methods are discussed with references in Reference 15.

Recent investigations [36] have employed ray-tracing studies to estimate the temporal development of wavefront distortion and have indicated the possible existence of diffraction. From plume flowfield data of electron density contours, a three dimensional model of the spatial variation and gradients of the complex refractive index has been developed. It was based on a three dimensional plume "tear drop" function sectioned by a plane surface. This enabled rapid progress by ray tracing leading to an investigation of the progressive wavefront distortion experienced by a plane wave propagated through the plume. The diffraction is dominated by a highly localised stationary phase region with a position that could be defined by inspection of refractive waveform compression. An equivalent diffractor was established having the form of an ideal absorbing disc and combining the GTD fields with that from a direct ray. The equivalent diffractor was replaced by an effective diffracting surface, positioned in the same way. Three dimensional ray-tracing of a large number of these rays and their truncation at a relative phase-time defined by the assumed location of this surface, was used to define secondary sources and represent in a more natural way, the stationary phase region within a discrete form of the Fresnel/Kirchkoff scalar diffraction integral. Account was taken of the very high lateral spatial refractive index gradients in the region between the effective diffracting surface and the plane of the receiver by incorporating geometrical masking into the diffraction calculation. For small angles, the effective diffractor approach was justified because the loss mechanism was dominated by the behaviour of the wavefront in a highly localised region. It is also strongly influenced by the masking effect of the intervening dense plasma and a non-abrupt interaction of the direct ray between transmitter and receiver. Figure 6-26 shows a sample comparison between calculated diffracted signal and measured attenuation for a high electron density plume from a double base propellant motor. The solid points are those of individual firings, the full line is that of the diffracted signal where Eo/Ei is the attenuation level in decibels. Work is still proceeding to evaluate this method for a range of rocket motors.

4.2.6 Refraction

4.2.6.1 Longitudinal Refraction

The refractive index of a medium is given by $n = c/v$, where v is the velocity of electromagnetic radiation in the medium and c is its velocity in a vacuum. In an absorbing medium the index of refraction is complex: $\underline{n} = n(1 + ik)$. Solutions to Maxwell's equations for a monochromatic plane wave in free space provide the propagation constant $\gamma = \alpha + i\beta$ which can be related to the complex refractive index ($\underline{n}$) since $\alpha = \omega nk/c$ and $\beta = \omega n/c$ where ω is the angular velocity of the wave

$$\therefore \underline{n} = \frac{\beta c}{\omega} + \frac{i\alpha c}{\omega}$$

The complex nature of the refractive index affects the path of the ray through an absorbing medium. Poynting's vector oscillates in such a medium, consequently the energy path cannot be obtained from this vector which leads to computations of considerable complexity. If absorption over one wavelength is not appreciable, then the complex law of diffraction deviates negligibly from Snell's law for absorbing media.

$$n_1 \text{ Sin } \theta_1 = n_2 \text{ Sin } \theta_2$$

where the subscripts refer to the media on either side of a boundary crossed by the radiation.

It is in the outer regions of the plume where refraction can occur with little attenuation of the incident wave, that energy in the wave leaving the exhaust can be at a high level. Calculation of refraction in these regions, where the refractive index gradients are low, can be achieved by the use of contours of constant refractive index. While recognising that the mean refractive index continually changes through the plume, as an approximation the path of the ray can be stepped through small volumes of constant refractive index changing direction at each interface. The step length can vary according to the local refractive index gradient and Snell's law can apply.

The results of several two-dimensional refraction calculations are shown in Figure 6-27. Oblique entering rays are refracted in the direction of increasing refractive index so strongly that they seem to almost glance off the plume. The fact that these rays emerge with little attenuation can result in multi-path effects in the field beyond the missile which may interfere with target tracking as indicated in Section 3.1.2 or with other missiles in salvo operation.

Multiple ray tracing as performed in References 34, 36 and 37 will provide a more rigorous method of calculating refractive effects over a range of rocket exhausts.

4.2.6.2 Transverse Refraction

The interaction of a focused microwave beam propagated transversely through a plume can be developed using the same method as that for the longitudinal case. Refraction of a single ray by a homogeneous plume will undergo a change in direction and path length. Summation of all such rays arriving at the receiver will result in a distorted wave pattern with variations of phase and amplitude across the wave front. A non-homogeneous plume increases the complexities of calculation since changes of refractive index gradients within the plume must be considered as the ray progresses through.

The energy in a focused microwave beam has been reported to vary as a first order Bessel function of the first kind.

Figure 6-28 compares experimental transverse attenuation data from firings of three motor sizes containing identical propellant with the results of the transverse refraction model. The refraction model agrees with the data far better than the simpler attenuation model. In using the model, a beam radius of 0.05m and beam focal length of 1.0m were assumed.

4.2.7 Emission

The physical processes governing thermal emission from rocket exhaust plumes at millimetric wavelengths have been examined by Sume. [6] The mechanisms considered were free-free electron emission (bremsstrahlung), molecular band emission, free-bound electron emission, and the emission from aluminium oxide particles in the exhaust. The dominant mechanism was found to be the free-free continuum emission from electrons, and is the only mechanism considered in this treatment.

The monochromatic emission intensity along a line of sight of path length L through a non-isotropic, non-isothermal medium is given by

$$I(\lambda) = \int_0^{\ell} \exp\left[-\int_0^{\ell} K(\ell')\, dL'\right] K(\ell)\, I_B(\ell, \lambda)\, d\ell \qquad (4.6)$$

where $I_B(\ell, \lambda)$ is the local black body emission and $K(\ell)$ is the absorption coefficient at wavelength λ. The absorption coefficient, at angular frequency ($\omega = 2\pi\omega c/\lambda$), of a plasma with no magnetic field present is given by Sume.

$$K = 2\omega\, n_2/c$$

where c is the velocity of light and n_2 is the imaginary part of the complex refractive index (n).
Following Sume

$$n^2 = (n_1 - i\, n_2)^2$$

$$= 1 - x\,(1 - i\, z)^{-1}$$

Assigning

$$x = \omega p^2\, \omega^{-2} \text{ and } z = \nu\omega^{-1}$$

with ν as the electron-neutral molecule collision frequency and ω_p as the plasma frequency given by

$$\omega_p^2 = N_e\, e^2/\epsilon_o m$$

where N_e is the electron density, e and m are the electronic charge and mass respectively and ϵ_o is the permittivity of free space, one now obtains :-

$$n_2 = \left[\frac{1}{2}\left(-\left(1 - \frac{x}{1+z^2}\right) + \ldots\ldots\ldots\right.\right.$$

$$\left.\left.\sqrt{\left(1 - \frac{x}{1+z^2}\right)^2 + \left(\frac{xz}{1+z^2}\right)^2}\right)\right]^{-1/2}$$

or if

$$\omega_p^2 \ll \nu^2 + \omega^2 \text{ and } \nu^2 \ll \omega^2, \text{ or if } \nu^2 \gg \omega^2$$

$$n_2 \cong \frac{x\,z}{2\,(1 + z^2)}$$

Hence, if temperature, electron concentration and electron-neutral molecule collision frequency are known along the line of sight, the emission can be calculated. The quantities can all be predicted for a rocket exhaust jet using plume programs such as REP or SPF.

The black body emission is given by the Planck equation

$$I_B = C_1 \lambda^{-5} \left\{ \exp\,(C_2/\lambda T) - 1 \right\}^{-1} \qquad (4.7)$$

Since apparent brightness temperatures are required, the black body emission equation is simplified by ignoring the first term (C_1/λ^{-5}), and the apparent brightness temperature is calculated.

The engineering quantity, Apparent Brightness Temperature, is here defined as that temperature which is required in Equation 4.7 to give the same output emission as in Equation 4.6 at wavelength λ.

A simplified three-dimensional geometry treatment is used to define the lines of sight. The position of any point along these lines of sight may be transformed into the plume frame of reference, and, using linear interpolation, the values of temperature, electron density and collision frequency at any point can be calculated from the plume output.

Provision can also be made for the possible transmission of background radiation from sources on the far side of the plume to the detector. A uniform apparent brightness temperature, specified by the user, is assumed for the background radiation. This is added to the total calculated emissions at the end of each line of sight, and is taken as the total emission for lines of sight which do not intersect the plume.

5.0 REDUCTION OF EXHAUST INTERFERENCE AND SIGNATURE

It should be the aim in rocket design to produce a motor that yields no guidance or tracking problems and offers minimal signature. Throughout the chapter microwave attenuation, scattering and emission have been directly associated with the presence of free electrons in the exhaust brought about by ionisation of impurities at exhaust temperature.

5.1 Chemical Modification

Readily ionisable alkali metal impurities are a major source of free electrons in rocket exhausts. Of these, sodium, potassium and calcium are commonly encountered, forming a small but significant constituent of the propellant. Typical concentrations of these metals in solid rocket motors would be 30ppm by weight of potassium and 100ppm of sodium (and even higher levels of calcium) depending upon the type of propellant and its method of manufacture. Complete removal of these impurities from propellants is difficult and prohibitively expensive.

Composite propellants incorporate calcium in the phosphate form to reduce agglomeration in ammonium perchlorate, while the hydroxide is used to counter the acidity of nitro-cellulose in double base propellants.

The ionisation process is very much dependent upon exhaust temperatures, should they be lowered the electron population will then show a marked decline, reducing the severity of microwave attenuation. Ultimately, if the plume is prevented from burning, very little or no attenuation is evident.

Exhaust combustion is supported by flame-propagation of free radicals like H and OH and rapid removal of these radicals is the aim of combustion suppression. Although paradoxical, potassium salts introduced into double base propellants as a small percentage of the propellant can stimulate the radical-removing reaction processes.

$$K + OH + M \rightarrow KOH + M$$
$$KOH + H \rightarrow K + H_2O$$

Sodium has similar reaction properties but, weight for weight, is unlikely to better potassium. An important aspect of flame suppression agents is that they should act in the gas phase rather than produce condensed products. Potassium compounds have been shown to be effective suppressants for double base propellants (38,39, 41].

Some alkaline earths have been considered, notably molybdenum, iron cobalt and tungsten. [40]

Suppression additives can be introduced in a variety of ways, the most common being as a propellant ingredient but other methods such as annular spray rings, ablating rods or collars and charge or throat coatings are possible. While static rocket firings are used to assess the performance of additives it must be cautioned that in critical 'burn/no-burn' cases the turbulence of forward velocity or other perturbations in flight may influence the onset of exhaust combustion. Wind-tunnel tests or ultimately flight tests may be necessary to ensure complete confidence.

The case for composite propellants is one where total suppression is unlikely to be successful. Some relief from attenuation can be achieved by the introduction of certain metallic compounds into the exhaust which will lower the free electron concentration. Two chemical mechanisms are suggested. One involves the process of electron attachment where free electrons are replaced by heavy, slow moving, negative ions which contribute very little to microwave absorption [43]. Using molybdenum as an example, such mechanisms could be :-

$$e^- + H_2MoO_4 \rightarrow HMoO_4^- + H$$

$$e^- + H_2MoO_4 \rightarrow MoO_3^- + H_2O$$

These reactions must over-ride the already active reaction

$$e^- + HCl \rightarrow Cl^- + H$$

The other mechanism has the object of lowering the free radical concentrations in the exhaust but not to the point of flame extinction. If chlorine is present in the plume then in general the ionisation of alkali metals(A) takes the form

$$ACl^- + 3H \rightarrow A^+ + e^- + HCl + H_2$$

where concentrations of electrons [e^-] can quickly fall if those of H (the hydrogen atom) drop [44]. It is important that the additive should remain in the gas phase in the exhaust, equally it should not form stable compounds with the chlorine.

With double base propellants it might be argued that any additive forming stable negative ions in the exhaust will, in some measure, reduce free electron concentrations, particularly since [Cl^-] is not being generated.

6.0 RECOMMENDATIONS

It has long been recognised that to fully evaluate the microwave properties of a rocket motor exhaust for a specific role, flight tests should be undertaken in the proposed operational environment. This is known to be very expensive when the full range of operating temperatures, altitudes and velocities are represented. Also missile manoeuvres and information on flight attitude at any instant can make the recording of accurate flight data a difficult task. Added to this is the fact that flight tests can only come at the post design stage when the programme is well advanced. Any fundamental changes at this point are often strongly resisted and a compromise enters the project. Theoretical plume studies offering reliable predictions at the time when design options are being considered would be the ideal way to optimise propulsion performance against plume effects. Although well progressed, plume technology has yet to reach the stage where modelling techniques preclude recourse to experiments. The aim of a plume study group must be to perfect these techniques supported by validation from well conceived experiments.

It is recommended that theoretical studies should be undertaken to understand the chemical and thermodynamic properties of the plume flowfield leading to its microwave signature and propagation characteristics. For any proposed propulsion system they must be backed by validation in test facilities of the kind discussed here and in Section 3.1.

6.1 Test Objectives

In order that research and missile projects can be supported, facilities for measuring rocket exhaust microwave properties should be broad ranging with maximum flexibility. The following requirements are offered as objectives :-

(i) To provide experimental data for new research concepts.

(ii) To conduct experiments for the validation of prediction codes.

(iii) To compare motors for specific mission objectives.

(iv) To measure the microwave characteristics of propellants containing a range of additives for plume suppression and other interference relief.

(v) To evaluate rocket motors for service acceptance.

6.2 Test Facilities

Test facilities are expensive and not all interested plume groups feel free to commit large sums of money to fund the options available. They fall into three main categories :-

(i) Static firings at sea-level.

(ii) Free flow velocity simulation using wind tunnels or high velocity sledge tracks.

(iii) Simulation of altitude and free flow velocity in chambers.

6.2.1 Static, Sea-level

Of the facilities, the most versatile is the open range, static firing site where short and long range microwave measurements can be conducted and where the various smoke and emission tests, outlined in the previous chapters, can also be accommodated. For example, some emission measurements with passive instrumentation can be combined with microwave measurements. Other combinations spring readily to mind.

It should be possible to fire a full range of motors, in both physical size and thrust and, to maximise site use, restrictions imposed by proximity to other installations or acoustic sensitive environments should be avoided.

Instrumentation should have ease of deployment and be able to view the plume from all aspect angles and from a variety of distances. For longitudinal microwave exhaust propagation experiments the propagation paths must be free from obstruction or any structure likely to introduce multipath reflections. This includes ground reflections, consequently an elevated thrust stand may be considered necessary to ensure integrity of measurement. Variation in aspect angle is often accomplished by rotation of the motor, which has the advantage of least disturbance to the microwave equipment and affords an economy in motors if they have burning times that allow angular sweep operation during firing. Obviously, antennae polar patterns should reflect this movement in that, for forward scatter, with the receiving antenna attached to the motor in the nozzle exit plane, the energy from the transmitter must illuminate the whole plume if true sideband noise levels are to be obtained. Polar patterns tailored to the location are advisable to avert the possibility of spurious reflections entering the receiver. Some beam shaping is seen in Figure 6-5 where the antenna was used on the elevated firing facility mentioned in Section 4.1.1.1.

Transverse plume measurements are usually made over very short distances between focused beams. They are normally of a diagnostic nature, as a research probe, for prediction validation or comparative measurement, one motor with another. Short signal paths bring the microwave equipment close to the rocket motor and its exhaust where ground-borne and air-borne vibrations can be a problem and radiant heat damage a possibility. A major facility requirement is that the support carriage bearing the microwave system should be able to travel the complete length of any rocket plume under test. Equally, the minimum vertical travel must take the microwave beam diameter through the full diametric range of the exhaust. For an exhaust having symmetry about the motor axis this need only be just beyond the radius, but it must be remembered that there may be angled or multiple nozzle motors. For both longitudinal and transverse measurements, where research versatility is important, the installation of a gas engine or liquid propellant engine can be of benefit. Variations of thrust, mixture ratio, length of burn and chemical seeding can be readily achieved. The initial installation costs of these engines may be quite high but running costs, assuming a good use rate, are low.

6.2.2 Free Flow Velocity Simulation

Longitudinal measurements are not often attempted in the confined space of a wind tunnel where access is difficult and give rise to scattering and multipath uncertainties in the experimental data obtained. Attempts have been made to provide internal absorption liners but these are harshly treated by the environment. However, wind tunnel exits can be fabricated to produce airflow over the missile body which simulate flight velocity conditions. Given that the wind tunnel exits to an open site area a range of

microwave measurements can be undertaken both transverse and longitudinal. It must be emphasised that for the latter case, spurious microwave reflections entering the receivers from any nearby objects or the ground must be made negligible, also any airflow interaction with the ground downstream of the tunnel exit may make conditions for longitudinal measurements unacceptable.

Sleds propelled by the rocket along high velocity tracks can simulate flight conditions but their use for longitudinal microwave measurements leave doubt about the results obtained. It must be kept in mind that although prefiring multipath reflections can be reduced, the dynamic case raises the possibility of plume refraction, diffraction or scattering causing unwanted returns from the track and nearby objects. This method of measurement should be approached with caution.

6.2.3 Altitude and Velocity Simulation

These measurements, again mainly transverse, more nearly represent those of flight. It might be argued that because of the control available, the amount of information gained is more useful and cost effective than that of flight trials where interpretation is difficult. Such facilities have good value in research and prediction validation when studying plume expansion with altitude, nozzles, base flow effects, propellants and additives. They provide the design team with confidence to proceed with a project backed by strong experimental evidence to support predictions which can then be translated to meet operational needs.

7.0 REFERENCES

1 Williams, H
Radio Propagation through Rocket Exhaust Jets:
Part 1. Electromagnetic Wave Propagation in an Ionised Medium.
RPE Report No 37, February 1959

2 Williams, H, Wilson, A S, Blake, C C
Scattering from a Turbulent Rocket Exhaust Jet Illuminated by Plane Wave
Electronics Letters Vol 7, No 189, Sept 1971

3 Smoot, L D, Underwood, D L
Prediction of Microwave Attenuation Characteristics of Rocket Exhausts
J Spacecraft and Rockets, Vol 3, No 3, March 1966

4 Smoot, L D, Seliga, T J
Rocket Exhaust Plume Radar Attenuation and Amplitude/Phase Noise
J Spacecraft and Rockets, Vol 4, No 6, June 1967

5 Victor, A C
Microwave Interference Characteristics of a Solid Rocket Motor Exhaust
NWC China Lake, California, NWCTP4199, Oct 1968

6 Sume, A
Millimetric Wavelengths Emissions from Solid Propellant Rocket Motor Plumes
Försvarets Forskingsanstalt Report C30291-E1, E3, Sept 1982

7 Ramsey, D A
The Evaluation of Radar Guidance
GEC Journal of Research, Vol 3, No 2, 1985

8 Cummings, G A McD, Lawrence, R E, Travers, B E L
Radio Interference due to Rocket Exhaust Jets. A Detailed Study of the Interference Characteristics of a Selected Propellant
RPE Tech Report 71/73, 1971

9 Cummings, G A McD, Travers, B E L, Wilson, A S
Radio Interference due to Rocket Exhaust Jets. The Study of Jet Structure Using Focused Microwave Beams
RPE Tech Report 71/72, 1971

10 Victor, A C, Mantz, J C
Interaction of Focused Microwave Beams with a Rocket Exhaust
NWC China Lake, California NWCTP5119, Feb 1972

11 Lawrence, R E
Radio Interference Caused by Rocket Exhaust Jets. The Measurement of Phase Modulation
RPE Tech Report No 70/9, Oct 1970

12 Cummings, G A McD, Lawrence, R E Travers, B E L.
Radio Interference due to Rocket Exhaust Jets: Study of Transverse Attenuation Characteristics at Simulated Altitudes

13 Buckley, F T, Williams, G M
Radar Attenuation Studies at Simulated Altitude.
CPIA Publication No 234, June 1973

14 Wilson, A S, Jensen D E
Prediction of Rocket Exhaust Flame Properties
Combustion and Flame 25, 43, 1975

15 Victor, A C
JANNAF Handbook on Rocket Exhaust Plume Technology
CPIA Publication 263, Chapter 4
John Hopkins University, MD, 1977

16 Dash, S M, Pergamont, H S, Thorpe, R D
The JANNAF Standard Plume Flowfield Model. Modular Approach and Preliminary Results
CPIA Publication 306, Vol 1, May 1979

17 Jensen, D E, Jones G A
Theoretical Aspects of Secondary Combustion in Rocket Exhausts
Combustion and Flame 41, 71, 1981

18 Pergamont, H S, Dash, S M, Verma, A K
Evaluation of Turbulent Models for Rocket and Aircraft Plume Flowfield Predictions
AIAA Paper 79-0359, Jan 1979

19 Dash, S M
Recent Developments in the Modelling of High Speed Jets, Plumes and Wakes
AIAA Paper 83-1616, July 1985

20 Cousins, J M, Jensen, D E
On the Computation of Ionization Levels in Rocket Exhaust Flames
Combustion and Flame 52, 111, 1983

21 Jensen, D E, Spalding, D B, Tatchell, D G, Wilson, A S
Computation of Structures of Flames with Recirculating Flow and Radial Pressure Gradients
Combustion and Flame 34, 309, 1979

22 Mace, A C H, Markatos, N C, Spalding, D B, Tatchell, D G
Analysis of Combustion in Recirculating Flow for Rocket Exhausts in Supersonic Streams
J Spacecraft and Rockets 19, 557, 1982

23 Tartarski, V I
Scattering from a Turbulent Medium
NY McGraw-Hill 1961

24 Salpeter, E E, Treiman, S B
Backscatter of Electromagnetic Radiation from a Turbulent Plasma
J Geophys 69, No 4, 869, 1964

25 Granatstein, V L, Buchsbaum, S J
Proceedings of Symposium on Turbulence of Fluids and Plasmas
Polytechnic Press NY, 1969

26 Graf, K A, Guthart, H, Douglas, D G
Scattering from a Turbulent Laboratory Plasma at 31GHz.
Radio Science Vol 6, No 7, 737-752, 1971

27 Graf, K A, Guthart, H
Application of a Simple Model for Calculating Scatter
Physics of Fluids Vol 14, No 2, 410-413, 1972

28 Guthart, H, Graf, K A
Scattering from a Turbulent Plasma
Radio Science, Vol 7, No 7, 1099-1118, 1970

29 Guthart, H, Graf, K A
Attenuation due to Scatter in Random Media
Physics of Fluids, Vol 15, No 7, 1972

30 Tremain, D E, Graf, K A, Guthart, H
Direct and Cross-Polarized Scatter from a Turbulent Laboratory Plasma
Radio Science, Vol 18, No 2, 281-287, 1983

31 Marlow, H C (Maj)
RAT-SCAT Radar Cross Section Measurements of 017-2, Rocket Exhaust Plumes
USAF, MDC-TR-66-37, (AD37935) Dec 1966

32 Pergamont, H S
Radar Cross Section of Rocket Exhaust Plumes
Aerochem, Princetown, NJ, AFRPL-TR-68-176 (AD394136) Oct 1968

33 Lee, M J, Victor, A C
Radar Cross Section Analysis for Rocket Plumes
18th JANNAF Exhaust Plume Technology Sub-committee Meeting, Monterey, Calif, 14-16 Nov 1989, to be published by CPIA

34 Golden, K E, Taylor, E C, Vincentie, F A
Diffraction by Rocket Exhausts
IEEE Trans AP 16, No 5, 614, 1968

35 Senol, A J, Romine, G L
Three-dimensional Refraction/Diffraction of Electromagnetic Waves Through Rocket Exhaust Plumes
J Spacecraft and Rockets 23, No 1, 39, 1986

36 Hall, C M, Strangeways, H J
Representation of Microwave Propagation Through High Electron-Density Rocket Exhaust Plumes by an Equivalent Diffracting Disc
Proc Int Conf on Electromagnetics in Aerospace Applications, Torino, Italy, 1989, pp 95-98

37 Molmud, P
RAYBEND - A Ray Tracing Program for Microwaves Propagating Through Rocket Plumes
JANNAF 12th Plume Technology Meeting, Oct 1980, pp 273-312

38 Smith, P K, Evans, G I
The Suppression of Secondary Combustion in Solid Propellant Motors
Imperial Metal Industries, Tech Note 82/5, 1982

39 McHale, E T
Flame Inhibition by Potassium Compounds
Combustion and Flame 24, 2377, 1975

40 Jensen, D E, Jones, G A
Theoretical Aspects of Secondary Combustion in Rocket Exhausts
Combustion and Flame, 41, pp 71-85, 1981

41 Jones, G A
Comparison of Predicted and Experimental Microwave Attenuation for a Flame-Suppressed Rocket Exhaust Plume
DRA Fort Halstead, RARDE Tech Report 13/85, Nov 1985

42 Jensen, D E, Webb, B C
Afterburning Predictions for Metal Modified Propellant Motor Exhausts
AIAA Journal Vol 14, No 7, 947, July 1976

43 Jensen, D E, Miller, W J
Electron Attachment and Compound Formation in Flames IV. Negative Ion and Compound Formation in Flames Containing Potassium and Molybdenum
Thirteenth Symp (Int) on Combustion (The Combustion Institute, Pittsburgh, 1971) p 363

44 Jensen, D E, Jones, G A
Mass-Spectrometric Tracer and Photometric Studies of Catalysed Radical Recombination in Flames
J Chem Soc Faraday Trans I, 71, 1975

45 Victor, A C
Calculations of Rocket Plume Afterburning Coupled to Reacting Base Recirculation Regions
J Spacecraft and Rockets Vol 14, No 9, 534, Sept 1977

FIGURES

TABLE OF CONTENTS

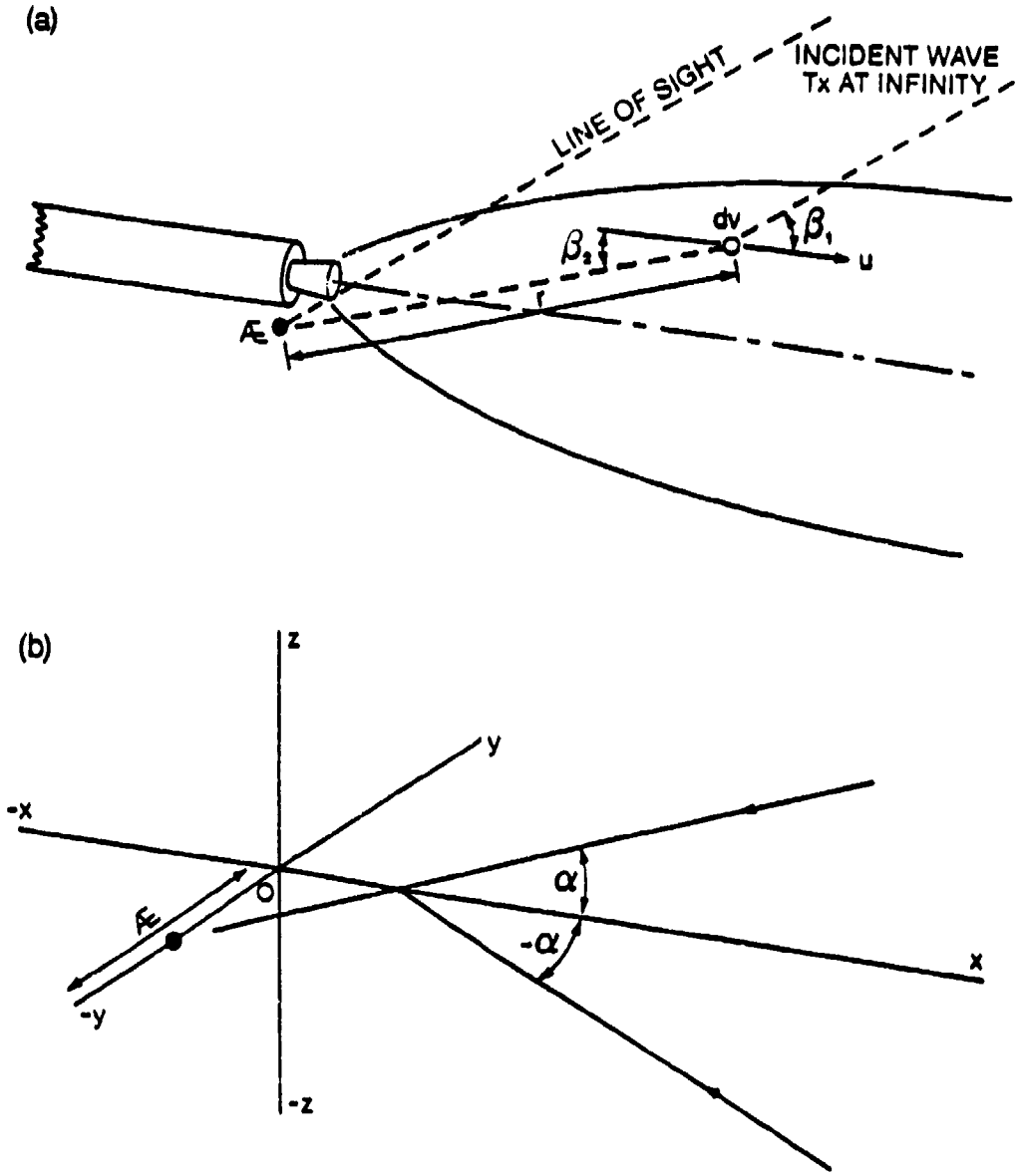

Fig. 6-1 Diagram Showing **(a)** Propagation Geometry
(b) Co-ordinate System

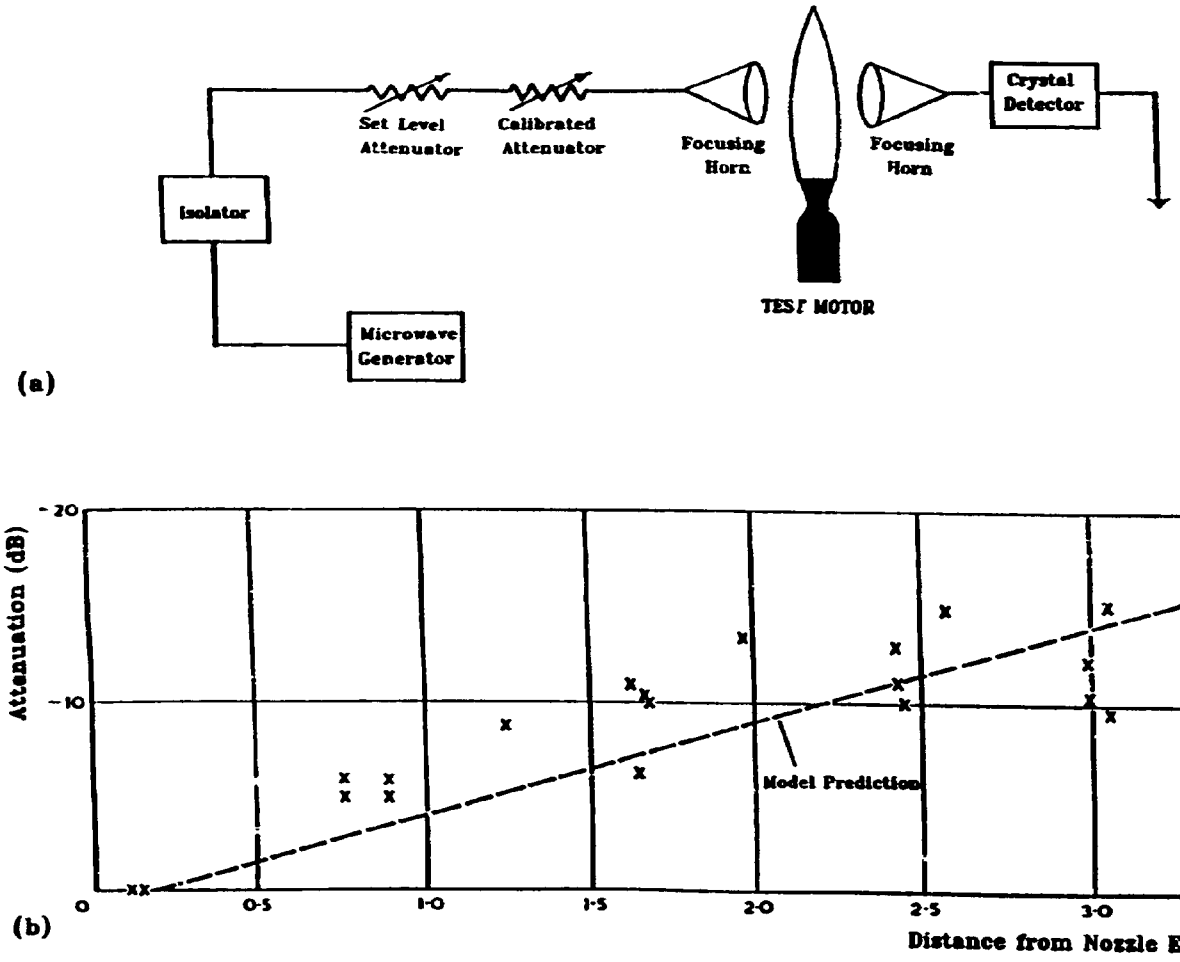

Fig. 6-2 (a) Transmitter and Receiver Assembly
(b) On axis Transverse Attenuation with Distance from Nozzle Exit

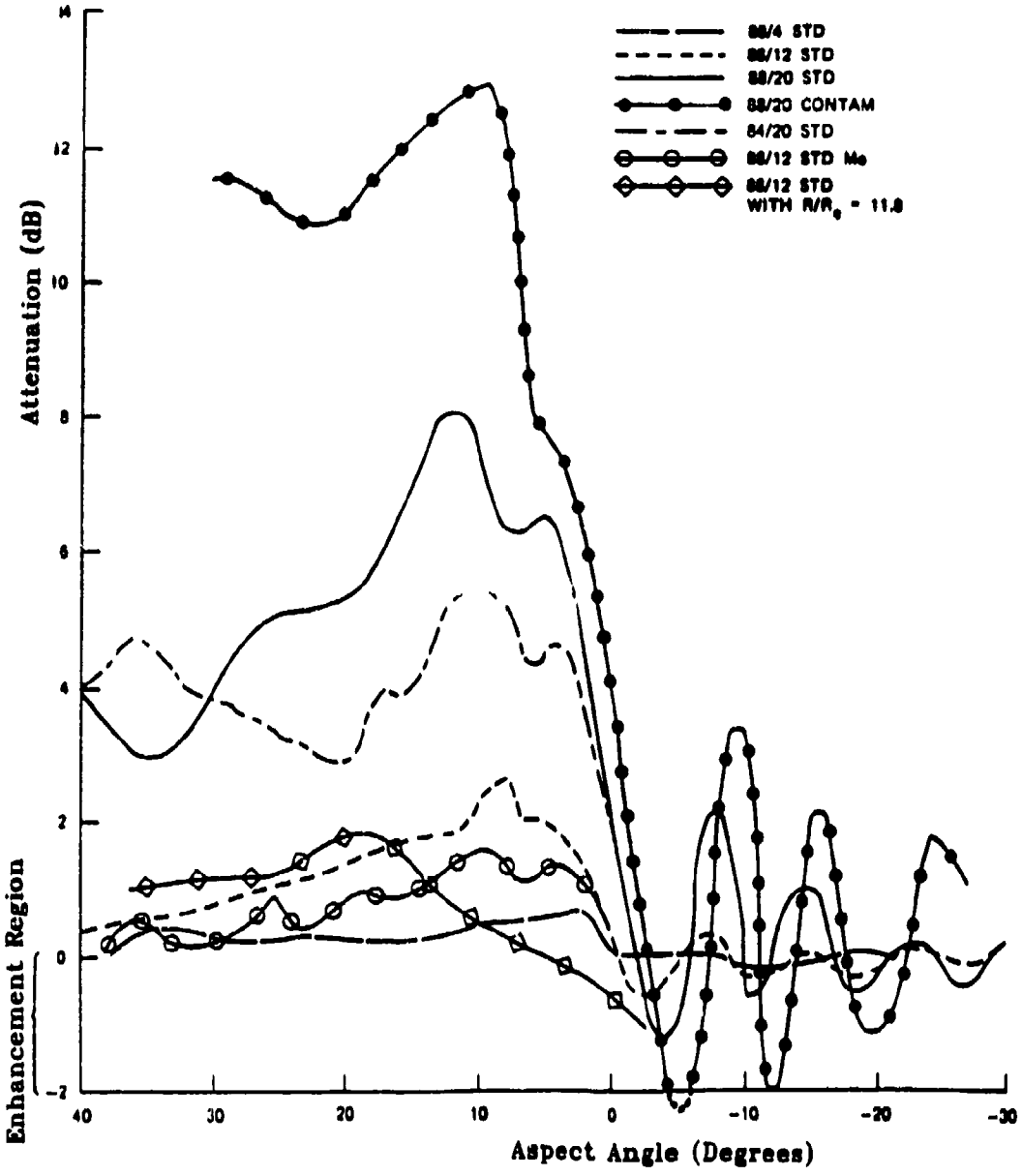

Fig. 6.3 Diagonal I-Band (Nominally 10GHz) Attenuation Data for Composite Propellant Motors. Static, Sea-Level Firing. 4.45kN Thrust, Transmitting Antenna in Exit Plane, 5 Exit Radii from Nozzle Centreline. (R/R_e=5).

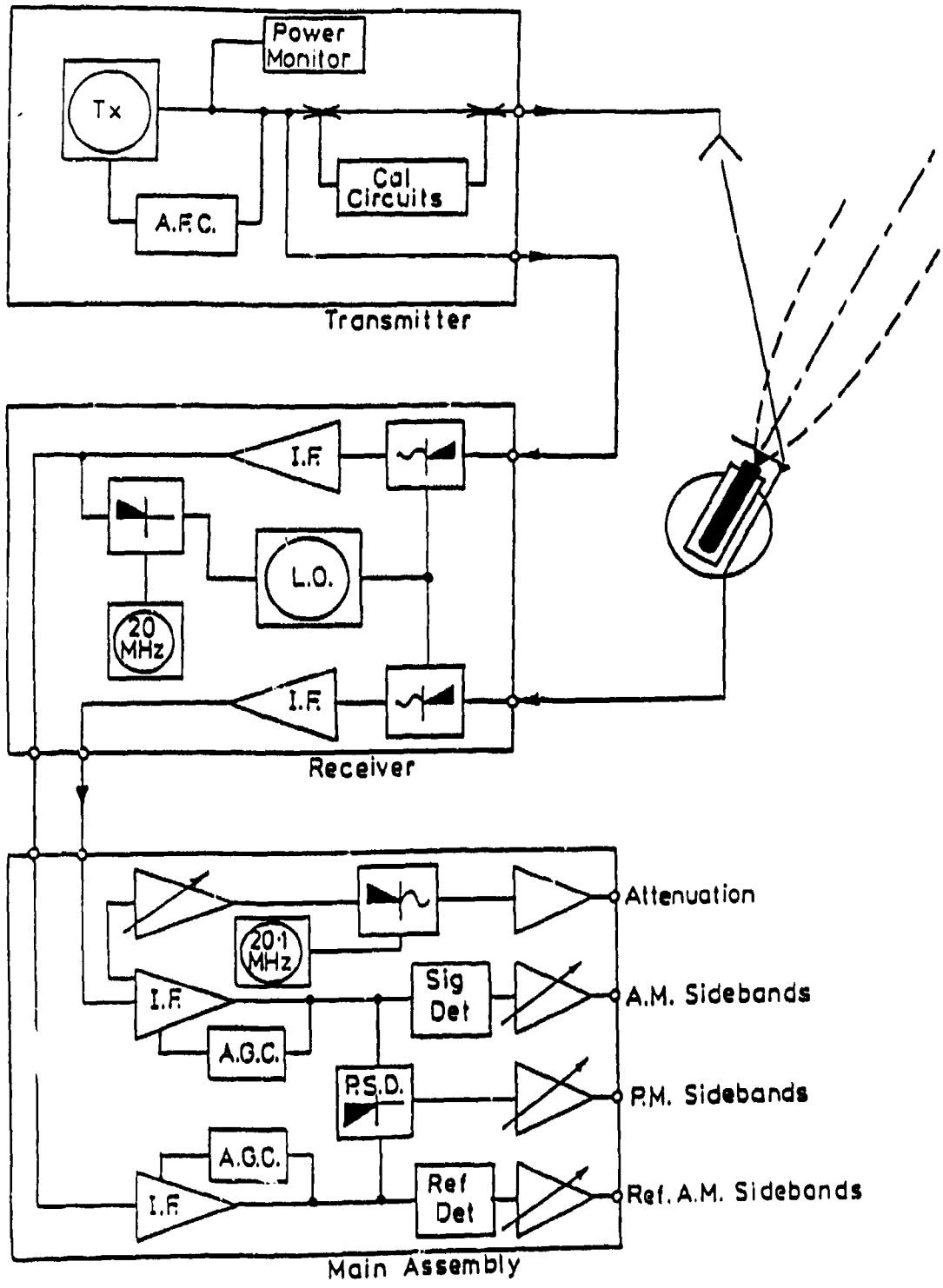

Fig. 6-4 Attenuation Measuring Equipment. Schematic Diagram

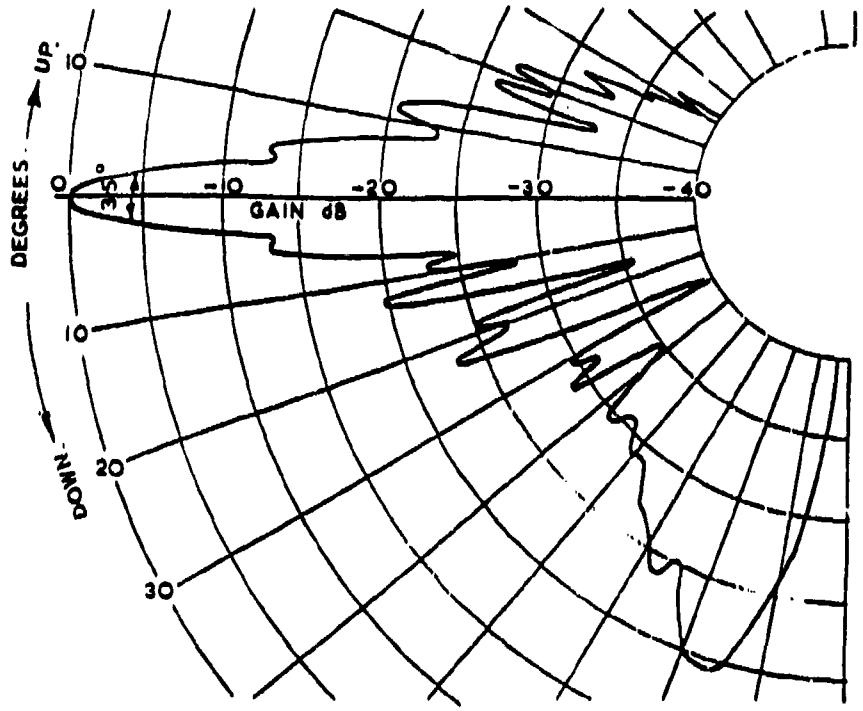

Vertical Plane

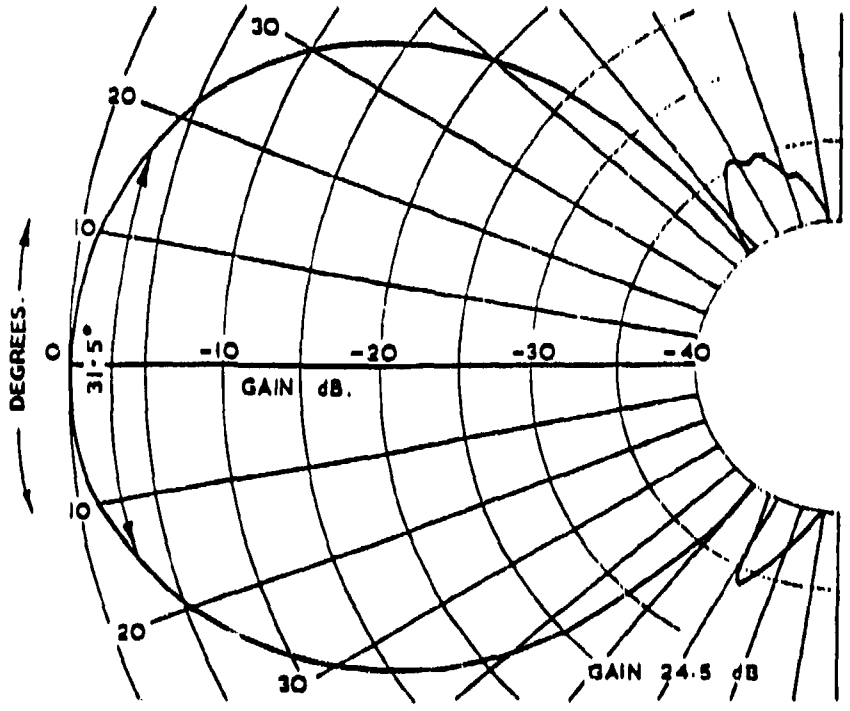

Horizontal Plane

Fig. 6-5 Tx.Antenna Polar Diagram. Vertical Polarization

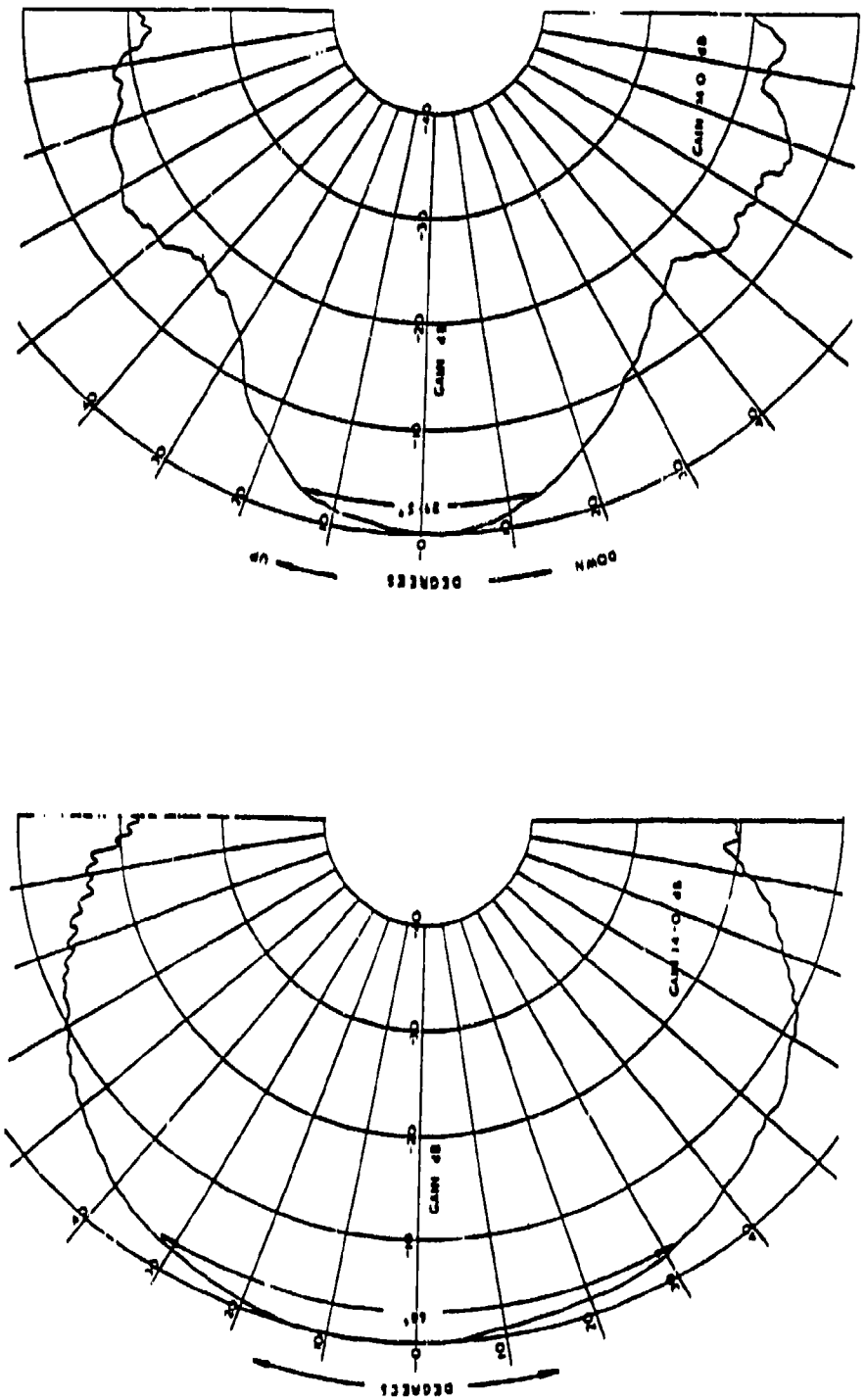

Fig. 6-6 Rx.Antenna Polar Diagram. Vertical Polarization

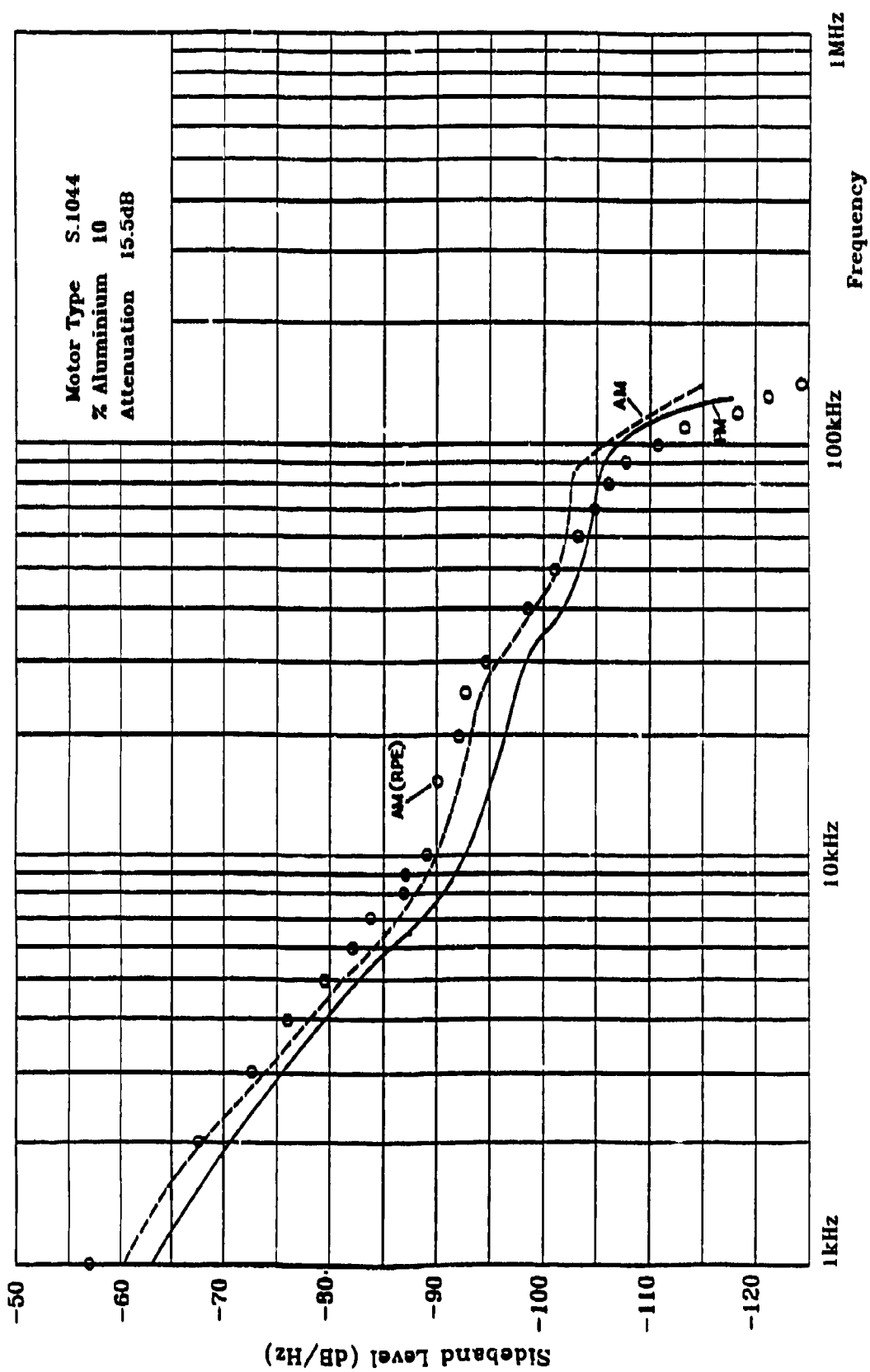

Fig. 6-7 Forward Scatter Spectra. AM and PM Noise Modulation

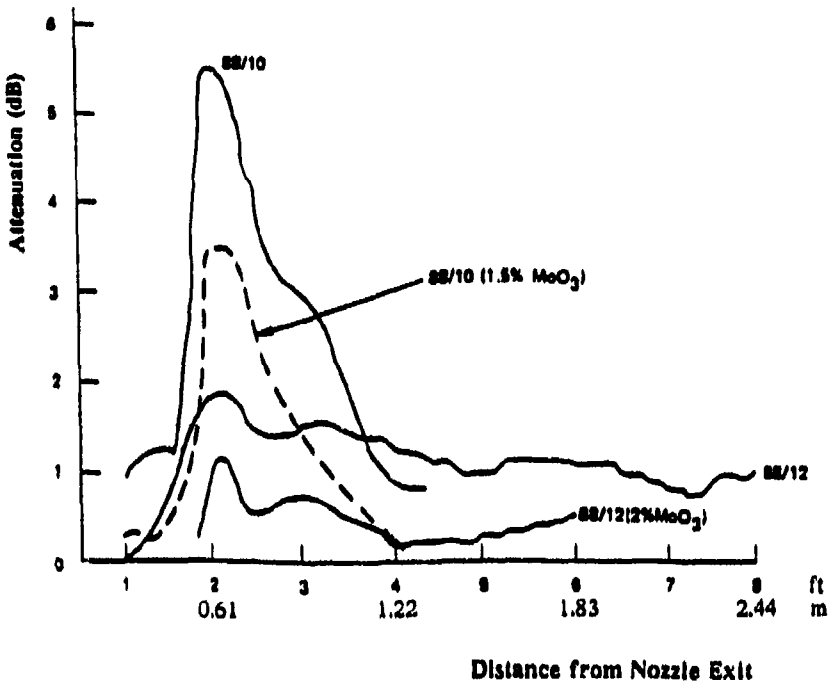

Fig. 6-8a Simulated Flight Data. Two Composite Propellants with and without Molybdenum. 8.53km Alt. M2.2

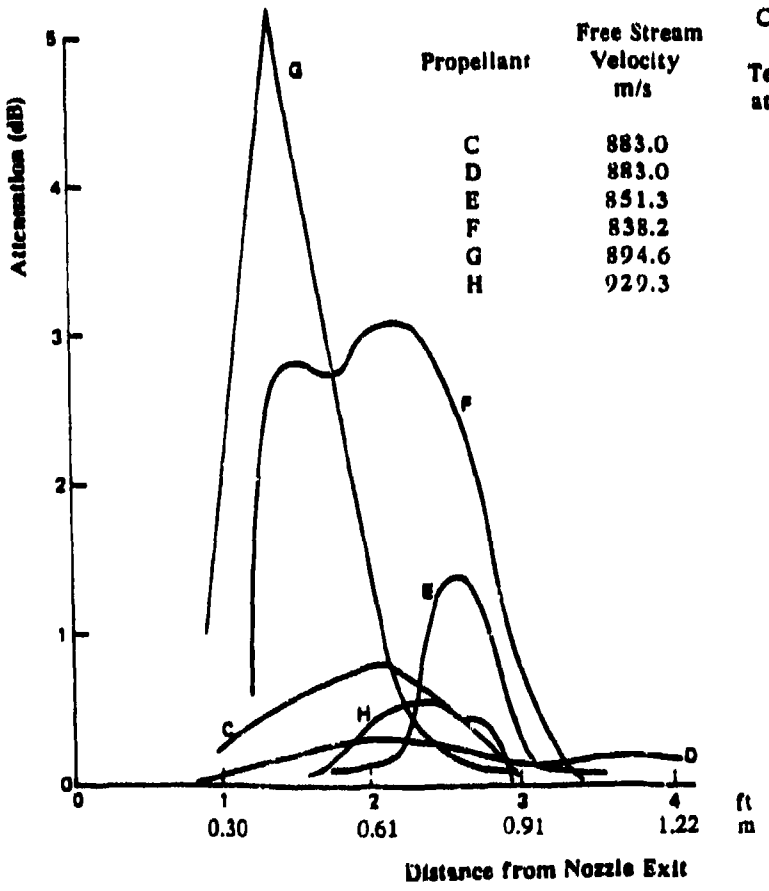

Propellant	Free Stream Velocity m/s	Calculated Chamber Temperature at 5.07MPa
C	883.0	2412K
D	883.0	2366K
E	851.3	1967K
F	838.2	1963K
G	894.6	2170K
H	929.3	2243K

Fig. 6-8b Simulated Flight Data for Six Propellants Thrust = 222.4N. Alt. = 10km to 11.6km

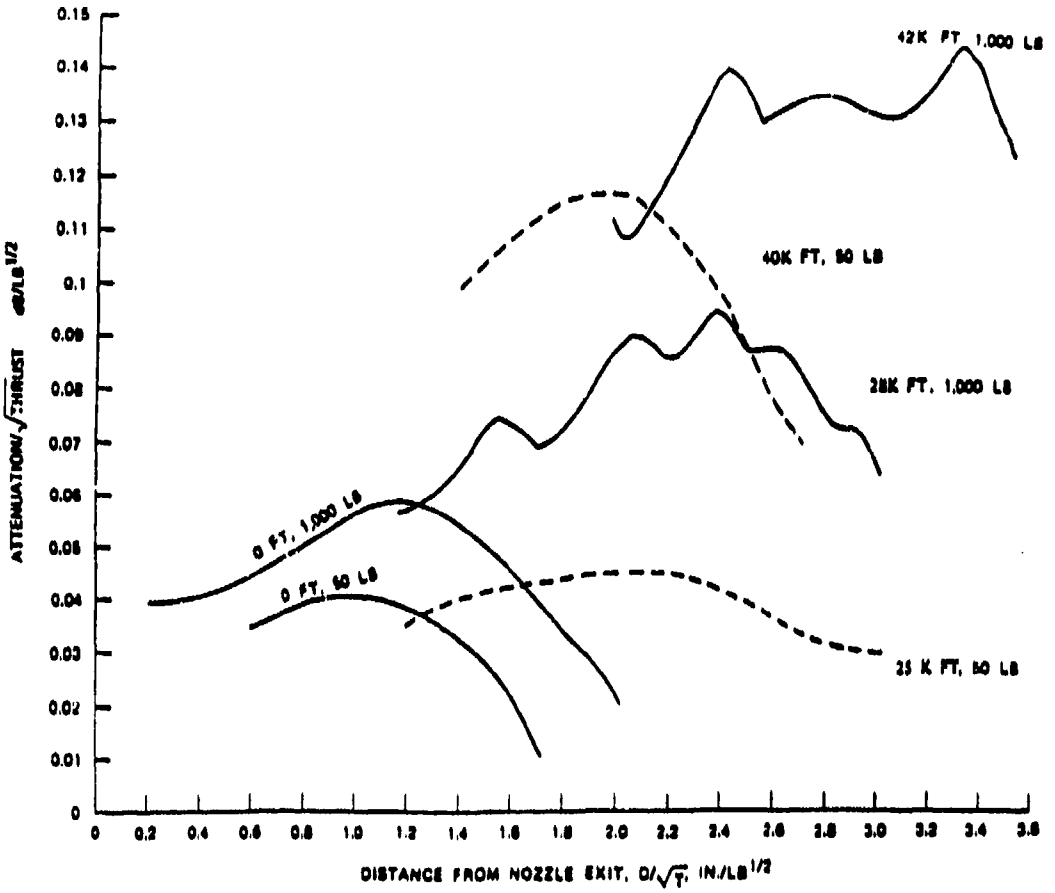

1.0lb thrust = 4.44822N

1.0ft = 0.3048m = 12 inches

Fig. 6-9 Measured Transverse Attenuation versus Altitude for the Plumes of Two Composite Motors. Frequency: Nominally 10GHz. (Scaled by inverse root-thrust).

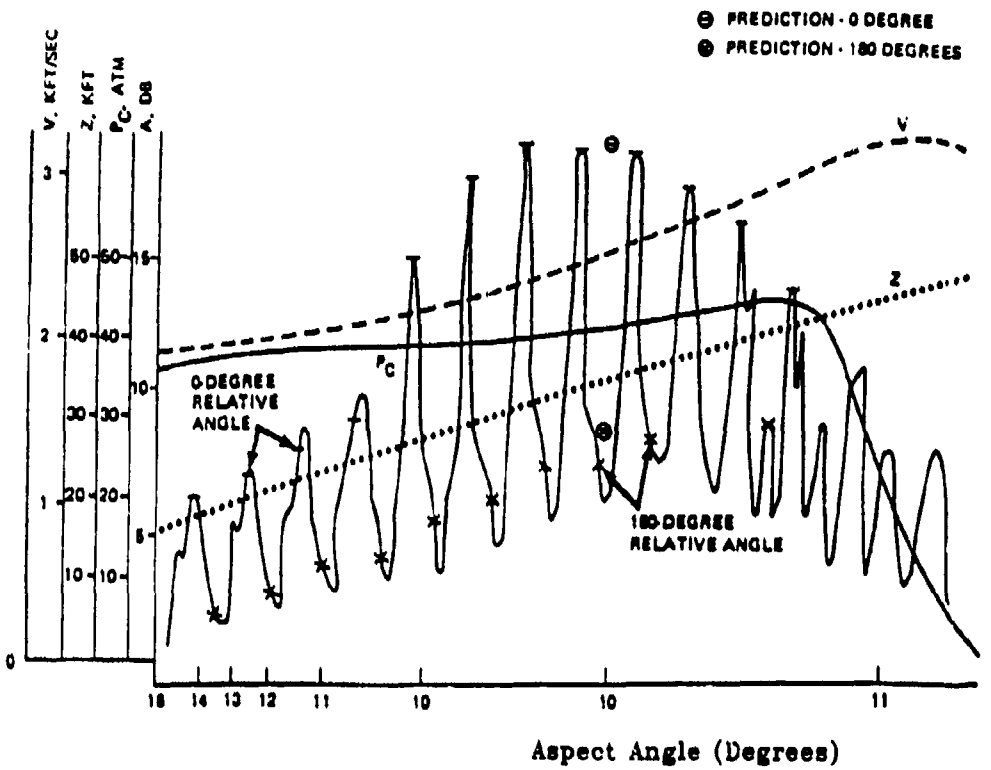

1.0Atm.= 101,325Pa
1.0FT. = 0.304m

Fig. 6-10 In-Flight Attenuation for Propellant "C" (Rolling Missile)

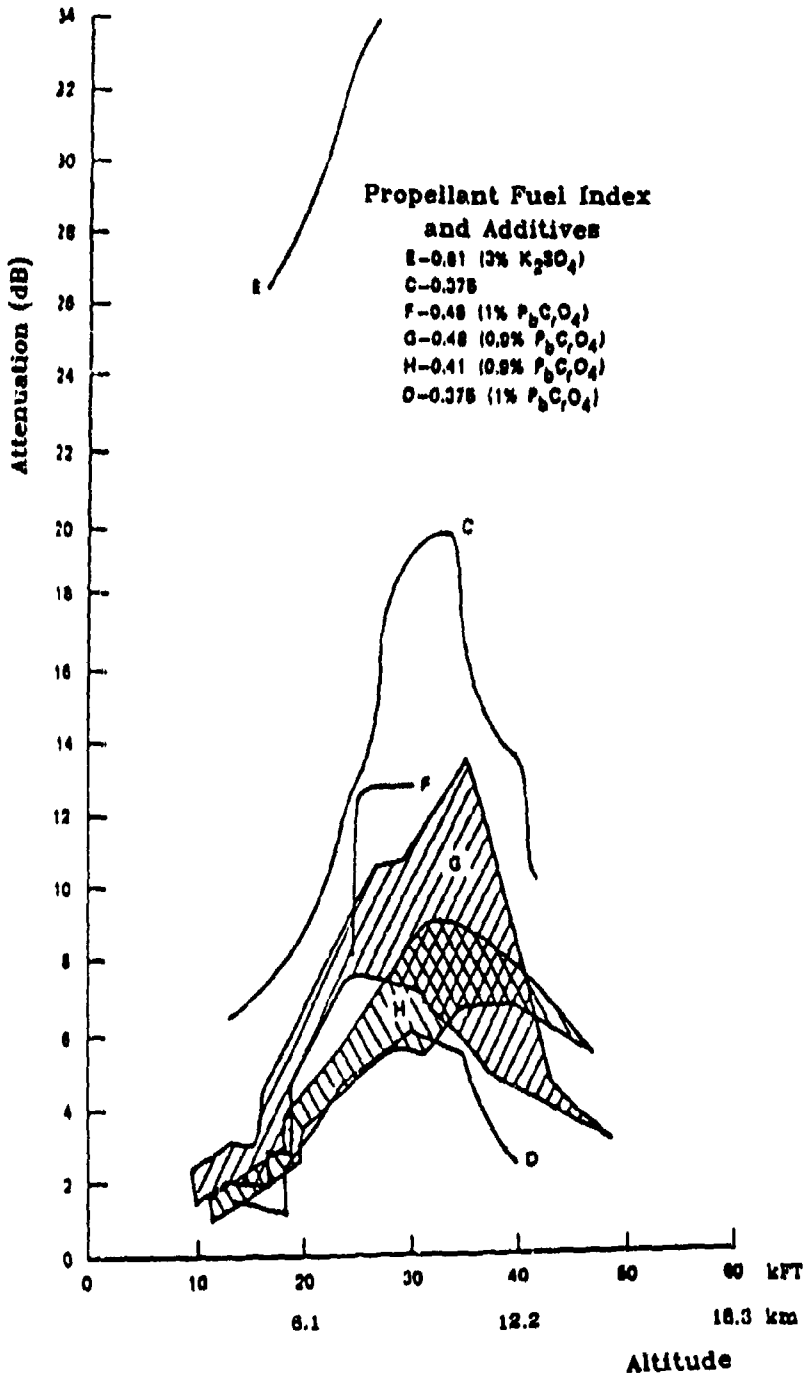

Fig. 6-11 Flight Attenuation for Propellant of Fig. 6-8b.
Aspect Angle Range: 2 degrees at 3.048km to 10 degrees at 10.67km and above

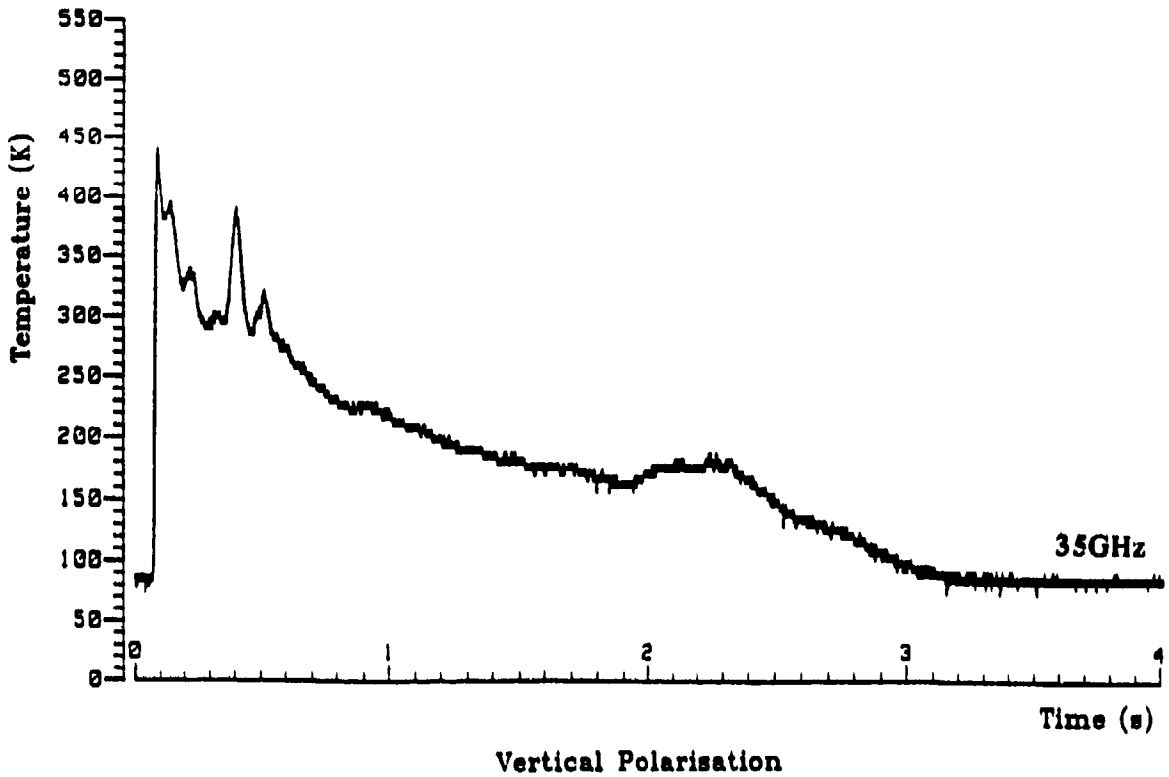

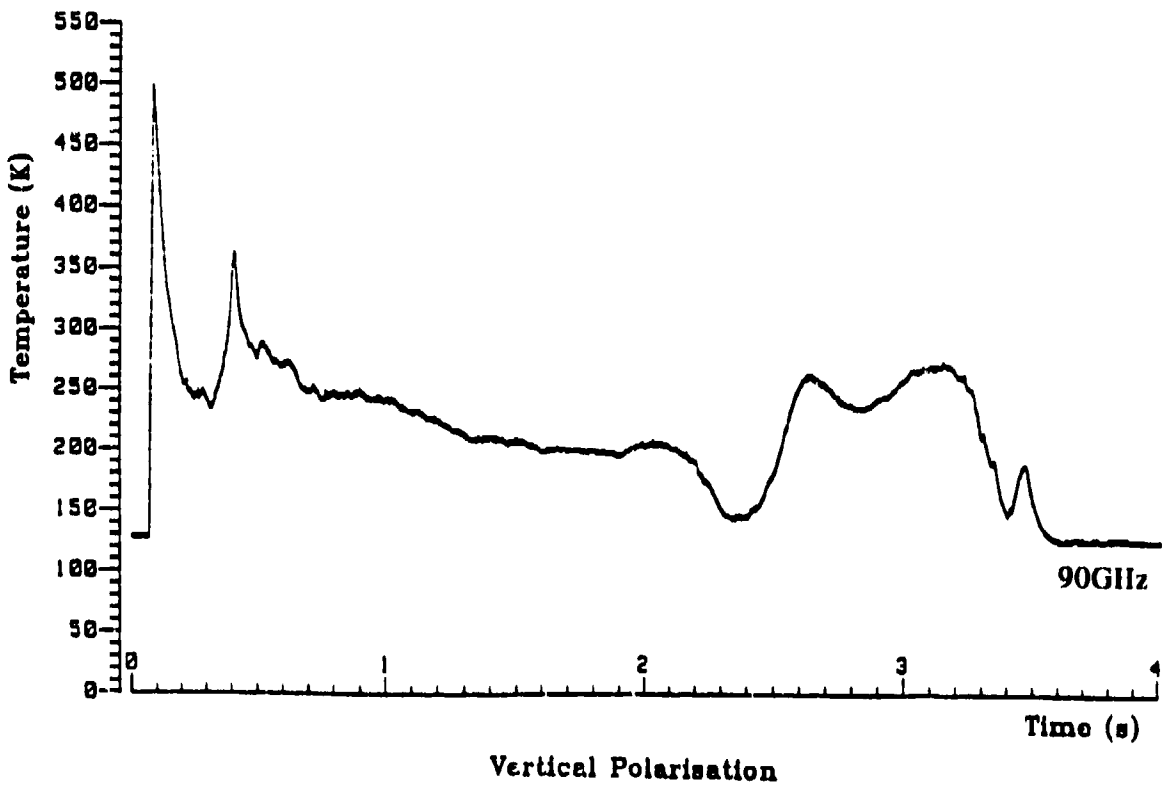

Fig. 6-12 Emission Apparent Brightness Temperatures for Composite Propellant Motor in Two Wavebands

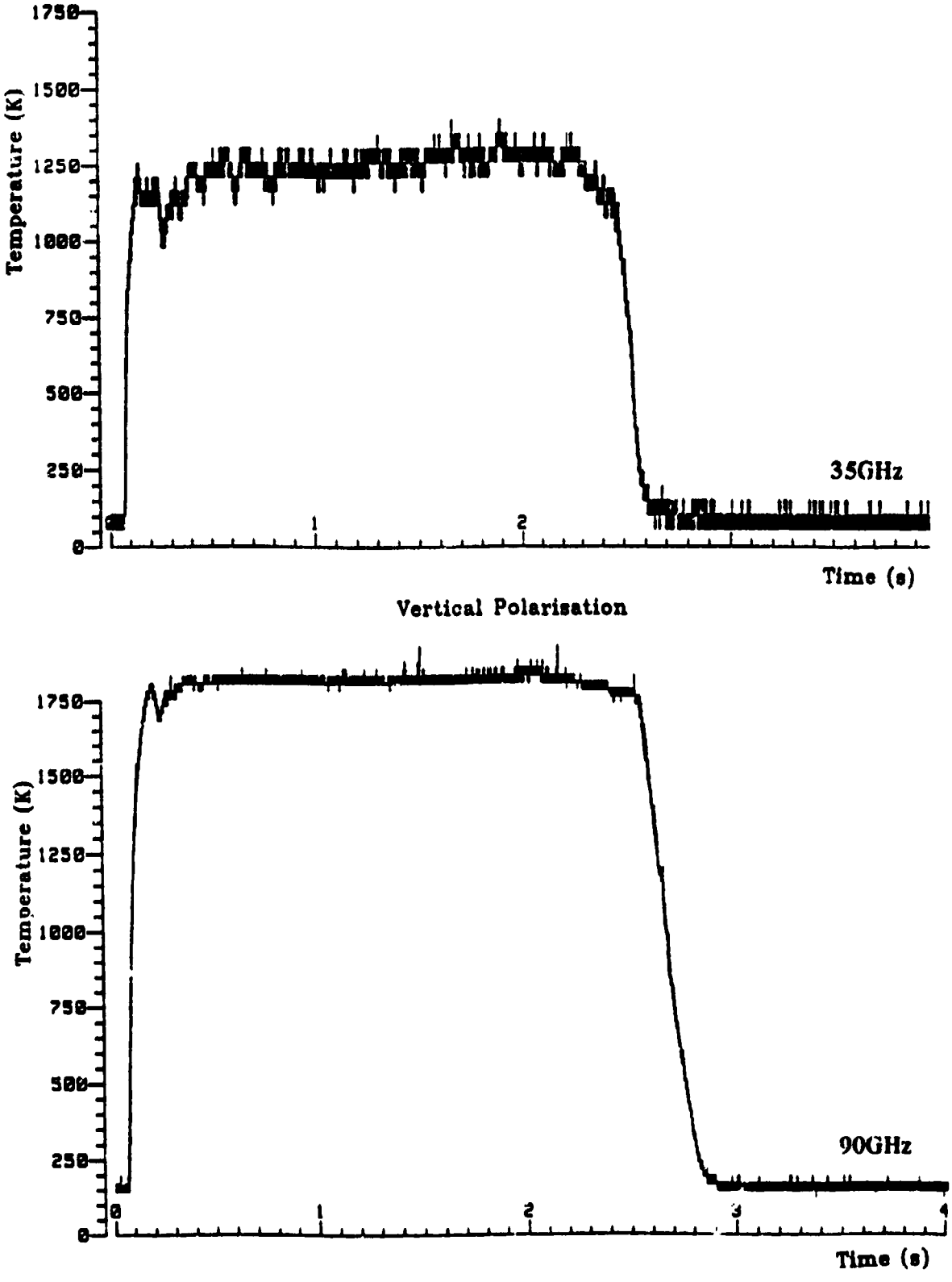

Fig. 6-13 Emission Apparent Brightness Temperatures for Double Base Propellant Motor in Two Wavebands

CONTOUR NO.	VE SEC^{-1}	GAS VELOCITY FT/SEC	ELECTRON DENSITY, CM^{-3}	ω_p RAD/SEC	TEMP K
1	1.6 (10^{11})	8,578	6.1 (10^{8})	7.9 (10^{9})	2313
2	1.7 (10^{11})	7,720	3.8 (10^{10})	1.1 (10^{10})	2393
3	1.7 (10^{11})	6,860	1.5 (10^{11})	2.2 (10^{10})	2576
4	1.7 (10^{11})	6,005	3.4 (10^{11})	3.31 (10^{10})	2707
5	1.7 (10^{11})	5,147	4.9 (10^{11})	3.95 (10^{10})	2784
6	1.6 (10^{11})	4,289	4.3 (10^{11})	3.69 (10^{10})	2794
7	1.6 (10^{11})	3,431	1.9 (10^{11})	2.48 (10^{10})	2718
8	1.5 (10^{11})	2,573	2.4 (10^{10})	8.66 (10^{9})	2510
9	1.4 (10^{11})	1,716	1.2 (10^{8})	6.22 (10^{8})	2099

VE = Electron Collision Frequency

1ft = 0.305m

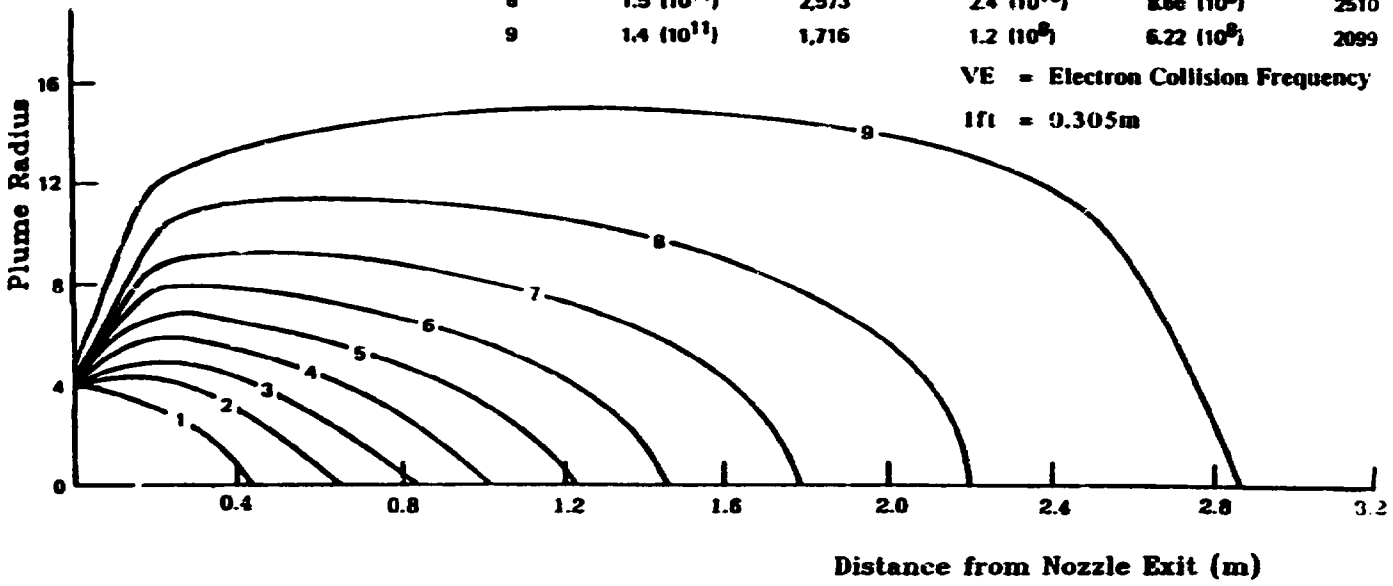

Fig. 6-14 Calculated Plume Properties for Motor Filled with Aluminised Composite Propellant. Static, Sea-level.

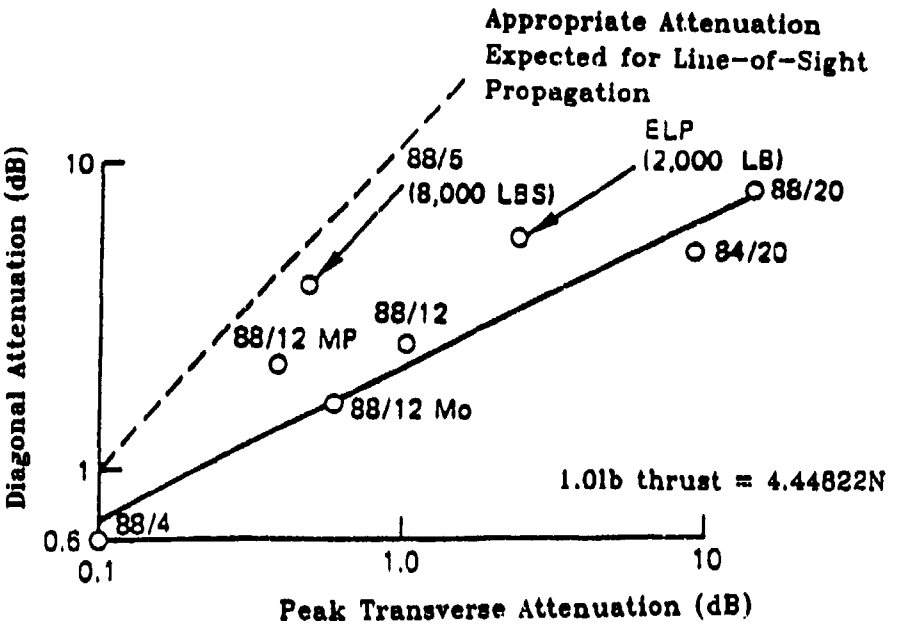

(a)

Interception angle, °	X-Band		J-Band		Q-Band	
	A dB	I dB	A dB	I dB	A dB	I dB
+ 3	-234	-15.0	-235	-18.0	-158	-19.0
+ 5	-185		-178	-22.0	-125	
+10	- 61	-22.0	- 58	-23.0	- 41	-30.0
+20	- 15.7	-13.5	- 15.1	-12.5	- 10.6	-

Nominal Frequencies: X(10GHz), J(16GHz), K(35GHz)

(b)

Fig. 6-15 (a) Attenuation Comparison between Longitudinal and Transverse Measurement for 4.45kN Thrust Motors (Except as noted)

(b) Comparison of Calculated Absorption Loss (A) with Experimental Insertion Loss (I)

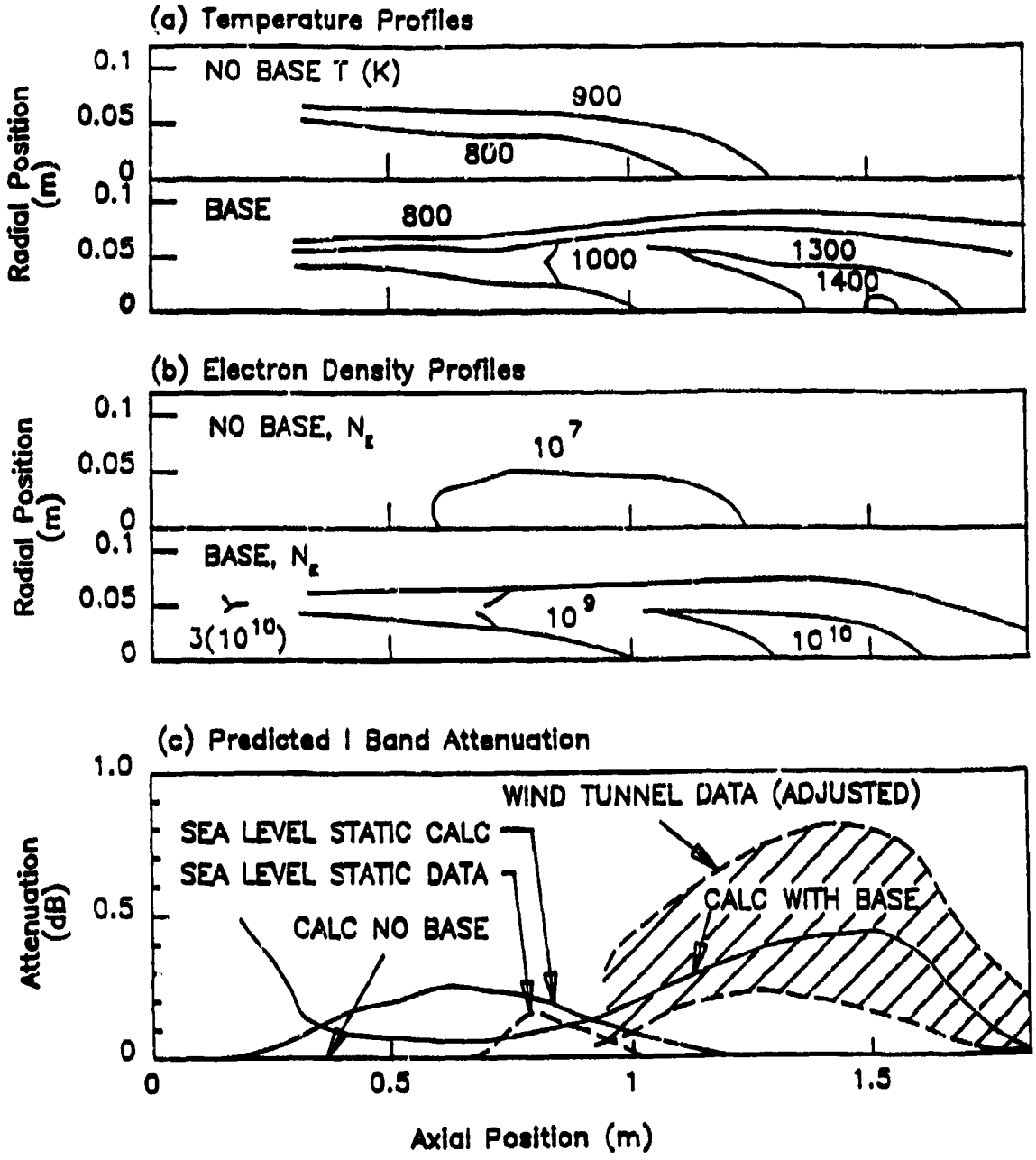

Fig. 6-16 Comparison of Calculated Plume Properties for Propellant "C". Effect of Base Recirculation

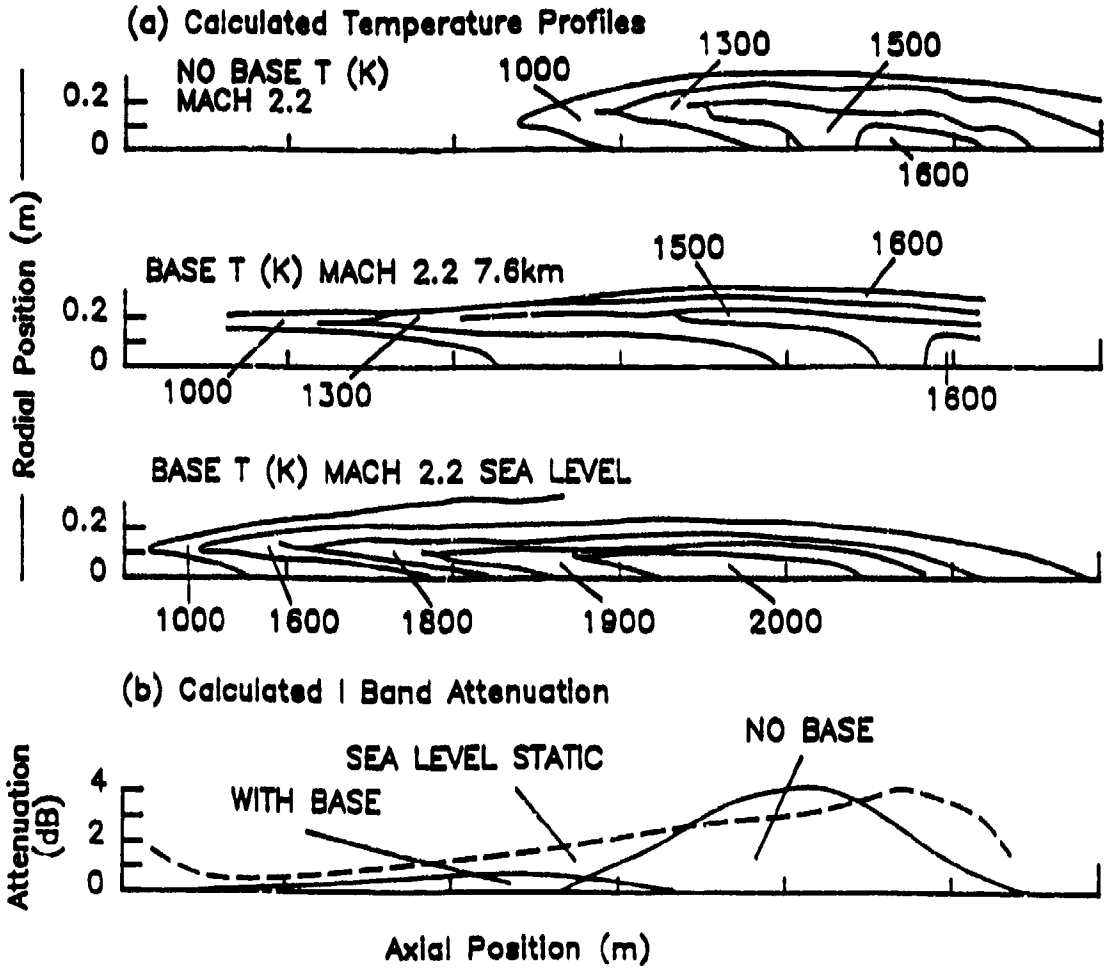

Fig. 6-17 Calculated Full-Scale Plume Properties for Propellant "C"

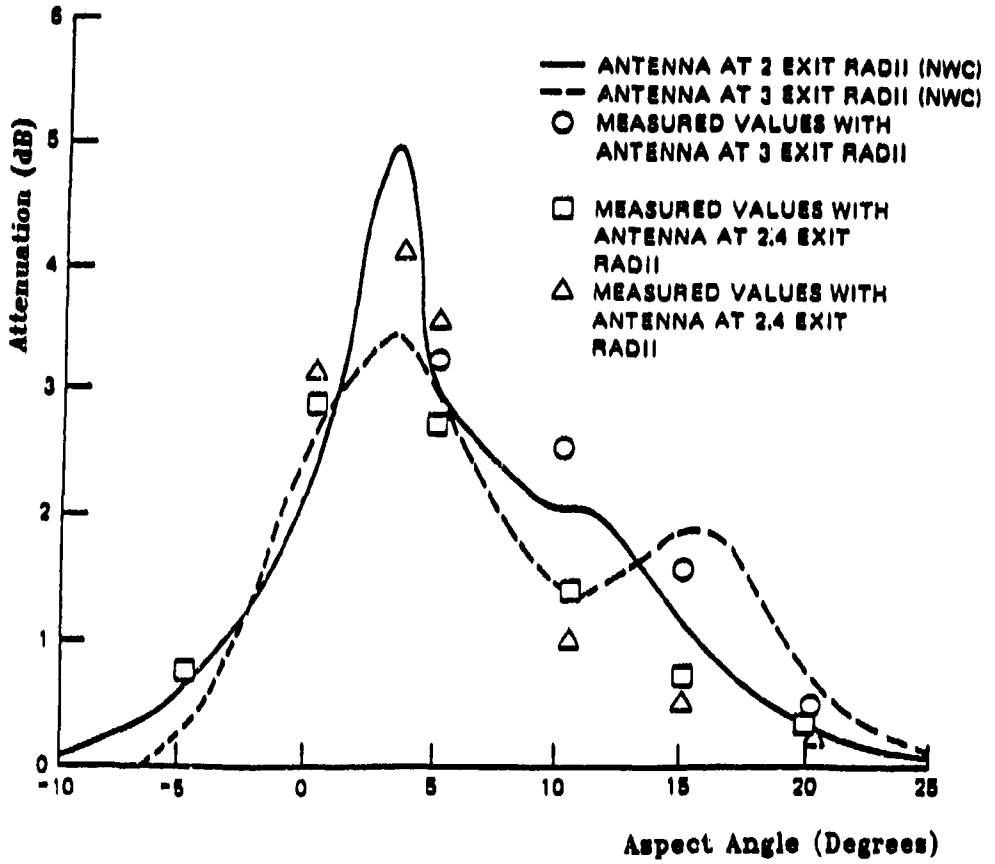

Fig. 6-18 Comparison of Measured and Calculated Longitudinal Attenuation for a Rocket Motor with 5%Al and 88% Solids Propellant Loading

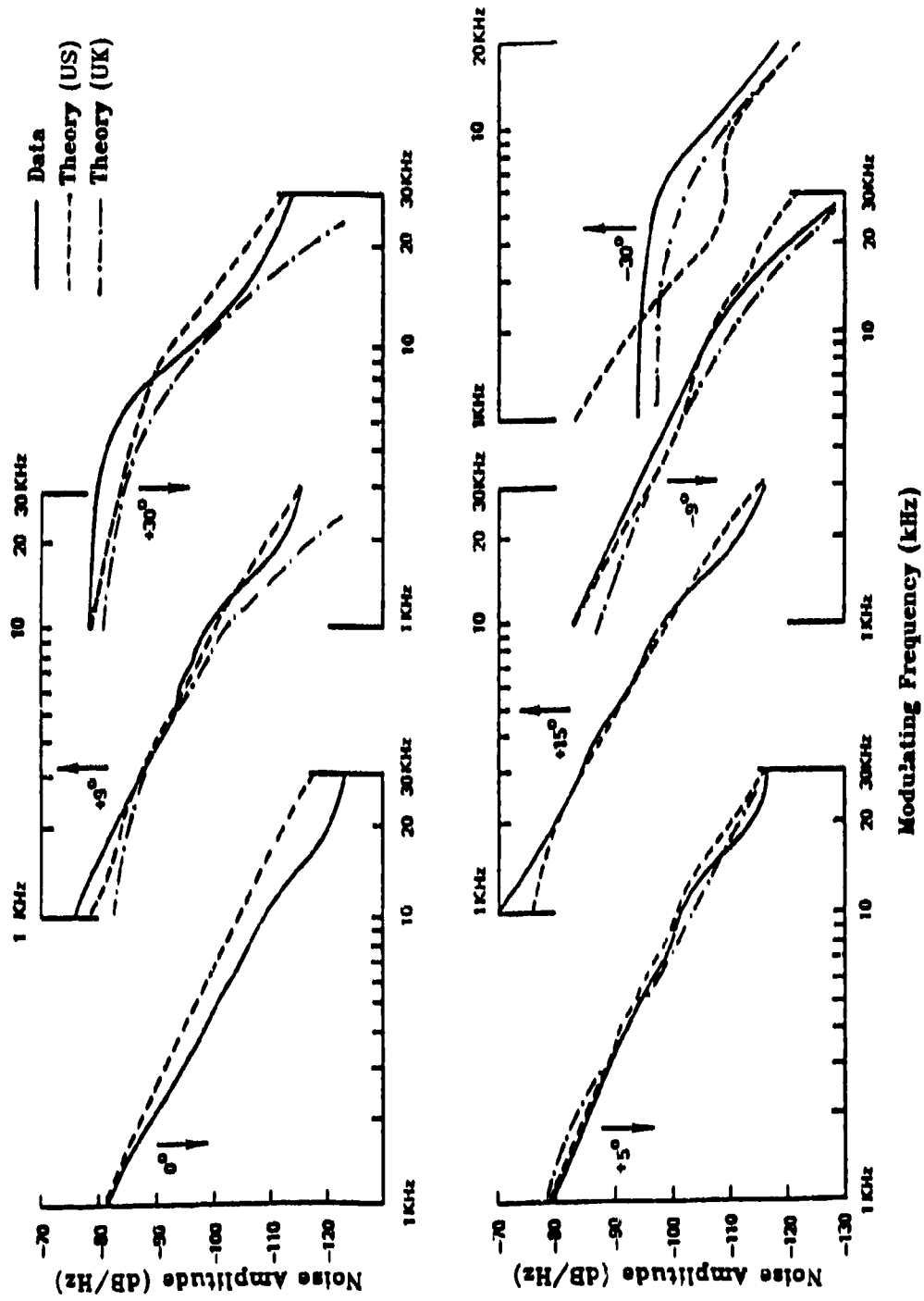

Fig. 6-19 Forward Scatter. Comparison between Measured Amplitude Modulated Noise and Prediction

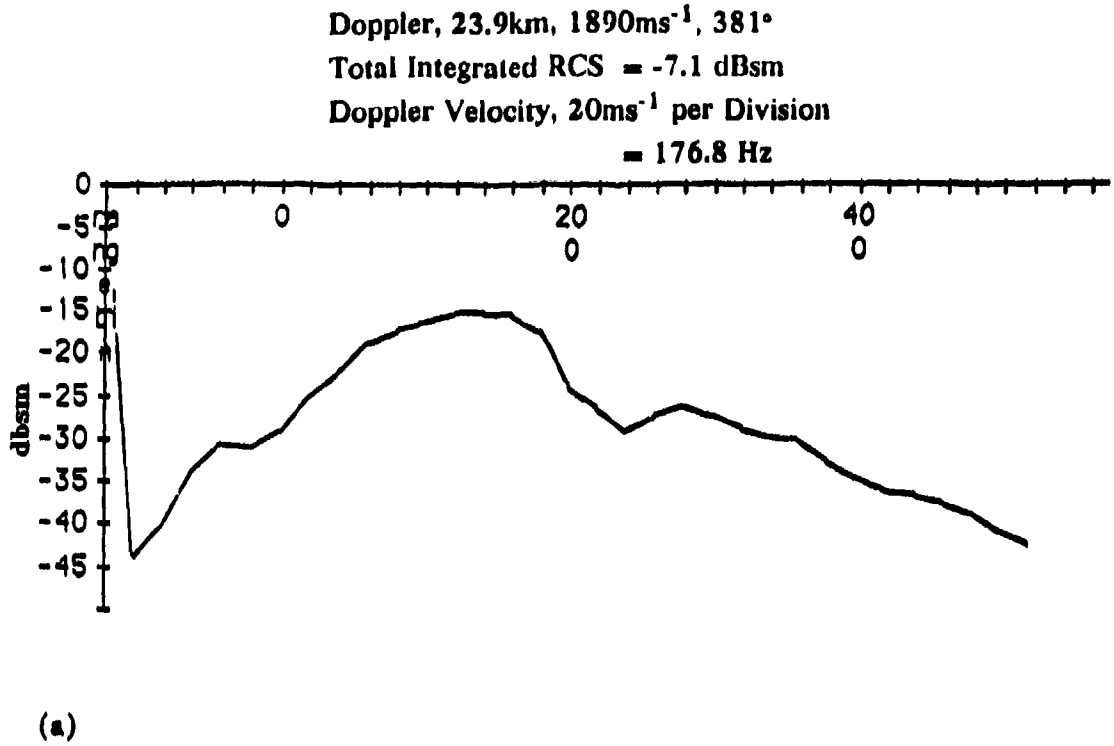

(a)

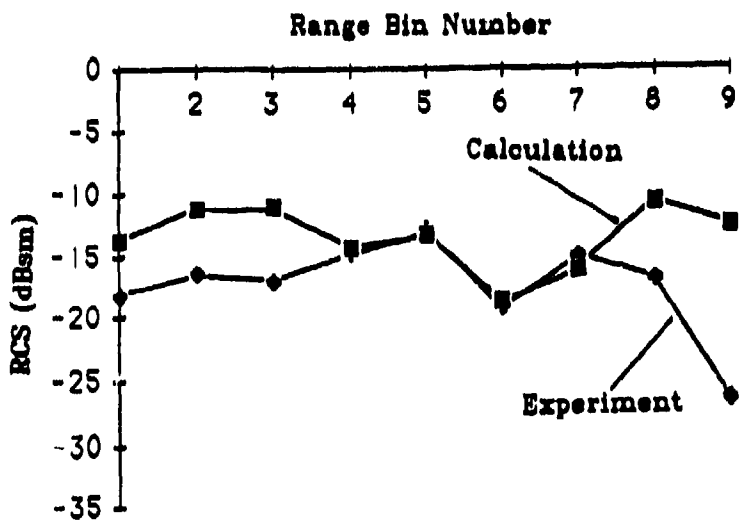

(b)

Fig. 6-20 (a) Total Doppler RCS Spectrum. US Motor (BB).
(b) RCS Spectra. Comparison Between Flight Data and Calculations. US Motor (BB)

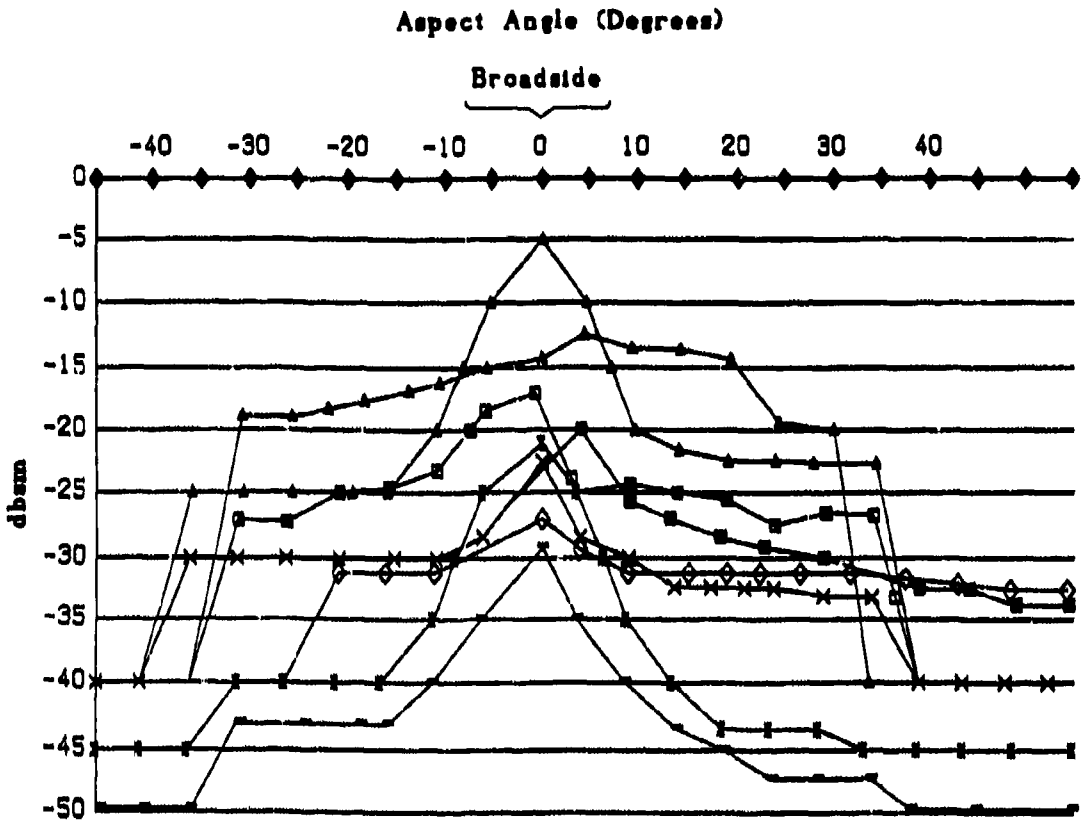

GHz	Al%	GHz	Al%
5	16	.45 (pr=.86)	16
1.25	16	2. (pr=.86)	16
.85	16	.45 (pr=.86)	5
.15	16	2. (pr=.86)	5

Fig. 6-21 RCS total Spectra (RATSCAT). Solid Rocket Motors Containing Aluminium

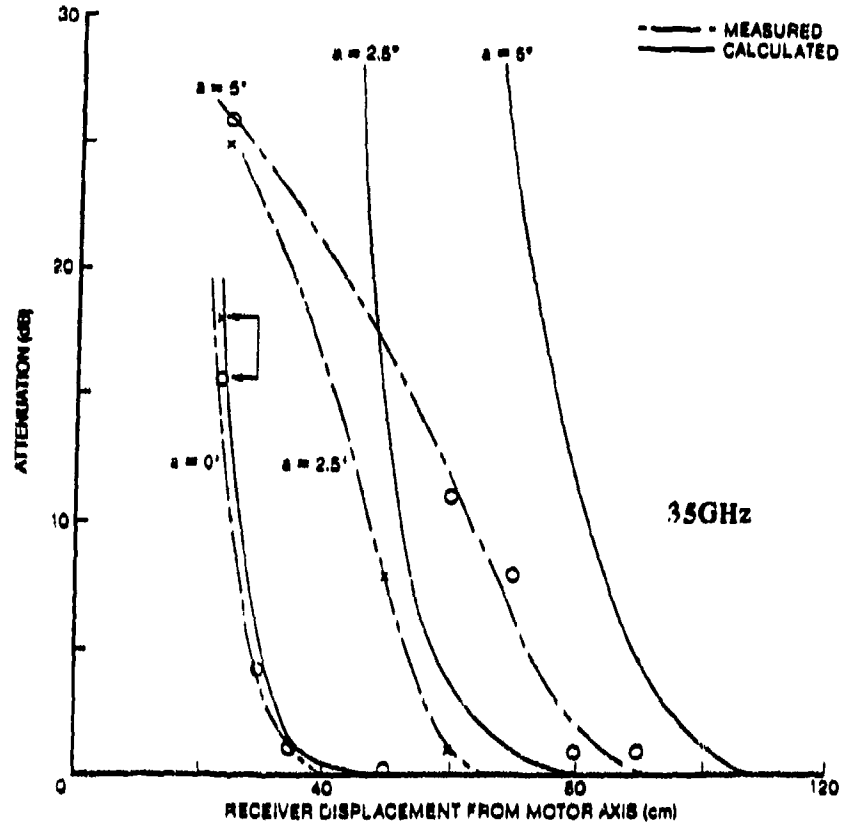

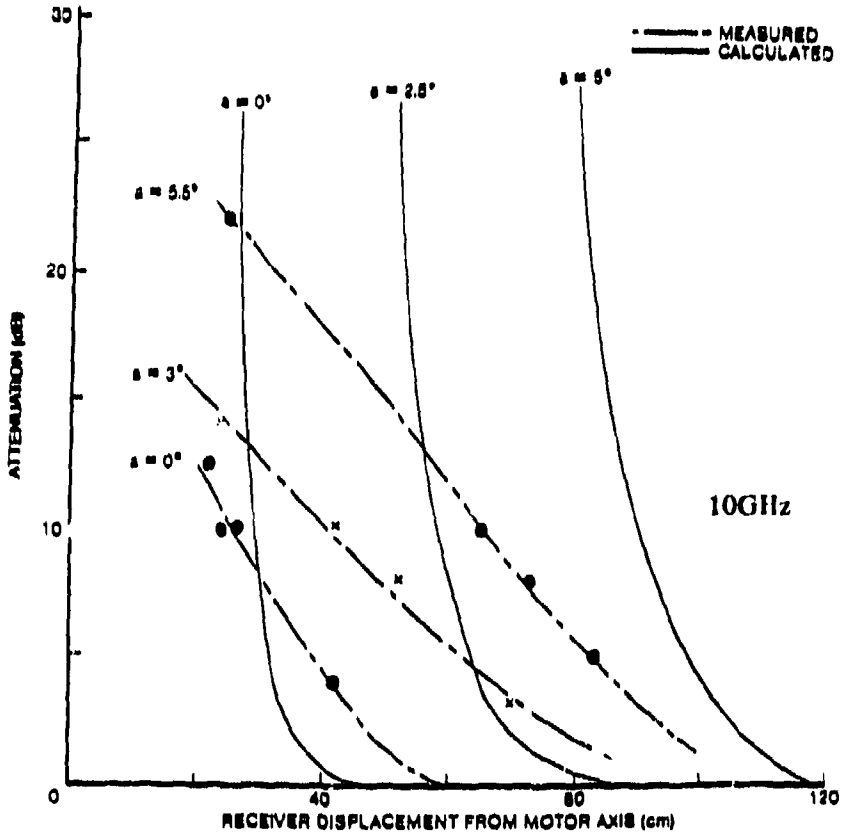

Fig. 6-22 K and I Band. Comparison of Predicted and Measured Attenuation Against Receiver Displacement for Three Aspect Angles

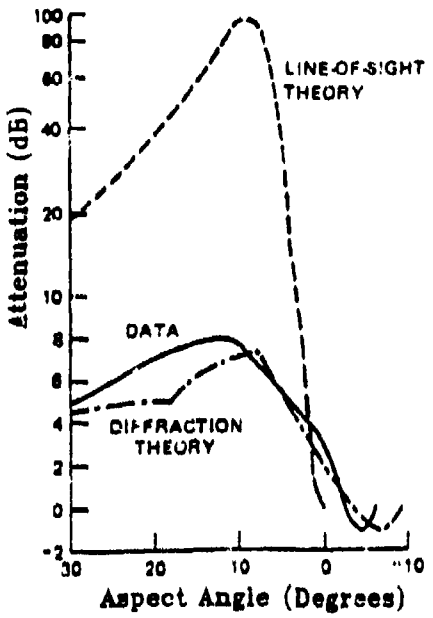

Fig. 6-23 Comparison of Line-of-Sight and Diffraction Calculations against Attenuation Measurement. Motor Propellant: 20%Al/88% Solids

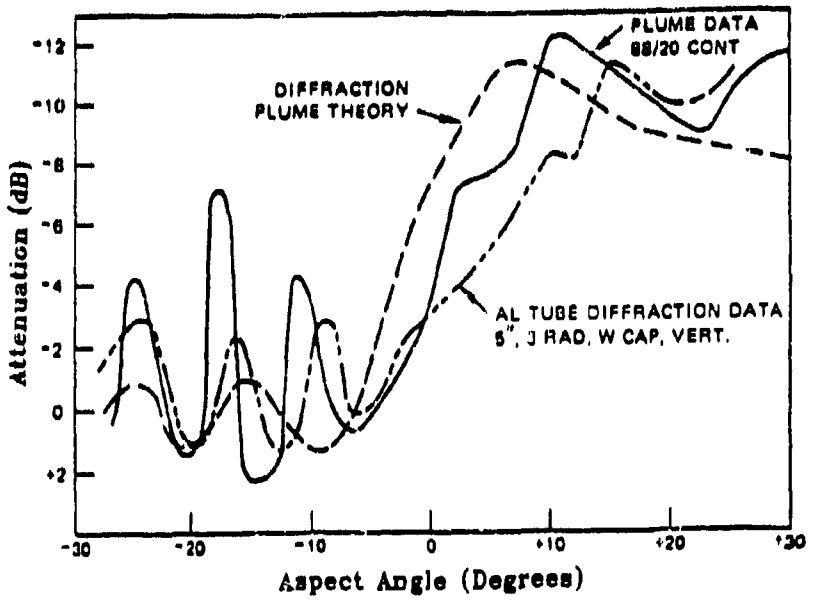

Fig. 6-24 Comparison of Measured Attenuation for a 20%Al/88% Solids Loaded Motor with Calculated Diffraction Theory for a Plume Model and a 0.127m (5") Diam Aluminium Cylinder.
(Frequency = Nominal 10GHz)

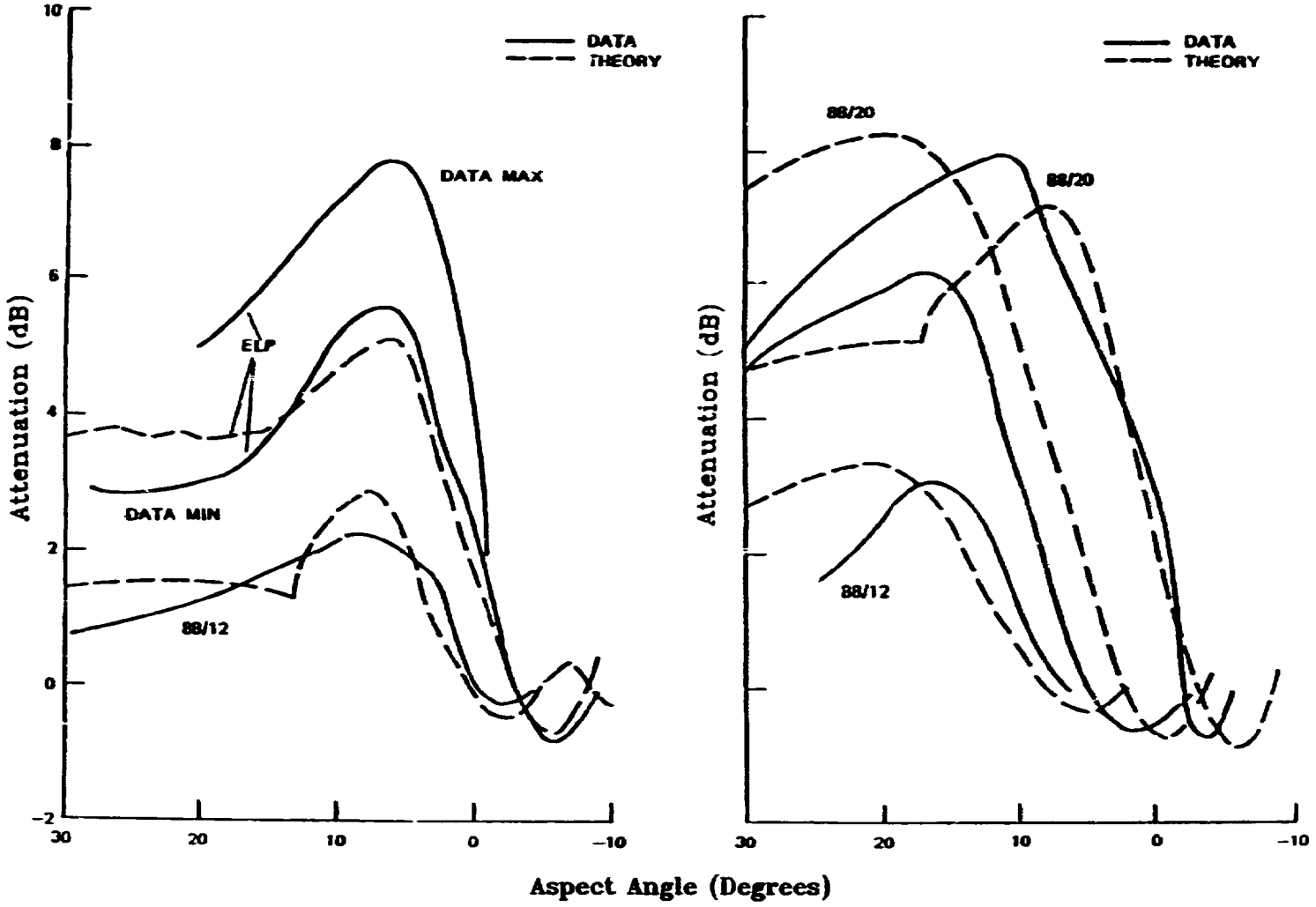

Fig. 6-25 Comparison between Measured Attenuation and Diffraction Theory for a Range of Rocket Motors

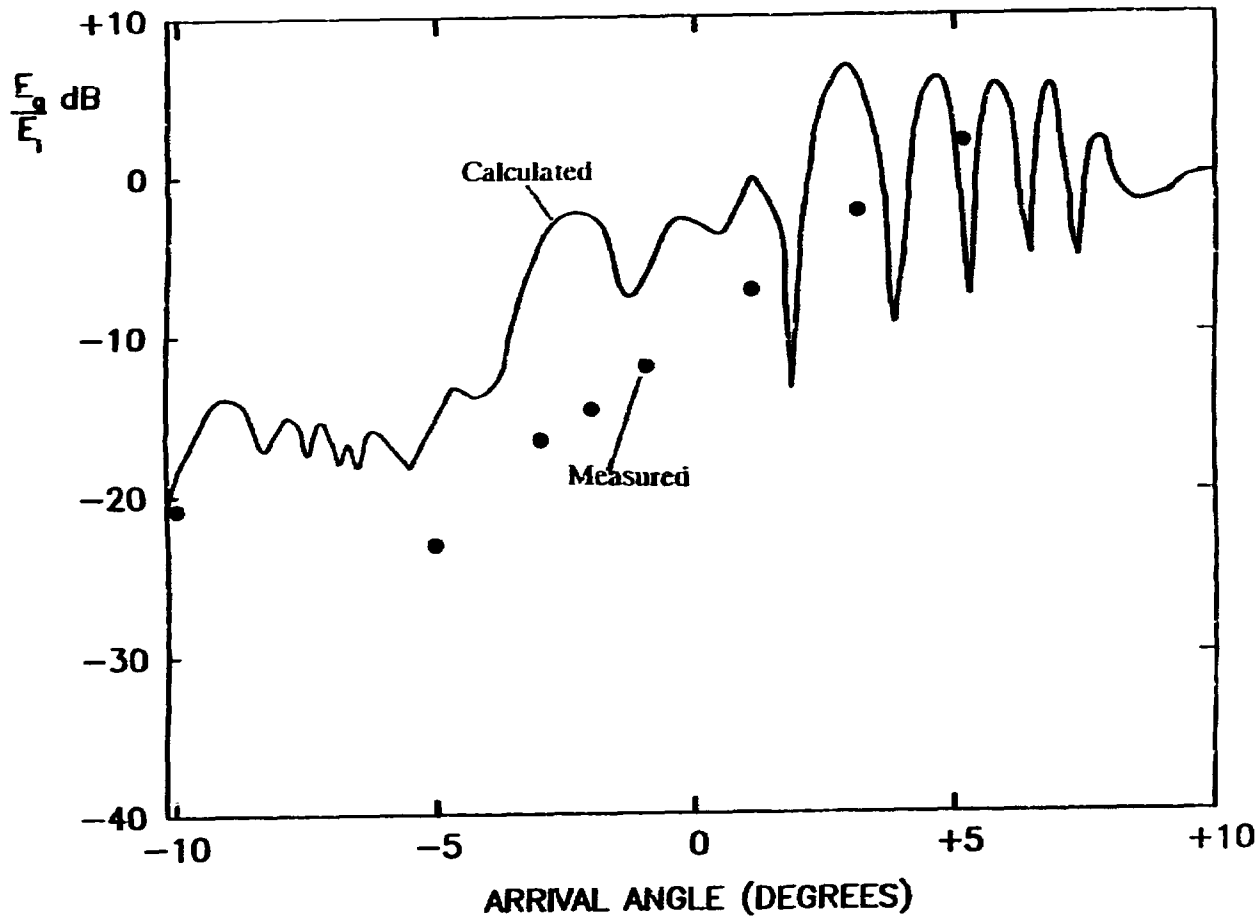

Fig. 6-26 Comparison between Calculated Diffraction Signal and Attenuation Measurement.
Double Base Motor, Thrust 30kN. Frequency 10GHz

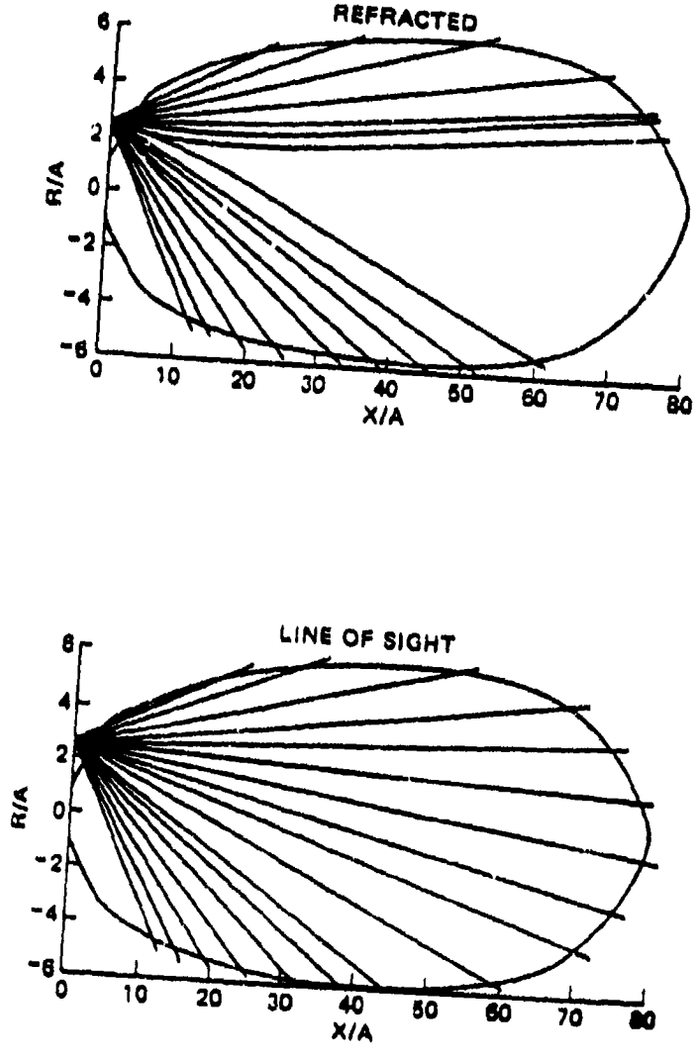

Fig. 6-27 Comparison of Line-of-Sight and Refracted Ray Calculations. Motor Propellant: 12%Al/88% Solids

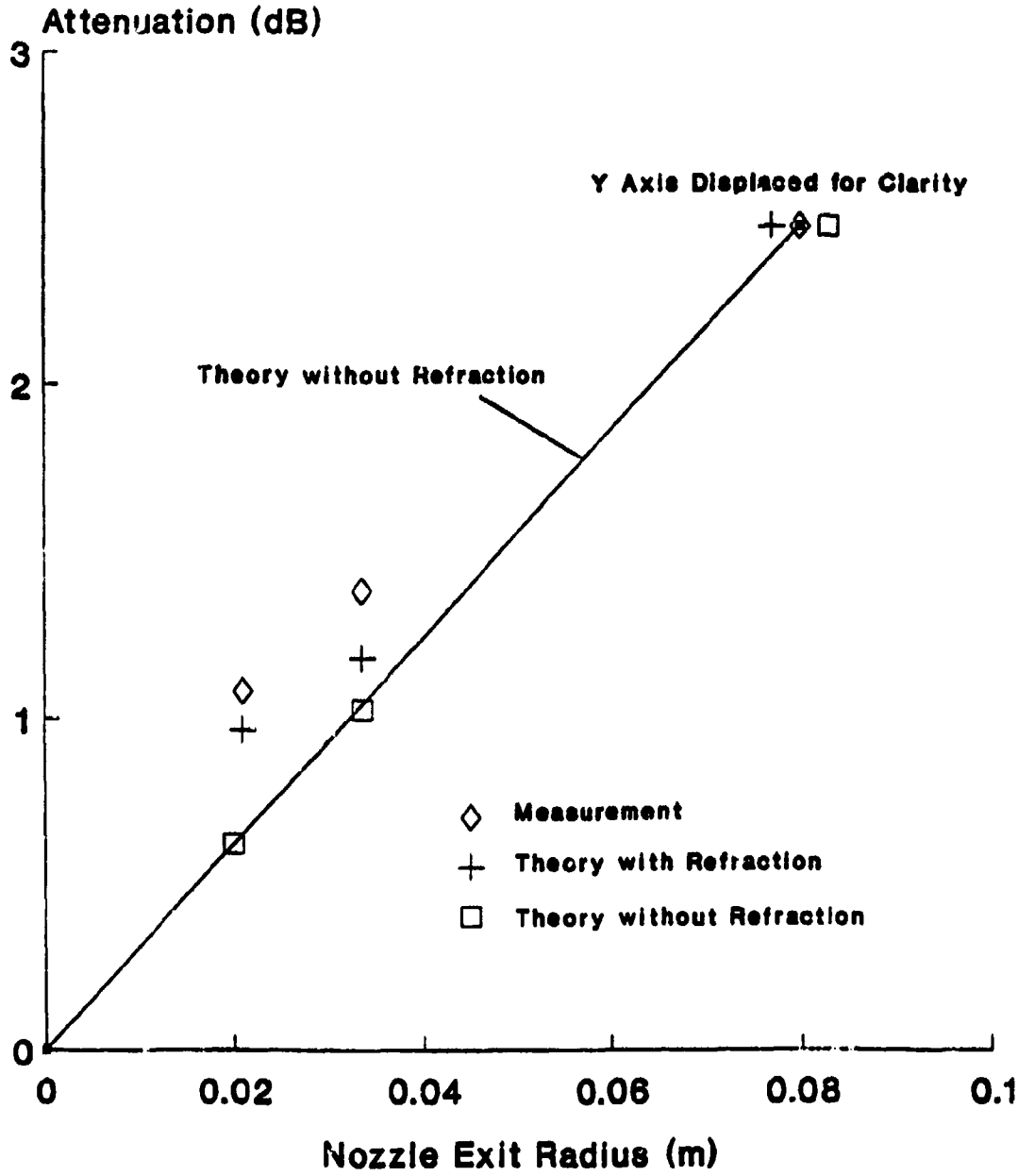

Fig. 6-28 Comparison between Measured Attenuation and Calculated Attenuation with and without Refraction

APPENDIX 1
Glossary

ACTIVE GUIDANCE - A form of missile guidance in which the missile emits radiation (usually RF) and subsequently homes in on the signal reflected from the target.

AFTERBURNING - Is the term applied to reignition and combustion of exhaust fuel products such as carbon monoxide or hydrogen in the mixing region of the rocket exhaust as they combine with oxygen and burns externally to the rocket motor.

AIRY DISC - In optics the diffraction pattern formed by a circular aperture consists of a bright central disk surrounded by fainter rings. The central disk is known as Airy's disk because he first described the mathematical solution for the intensity distribution.

ALBEDO - A measure of the reflecting power of an object, defined as the ratio of the radiation reflected from an object to the total amount incident upon it. The albedo from the earth is generally considered to be approximately 50% but local variations, i.e. water surfaces, may be as high as 80%.

ALMPS - A code used by US Air Force for the generation of statistical climatic data.

AMMONIUM PERCHLORATE - An oxidiser compound commonly found in composite propellants. The decomposition products include hydrogen chloride which contributes to secondary smoke condensation through reduction of the saturation vapour pressure of ambient water.

ATTENUATION - A term that describes the decrease in intensity of a beam of energy propagated through a medium, e.g. exhaust plume, as a result of absorption, scattering, or a combination of both.

ATMOSPHERIC WINDOWS - Are regions of the electromagnetic radiation spectrum in which the atmosphere is relatively transparent.

AUTONOMOUS - Describes a missile guidance scheme in which the detection and target tracking systems are entirely onboard the missile, e.g. an IR seeker system.

BANC OPACIMETRIQUE - An SNPE motor test facility based on an open firing room instrumented for smoke measurements.

BASE FLOW - Is the aerodynamic flow phenomenon that produces pressure disturbance, flow field separation or recirculation effects in missile flight plumes which cannot be predicted by analysis of static firing plumes.

BEER-LAMBERT EQUATION - Also known as the Lambert-Beer, Beer's or Bouguer equation which relates the log of the transmittance to an extinction coefficient times the thickness of the transmitting medium. When the medium is a cloud of particles the extinction becomes a function of the projected area concentration, i.e. number density, path length, size distribution, and extinction efficiency of the particles.

BRIGHTNESS - In photometry brightness of luminance is the visible flux emitted per unit surface area per unit solid angle. The SI unit of luminance is cd/m^2. There is no numerical equivalence between photometric luminance and radiometric radiance because of variations in source and receiver sensitivity versus wavelength.

CHEMILUMINESCENCE - Describes the radiation process caused by excitation of atoms or molecules through chemical reaction within the exhaust plume.

CHOKING - A condition which arises when a compressible fluid has reached its maximum limit of mass flow In a De Laval nozzle choking limits the flow to Mach 1 at the throat and the flow velocity can only be increased in the diverging section.

CIE - Commission Internationale de l'Eclairage (International Commission on Illumination).

CLOS (Command to Line of Sight) - A form of guidance in which the missile is commanded to fly a target intercept trajectory relative to the direction defined by a target/missile tracker. This method requires two way communication with the missile either by means of an IR, RF, wire, or fibre optic link.

COLLISION BROADENING - Is a spreading of the frequency distribution about a particular emission or absorption spectral line caused by interaction with other molecules. The collision broadened line may be described by the Lorentz line shape.

COMBUSTION INSTABILITY - Acoustical vibration energy in a rocket motor that may be observed as pressure oscillations capable of propellant extinguishment, fracture, or pressure bursts. The addition of metal or refractory powders in small amounts has been found to

reduce the oscillations that lead to combustion instability.

COMPOSITE PROPELLANT - A grain of heterogeneous mixture with oxidizer crystals and possibly powdered fuel (usually aluminium) held together by a matrix of synthetic rubber or plastic.

CONDENSATION NUCLEI - Submicron particles consisting mostly of condensed solids that serve as seed particles for vapour condensation and growth of secondary smoke.

CONTINUUM - Refers to the radiation spectral energy distribution exhibited by solids (or exhaust particulates) as described by the Plank distribution function.

CONTRAIL - UK code for calculation of the visual contrast of a smoke or condensation trail

CONTRAST - A mathematical expression of the relative brightness difference between a target and its background ratioed to the brightness of the background.

CRITICAL RADIUS - Is the minimum size for stability of a droplet as determined by ambient temperature, pressure and humidity.

CURTIS-GODSON APPROXIMATION - An approximate technique for the calculation of transmissivity of inhomogeneous gases using a multiplicative procedure.

DIFFRACTION - Is the term used to describe the interference (phase cancellation) effects that occur when radiation encounters an aperture or other partial obstruction e.g., a rocket plume. In optics see Fraunhofer or Fresnel diffraction.

DOPPLER BROADENING - Is the spectral line broadening that is a result of the spread in frequency due to thermal motion of the atoms or molecules.

DOUBLE-BASE PROPELLANT (DB) - A propellant consisting of nitrocellulose and nitroglycerin with burning rate or combustion instability additives. Two subgroups are Extruded Double Base (EDB) and Cast Double Base (CDB) propellants.

DROP - Code for the prediction of secondary smoke formation developed at US Army MICOM

ECARTOMETRY - A guidance system in which the underlying principle is command to line of sight. An operator or "servant" designates the target optically while the missile follows the established line of sight.

ELASTOMER - A polymeric material such as rubber which will stretch under stress and return to approximately its original length when the stress is removed.

ELECTRICAL PLUME - A general term referring to the free electrons and ions that affect electromagnetic beam propagation through and around the plume.

ELECTRON DENSITY - Refers to the number of free electrons per unit volume in a rocket exhaust plume. ED has a direct correlation with microwave radiation attenuation loss.

EMCDB - Acronym for Elastomer Modified Cast Double Base, a subgroup of the double base family of propellants offering enhanced mechanical properties at low temperatures.

ENERGETIC BINDERS - A combination of ingredients consisting of prepolymers, curing agents, energetic plasticizers, or bonding agents that not only gives strength to a solid propellant grain but contains energy producing molecules, e.g. nitroglycerin.

EROSIVE BURNING - The accelerated burning of solid propellant due to action of gas flow parallel to the burning surface.

FAR FIELD - A general term describing the relative scale effects of energy diffraction patterns as a function of the ratio of object diameter to wavelength. In the far field the diffraction patterns are not as well defined as in the near field.

FLASH - A term used to describe the visible emission or luminous intensity of a rocket exhaust that may reveal the launch site to an enemy observer. Afterburning flash is particularly a problem for night firings and can be reduced through the use of suppressants.

FREE-FREE EMISSION - Is the radiative process whereby free electrons collide with other electrons and ions and produce continuum radiation called Bremsstrahlung.

FTIR - Acronym for Fourier Transform Infrared spectrometer which is based on Fourier analysis of interferometer signals to determine the spectral

distribution of radiation. The instrument may also be classed as a spectroradiometer which is calibrated to measure radiation intensity versus wavelength.

FUMIMETRE - A French (SNPE) motor smoke test facility that uses a fan driven wind tunnel.

HCT - Also MCT or HgCdTe, Mercury Cadmium Telluride semiconductor material used for detection of far infrared wavelengths.

HETEROGENEOUS CONDENSATION - Is the process whereby condensation occurs on solid particles which act as nuclei for the liquid droplet. If the nuclei are soluble the process is enhanced through lowering of the ambient water vapour pressure. Homogeneous condensation and growth of pure water droplets is less likely to occur in a plume environment.

HITRAN - A computer model that calculates high resolution atmospheric absorption of radiation.

IFTA - In Flight Transmission Analysis model, an empirical computer model developed at MICOM to predict laser transmission through an exhaust plume.

INSENSITIVE MUNITIONS - A term applied to munitions which have been designed to have reduced sensitivity to accidental initiation and subsequent violent collateral damage. In the US military IM refers to munitions which pass a specific series of test defined by DoD Std 2105A.

IR - An acronym for infrared radiation which is the band of wavelengths between approximately .7 and 100 micrometers. Plume IR sources may be both continuous and selective radiators but are generally dominated by rotation-vibration transitions. They may include both pure rotational and some electronic transitions of molecules.

JANNAF - Joint US Army-Navy-NASA-Air Force Interagency Propulsion Committee chartered to co-ordinate technology programs and promote technical exchange within US propulsion community.

LAPP - Low Altitude Plume Program, an early plume flow code used in the USA

LOWTRAN - A computer model that calculates low resolution (20 wavenumbers) atmospheric absorption of radiation from 0.2 to 20 micrometers.

MICOM - Acronym for the US Army Missile Command located at Redstone Arsenal, Alabama.

MICROWAVE - A region of the electromagnetic spectrum generally in the 10^9 - 10^{12} Hz frequency range. No universally accepted standard exists for the definition of microwave frequencies.

MICROWAVE PROPERTIES - of a rocket exhaust plume are those properties that enhance or hinder the detection or tracking of a missile by microwave radiation. The attenuation of a signal by free electrons is a microwave property of the plume.

MIE SCATTERING - Refers to light scattering by particles approximately equal to or greater than the wavelength of the light. The Mie equation reduces to the Rayleigh equation in the limiting case for small particles less than one tenth of the wavelength

MINIMUM SMOKE - A term used to describe a family of propellants whose characteristic is to produce the least amount of smoke under specified conditions. Differences in the application of the term to certain propellants has led AGARD to propose a standard classification procedure for NATO countries. An AGARD class AA may be used to identify this type of propellant.

MODULATION - Is any process that varies a characteristic of a carrier beam, i.e. pulse modulation, frequency modulation, amplitude modulation, etc.

NATURAL LINE BROADENING - Limits the sharpness of a spectral line due to the inherent energy decay of the radiating oscillator.

NAVIER-STOKES EQUATION - The complete classical continuum fluid mechanic equation of motion including inertial forces, pressure gradients, body forces, and viscosity. The differential equation of fluid flow can be solved by finite difference methods.

OBSCURATION - The process of blocking the electromagnetic energy emanating from a potential target thereby preventing detection of the target. An example is prevention of a second shot capability through obscuration by the post firing smoke cloud.

OLIVER CURVE - Is a plot of relative humidity vs temperature which predicts the condensation boundary for secondary smoke occurrence for a

particular type of propellant. The theory developed by R C Oliver is based on equilibrium thermochemistry.

OPTICAL DENSITY - See optical depth.

OPTICAL DEPTH - The exponent of the Beer-Lambert extinction equation. If the optical depth exceed a value of 0.5 consideration must be given to multiple scattering effects.

OSA - Optical Signal Attenuation code used in the US for the prediction of signal extinction by a rocket plume

OTH - "Over The Horizon" radar system

PARTICLE SIZE DISTRIBUTION - The particle number density or size parameter vs particle count in each bin of a particle analyser instrument. Also an analytical approximation or expression used to fit the measured data.

PASSIVE GUIDANCE - A form of missile guidance in which the missile homes on natural radiation from the target (e.g. RF, IR or visible). The missile contains an autonomous seeker that requires no external illumination of the target.

PLUME INSERTION LOSS - Refers to the loss of microwave energy observed at the detector as a result of the presence of the plume in the microwave link. The loss mechanisms are many. See attenuation, refraction, diffraction, backscatter, absorption, etc.

PMT - Photomultiplier tubes, i.e. high gain detectors used for detection of UV and visible radiation. PMT's usually consist of cascading dynodes which amplify the photoelectron.

PROPORTIONAL GUIDANCE SCHEME - Refers to a missile guidance system in which the controlling force i.e. airfoil, gas generator etc. is proportional to the deviation from the intended line of flight or trajectory

PRIMARY SMOKE - Consists of solid particulates from the rocket motor combustion and/or afterburning products. Metal fuels and other combustion control additives contribute significantly to primary smoke.

RADIOMETER - A device usually consisting of collector optics in combination with a transducer that converts radiant energy of a given bandwidth to an electrical signal proportional to the intensity of the received energy.

RAYLEIGH SCATTERING LIMIT - Particles which are larger in diameter than about one tenth the wavelength of the incident light are approaching the Rayleigh limit beyond which the general theory must be applied. See Mie Scattering.

RCS - Radar cross-section refers to the equivalent perpendicular area of reflection that duplicates the actual signal received from a target.

REDUCED SMOKE - A description for propellants that have been tailored to produce less smoke than previous formulations that contained binder with large amounts of aluminium and ammonium perchlorate. An AGARD class AC or BC may be used as an alternative to this term.

REFRACTION - Deviation of electromagnetic waves from straight line propagation due to velocity differences (refractive index changes) in the propagating medium.

REP - a plume flow code used in the UK

RF GUIDANCE - Radio frequency guidance, a general term used to describe electromagnetic radiation wavelengths greater than infrared, for example, radar, microwave, millimeter wave etc. that may be used for transmitting guidance signals.

ROS - Acronym for Royal Ordnance Summerfield, a British Aerospace Company located near London, England.

SCATTERING - one of two loss mechanisms (the other is absorption) in the propagation of radiation. Scattering is a change in direction or reradiation of incident photons caused by discontinuities (particles or electrons) in electrical properties of the propagation medium. The direction and intensity of scattered radiation depends upon the incident wavelength, the size, shape and refractive index of the particle.

SCF - Signature Characterisation Facility for ranking of propellant smoke, radiation emission and absorption, based on small rocket motor firings within a climatic chamber located at Army Missile Command, Redstone Arsenal, Alabama.

SCINTILLATION - Random signal fluctuation from a target being tracked by radar or laser. Scintillation may be caused by real motion of the source or by variations in refractive index of the atmosphere.

SEARCHLIGHT EFFECT - Is the term used to describe the motor chamber and nozzle emission continuum scattered by plume particles and detected as having an origin within the plume.

SECSMOKE - UK code for the prediction of secondary smoke

SECONDARY SMOKE - Is smoke that occurs when exhaust gases mix with ambient atmospheric water and condense on submicron particles that serve as nuclei for droplet formation. Secondary smoke is enhanced at low temperatures and high relative humidity and by the presence of acid vapours (typically HCl) and soluble nuclei that lower the saturation pressure of ambient water.

SELF ABSORPTION - Refers to radiation that is emitted in the core region of the plume and reabsorbed in the boundary layer or colder mixing regions. The observed bands show greater absorption in the band centres and less in the wings.

SEMI-ACTIVE - A form of missile guidance in which the target is illuminated by a friendly emitter (e.g. a radar or laser illuminator) and the missile homes on the signal reflected from the target.

SENSITIVITY - Refers to the hazardous potential for inadvertent initiation or detonation of energetic materials or munitions by unplanned thermal, mechanical or electrical stimuli.

SIGNATURE - A term which includes any or all the properties or characteristics of a system or a rocket motor exhaust that may be used for detection, identification or interception of a launch platform or missile at some time during its mission. Plume signature characteristics include smoke, radiation emissions, visibility, radar absorption etc.

SMOKE - A general term that refers to the effluent of rocket motor combustion which is made visible by light scattered or absorbed by condensed solid and liquid particulates. Smoke is a concern to rocket users who desire a low signature.

SMOKY PROPELLANT - Describes propellants with high aluminium and ammonium perchlorate content. An AGARD class CC may be used to describe this propellant.

SNPE - Acronym for Societe Nationale des Poudres et Explosifs, a French company which deals with research and development of energetic materials (high explosives, guns and rocket propellants) for military use.

SOLAR BLIND REGION - Is the portion (200 - 300nm) of the ultraviolet spectrum which lies outside the solar radiation region.

SPECTRAL RADIANCE - Refers to the radiant power emitted per unit area per unit solid angle per unit wavelength interval by a source such as a rocket plume. The units are Watts-meter-2-steradian-1-nanometer-1 (SI) and Watts-cm-2-steradian-1-micrometer-1 (JANNAF)

SPF - Standardised Plume Flowfield computer model whose development was sponsored by JANNAF.

THERMAL LAG - Describes the thermal inertia or delay of large particles within the plume to reach thermal equilibrium with the gaseous surroundings.

TRANSMISSIVITY - In propagation through an attenuating medium, transmissivity is the ratio of the transmitted beam intensity to the incident beam intensity. See the Beer-Lambert law for additional information.

TRANSMISSOMETER - An instrument for measuring the transmission of radiation passing through a medium

VALIDATION - The process of comparison of an analytical model with experimental data to confirm the accuracy of future predictions. Post correlation of model results with one set of test data should not constitute validation.

UV - Acronym for UltraViolet electromagnetic radiation which is defined by JANNAF to be the region between 100 and 400 nanometers. UV radiation sources arise from transitions between the electronic states of molecules.

VISIBILITY - A general term that relates to the probability of target detection by a human observer in a given scenario. The visibility of a target depends upon the target size, shape and colour; its contrast with the background; its orientation with respect to solar radiation; the visual acuity of the observer and the atmospheric visual range.

VISIG - Visual SIGnature, a commercial code for the calculation of plume visibility

XLDB - Acronym for cross-linked double base, a high energy subgroup of the double base family of propellants incorporating energetic fillers.

APPENDIX 2

Main Families of Solid Propellant

MAIN FAMILIES OF SOLID PROPELLANT

Propellant Family	Propellant Type	Main Ingredients	Additives (less than 5%)		
			Burning Rate Modifiers	Pressure Stabilizers	Signature Suppressants
Double Base	Extruded Double Base Cast Double Base	Nitrocellulose Nitroglycerine	Lead and Copper derivatives (mainly salts or oxides) (possibly Tin derivatives)	Refractories eg Zirconium carbide Zirconium silicate Zirconium oxide Metals eg Aluminium	Potassium salts eg Potassium sulphate (K_2SO_4) Potassium cryolithe (K_3ALF_6) Other Alkali salts
Composite	Aluminized (some Zirconium or Berylium envisaged)	Aluminium Ammonium perchlorate (AP) Inert binder (typically HTPB based)	Ferrocenic derivatives eg catocene Ferric oxide Copper chromite	-	Molybdenum trioxide (MoO_3)
	Non or slightly aluminized	Some Aluminium Ammonium perchlorate(AP) Inert binder (typically HTBP based)		Aluminium Refractories eg Zirconium carbide Zirconium silicate Zirconium oxide	Molybdenum trioxide (MoO_3)
High Energy Composite	High Energy (NEPE type) Nitrate-ester Polyether or Polyester	Aluminium Ammonium perchlorate (RDX) or (HMX) Energetic binder based on inert polymer plasticized with liquid nitrate-ester	-	-	Molybdenum trioxide (MoO_3)

MAIN FAMILIES OF SOLID PROPELLANT (CONTINUED)

Propellant Family	Propellant Type	Main Ingredients	Additives (less than 5%)		
			Burning Rate Modifiers	Pressure Stabilizers	Signature Suppressants
Composite Double Base	Cross Linked Double Base (XLDB)	(RDX) or (HMX) Energetic binder based on inert polymer plasticized with liquid nitrate-ester. Some ammonium perchlorate may be added	Lead and copper derivatives	Aluminium Refractories eg Zirconium carbide Zirconium silicate Zirconium oxide	Potassium salts eg Potassium sulphate (K_2SO_4) Potassium cryolithe (K_3ALF_6) Other Alkali salts
	Composite Modified Double Base (CMDB)	Nitrocellulose Nitroglycerin (RDX) or HMX) (Possibly some aluminium and ammonium perchlorate)	Lead and copper derivatives (possibly tin derivatives)	Aluminium Refractories eg Zirconium carbide Zirconium silicate Zirconium oxide	Potassium salts eg Potassium sulphate (K_2SO_4) Potassium cryolithe (K_3ALF_6) Other Alkali salts
	Elastomeric Modified Cast Double Base (EMCDB) (or filled double base)	Nitrocellulose Nitroglycerin Inert Prepolymer curing agent (RDX) or (HMX) (Possibly some aluminium and ammonium perchlorate)	Lead and copper derivatives (possibly tin derivatives)	Aluminium Refractories eg Zirconium carbide Zirconium silicate Zirconium oxide	Potassium salts eg Potassium sulphate (K_2SO_4) Potassium cryolithe (K_3ALF_6) Other Alkali salts

APPENDIX 3

List of Numerical Codes Used In The Calculation of Plume Signatures

APPENDIX 3

List of Numerical Codes Used In The Calculation of Plume Signatures

NOTE: The codes herein do not represent the total in existence. It is important to acknowledge advanced research codes that reflect the latest technology and methods. These codes attract high investment costs and some may involve sensitive national interests thereby preventing general release. The contact address should reveal the status of codes and their availability.

COUNTRY	CANADA
ORGANISATION OR COMPANY	Defence Research Establishment Valcartier, Quebec, Canada
NAME OF THE CODE	Missile Launch Cloud Prediction
PURPOSE OF THE CODE	To predict formation, motion, dispersion, and IR signal attenuation properties of primary smoke clouds (not plumes) that form upon vertical missile launches from ships
INPUTS (and possibly the name of the codes which give the inputs)	Ambient temperature, pressure, wind speed and direction, and atmospheric stability, missile thrust and mass, nozzle exit plane conditions (temperature, pressure, velocities, mass fraction of attenuating material from NASA-Lewis SP-273), maximum temperature of afterburning from REP-3, and ship speed and direction, mass extinction coefficients of attenuating material
OUTPUTS (and possibly the name of the codes which use the outputs)	Size, rise, position and concentration of cloud with time, and attenuation capability of the cloud
CHEMICAL SPECIES TAKEN IN ACCOUNT (precise if they are gaseous, liquid or solid)	Presently set up for HTPB-AP propellant smoke, either aluminized or non-aluminized, for attenuation in the visible and 3 to 5 μm and 8 to 14 μm infrared regions.
PHYSICAL PHENOMENA TAKEN IN ACCOUNT AND PHYSICAL LIMITATIONS	Treats clouds as homogeneous spheres at their formation and while they move and disperse. Must enter mass extinction coefficient of material of interest (except for HTPB-AP-Al propellant smoke), steady ship and wind speeds and directions only
SIMULATED ALTITUDE AND EXTENT OF THE PLUME	For missile launch clouds rather than comparatively well-defined, well-structured plumes
COMPUTING TIME DURING A RUN (indicate the kind of computer)	A few seconds on a 386 SX PC. The program is set up on a SYMPHONY spreadsheet
NUMERICAL METHOD AND GRID	Several equations set up on a spreadsheet to do a time-line analysis
AVAILABILITY (indicate if it is fully commercially available or if only a few runs may be performed)	Not commercially available, research tool only, contact DREV
CONTACT ADDRESS	Defence Research Establishment Valcartier PO Box 8800 Courcellette, Quebec, Canada GOA 1RO

COUNTRY	CANADA
ORGANISATION OR COMPANY	Defence Research Establishment Valcartier, Quebec, Canada
NAME OF THE CODE	FREEJET, Naval Weapons Center, Chinalake
PURPOSE OF THE CODE	Predicts formation of secondary smoke in plumes
INPUTS (and possibly the name of the codes which give the inputs)	Ambient temperature, relative humidity, and properties of plume at a point where there is less than 10% exhaust in the plume (temperature, pressure, velocities of jet and air, mole fractions of acid and water, nucleation particle sizes and whether or not they are soluble)
OUTPUTS (and possibly the name of the codes which use the outputs)	Position, temperature, mass fractions, velocities, saturation ratio, particle radii, particle concentration, mass fraction of acid in particles, on a two-dimensional grid
CHEMICAL SPECIES TAKEN IN ACCOUNT (precise if they are gaseous, liquid or solid)	H_2O, HCl, HF all gaseous or liquid
PHYSICAL PHENOMENA TAKEN IN ACCOUNT AND PHYSICAL LIMITATIONS	Two-dimensional axisymmetric grid, considers only four different streamlines in plume, can choose only six different sizes of nuclei, considers both soluble and insoluble nuclei, no turbulence modelling
SIMULATED ALTITUDE AND EXTENT OF THE PLUME	
COMPUTING TIME DURING A RUN (indicate the kind of computer)	A few minutes on a Honeywell CP-6
NUMERICAL METHOD AND GRID	Two-dimensional axisymmetric grid
AVAILABILITY (indicate if it is fully commercially available or if only a few runs may be performed)	Contact NWC, Chinalake
CONTACT ADDRESS	Defence Research Establishment Valcartier PO Box 8800 Courcelette, Quebec, Canada G0A 1R0

COUNTRY	CANADA
ORGANISATION OR COMPANY	Defence Research Establishment Valcartier, Quebec, Canada
NAME OF THE CODE	IPHASE (Integrated Program Host for Absorption, Scattering, and Extinction Calculations)
PURPOSE OF THE CODE	To compute extinction, scattering, and absorption efficiencies plus phase function for many shapes and size distributions
INPUTS (and possibly the name of the codes which give the inputs)	Refractive index (possibly from Drude models) shape, orientation, size, polarization
OUTPUTS (and possibly the name of the codes which use the outputs)	Extinction, scattering, and absorption efficiency, phase function
CHEMICAL SPECIES TAKEN IN ACCOUNT (precise if they are gaseous, liquid or solid)	Aerosols of any material
PHYSICAL PHENOMENA TAKEN IN ACCOUNT AND PHYSICAL LIMITATIONS	EM scattering from spheres, coated spheres, anisotropic coated spheres, infinite cylinders, coated infinite cylinder, finite cylinders and some irregular shapes
SIMULATED ALTITUDE AND EXTENT OF THE PLUME	
COMPUTING TIME DURING A RUN (indicate the kind of computer)	For monidispersions, typically $\ll$ 1 s on a 486 PC with Weitek chip Can be minutes to tens of minutes for wide polydispersions and cylinders
NUMERICAL METHOD AND GRID	For regular shapes codes are exact Irregular shapes are semi-empirical
AVAILABILITY (indicate if it is fully commercially available or if only a few runs may be performed)	Available. Code is copyrighted by DND
CONTACT ADDRESS	Defence Research Establishment Valcartier PO Box 8800 Courcelette, Quebec, Canada GOA 1RO

COUNTRY	FRANCE
ORGANISATION OR COMPANY	SNPE
NAME OF THE CODE	EMIR
PURPOSE OF THE CODE	IR radiation signature
INPUTS (and possibly the name of the codes which give the inputs)	Values of thermodynamical and chemical parameters (given by AJAX code)
OUTPUTS (and possibly the name of the codes which use the outputs)	Any result about IR radiation in any given band between 1.3 to 8.7 μm
CHEMICAL SPECIES TAKEN IN ACCOUNT (precise if they are gaseous, liquid or solid)	H_2O, CO_2, CO, HCl
PHYSICAL PHENOMENA TAKEN IN ACCOUNT AND PHYSICAL LIMITATIONS	Gaseous emission are evaluated by Goody hypothesis Heterogeneous mixture effects are formulated with Curtis-Godson approximation Particle radiation is considered as obeying an isotropic model
SIMULATED ALTITUDE AND EXTENT OF THE PLUME	
COMPUTING TIME DURING A RUN (indicate the kind of computer)	
NUMERICAL METHOD AND GRID	Computation of integrals along a path
AVAILABILITY (indicate if it is fully commercially available or if only a few runs may be performed)	Runs at SNPE for an outside customer are possible
CONTACT ADDRESS	Monsieur le Directeur Centre de Recherches du Bouchet SNPE BP No 2 91710 Vert-Le-Petit France

COUNTRY	FRANCE
ORGANISATION OR COMPANY	SNPE
NAME OF THE CODE	AJAX
PURPOSE OF THE CODE	Computing the close flowfield
INPUTS (and possibly the name of the codes which give the inputs)	Nozzle exit conditions
OUTPUTS (and possibly the name of the codes which use the outputs)	Values of thermodynamical and chemical parameters in the exhaust plume (used by EMIR code)
CHEMICAL SPECIES TAKEN IN ACCOUNT (precise if they are gaseous, liquid or solid)	Any chemical species However, only two finite rate reactions with CO and H_2 are taken into account
PHYSICAL PHENOMENA TAKEN IN ACCOUNT AND PHYSICAL LIMITATIONS	Two-dimensional Steady state Ke turbulence closure account of pressure gradients in Navier-Stokes equations simplified chemistry (see above)
SIMULATED ALTITUDE AND EXTENT OF THE PLUME	Low altitude
COMPUTING TIME DURING A RUN (indicate the kind of computer)	More than one hour on VAX 8530
NUMERICAL METHOD AND GRID	Finite differences
AVAILABILITY (indicate if it is fully commercially available or if only a few runs may be performed)	Runs at SNPE for an outside customer are possible
CONTACT ADDRESS	Monsieur le Directeur Centre de Recherches du Bouchet SNPE BP No 2 91710 Vert-Le-Petit France

COUNTRY	UNITED KINGDOM
ORGANISATION OR COMPANY	DRA, Fort Halstead
NAME OF THE CODE	BANDIR (Application Code)
PURPOSE OF THE CODE	Computes Narrow Band Spectral Infrared plume emissions selected from the range 1 to 15 μm
INPUTS (and possibly the name of the codes which give the inputs)	Output from REP3-90 via interfacing program. Atmospheric data, range, aspect angle, band model data
OUTPUTS (and possibly the name of the codes which use the outputs)	Provides band radiation intensity spectra over a selected wavelength band range (not line-by-line). Computes total radial intensity and irradiance
CHEMICAL SPECIES TAKEN IN ACCOUNT (precise if they are gaseous, liquid or solid)	Multispecies operation providing band spectral data. Principally CO, CO_2, H_2O
PHYSICAL PHENOMENA TAKEN IN ACCOUNT AND PHYSICAL LIMITATIONS	Atmospheric conditions included Particle emission not considered Body obscuration effects included (Note: 3D version coming on line)
SIMULATED ALTITUDE AND EXTENT OF THE PLUME	Multiple aspect angle
COMPUTING TIME DURING A RUN (indicate the kind of computer)	40 mins per aspect angle PC, Encore, VAX
NUMERICAL METHOD AND GRID	Spectral band model
AVAILABILITY (indicate if it is fully commercially available or if only a few runs may be performed)	Availability restricted
CONTACT ADDRESS	MTC4 Plume Science Defence Research Agency Fort Halstead, Sevenoaks Kent, England

COUNTRY	UNITED KINGDOM
ORGANISATION OR COMPANY	DRA, Fort Halstead
NAME OF THE CODE	REP3-90 (incorporating CCS, NEWFEC and FIRAC)
PURPOSE OF THE CODE	Plume flowfield calculation with secondary combustion
INPUTS (and possibly the name of the codes which give the inputs)	Nozzle exit plane conditions consisting of gas chemical composition, temperature, pressure and velocity given by FIRAC. Kinetic rate reactions and thermodynamic data. Turbulence model Kω or Kε. Flight free stream condition
OUTPUTS (and possibly the name of the codes which use the outputs)	Axisymmetric jet of time avereged quantities, chemical species and gas dynamic properties. This supplies data for all application codes
CHEMICAL SPECIES TAKEN IN ACCOUNT (precise if they are gaseous, liquid or solid)	System orientated chemical species. Ranging from chemistry of mono and bi-propellant liquid engines to those of solid composites and double base variants
PHYSICAL PHENOMENA TAKEN IN ACCOUNT AND PHYSICAL LIMITATIONS	Full finite rate chemistry Turbulence model Kω and Kε Single phase, time averaged axisymmetric variable grid parabolic code Predicts shock structure, position and magnitude of mach disc Does not represent particle flow
SIMULATED ALTITUDE AND EXTENT OF THE PLUME	Up to 50 km. Size governed by input to program
COMPUTING TIME DURING A RUN (indicate the kind of computer)	PC, VAX, ENCORE, say 45 mins. Problem dependent
NUMERICAL METHOD AND GRID	Solves parabolic/hyperbolic equations with implicit marching procedure on an expanding grid as calculation proceeds
AVAILABILITY (indicate if it is fully commercially available or if only a few runs may be performed)	Availability restricted
CONTACT ADDRESS	MTC4 Plume Science Defence Research Agency Fort Halstead, Sevenoaks Kent, England

COUNTRY	UNITED KINGDOM
ORGANISATION OR COMPANY	DRA, Fort Halstead
NAME OF THE CODE	BAFL2
PURPOSE OF THE CODE	To calculate early stages of flowfield to account for base recirculation.
INPUTS (and possibly the name of the codes which give the inputs)	Nozzle exit plane conditions consisting of gas chemical composition, temperature, pressure and velocity given by FIRAC. Kinetic rate reactions and thermodynamic data. Turbulence model Kω or Kε. Flight free stream condition Dedicated grid structure
OUTPUTS (and possibly the name of the codes which use the outputs)	Axisymmetric jet of time averaged quantities, chemical species and gas dynamic properties. This supplies data for all application codes. To interface with REP3-90
CHEMICAL SPECIES TAKEN IN ACCOUNT (precise if they double base variants are gaseous, liquid or solid)	Gaseous species dependant upon initial selection. System orientated chemical species. Ranging from chemistry of mono and bi-propellant liquid engines to those of solid composites and double base variants
PHYSICAL PHENOMENA TAKEN IN ACCOUNT AND PHYSICAL LIMITATIONS	Time averaged only Gas phase Fixed grid domain Finite rate chemistry Turbulence model laminar and Kε Axisymmetric
SIMULATED ALTITUDE AND EXTENT OF THE PLUME	Usually in early stages of plume calculation where axial diffusion is important
COMPUTING TIME DURING A RUN (indicate the kind of computer)	60+ mins VAX, PC, ENCORE
NUMERICAL METHOD AND GRID	Fixed grid set up at start of run. Elliptic code using upwind differencing
AVAILABILITY (indicate if it is fully commercially available or if only a few runs may be performed)	Availability restricted
CONTACT ADDRESS	MTC4 Plume Science Defence Research Agency Fort Halstead, Sevenoaks Kent, England

COUNTRY	UNITED KINGDOM
ORGANISATION OR COMPANY	DRA, Fort Halstead
NAME OF THE CODE	VISRAD (Application Code)
PURPOSE OF THE CODE	Computes visible radiation intensity distribution, eg sodium 'D' lines etc
INPUTS (and possibly the name of the codes which give the inputs)	Output from REP3-90 via interfacing program for excited states of of sodium and potassium
OUTPUTS (and possibly the name of the codes which use the outputs)	Visible radiation due to Na and K species only
CHEMICAL SPECIES TAKEN IN ACCOUNT (precise if they are gaseous, liquid or solid)	Na and K
PHYSICAL PHENOMENA TAKEN IN ACCOUNT AND PHYSICAL LIMITATIONS	Radiation of excited species. Currently Na and K but in principle other species can be considered
SIMULATED ALTITUDE AND EXTENT OF THE PLUME	
COMPUTING TIME DURING A RUN (Indicate the kind of computer)	30 mins VAX, ENCORE, PC. Problem dependant
NUMERICAL METHOD AND GRID	
AVAILABILITY (Indicate if it is fully commercially available or if only a few runs may be performed)	Availability restricted
CONTACT ADDRESS	MTC4 Plume Scien Defence Research Agency Fort Halstead, Sevenoaks Kent, England

COUNTRY	UNITED KINGDOM
ORGANISATION OR COMPANY	DRA, Fort Halstead
NAME OF THE CODE	RCS (Application Code)
PURPOSE OF THE CODE	To calculate the radar cross section of any flowfield
INPUTS (and possibly the name of the codes which give the inputs)	REP3-90 interface code including free electron concentrations, turbulence data and electron collision frequency
OUTPUTS (and possibly the name of the codes which use the outputs)	Radar cross section for given aspect angle
CHEMICAL SPECIES TAKEN IN ACCOUNT (precise if they are gaseous, liquid or solid)	[e⁻]
PHYSICAL PHENOMENA TAKEN IN ACCOUNT AND PHYSICAL LIMITATIONS	Back scattering process of plume
SIMULATED ALTITUDE AND EXTENT OF THE PLUME	
COMPUTING TIME DURING A RUN (indicate the kind of computer)	20 mins per aspect angle. PC. VAX, ENCORE. Problem dependent.
NUMERICAL METHOD AND GRID	
AVAILABILITY (indicate if it is fully commercially available or if only a few runs may be performed)	Availability restricted
CONTACT ADDRESS	MTC4 Plume Science Defence Research Agency Fort Halstead, Sevenoaks Kent, England

COUNTRY	UNITED KINGDOM
ORGANISATION OR COMPANY	DRA, Fort Halstead
NAME OF THE CODE	EPIC-90
PURPOSE OF THE CODE	To model plume for multi-nozzle, non axisymmetric flows. Finite rate chemistry. Single phase. No particles.
INPUTS (and possibly the name of the codes which give the inputs)	Nozzle exit plane conditions consisting of gas chemical composition, temperature, pressure and velocity. Kinetic rate reactions and thermodynamic data. Turbulence model Kω or Kϵ. Flight free stream condition.
OUTPUTS (and possibly the name of the codes which use the outputs	3-D spatial plume flowfield. Time averaged quantities, chemical species and gas dynamic properties. This supplies data for all application codes.
CHEMICAL SPECIES TAKEN IN ACCOUNT (precise if they are gaseous, liquid or solid)	System orientated chemical species. Ranging from chemistry of mono and bi-propellant liquid engines to those of solid composite and double base variants.
PHYSICAL PHENOMENA TAKEN IN ACCOUNT AND PHYSICAL LIMITATIONS	Full finite rate chemistry Turbulence model Kω and Kϵ Single phase, 3-D code with complex geometry Predicts shock structure, position and magnitude of mach disc
SIMULATED ALTITUDE AND EXTENT OF THE PLUME	Up to 70 km. Plume length variable.
COMPUTING TIME DURING A RUN (indicate the kind of computer)	In excess of two hours. WORK STATION, VAX, ENCORE.
NUMERICAL METHOD AND GRID	Finite difference, flexible grid. Uses eliptic code.
AVAILABILITY (indicate if it is fully commercially available or if only a few runs may be performed)	Availability restricted
CONTACT ADDRESS	MTC4 Plume Science Defence Research Agency Fort Halstead, Sevenoaks Kent, England

COUNTRY	USA
ORGANISATION OR COMPANY	Joint-Army-Navy-Nasa-Air Force (JANNAF) US Government
NAME OF THE CODE	Standard Infrared Radiation (2 to 25 μm) Model-SIRRM
PURPOSE OF THE CODE	Computing the IR radiation 2 to 25 μm from the gas and particle laden plume flowfields
INPUTS (and possibly the name of the codes which give the inputs)	1 Flowfield property map of plume domain, static T, P, and IR (active species = f (x, y)) usually provided by Standard Plume Flowfield, model (SPF) 2 Gaseous band model file 3 Particulate optical property file 4 Atmosphere property file
OUTPUTS (and possibly the name of the codes which use the outputs)	Spectral and in band local radiance, station radiation, radiant intensity-both apparent and source
CHEMICAL SPECIES TAKEN IN ACCOUNT (precise if they are gaseous, liquid or solid)	26 gaseous species H_2, CO_2, O_3, N_2O, CH_4, HNO_3, BO, BF, BCl, BFO, BClO, BHO, BO_2, BF_2, BClF, B_2O_2, B_2O_3, $B(OH)_2$, HBO_2, BF_3, HF, HCl, CO, ClF, OH, NO Al_2O_3, C(S), MgO and ZrO_2 condensables radii from 1 to 30 μm
PHYSICAL PHENOMENA TAKEN IN ACCOUNT AND PHYSICAL LIMITATIONS	Atmospheric attenuation and emission included for numerous atmospheric models Axisymmetric flowfield Particulate scattering - 2 flux and 6 flux approximation Curtis-Godson approximation for band model radiation from inhomogeneous gas paths Coupled gas/particle treatment of radiative transfer Incorporation of missile body obscuration near nose aspect Moderate resolution (5 cm^{-1})
SIMULATED ALTITUDE AND EXTENT OF THE PLUME	Multiple aspect angle, variable observer/target position
COMPUTING TIME DURING A RUN (indicate the kind of computer)	Wide range of computing time depending on problem. Executes on CDC 6600 and 7600, UNIVAX and IBM Minimum 5 min for simple LOS execution
NUMERICAL METHOD AND GRID	Band model formulation for gaseous emission, heavy gas, 2 flux and 6 flux scattering and emission for particulate radiation
AVAILABILITY (indicate if it is fully commercially available or if only a few runs may be performed)	Code export controlled Reports and permission to reproduce through CPIA Chemical Propulsion Information Agency John Hopkins University John Hopkins Road Laurel, Maryland 20707
CONTACT ADDRESS	Mr Thomas Smith OL-AC PL/RKFT Edwards AFB, CA 93524-7003

COUNTRY	USA
ORGANISATION OR COMPANY	Dr Eugene Miller, PO Box 4361, Incline Village, Nevada 89450, USA
NAME OF THE CODE	VISIG, DROP and OSA
PURPOSE OF THE CODE	**VISIG** predicts visible signature of rocket exhaust plumes due to scattering of ambient light by primary and secondary smoke **DROP** calculates formation of secondary smoke in solid rocket plumes based on SPF plume code (earlier version used LAPP as basis or plume flowfield) **OSA** calculates optical signal attenuation in solid rocket plumes
INPUTS (and possibly the name of the codes which give the inputs)	VISIG/OSA input includes particle size, type and spacial distribution and atmospheric transmission DROP input includes SPF/LAPP and climate (temperature/humidity)
OUTPUTS (and possibly the name of the codes which use the outputs)	See purpose of Code
CHEMICAL SPECIES TAKEN IN ACCOUNT (precise if they are gaseous, liquid or solid)	Optical properties of water, HCl-water, alumina and zirconia
PHYSICAL PHENOMENA TAKEN IN ACCOUNT AND PHYSICAL LIMITATIONS	Temperature, humidity, primary and secondary smoke particles, atmospheric transmission. Does not account for HF effects or soluble salts
SIMULATED ALTITUDE AND EXTENT OF THE PLUME	Limited only by plume flowfield calculation limits
COMPUTING TIME DURING A RUN (indicate the kind of computer)	Available for PC with MSDOS or PCDOS system
NUMERICAL METHOD AND GRID	
AVAILABILITY (indicate if it is fully commercially available or if only a few runs may be performed)	For sale by Dr Eugene Miller, PO Box 5461, Incline Village Nevada 89450, USA (Tel: 1-702-831-0429) Ensure correct export licence has been obtained.
CONTACT ADDRESS	See availability

APPENDIX 4

AGARD PEP WG-21 Climate Data Base

APPENDIX 4

AGARD PEP WG-21 CLIMATE DATA BASE

1 The temperature-Dew Point Model, referred to hereafter as the "Climate Database," is a computer code and database provided by the National Climatic Data Center, Federal Building, Ashville, North Carolina, 288180, USA, (ATTN: Mr M Changery E/CC22–telephone (704) 259-0765)), and described by them as a "Gridded Upper Air Climatology." The Climate Database was initially developed for the Naval Weapons Center (NWC) for its use and for promulgation to AGARD as a standard for uniform probability estimates of secondary-smoke formation by rocket exhausts.

2 The package comprising the model and database consists of thirteen 9-track, 6250 bpi, unlabelled ASCII tapes with 380 characters per record and 10 records per block on which data was generated from a UNIVAC 1100 computer. On the first of these tapes, Tape (1), is the program that reads the required data from the other tapes and formats it properly in an output file. The code listing, a brief output, and a sample input are attached.

3 The other twelve tapes contain climate data stored one month per tape. Because of differences between the UNIVAC and the VAX (at NWC), the files on the tapes had to be reformatted before they could be read by the computer code.

4 Each monthly climatology tape consists of five files. These files are determined by the latitude bands listed below in degrees:

i)	90.0 N	-	57.5 N
ii)	55.0 N	-	20.0 N
iii)	17.5 N	-	17.5 N
iv)	20.0 S	-	55.0 S
v)	57.5 S	-	90.0 S

Longitude is covered from 0.0 to 360.0 degrees for every file, and the limits of atmospheric pressure ("surface level") extend from 1000.0 to 30.0 millibars.

5 To run the program, one, and only one, of the sixty possible climatology input files can be attached. The user is prompted to give the limits for the surface level in the atmosphere, the longitude, and the latitude within the limits of the attached data file. Specific points may be entered. For example, latitude may be entered to range from 55.0 N to 55.0 N; and thus restrict the range considered to one particular latitude.

6 Latitude and longitude may be entered in multiples of 2.5 degrees. The altitude level is most easily entered as a range of values, but may be entered as an exact value. Data are stored in the files at the following "altitudes" levels in millibars: 1000.0, 850.0, 700.0, 500.0, 400.0, 300.0, 250.0, 100.0, 70.0, 50.0, and 30.0.

7 Within the database there are approximately 30 data points for temperature and dew point depression over a two-week period for a specific month, altitude, latitude and longitude, on which the statistics are based.

8 The attached output listing shows statistical summaries printed for each of the years 1980 through 1985 for January (1st month), both first two-week period and second two-week period for -20 degrees latitude and 120 degrees longitude at 100, 70, 50 and 30 millibars. Temperature and dew point depression are listed in °C with their one-, two-, and three-sigma variations added to and subtracted from the mean. No dew point depression data were included at these altitudes (such data are included in the database only from 1000 to 300 mb). A partial input tape listing with limited annotation, for December (12th month) is also included for 100 mb, 87.5 degrees latitude and 0-15 degrees longitude. Number of observations, mean temperature, mean dew point depression and one-sigma values for

temperature and dew point depression are given. Clearly the six-year data base, first and last half of the month is included, but without the code one cannot determine which data are which. From examining both of these listings, it is clear that a linear curve of variation is assumed in the statistical analysis of temperature. A linear variation of dew point depression is also used, below 300 mb.

9 A set of the Climate Database tapes for VAX computers is available on loan (for copying and return) from the AGARD office (address given in the Introduction to this report). The Climate Database tapes can be purchased from the National Climatic Data Center address given above. The National Climatic Data Center is currently updating its climate database and incorporating more precise ground-level data than are in the current database.

```
      PROGRAM PHERE
      CHARACTER CBUF*360
      DIMENSION RLIM(6)
      DIMENSION TEMP(12), SIGT(12), DPD(12), SIGD(12)
      INTEGER NOBS(12)

      DATA RLIM(1)/90.0/
      DATA RLIM(2)/55.0/
      DATA RLIM(3)/17.5/
      DATA RLIM(4)/-20.0/
      DATA RLIM(5)/-57.5/
      DATA RLIM(6)/-92.5/

      OPEN(UNIT=2,FILE='CBUF.DAT',STATUS='NEW')

      OPEN(UNIT=9,FILE='WETHR.DAT',STATUS='NEW')

      OPEN(UNIT=8,FILE='JAN.FL4',STATUS='OLD',ERR=800,
     *       FORM='FORMATTED',ACCESS='SEQUENTIAL',IOSTAT=IERR)

C     ************************************************************************
      READ(8,1000,IOSTAT=IERR,ERR=800,END=999) INMTH,LEVEL,TLAT,
     *  TLON,CBUF

1000  FORMAT(I2,I6,2F6.1,A360)

      WRITE(2,*)CBUF

      IF(TLAT.GT.RLIM(2)) THEN
        LBIND = 1
      ELSE IF (TLAT.GT.RLIM(3)) THEN
        LBIND = 2
      ELSE IF (TLAT.GT.RLIM(4)) THEN
        LBIND = 3
      ELSE IF (TLAT.GT.RLIM(5)) THEN
        LBIND = 4
      ELSE
        LBIND = 5
      END IF
      RLIM1 = RLIM(LBIND)
      RLIM2 = RLIM(LBIND+1) + 2.5
      WRITE(6,1100) INMTH,RLIM1,RLIM2
1100  FORMAT(' CURRENTLY EXAMINING UNIT=8 MONTH=',I4 ,
     *  '  LATITUDE LIMITS =',F6.1,' TO ',F6.1)
    5 WRITE(6,1200)
1200  FORMAT(' ENTER LOWER AND UPPER LEVELS (1000 TO 30)')
      READ (5,*) ILEV1,ILEV2
      WRITE(6,*) ILEV1,ILEV2
      IF (ILEV1 .EQ. 0) THEN
        WRITE(6,1300)
1300    FORMAT(' END OF PROGRAM ')
      END IF

    7 WRITE(6,1500) RLIM1,RLIM2
1500  FORMAT(' ENTER TOP AND BOTTOM LATITUDES (',F6.1,' TO ',F6.1,')')
      READ  (5,*)  ALAT1,ALAT2
      WRITE (6,*)  ALAT1,ALAT2
```

```
      IF(ALAT1.GT.RLIM1 .OR. ALAT2.LT.RLIM2 .OR. ALAT1.LT.ALAT2) THEN
       WRITE(6,1600)
1600   FORMAT(' INVALID LATITUDE RANGE, PLEASE TRY AGAIN')
       GO TO 7
      END IF

    8 WRITE(6,1700)
1700  FORMAT(' ENTER LEFT AND RIGHT LONGITUDES (0 TO 360)')
      READ  (5,*) ALON1,ALON2
      WRITE (6,*) ALON1,ALON2
      IF(ALON1 .LT. 0. .OR. ALON2 .GT. 360. .OR. ALON1 .GT. ALON2) THEN
       WRITE(6,1800)
1800   FORMAT(' INVALID LONGITUDE RANGE, PLEASE TRY AGAIN')
       GO TO 8
      END IF

   10 IF(LEVEL .LE. ILEV1 .AND. LEVEL .GE. ILEV2) THEN
       IF(TLAT .LE. ALAT1 .AND. TLAT .GE. ALAT2) THEN
        IF(TLON .GE. ALON1 .AND. TLON .LE. ALON2) THEN
C         FOUND DATA WITHIN RANGE LIMITS, DECODE, CALCULATE, AND
C         OUTPUT TO UNIT 6
          READ(CBUF,2000) (NOBS(I),TEMP(I),SIGT(I),DPD(I),SIGD(I),
     *     I=1,12)
2000      FORMAT(12(I4,2(F7.2,F6.2)))
          I = 0
          WRITE(9,3000) INMTH,LEVEL,TLAT,TLON
3000      FORMAT(' MONTH ',I2,'; LEVEL ',I4,' MB; LATITUDE ',
     *     F6.1,'; LONGITUDE',F6.1,/,' YEAR HALF',
     *     '   TEMP    + 1SIG -          + 2SIG -     +3SIG     -   ',
     *     ' DEPRES   + 1SIG -          + 2SIG -     +3SIG     -   ')
          DO 30 IYR = 1980,1985
           DO 20 IHLF = 1,2
             I = I + 1
             IF(NOBS(I) .NE. 0) THEN
              SIGT1P = TEMP(I) + SIGT(I)
              SIGT1M = TEMP(I) - SIGT(I)
              SIGT2P = TEMP(I) + SIGT(I)*2.
              SIGT2M = TEMP(I) - SIGT(I)*2.
              SIGT3P = TEMP(I) + SIGT(I)*3.
              SIGT3M = TEMP(I) - SIGT(I)*3.
              SIGD1P = DPD(I) + SIGD(I)
              SIGD1M = DPD(I) - SIGD(I)
              IF(SIGD1M .LT. 0.) SIGD1M =0.
              SIGD2P = DPD(I) + SIGD(I)*2.
              SIGD2M = DPD(I) - SIGD(I)*2.
              IF(SIGD2M .LT. 0.) SIGD2M =0.
              SIGD3P = DPD(I) + SIGD(I)*3.
              SIGD3M = DPD(I) - SIGD(I)*3
              IF(SIGD3M .LT. 0.) SIGD3M =0.
              WRITE(9,3100) IYR,IHLF,TEMP(I),SIGT1P,SIGT1M,SIGT2P,
     *         SIGT2M,SIGT3P,SIGT3M,DPD(I),SIGD1P,SIGD1M,SIGD2P,
     *         SIGD2M,SIGD3P,SIGD3M
3100          FORMAT(2I5,2(F8.2,6F7.2))
             END IF
   20       CONTINUE
   30      CONTINUE
           IF(LEVEL .LE. ILEV2 .AND. TLAT .LE. ALAT2 .AND.
     *      TLON .GE. ALON2) THEN
```

```
            WRITE(9,3200)
3200        FORMAT(' AT END OF DESIRED RANGE')
          GO TO 999
         END IF
        END IF
       END IF
      END IF
      READ(8,1000,IOSTAT=IERR,ERR=800,END=999) INMTH,LEVEL,TLAT,
     *   TLON,CBUF
      GO TO 10



 800  IF(IERR .NE. 0) THEN
       WRITE (6,3500) IERR
3500   FORMAT(' READ ERR UNIT=8 : ERROR=',I8)
      END IF

 999  WRITE(6,3900)
3900  FORMAT(' END OF PROCESSING')

      WRITE(2,*)CBUF

      CLOSE(UNIT=8,STATUS='KEEP')
      CLOSE(UNIT=9,STATUS='KEEP')
      CLOSE(UNIT=2,STATUS='KEEP')

      STOP
      END
```

INPUT TAPE = GIBBS - TAPE-WO5121 TEST RUN
OUTPUT FILE = WO5121.TST

[Month] [Alt] [Lat] [Long] [No of Observations] [Temperature C] [One Standard Deviation of Temperature] [Dewpoint. Depression C] [One Standard Deviation of Dewpoint Depression]

12 1000 90.0 .0 30 -23.24 2.58 3.77 1.85 32 -24.67 1.86 3.80 1.62 30 -29.16 5.13 7.11 1.81 32 -24.34 4.53 5.
98 2.79 30 -25.74 4.39 1.64 1.11 32 -25.54 3.76 1.88 1.62 30 -22.93 4.92 3.74 2.61 32 -29.48 3.22 2.69 2.67 30
-28.11 2.58 3.25 2.92 32 -23.01 4.36 4.53 4.35 30 -24.44 3.37 1.12 .88 32 -23.07 3.64 1.79 1.69

12 1000 87.5 0 30 -23.48 2.43 0.56 0.81 32 -23.81 2.12 0.75 1.00 30 -28.46 4.56 1.01 1.69 32 -23.98 4.28 1.
67 2.99 30 -25.09 3.60 1.25 1.15 32 -25.65 2.84 1.22 1.37 30 -23.55 4.54 3.81 3.95 32 -28.23 2.12 2.76 2.76 30
-26.57 2.00 2.54 2.08 32 -21.92 4.39 3.70 3.43 30 -22.94 4.01 1.01 1.03 32 -23.21 2.95 1.37 1.38

12 1000 87.5 2.5 30 -23.43 2.43 .53 0.78 32 -23.78 2.13 0.73 1.00 30 -28.46 4.52 0.97 1.60 32 -24.01 4.29 1.
64 3.00 30 -25.12 3.54 1.22 1.13 32 -25.61 2.83 1.21 1.37 30 -23.63 4.50 3.81 3.97 32 -28.20 2.10 2.76 2.76 30
-26.56 1.95 2.51 2.01 32 -21.91 4.31 3.69 3.54 30 -22.82 4.01 .99 1.00 32 -23.34 2.95 1.33 1.34

12 1000 87.5 5.0 30 -23.49 2.43 .50 0.75 32 -23.74 2.14 0.70 0.99 30 -28.44 4.48 0.92 1.52 32 -24.03 4.30 1.
63 3.00 30 -25.15 3.48 1.18 1.10 32 -25.57 2.32 1.21 1.36 30 -23.71 4.47 3.81 3.97 32 -28.18 2.08 2.75 2.78 30
-26.56 1.91 2.48 1.94 32 -21.90 4.24 3.69 3.61 30 -22.72 4.02 .95 .97 32 -23.47 2.95 1.28 1.30

12 1000 87.5 7.5 30 -23.49 2.42 .48 0.73 32 -23.71 2.15 0.68 0.99 30 -28.43 4.45 0.88 1.45 32 -24.05 4.31 1.
62 3.01 30 -25.18 3.41 1.15 1.08 32 -25.53 2.81 1.20 1.35 30 -23.79 4.43 3.81 3.97 32 -28.16 2.06 2.75 2.81 30
-26.56 1.87 2.47 1.88 32 -21.91 4.16 3.69 3.69 30 -22.62 4.02 .92 .94 32 -23.62 2.96 1.24 1.26

12 1000 87.5 10.0 30 -23.48 2.42 .45 .71 32 -23.68 2.15 0.65 0.98 30 -28.40 4.42 0.85 1.38 32 -24.05 4.32 1.
61 3.02 30 -25.20 3.35 1.12 1.05 32 -25.48 2.30 1.20 1.35 30 -23.87 4.39 3.79 3.94 32 -28.15 2.05 2.74 2.86 30
-26.57 1.84 2.46 1.84 32 -21.91 4.08 3.70 3.77 30 -22.53 4.02 .90 .91 32 -23.76 2.96 1.20 1.22

12 1000 87.5 12.5 30 -23.48 2.42 .42 .69 32 -23.64 2.16 0.62 0.97 30 -28.37 4.39 0.82 1.32 32 -24.05 4.34 1.
61 3.03 30 -25.22 3.30 1.10 1.03 32 -25.43 2.80 1.20 1.34 30 -23.96 4.35 3.76 3.91 32 -28.14 2.05 2.72 2.92 30
-26.58 1.81 2.46 1.81 32 -21.92 4.00 3.73 3.85 30 -22.45 4.01 0.87 .89 32 -23.91 2.96 1.16 1.19

12 1000 87.5 15.0 30 -23.47 2.41 0.40 0.68 32 -23.61 2.17 0.60 0.95 30 -28.33 4.37 .80 1.27 32 -24.05 4.36 1.
63 3.04 30 -25.23 3.24 1.07 1.00 32 -25.88 2.80 1.20 1.33 30 -24.04 4.31 3.27 3.56 32 -28.13 2.05 2.70 3.30 30
-26.59 1.79 2.48 1.80 32 -21.63 3.82 3.76 3.93 30 -22.38 4.00 .84 .87 32 -24.05 2.96 1.12 1.15

OUTPUT FILE

MONTH 1: LEVEL 100 MB: LATITUDE -20.0: LONGITUDE 120.0

YEAR	HALF	TEMP	+ 1SIG -		+ 2SIG -		+3SIG -		DEPRES	+ 1SIG -		+ 2SIG -		+ 3SIG -	
1980	1	-75.77	-75.00	-76.54	-74.23	-77.31	-73.46	-78.08	0.00	0.00	0.00	0.00	0.00	0.00	0.00
1980	2	-74.88	-73.57	-76.19	-72.26	-77.50	-70.95	-78.81	0.00	0.00	0.00	0.00	0.00	0.00	0.00
1981	1	-77.95	-77.28	-78.62	-76.61	-79.29	-75.94	-79.76	0.00	0.00	0.00	0.00	0.00	0.00	0.00
1981	2	-78.30	-77.71	-78.89	-77.12	-79.48	-76.53	-80.07	0.00	0.00	0.00	0.00	0.00	0.00	0.00
1982	1	-77.08	-76.14	-78.02	-75.20	-78.96	-74.26	-79.90	0.00	0.00	0.00	0.00	0.00	0.00	0.00
1982	2	-78.03	-76.91	-79.15	-75.79	-80.27	-74.67	-81.39	0.00	0.00	0.00	0.00	0.00	0.00	0.00
1983	1	-76.25	-75.17	-77.33	-74.09	-78.41	-73.01	-79.49	0.00	0.00	0.00	0.00	0.00	0.00	0.00
1983	2	-74.10	-73.23	-74.97	-72.36	-75.84	-71.49	-76.71	0.00	0.00	0.00	0.00	0.00	0.00	0.00
1984	1	-75.74	-75.12	-76.36	-74.50	-76.98	-73.88	-77.60	0.00	0.00	0.00	0.00	0.00	0.00	0.00
1984	2	-75.74	-74.65	-75.65	-74.15	-76.15	-73.65	-76.65	0.00	0.00	0.00	0.00	0.00	0.00	0.00
1985	1	-74.40	-73.97	-74.83	-73.54	-75.26	-73.11	-75.69	0.00	0.00	0.00	0.00	0.00	0.00	0.00
1985	2	-75.54	-75.03	-76.05	-74.52	-76.56	-74.01	-77.07	0.00	0.00	0.00	0.00	0.00	0.00	0.00

MONTH 1: LEVEL 70 MB: LATITUDE -20.0: LONGITUDE 120.0

YEAR	HALF	TEMP	+ 1SIG -		+ 2SIG -		+3SIG -		DEPRES	+ 1SIG -		+ 2SIG -		+ 3SIG	
1980	No Data														
1981	1	-73.98	-73.02	-74.94	-72.06	-75.90	-71.10	-76.86	0.00	0.00	0.00	0.00	0.00	0.00	0.00
1981	2	-75.20	-74.43	-75.97	-73.66	-76.74	-72.89	-77.51	0.00	0.00	0.00	0.00	0.00	0.00	0.00
1982	1	-74.64	-73.66	-75.62	-72.68	-76.60	-71.70	-77.58	0.00	0.00	0.00	0.00	0.00	0.00	0.00
1982	2	-76.52	-75.27	-77.77	-74.02	-79.02	-72.77	-80.27	0.00	0.00	0.00	0.00	0.00	0.00	0.00
1983	1	-72.48	-71.09	-73.87	-69.70	-75.26	-68.31	-76.65	0.00	0.00	0.00	0.00	0.00	0.00	0.00
1983	2	-71.16	-70.43	-71.89	-69.70	-72.62	-68.97	-73.35	0.00	0.00	0.00	0.00	0.00	0.00	0.00
1984	1	-73.27	-72.50	-74.04	-71.73	-74.81	-70.96	-75.58	0.00	0.00	0.00	0.00	0.00	0.00	0.00
1984	2	-72.06	-71.53	-72.59	-71.00	-73.12	-70.47	-73.65	0.00	0.00	0.00	0.00	0.00	0.00	0.00
1985	1	-71.26	-70.27	-72.25	-69.28	-73.24	-68.29	-74.23	0.00	0.00	0.00	0.00	0.00	0.00	0.00
1985	2	-72.74	-72.00	-73.48	-71.26	-74.22	-70.52	-74.96	0.00	0.00	0.00	0.00	0.00	0.00	0.00

MONTH 1: LEVEL 50 MB: LATITUDE -20.0: LONGITUDE 120.0

YEAR	HALF	TEMP	+ 1SIG -		+ 2SIG -		+3SIG -		DEPRES	+ 1SIG -		+ 2SIG -		+ 3SIG	
1980	1	-68.87	-67.83	-69.91	-66.79	-70.95	-65.75	-71.99	0.00	0.00	0.00	0.00	0.00	0.00	0.00
1980	2	-69.05	-68.21	-69.89	-67.37	-70.73	-66.53	-71.57	0.00	0.00	0.00	0.00	0.00	0.00	0.00
1981	1	-64.76	-63.83	-65.69	-62.90	-66.62	-61.97	-67.55	0.00	0.00	0.00	0.00	0.00	0.00	0.00
1981	2	-66.26	-65.59	-66.93	-64.92	-67.60	-64.25	-68.27	0.00	0.00	0.00	0.00	0.00	0.00	0.00
1982	1	-68.74	-67.91	-69.57	-67.08	-70.40	-66.25	-71.23	0.00	0.00	0.00	0.00	0.00	0.00	0.00
1982	2	-70.88	-69.59	-72.17	-68.30	-73.46	-67.01	-74.75	0.00	0.00	0.00	0.00	0.00	0.00	0.00
1983	1	-65.82	-64.64	-67.00	-63.46	-68.18	-62.28	-69.36	0.00	0.00	0.00	0.00	0.00	0.00	0.00
1983	2	-65.49	-64.81	-66.17	-64.13	-66.85	-63.45	-67.53	0.00	0.00	0.00	0.00	0.00	0.00	0.00
1984	1	-63.84	-63.33	-64.35	-62.82	-64.86	-62.31	-65.37	0.00	0.00	0.00	0.00	0.00	0.00	0.00
1984	2	-62.94	-62.54	-63.34	-62.14	-63.74	-61.74	-64.14	0.00	0.00	0.00	0.00	0.00	0.00	0.00
1985	1	-62.44	-61.93	-62.95	-61.42	-63.46	-60.91	-63.97	0.00	0.00	0.00	0.00	0.00	0.00	0.00
1985	2	-63.29	-62.74	-63.84	-62.19	-64.39	-61.64	-64.94	0.00	0.00	0.00	0.00	0.00	0.00	0.00

OUTPUT FILE (CONTINUED)

MONTH 1: LEVEL 30 MB: LATITUDE -20.0: LONGITUDE 120.0

YEAR	HALF	TEMP	+ 1SIG -		+ 2SIG -		+3SIG -		DEPRES	+ 1SIG -		+ 2SIG -		+ 3SIG	
1980	1	-60.58	-59.97	-61.19	-59.36	-61.80	-58.75	-62.41	0.00	0.00	0.00	0.00	0.00	0.00	0.00
1980	2	-60.94	-60.54	-61.34	-60.14	-61.74	-59.74	-62.14	0.00	0.00	0.00	0.00	0.00	0.00	0.00
1981	1	-48.93	-48.13	-49.73	-47.33	-50.53	-46.53	-51.33	0.00	0.00	0.00	0.00	0.00	0.00	0.00
1981	2	-50.21	-49.65	-50.77	-49.09	-51.33	-48.53	-51.89	0.00	0.00	0.00	0.00	0.00	0.00	0.00
1982	1	-58.85	-58.14	-59.56	-57.43	-60.27	-56.72	-60.98	0.00	0.00	0.00	0.00	0.00	0.00	0.00
1982	2	-60.79	-59.65	-61.93	-58.51	-63.07	-57.37	-64.21	0.00	0.00	0.00	0.00	0.00	0.00	0.00
1983	1	-55.65	-54.96	-56.34	-54.27	-57.03	-53.58	-57.72	0.00	0.00	0.00	0.00	0.00	0.00	0.00
1983	2	-56.45	-55.65	-57.25	-54.85	-58.85	-58.05	-58.85	0.00	0.00	0.00	0.00	0.00	0.00	0.00
1984	1	-54.40	-53.74	-55.06	-53.08	-55.72	-52.42	-56.38	0.00	0.00	0.00	0.00	0.00	0.00	0.00
1984	2	-53.83	-53.27	-54.39	-52.71	-54.95	-52.15	-55.51	0.00	0.00	0.00	0.00	0.00	0.00	0.00
1985	1	-53.63	-53.32	-53.94	-53.01	-54.25	-52.70	-54.56	0.00	0.00	0.00	0.00	0.00	0.00	0.00
1985	2	-53.84	-53.26	-54.42	-52.68	-55.00	-52.10	-55.58	0.00	0.00	0.00	0.00	0.00	0.00	0.00

AT END OF DESIRED RANGE

REPORT DOCUMENTATION PAGE

1. Recipient's Reference	2. Originator's Reference	3. Further Reference	4. Security Classification of Document
	AGARD-AR-287	ISBN 92-835-0699-5	UNCLASSIFIED/ UNLIMITED

5. Originator Advisory Group for Aerospace Research and Development
North Atlantic Treaty Organization
7 Rue Ancelle, 92200 Neuilly sur Seine, France

6. Title
TERMINOLOGY AND ASSESSMENT METHODS OF SOLID PROPELLANT ROCKET EXHAUST SIGNATURES

7. Presented at

8. Author(s)/Editor(s)	9. Date
Various	February 1993
10. Author's/Editor's Address	**11. Pages**
Various	278

12. Distribution Statement There are no restrictions on the distribution of this document. Information about the availability of this and other AGARD unclassified publications is given on the back cover.

13. Keywords/Descriptors

Assessment methods
Detection requirements
Exhaust of rockets
Expansion nozzles
Ionisation of plumes
Ingredients of propellants
Microwave effects
Plume properties
Signature of rockets
Smoke signatures
Solid propellants
Terminology of rockets
Radiation of exhaust

14. Abstract

The Propulsion and Energetics Panel's Specialists' Meeting in autumn 1985 on Smokeless Propellants demonstrated that no common standard was available in this field and that the lack of common understanding led to misunderstanding amongst the NATO community.

After some preparatory discussion, the Panel, therefore, formed Working Group Number 21 with the objectives of defining methods for the assessment of rocket motor exhaust optical properties in the visible and in the infrared range, and of recommending a terminology based on quantitative criteria.

The Working Group discussed the subject in a total of eight sessions and prepared this Advisory Report. Following an Introduction and Summary there are six chapters, commencing with an Overview and continuing with Propellant Smoke Classification, Plume Primary Smoke, Plume Secondary Smoke, Plume Radiation and Plume Microwave Properties. In most cases, the conclusions and recommendations follow the chapters and are not repeated at the end of the Report.

AGARD Advisory Report 287
Advisory Group for Aerospace Research and Development, NATO
TERMINOLOGY AND ASSESSMENT METHODS OF SOLID PROPELLANT ROCKET EXHAUST SIGNATURES
Published February 1993
278 pages

The Propulsion and Energetics Panel's Specialists' Meeting in autumn 1985 on Smokeless Propellants demonstrated that no common standard was available in this field and that the lack of common understanding led to misunderstanding amongst the NATO community.

After some preparatory discussion, the Panel, therefore, formed Working Group Number 21 with the objectives

P.T.O.

AGARD-AR-287

Assessment methods
Detection requirements
Exhaust of rockets
Expansion nozzles
Ionisation of plumes
Ingredients of propellants
Microwave effects
Plume properties
Signature of rockets
Smoke signatures
Solid propellants
Terminology of rockets
Radiation of exhaust

AGARD Advisory Report 287
Advisory Group for Aerospace Research and Development, NATO
TERMINOLOGY AND ASSESSMENT METHODS OF SOLID PROPELLANT ROCKET EXHAUST SIGNATURES
Published February 1993
278 pages

The Propulsion and Energetics Panel's Specialists' Meeting in autumn 1985 on Smokeless Propellants demonstrated that no common standard was available in this field and that the lack of common understanding led to misunderstanding amongst the NATO community.

After some preparatory discussion, the Panel, therefore, formed Working Group Number 21 with the objectives

P.T.O.

AGARD-AR-287

Assessment methods
Detection requirements
Exhaust of rockets
Expansion nozzles
Ionisation of plumes
Ingredients of propellants
Microwave effects
Plume properties
Signature of rockets
Smoke signatures
Solid propellants
Terminology of rockets
Radiation of exhaust

AGARD Advisory Report 287
Advisory Group for Aerospace Research and Development, NATO
TERMINOLOGY AND ASSESSMENT METHODS OF SOLID PROPELLANT ROCKET EXHAUST SIGNATURES
Published February 1993
278 pages

The Propulsion and Energetics Panel's Specialists' Meeting in autumn 1985 on Smokeless Propellants demonstrated that no common standard was available in this field and that the lack of common understanding led to misunderstanding amongst the NATO community.

After some preparatory discussion, the Panel, therefore, formed Working Group Number 21 with the objectives

P.T.O.

AGARD-AR-287

Assessment methods
Detection requirements
Exhaust of rockets
Expansion nozzles
Ionisation of plumes
Ingredients of propellants
Microwave effects
Plume properties
Signature of rockets
Smoke signatures
Solid propellants
Terminology of rockets
Radiation of exhaust

AGARD Advisory Report 287
Advisory Group for Aerospace Research and Development, NATO
TERMINOLOGY AND ASSESSMENT METHODS OF SOLID PROPELLANT ROCKET EXHAUST SIGNATURES
Published February 1993
278 pages

The Propulsion and Energetics Panel's Specialists' Meeting in autumn 1985 on Smokeless Propellants demonstrated that no common standard was available in this field and that the lack of common understanding led to misunderstanding amongst the NATO community.

After some preparatory discussion, the Panel, therefore, formed Working Group Number 21 with the objectives

P.T.O.

AGARD-AR-287

Assessment methods
Detection requirements
Exhaust of rockets
Expansion nozzles
Ionisation of plumes
Ingredients of propellants
Microwave effects
Plume properties
Signature of rockets
Smoke signatures
Solid propellants
Terminology of rockets
Radiation of exhaust

of defining methods for the assessment of rocket motor exhaust optical properties in the visible and in the infrared range, and of recommending a terminology based on quantitative criteria.

The Working Group discussed the subject in a total of eight sessions and prepared this Advisory Report. Following an Introduction and Summary there are six chapters, commencing with an Overview and continuing with Propellant Smoke Classification, Plume Primary Smoke, Plume Secondary Smoke, Plume Radiation and Plume Microwave Properties. In most cases, the conclusions and recommendations follow the chapters and are not repeated at the end of the Report.

ISBN 92-835-0699-5

of defining methods for the assessment of rocket motor exhaust optical properties in the visible and in the infrared range, and of recommending a terminology based on quantitative criteria.

The Working Group discussed the subject in a total of eight sessions and prepared this Advisory Report. Following an Introduction and Summary there are six chapters, commencing with an Overview and continuing with Propellant Smoke Classification, Plume Primary Smoke, Plume Secondary Smoke, Plume Radiation and Plume Microwave Properties. In most cases, the conclusions and recommendations follow the chapters and are not repeated at the end of the Report.

ISBN 92-835-0699-5

of defining methods for the assessment of rocket motor exhaust optical properties in the visible and in the infrared range, and of recommending a terminology based on quantitative criteria.

The Working Group discussed the subject in a total of eight sessions and prepared this Advisory Report. Following an Introduction and Summary there are six chapters, commencing with an Overview and continuing with Propellant Smoke Classification, Plume Primary Smoke, Plume Secondary Smoke, Plume Radiation and Plume Microwave Properties. In most cases, the conclusions and recommendations follow the chapters and are not repeated at the end of the Report.

ISBN 92-835-0699-5

of defining methods for the assessment of rocket motor exhaust optical properties in the visible and in the infrared range, and of recommending a terminology based on quantitative criteria.

The Working Group discussed the subject in a total of eight sessions and prepared this Advisory Report. Following an Introduction and Summary there are six chapters, commencing with an Overview and continuing with Propellant Smoke Classification, Plume Primary Smoke, Plume Secondary Smoke, Plume Radiation and Plume Microwave Properties. In most cases, the conclusions and recommendations follow the chapters and are not repeated at the end of the Report.

ISBN 92-835-0699-5